Design, Validation and Assessment of Vibratory Mat for Stochastic Resonance Applications

By

Camilo Giraldo

Submitted to the graduate program in Mechanical Engineering and the Graduate Faculty of the University of Kansas in partial fulfillment of the requirements for the degree of Doctor of Philosophy.

_____
Chairperson Carl Luchies, Ph.D.

_____
Elizabeth Friis, Ph.D.

_____
Lorin Maletsky, Ph.D.

_____
Sara Wilson, Ph.D.

_____
John Keighley, Ph.D.

_____
Caroline Bennett, Ph.D.

Date Defended: June 8, 2021

The Dissertation Committee for Camilo Giraldo certifies that this is the approved version of the following dissertation:

Design, Validation and Assessment of Vibratory Mat for Stochastic Resonance Applications

_____

Chairperson Carl Luchies, Ph.D.

Date Approved: June 11, 2021

Abstract

Falls in people over the age of 65 is a problem that has a significant and negative impact on a country's economy and faller's quality of life. Despite the positive efforts to reduce falls, this problem is still in need of a solution. Some of the efforts to improve postural stability (i.e., reduce fall risk) are physical therapy, medication, and medical devices, all showing significant improvements in people's postural stability. However, in the case of medical devices, some (canes, wheelchairs, etc.) create a stigma of *weakness* on the user, causing them to often choose to take chances by not using the suggested medical device. Stochastic resonance, a relative new technology, has shown positive results towards improving the somatosensory (sensation) feedback in humans, which is one type of sensory feedback used in postural stability. Stochastic resonance can be introduced in humans through mechanically vibrating their feet, making this potential medical device one that does not create a stigma of *weakness* among their users (i.e., it would not be visible to the public). This dissertation covers the design, manufacturing, validation, and performance assessment of a new vibratory mat that introduces stochastic resonance to the user.

In the first study, the most-reported vibratory device in stochastic resonance studies was compared to the vibratory mat that is proposed in this dissertation. By asking various questions that addressed current design requirements, and new ones that increase the likelihood of being used by the targeted populations, both vibratory devices (i.e., the one developed here and the one most-reported in the literature) were assessed. It was found that our vibratory mat follows all designed requirements and has as much potential (and possibly more) to be successful in stochastic resonance studies.

In the second study, our vibratory mat was quantified and validated by measuring the forces and frequencies it exerted at various power levels, as well as by analyzing the quality of its vibrations. Using all configurations in the vibratory mat, the exerted forces and frequencies were recorded and fitted by

quadratic regression equations. The obtained regression equations accurately quantified the forces and frequencies since their fitting coefficients were $R^2 \geq 0.87$ and $R^2 \geq 0.70$, respectively. In addition, it was validated through experimental data if the vibratory mat could accurately execute white, pink, and brown vibrations. It was found that our vibratory mat can exert white, pink, and brown vibrations, and that the quality of the signals increase as larger motors and power levels are used.

The final study of this dissertation consisted of quantifying the impact of subthreshold vibration (i.e., stochastic resonance) in small groups of healthy older adults and healthy younger adults who stood on a 1-inch foam to simulate a sensory deficit. This was tested by introducing white, pink, brown, and placebo vibrations across 4 different visits, and recording their center of pressure prior, during and after the vibration. The first result from this study was that the use of 1-inch foam in healthy younger participants has the potential to simulate aging in future stochastic resonance studies. The second significant result is that subthreshold vibration is dependent on the state of postural stability prior to the vibration. Indicating that it is possible that more than one type of vibration could benefit people's postural stability, and that the most beneficial vibration to a participant could change day-to-day depending on the participant's state of postural stability. This implies a personalized medicine approach, in which the vibration treatment is customized for the individual on the day of the treatment. Finally, our results agreed with previous stochastic resonance studies towards the evidence that subthreshold vibration reduces postural sway magnitude and increases predictability.

Acknowledgements

I am widely grateful for everybody in my life who helped me complete my graduate career at The University of Kansas. This experience has indeed taught me lessons that I am going to hold close in my future professional career. I would like to thank a few people in particular:

- Dr. Carl Luchies, my adviser and committee chair. I had the pleasure of working with you during my MS and PhD studies, and during this time you taught me more than just biomechanics. Thanks for all the life lessons and for all the knowledge on engineering education.
- My committee members, Dr. Sara Wilson, Dr. Elizabeth Friis, Dr. Lorin Maletsky, Dr. Caroline Bennett and Dr. John Keighley. You might think our conversations were short and easy; however, I valued those conversations greatly. Thanks for your advice, expertise, and suggestions throughout my dissertation.
- My lab colleagues, Melanie Weilert, Logan Sidener, Eryn Gerber, Paris Nichols, Brett Whorley, Alex Wilson, Jessica Kirchner, Scott Ring, Zaccur Nkrumah, Victoria Blackwood and Di Bin. Thanks for bouncing ideas with me, and for your comments and suggestions on my work.
- The faculty and staff of the Mechanical Engineering graduate studies, Kate Maisch, Ansel Armstrong, Will Vincent, Josie Nixon, Dr. Chris Depcik, and Dr. Robert Sorem. Thanks for helping me navigate my graduate education from the logistical point of view.
- The faculty and staff outside the School of Engineering, Dr. Ward Lyles, Dr. Daniel Tapia, Dr. Jennifer Delgado, Dr. Matthew Richard, Dr. Mark Mort, Dr. Andrea Follmer Greenhoot, Kristin Rennells and Judy Eddy. Your advice, financial support through GRA appointments, and lessons outside biomechanics enhanced my graduate engineering education.
- Everybody in the engineering department at Olivet Nazarene University. Thanks for your understanding and flexibility while I completed my graduate education.

- My family, Oscar Giraldo, Amparo Grisales, Sebastian Giraldo, Maria Clara Madrigal, Deron Soendlin, Rhonda Soendlin, and Bradley Soendlin. Thanks for always believing in me.
- Finally, my wife Katelynn Giraldo. I would have **never made it** without your conversations, advice, help and encouragement.

Table of Content

List of Figures

List of Tables

Abbreviations

α	Slope of linear fit from log-log Detrended Fluctuation Analysis' plot
ANOVA	Analysis of Variance
AP	Anterior-Posterior

AppEn	Approximate Entropy
BF	Both Feet
COM	Center of Mass
COP	Center of Pressure
DFA	Detrended Fluctuation Analysis
EMG	Electromyography
HO	Healthy Old
HY	Healthy Young
LF	Left Foot
ML	Medial-Lateral
PS	Postural Stability
RF	Right Foot
RMS	Root Mean Square
RMSE	Root Mean Squared Error
SampEn	Sample Entropy
SDA	Stabilogram Diffusion Analysis
SN	Signal-to-Noise
SR	Stochastic Resonance

Chapter 1: Introduction

Introduction and Motivation

One in three people over the age of 65 is expected to fall once per year, significantly changing their quality of life and resulting in significant health care costs. In 2017, the US Department of Housing and Urban Development predicted that by the year of 2020, $59.7 billion were going to be used to cover fall-related injuries. While we know that the cause of falls is multifactorial, one cause is due to low postural stability (PS) which is defined as the integration and processing of all types of sensory feedback (visual, proprioceptive, vestibular and somatosensory), and the correct execution by the central nervous system of a biomechanical task (standing, walking, chair rise, etc.). A loss of performance in any of the types of sensory feedback or in the central nervous system results in low PS and an increased fall risk. Canes, wheelchairs, and walkers are examples of strategies to improve PS and reduce fall risk. Despite the PS improvements these devices offer, people often choose not to use them since they create a stigma of "weakness". Introducing vibration on the plantar foot surface has shown potential to improve PS without the social stigma.

Vibratory mats or insoles improve PS since they introduce stochastic resonance (SR) in the somatosensory feedback (i.e., sensation). The ability to sense touch stimuli is strictly dependent on the neurons at the skin crossing the sensing threshold level. This means that sensation is only recorded by the brain if the touch stimulus at the skin makes the neurons cross the sensing threshold level. SR is the addition of noise to a system, so that the system with the noise can cross a threshold level that the system alone could not cross. Given that older adults and those affected by diabetes and stroke often experience loss of somatosensory feedback, vibratory devices that introduce SR at the bottom of the feet are strong candidates to improve PS without creating a stigma of "weakness".

Specific Aim 1: Design and Manufacturing of a Vibratory Mat

The most recent SR studies that have assessed the effect of vibration under the feet on PS have used vibratory insoles. Current design requirements followed by these insoles cover the essential features that any vibratory device should have. However, they do not cover features that increase the probability of vibratory devices being used by people with low PS. This specific aim is to create a modified set of design requirements that should be considered by future vibratory devices. Also, this specific aim is to propose a vibratory mat that meets the current and new design requirements and has the potential of being preferred over existing vibratory insoles.

Specific Aim 2: Validation of Vibratory Mat's Output

Most of the SR studies that have assessed the effect of vibration under the feet on PS report their vibrating outputs in units that are attached to their systems or participants (e.g., 70% power level, or 40% of the participant's sensing threshold). In addition, all SR studies have claimed that their outputs are constant or follow white noise patterns. It is proposed that all vibratory devices should have an experimental validation on their outputs, since the assumption, *whatever is input, it is the output*, is highly questionable. In fact, it is hypothesized that a vibrating output's quality is dependent on the system's power level and/or participant's weight. This specific aim is to establish a thorough and robust validation process to be used on all vibratory systems. The results of this validation process will enable the performance of different vibration systems to be directly compared.

Specific Aim 3: Impact of Vibratory Mat on Postural Stability

SR studies that have assessed the effect of plantar foot surface vibration on PS compare people's balance when vibration is and is not present. In fact, these studies make PS comparisons between the before, during, and after the vibration has been administered. All studies that we found in the literature have used vibrations that are constant or follow a white noise pattern. It is proposed that the effect of vibration under the feet cannot be only described by whether vibration is present, and by when it is

administered. Instead, it is hypothesized that the effect of vibration under the feet is also dependent on the participant's balance before the treatment, and the efficacy of the treatment depends on the type of vibration that is administered.

Dissertation Content

This dissertation is comprised of 6 chapters:

- Chapter 1 introduces the current issue that is targeted by the three studies of the dissertation (Chapters 3 to 6).
- Chapter 2 is an in-dept background and literature review of all relevant peer-reviewed papers related to the issue introduced in Chapter 1.
- Chapter 3 addresses Specific Aim 1 by proposing new design requirements for future vibratory devices, and a new vibratory mat that follows all requirements better than the most-reported vibratory insoles.
- Chapter 4 covers Specific Aim 2 by quantifying the magnitude and quality of the new vibratory mat's outputs.
- Chapter 5 targets Specific Aim 3 by assessing how different types of subthreshold vibrations under the feet affect people's PS. Due to the COVID-19 pandemic, this chapter consists of a pilot study (i.e., low sample size).
- Finally, Chapter 6 summarizes the most significant findings, any limitations within the studies and future projects that could continue the work started by this dissertation.

Chapter 2: Background

Falls and Postural Stability

Falls among older adults in the United States is a problem best described by its cost. In 2006, $19.2 billion were used to cover fall related injuries among people over the age of 65 [1]. In 2017, the U.S. Department of Housing and Urban Development stated that $40 billion were used to cover fall related injuries among people over the age of 65, and predicted that by 2020, this would rise to $59.7 billion [2]. The increase of cost can be explained by the fact that around 1 in 3 adults over the age of 65 fall at least once each year [2], and that the "baby boomer" population (around 76 million in the US) is above 74 years old, half of whom qualify for Medicare [3]. An increase on the number of people above the age of 65, and the lack of effective interventions to prevent falls yields more spending on reactive treatments (e.g., emergency room visits).

Exercising, home modifications, vitamin D supplements, and medical devices are examples of interventions available today that reduce falls in populations at risk [4], [5]. Physical therapy and home exercises have been shown to reduce falls; however, they do not reduce falls that occur due to the sudden loss of balance (e.g., tripping on a rug or uneven surfaces). Physical therapy and home exercises strengthen muscles needed to keep a healthy balance, but they do not train the quick reaction time and muscle activation needed when humans lose their balance suddenly [6]. In addition, physical therapy and home exercises are most effective when they are tailored to the participant, requiring time and resources from a physical therapist and other health experts [5]. Home modifications and vitamin D supplements have shown to be as or more effective on reducing falls when compared to exercising on higher risk populations (i.e., people with large history of falls or vitamin D deficiency). Even though home modifications and vitamin D supplements are effective, they are more targeted to populations who have needed an intervention for a while. Finally, medical devices (canes, walkers, wheelchairs, etc.) improve balance significantly when users and non-users are compared [7]. However, they also create a

stigma of *weakness* on the users, resulting in medical device users often taking a "chance" on living without the needed medical device [8]. Despite the variety of intervention approaches available to reduce falls, all of them share an equal goal of improving postural stability (PS).

Humans' PS can be defined as the integration and processing of visual, proprioceptive, vestibular and somatosensory information, and the correct execution of a biomechanical task (e.g., standing or walking) (Figure 1) [9]. As humans age, sensory feedback (visual, proprioceptive, vestibular and somatosensory) decays, increasing postural instability and risk of falling [10]–[20]. Given that aging is natural and inevitable, the body's natural response is to compensate the loss of one feedback system, by increasing the importance of another one. For example, if vision starts to decay on our bodies, our natural reaction to avoid falls is to pay more attention to how we feel our surroundings via the sensory system. However, this natural compensation proves to be insufficient when damage to the sensory feedback or central nervous system is too large [9]. Postural instability due to insufficient compensation occurs at high ages, as well as in the presence of neuromuscular diseases such as diabetes [21]–[23], stroke [22], [24], vestibular deficiency [25], and Parkinson's, or in the presence of simulated low PS [26]–[28].

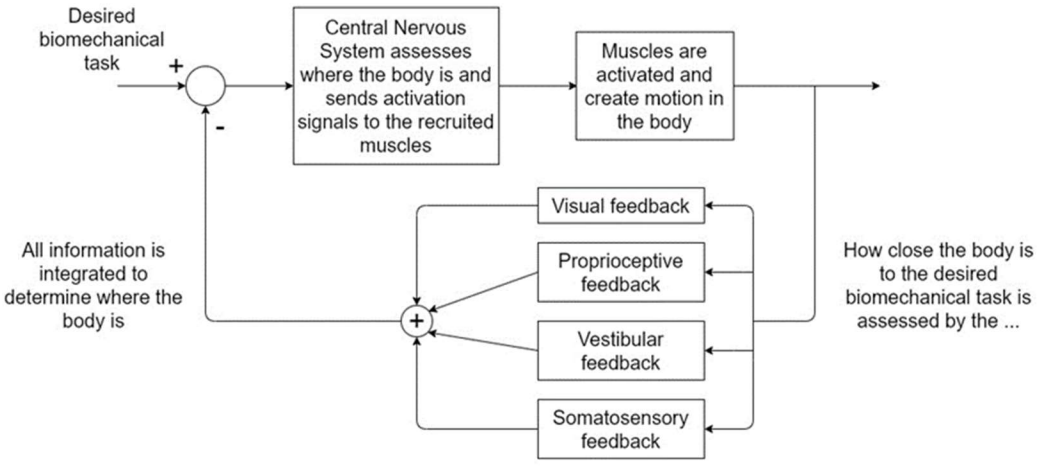

Figure 1: Postural stability feedback loop

Postural stability in a biomechanical task can be roughly explained as the action sent to the central nervous system, which activates the required muscles to perform such task. Throughout this process, the sensory feedback (vision, proprioceptive,

vestibular, and somatosensory) tells the central nervous system how close the body is to the desired biomechanical task, which eventually leads the central nervous system to stop sending activation signals to the required muscles.

Assisting the natural compensation that maintains PS as humans age can be achieved by improving the central nervous system and/or the sensory feedback. Deep brain stimulation is an example of a surgical intervention that improves the accuracy of the central nervous system's decision-making process [29]. Despite the positive results of central nervous system interventions, the scope of the dissertation will be on the improvement of one form of sensory feedback. There is not a general treatment to improve all types of sensory feedback. Vision feedback can be improved with glasses, which re-center the eyes' focal point. Proprioceptive feedback can be improved through healthy levels of exercise, which helps joints, muscles, tendons and/or ligaments to keep their optimal viscoelastic properties. In the case of improving the somatosensory feedback (i.e., dissertation's scope), the goal is to regain the ability to sense touch stimuli that no longer are felt due to aging, neuromuscular diseases, or simulated low PS.

Stochastic Resonance

Stochastic resonance (SR) is the addition of noise to a signal that is below a threshold level so that the signal with the noise's assistance can cross the threshold level that it could not cross before (Figure 2) [16]. This makes SR a strong candidate to improve the somatosensory feedback, thus improving PS [30]–[46]. SR's strong potential is explained by how neurons in the skin (skin's mechanoreceptors) are activated, as well as by the leading theory on how SR interacts with skin's mechanoreceptors. The somatosensory feedback in humans starts with the skin's mechanoreceptors in a resting potential waiting for an external input to activate them (Part 1, Figure 3). Next, (ideally) the input creates a strong source of voltage that makes the skin's mechanoreceptors cross the firing threshold, which initiates the climb to an action potential (depolarization) which eventually creates sensation in humans (Part 2 and 3, Figure 3). It must be pointed out that skin's mechanoreceptors only get excited (i.e., produce sensation), if the external input creates enough voltage to pass the neuron's firing threshold (Part 2, Figure 3). After

the peak action potential is reached, the skin's mechanoreceptors start their decay to the resting potential (i.e., repolarization), passing first through a hyperpolarization stage (Part 4 and 5, Figure 3). Once the skin's mechanoreceptors are in the resting potential, they can receive a new input and start the described process again. The leading theory on how SR interacts with the neuron activation process is through the addition of voltage in the resting potential stage, so external inputs can receive assistance on crossing the firing threshold and eventually create sensation in humans [10]–[28], [47]–[53].

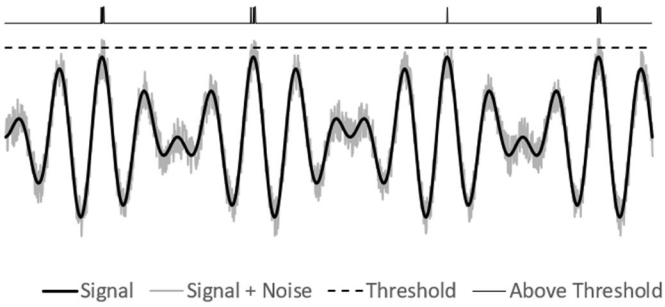

Figure 2: Stochastic resonance graphical description

Stochastic resonance (SR) is the addition of noise to a signal that is below a threshold level so that the signal with the noise's assistance can cross the threshold level that it could not cross before.

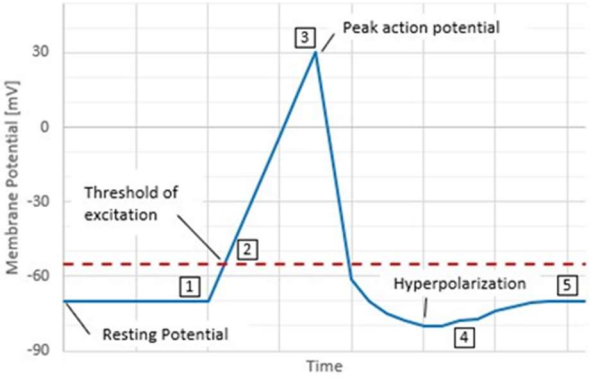

Figure 3: Neuron activation process

The natural state of a neuron in the skin is the resting potential, and the neuron will only send a signal to the brain (peak action potential), if a touch stimulus makes the neuron cross the threshold of excitation.

SR's assistance to the skin's mechanoreceptors is a multidimensional phenomenon since it can be described by its input category, magnitude, and application point (i.e., body part), as well as by the device that hosts the SR source (Table 1). Mechanical, electrical, and magnetic inputs on human skin increase the neuron's voltage in its resting potential stage, so it is understandable that all methodologies

are explored by researchers. The input magnitude can be below the human's sensing threshold (subthreshold) or above their sensing threshold (suprathreshold). Both strategies, subthreshold [16] and suprathreshold [54], have shown to be effective methods that increase PS, but there are no current theories that separate how each works. A non-validated theory states that subthreshold inputs "train" humans to improve PS, while suprathreshold inputs "alert" humans during postural instability. The application point is decided based on the targeted skin mechanoreceptors. However, there is evidence that SR can have a chain effect in the body, meaning that an input at the feet can affect behavior at the hips [55]. Finally, in the case of SR at the feet, housing the SR source can be portable and always present (e.g., shoe insole), or static (e.g., mat at home). Currently, there are supporting arguments for both devices, and there is no evidence to rule out one and support the other. There are various acceptable designs to introduce SR in the body with the goal to improve the somatosensory feedback in humans, and therefore PS.

Table 1: Stochastic resonance various designs to assist the somatosensory feedback

<table>
<tr><th>Input Category</th><th>Input's Magnitude</th><th>Application Point</th><th>Device
(Feet Only)</th></tr>
<tr><td>Mechanical [10]–[28], [47]–[63]</td><td rowspan="2">Subthreshold [10]–[24], [26]–[28], [47]–[53], [64], [65]</td><td rowspan="2">Feet [10]–[28], [47]–[61], [63], [64], [66], [67]</td><td>Shoe Insole [10], [14], [15], [17]–[24], [26]–[28], [47]–[49], [51], [52], [55], [63]</td></tr>
<tr><td>Electrical [64], [65]</td><td rowspan="2">Mat [11]–[13], [16], [25], [54], [56]–[61], [66], [67]</td></tr>
<tr><td>Magnetic [66], [67]</td><td rowspan="2">Suprathreshold [20], [24], [25], [52], [54]–[64]</td><td rowspan="2">Leg [24], [55], [58], [64], [65]
Torso [62]</td></tr>
<tr><td></td><td>Motor/Device on Skin [24], [50], [53], [58], [64]</td></tr>
</table>

Subthreshold Vibratory Mat

The goal of this dissertation is to demonstrate the potential of a proactive, easy-to-use, and inexpensive medical device that increases PS through SR at the feet. A subthreshold vibratory mat (Figure 4) was the chosen device to explore, and its reasons are listed below.

- Mechanical vibrating components are usually cheaper when compared to magnetic sources.

- Mechanical vibrating input to humans are most likely to have fewer medical regulations when compared to electrical or magnetic inputs.
- Despite being an unvalidated theory, subthreshold mechanical vibration in humans might have more potential to be a daily-used proactive intervention for postural instability. For example, one study found that suprathreshold mechanical vibrations corrected human posture; however, they reduced human cognitive reaction time [62].
- The sole of the foot is the main source of contact between the environment and the body. Therefore, a medical device that targets the feet's soles could have higher chances of success when compared to a medical device that targets other body parts.
- People over the age of 65 (targeted population due to fall risk [1]–[3]) are often more cautious to adapt to new technologies (e.g., vibrating insoles). Therefore, a vibrating mat, which can be seen as a bathroom scale, could have higher chances of being accepted and used.

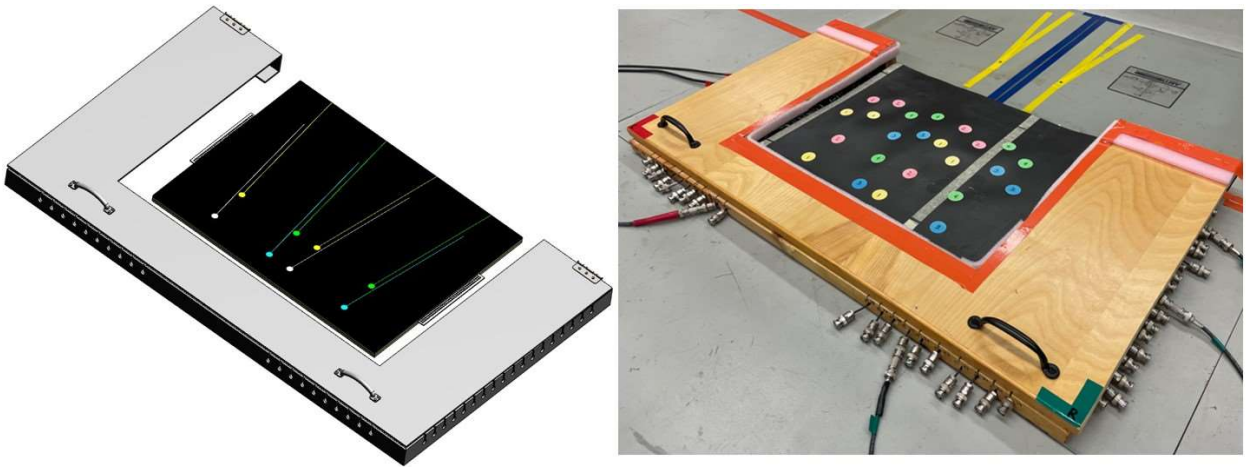

Figure 4: New vibratory mat (schematic and manufactured)

Vibratory mat controlled by custom-built Arduino code that uses validated white, pink, and brown inputs for each of the offered motors. Four sets of motors (307-105, 310-003, 306-10H and 307-103 from Precision Microdrives, UK) are embedded in a 10-mm think Shore A50 silicone, and each set of motors accommodate multiple shoe sizes by offering three ranges of shoe sizes. Finally, the mat directs participants to follow a standardized stance. Further details in Chapter 3 of this dissertation.

Since a new vibratory mat that introduces SR is proposed, its design and manufacturing must be justified, its outputs must be validated, and its effect on PS needs to be compared with current vibratory

devices. That is why the next three sections (Design, Vibrating Output, and Performance Assessment on Postural Stability) describe the relevant publications for the mentioned three stages of the dissertation (Design, Validation and Performance of a new vibratory mat). The Design section covers the vibratory devices that have been manufactured when investigators wanted to introduce SR at the feet, as well as the design requirements that justified the investigators' manufacturing process. The Vibrating Output section covers the features that make an output valid among the investigators that study vibratory devices, and it compares these features with the expectations and requirements held by the larger research community (i.e., human biomechanics and neurophysiology). Finally, the Performance Assessment of Postural Stability section describes the latest reported effects when people are introduced with SR through vibration at the feet, and how these effects have been analyzed.

Design

This section shows the current and accepted design requirements for vibratory devices, and how the current devices meet them. Finally, the section proposes new design requirements that have not been considered by previous investigators.

Current Design Requirements and Suggestions

Despite the large number of research studies on SR through vibratory mats or insoles, and their effect on human PS [10]–[28], [47]–[61], [63], only two peer-reviewed papers have detailed the design of the vibratory device [68], [69]. While most of the research studies mention the vibrating device's features (motors' choice and location, insole's/mat's material and thickness, etc.), the design papers [68], [69] mention their device's features as well as their justifications. Both design papers involve vibratory insoles as opposed to a vibratory mat (i.e., dissertation's choice); however, features from vibratory insoles are applicable to a vibratory mat, and vice versa, as long as the thickness of both devices is less than or equal to 16 mm [68]. Both design papers agree on their design requirements and suggestions, and they are listed below.

1. Motor Selection: The vibrating component should not exceed a thickness of 16 mm, since large thicknesses (16 to 27 mm) could be associated with balance deficiencies [68]. Examples of possible vibrating components (indenters, eccentric rotating mass motors, or piezo-electric actuators) are: C1026B200F (KOTL, Jinlong Machinery, China) [68], [69], C-2 Tactors (Engineering Acoustics, FL) [68], B5A-11W [68], P-289 (PI, MA) [68], APA400M (Cedrat Technologies, France) [68], and VBW32 (Tactaid, China) [68].
2. Motor Location: The vibrating components should be under the most crucial mechanoreceptors [68], [69], therefore it is suggested to have the vibrating components at the heel, big toe, first and fifth metatarsal.
3. Power Generator: The power generator should be able to move all the vibrating components in each foot (i.e., at least one power generator per foot) [68]. Potential power generators are commercial microcontrollers (Arduino, Raspberry Pi, etc.) powered by at least a 7-volt battery [69].
4. Noise Generator: The amplitude and frequency of the vibrating components need to be adjustable, so the vibrating output can be adjusted to different people's sensing thresholds [68], [69]. In addition, the noise generator should be able to output white noise [69], among other types [68].
5. Material: The main body that encases the vibrating components of the device should be a hard silicone (Shore A50, such as polyurethane and ethylene vinyl acetate), covered on top by two thin layers. The first layer being a harder material (Shore A55, such as cork), while the second layer being a softer one (Shore A30, such as soft leather) [68], [69]. The order of the layers from ground up are main body (Shore A50), first layer (Shore A55), and second layer (Shore A30).

Studies that use vibratory mats or insoles to improve PS through SR [10]–[23], [25]–[28], [47]–[49], [51], [52], [54], [55], [57]–[61], [63] (31 studies) follow most of the published design requirements and

recommendations [68], [69] (Table 2). A description when each design requirement is observed individually is given below.

1. Motor Selection: All thirty-one studies used either indenters, eccentric rotating mass motors, or piezo-electric actuators. From the list of possible motors [68], only the C-2 Tactors (Engineering Acoustics, FL) were used, and 10 studies [11]–[15], [17], [20], [22], [51], [52] chose them as their vibrating components. Fifteen studies [10], [16], [18], [19], [23], [25], [26], [28], [47]–[49], [55], [59]–[61] did not provide a detailed reference to their vibrating components, and 6 studies [21], [27], [54], [57], [58], [63] used vibrating components not listed as possible motors [68]. In addition, 20 studies followed the thickness suggestion (i.e., 16 mm or less) [68]. In fact, 9 studies [10]–[14], [17], [20]–[22] stated that their vibratory mat or insoles had thicknesses equal to or less than 16 mm, while 11 studies [15], [18], [19], [27], [28], [47]–[49], [51], [52], [63] used commercial insoles which most likely have thicknesses less than 16 mm. Four studies [23], [26], [55], [59] did not state the thickness of their device, and 7 studies [16], [25], [54], [57], [58], [60], [61] (i.e., Thickness = N/A in Table 2) did not have to follow the thickness suggestion since they used large vibratory platforms.
2. Motor Location: Only 1 study [10] followed all placement suggestions [68], [69] (heel, big toe, first and fifth metatarsal). Twenty-five studies [11]–[15], [17]–[23], [26], [27], [47], [51], [52], [54], [55], [57]–[61], [63] partially followed the placement suggestions by installing their vibrating components under the heel, first and fifth metatarsals. The remaining five studies applied vibration to the entire sole of the foot [16], just the metatarsals [25], and the medial arch area [28], [48], [49].
3. Power Generator: Twenty-three studies [11], [16]–[20], [22], [23], [25]–[28], [47]–[49], [54], [55], [57]–[61], [63] used a custom-built power generator, suggesting that they all performed as required [68], [69] (i.e., at least enough power to move all motors providing vibration to the

foot), since the 23 studies yielded results accepted in the literature. Six studies [12]–[15], [51], [52] used the Engineering Acoustics Controller (Engineering Acoustics, FL), while 2 studies used commercial microcontrollers [10], [21] (Arduino Nano, Arduino, MA and USB-DAQ, National Instruments, TX) [69].

4. Noise Generator: Ten studies (i.e., Noise Gen = N/A in Table 2) did not have to list their noise generator since their vibratory components produced a sinusoidal vibration (i.e., voltage was constant) [25], [52], [54], [55], [57]–[61], [63]. The remaining studies (21) used noise generators that produced white (random) noises, and they were divided into 9 studies [16], [18], [19], [23], [26]–[28], [48], [49] that used a custom-built noise generator, 4 studies [11], [17], [20], [22] that used an ISD2560 Chip (Winbound Electronics, Taiwan), 5 studies [12]–[15], [51] that used the Engineering Acoustics Controller (Engineering Acoustics, FL), 2 studies [10], [47] that used MATLAB (MathWorks, MA), and 1 study [21] that used LabVIEW (National Instruments, TX). All noise generators were adjustable and produced white noise [68], [69]; however, none of the noise generators claimed to yield other types of noise [68].
5. Material: Ignoring the 7 studies [16], [25], [54], [57], [58], [60], [61] that used large platforms (i.e., Thickness = N/A in Table 2), 21 studies [10]–[15], [17]–[22], [26]–[28], [47]–[49], [51], [52], [63] followed the material suggestions [68], [69] (i.e., Shore A50, Shore A55, or commercial insoles), and 3 studies [23], [55], [59] did not state their encapsulating material.

Table 2: Design specifications of existing vibratory mat and insoles

Reference(s)	Motor Type	Motor Reference	Thickness	Motor Location	Power Generator	Noise Generator	Material
[54], [57], [58]	Indenter	201	N/A	Heel + Meta	Custom-built	N/A	Metal
[25]	Indenter	Undefined	N/A	Meta	Custom-built	N/A	Metal
[16]	Indenter	Undefined	N/A	Entire sole	Custom-built	Custom-built	Metal
[55], [59]	ECR	Undefined	Undefined	Heel + Meta	Custom-built	N/A	Undefined
[11], [17], [20], [22]	Indenter	C-2 Tactor	16 mm	Heel + Meta	Custom-built	ISD2560	Shore A50
[63]	ECR	2890W11	Commercial	Heel + Meta	Custom-built	N/A	Commercial
[21]	Piezo	EPZ35-MS29	6 mm	Heel + Meta	USB-DAQ	LabVIEW	Shore A55
[15], [51]	Indenter	C-2 Tactor	Commercial	Heel + Meta	EA Controller	EA Controller	Commercial
[18], [19]	ECR	Undefined	Commercial	Heel + Meta	Custom-built	Custom-built	Commercial
[47]	ECR	Undefined	Commercial	Heel + Meta	Custom-built	MATLAB	Commercial
[12]–[14]	Indenter	C-2 Tactor	16 mm	Heel + Meta	EA Controller	EA Controller	Shore A50
[28], [48], [49]	Piezo	Undefined	Commercial	Medial Arch	Custom-built	Custom-built	Shore A50
[52]	Indenter	C-2 Tactor	Commercial	Heel + Meta	EA Controller	N/A	Commercial
[10]	ECR	Undefined	16 mm	Heel + Meta + Big Toe	Arduino Nano	MATLAB	Shore A55
[60], [61]	ECR	Undefined	N/A	Heel + Meta	Custom-built	N/A	Undefined
[23]	ECR	Undefined	Undefined	Heel + Meta	Custom-built	Custom-built	Undefined
[26]	ECR	Undefined	Undefined	Heel + Meta	Custom-built	Custom-built	Shore A50
[27]	Piezo	20-2225	Commercial	Heel + Meta	Custom-built	Custom-built	Commercial

Abbreviations: ECR = Eccentric Rotating Mass, 201 = 201 (Ling Dynamic Systems), C-2 Tactor = C-2 Tactor (Engineering Acoustics, FL), 2890W11 = Optec 2890W11 (Optec, Japan), 20-2225 = Disc Benders-Bimorphs 20-2225 (APC, PA), Commercial = Commercial Insole, Meta = Metatarsals, USB-DAQ = USB-DAQ (National Instruments, TX), EA Controller = Engineering Acoustics Controller (Engineering Acoustics, FL), Arduino Nano = Arduino Nano (Arduino, MA), ISD2560 = ISD2560 (Winbound Electronics, Taiwan), LabVIEW = LabVIEW (National Instruments, TX), MATLAB = MATLAB (MathWorks, MA).

When the design specifications [68], [69] are observed as a group (i.e., complete vibratory design), the three most used designs for a vibratory mat or insole are described below.

- Design 1: 16-mm insoles made from Shore A50 silicone with C-2 Tactors (Engineering Acoustics, FL) under the heel, first and fifth metatarsal powered and controlled by a custom-built power generator and an ISD2560 (Winbound Electronics, Taiwan) noise generator [11], [17], [20], [22].

- Design 2: 16-mm insoles made from Shore A50 silicone with C-2 Tactors (Engineering Acoustics, FL) under the heel, first and fifth metatarsal powered and controlled by the Engineering Acoustics Controller (Engineering Acoustics, FL) [12]–[14].
- Design 3: Insoles made from Shore A50 silicone with piezo-electric actuators under the medial arch powered and controlled by a custom-built power and noise generators [28], [48], [49].

Given the accepted design requirements [68], [69], designs 1 and 2 meet almost all requirements, while design 3 does not meet the Motor Location requirement. Design 3 placed their vibrating components at the medial arch of the foot, when it is recommended to place the vibrating components at the heel, big toe first and fifth metatarsal. Designs 1 and 2 meet all requirements except for placing a vibrating component under the big toe.

Proposed Design Requirements and Suggestions

The accepted design specifications and requirements [68], [69] allow the development of vibratory mats or insoles that can improve PS through SR; however, it is proposed by this dissertation that additional design specifications and requirements are needed to assure that vibratory devices are used by the targeted population [1]–[3]. The suggested design specifications and requirements, as well as their justifications are described under.

1. Multiple Shoe Sizes: People over the age of 65 have different shoe sizes, and they differ based on gender. In a study of 158 men and 154 women (most over the age of 65), it was found that men's US shoe sizes range from 8.5 to 15, while women's US shoe sizes range from 4.5 to 13 [70]; both ranges following Gaussian distributions. Given that there is not a narrow distribution for men's and women's US shoe sizes, the vibratory mat or insoles must accommodate for this variability and place their vibrating components at the heel and metatarsals of multiple US shoe

sizes. Misplacing the vibrating components under the foot sole could impact the sensing threshold [71], [72], or the targeted mechanoreceptors (heel and metatarsals) [73].

2. Multiple Motors: Human sensation threshold changes with age [74], body temperature [75], contact area [76], among other factors, making the sensing threshold non-constant. Therefore, it is suggested for the vibratory mat or insoles to have multiple motors that cover different ranges of amplitude and frequency. Frequencies between 200 Hz and 300 Hz are preferable since they cover the Pacinian Corpuscles (Fast Adapting Type II), which are the skin mechanoreceptors that should be targeted by vibratory devices that introduce SR [71]–[73].
3. Cost: Knowing that falls increase in people over the age of 65 [1]–[3] or people with a neuromuscular disease [21]–[28], it is required for the vibratory mat or insoles to be marketed at a cost that the public can afford. As a reference (November 2020), current vibratory insoles (e.g., Vibratothics https://www.vibrathotics.com/) cost around $100, whole-body vibrating equipment (e.g., LifePro Turbo 3D https://lifeprofitness.com/) costs around $300, and physical therapy equipment that enhances PS (e.g., Korebalance 19 https://www.korebalance.com/index.htm) costs around $16,000. It is suggested for the final vibratory device to not exceed the cost of a whole-body vibrating equipment, since there is evidence that people feel comfortable spending that sum of money to improve their PS.
4. Robust Sensing Threshold: Given the natural variability in human sensation threshold [74]–[76], and the difference between suprathreshold [54], [57], [58] and subthreshold studies [16], [17], [22], a robust method to find people's sensing threshold must be part of the vibratory mat or insoles [77]. Not having a clear differentiation between subthreshold and suprathreshold vibration could impact PS in unexpected ways [20], [52].
5. Robust Manufacturing: Unless a patent is under application, the manufacturing process (beyond the list of materials) for vibratory mats or insoles should be complete and reproducible. This

allows other studies to fabricate existing vibratory mats or insoles, replicate results and analyze aspects that have not been considered.

Vibrating Output

This section explains the dimensions used in SR studies to describe their vibratory outputs, as well as states the limitations on the outputs' units and validity. Finally, the section describes the data manipulation required to study these dimensions on any vibratory output.

Studies that assess the effect of SR through foot-sole vibration on human PS [10]–[28], [47]–[61], [63] define their vibrating outputs based on their magnitude and type (Table 3). Regarding the vibrating output's magnitude, 9 studies (out of 35) [24], [25], [52], [54]–[59] use indentation depth and frequency (i.e., universal units). Out of these 9 studies, 6 studies [25], [54], [56]–[59] go further by specifying the indenter's contact area, which affects human sensing threshold [76]. Also, from the same 9 studies, 4 studies [54], [56]–[58] define their vibratory system. A vibratory system is *Defined* if the vibrating motor reference, mat/insole thickness, motor location, and mat/insole material are given in Table 2. Besides these 9 studies (i.e., 26 studies), 21 studies [10]–[23], [26]–[28], [47]–[49], [51] express their vibrating output's magnitude as a percentage of the participant's sensing threshold, while 5 studies [50], [53], [60], [61], [63] express their vibrating output's magnitude as a voltage or power level relative to their vibratory system. From these 26 studies whose vibrating output's magnitude is either a percent of the participant's threshold or a power level of their equipment, 9 studies [11]–[14], [17], [20]–[22], [53] define their vibratory system. Regarding the vibrating output's type, 19 studies [10]–[18], [20]–[23], [26], [28], [47]–[49], [51] use white noise (random noise) as the plantar vibratory stimulus, 15 studies [24], [25], [27], [50], [52]–[61], [63] use a constant power level yielding a sinusoidal vibratory output, and 1 study [19] does not express their output's type. Even though it seems that most studies objectively express their vibrating outputs, it is suggested by this dissertation that there are two unresolved issues: 1) the vibrating outputs' magnitudes do not use universal units, and 2) the vibrating

output's types have not been assessed to determine if they are constant (i.e., sinusoidal) or white. Each unresolved issue will be further described by the following two sections.

Table 3: Vibratory outputs' magnitude and type characterization

Reference(s)	Defined Vibratory System?	Output's Magnitude	Output's Type
[10], [15], [16], [18], [23], [26], [28], [47]–[49], [51]	Undefined	Percent of sensing threshold	White
[11]–[14], [17], [20]–[22]	Defined	Percent of sensing threshold	White
[54], [56]–[58]	Defined	Indentation depth, Frequency, Contact area	Sinusoidal
[50], [60], [61], [63]	Undefined	Constant and set voltage	Sinusoidal
[24], [52], [55]	Undefined	Indentation depth, and Frequency	Sinusoidal
[25], [59]	Undefined	Indentation depth, Frequency, Contact area	Sinusoidal
[53]	Defined	Constant and set voltage	Sinusoidal
[19]	Undefined	Percent of sensing threshold	Undefined
[27]	Undefined	Percent of sensing threshold	Sinusoidal

Note: A study is labeled as a *Defined* system if the vibrating motor reference, mat/insole thickness, motor location, and mat/insole material is given in Table 2. Otherwise, the vibratory system is labeled as an *Undefined* system.

Use of Universal Units for Vibrating Outputs

Using universal units to quantify the magnitude of any vibrating output allows comparison among multiple researchers and aligns with practices from neurophysiology studies on human sensing threshold. Neurophysiology studies had been and are using universal units to quantify their system outputs' magnitudes when measuring human sensing threshold. SR studies on PS that do not use universal units [10]–[23], [26]–[28], [47]–[51], [55], [60], [61], [63] require new researchers to manufacture previous studies' vibratory systems if it is desired to compare vibrating outputs and participants' sensing thresholds. Given that outputs' magnitudes quantified without universal units are measured in reference to the vibratory system (i.e., percent of sensing threshold or power level), the only way for new researchers to compare results with previous studies that do not use universal units is by having the same vibratory system. To date, it is only possible to do this with 9 out of 26 studies [11]–[14], [17], [20]–[22], [53], since only 9 studies define their vibratory system's design. On the other hand,

if a future researcher wants to compare vibrating outputs and sensing thresholds with studies that use universal units [24], [25], [52], [54]–[59] (i.e., indentation depth, frequency, and/or contact area), new researchers can build their vibratory system either using existing designs [54], [56]–[58], or their own as other studies have done [24], [25], [52], [55], [59]. In addition, PS enhancement through SR studies that do not use universal units [10]–[23], [26]–[28], [47]–[51], [55], [60], [61], [63] miss a possible connection with neurophysiology studies on human sensing threshold [71]–[76], [78]. Even though both fields of study have different goals; effect of SR through feet vibration on PS [10]–[28], [47]–[61], [63], and understanding of the afferent/efferent neural system through human sensation [71]–[76], [78], both fields of study measure human sensing threshold (i.e., share a step on their methodology). If both fields of study (SR on human PS and neurophysiology) were to use universal units (distance, frequency, contact area, force, etc.) to quantify the stimulus given to humans, it would be possible to relate both fields' results and discoveries.

Validating the Vibrating Output's Type

Verifying the vibrating output's type removes the assumption, *whatever is input to the vibrating component, is output by the vibrating component*, as well as yields good practices knowing the sensitivity of human PS towards different noise types. A vibrating component (e.g., eccentric rotating mass motor) is a complex electro-mechanical system that when modeled requires at least a resistor, an inductor, a conversion factor from electrical to mechanical energy, a mass moment of inertia, a friction coefficient and a damping coefficient. This complexity increases when the vibrating component is embedded in a mat or insole due to the insolation provided by the embedding material, proximity to other vibrating components and the participant's weight compressing it. Even though it is possible to design controllers that allow researchers to use the assumption, *whatever is input to the vibrating component, is output by the vibrating component*, it is reasonable to verify the vibrating output's type since human PS is sensitive towards different noise types. A time series' (e.g., vibrating output, Figure 5

Middle Row) type is defined by the slope of the linear fit on the log-log plot (α), resultant of a Detrended Fluctuation Analysis (DFA) (Figure 5 Bottom Row) [79]. Time series (e.g., vibrating outputs) with α's equal to 0.5, 1.0, and 1.5 are referred to respectively as white, pink and brown noises [80]. The quality of α is described by the R^2 extracted from the linear fit, meaning that R^2 values close to 1 correspond to reliable α's. With that said, a hearing study found that different types (i.e., white, pink or brown) of tempo-audio outputs given to a human while walking affected their gait variability differently [81], suggesting that special attention should be given to the outputs' types given to humans in PS studies. More specifically, a SR study on PS through feet vibration mentioned the importance and potential of multiple types of vibrating outputs given to humans [82]. Using DFA on sway Center of Pressure (COP) time series from [17], it was suggested that vibratory insoles or mats should be able to output multiple types of vibration (white, pink or brown) because there is evidence that one noise type may not improve all participants' PS [82]. Previous studies have either used white noise [10]–[18], [20]–[23], [26], [28], [47]–[49], [51] or sinusoidal [24], [25], [27], [50], [52]–[61], [63] vibrating outputs, ignoring previous design recommendations [68], conclusions [15], [81], [82] and the importance of complexity and predictability in human PS [11], [81], [82]. Therefore, it is evident that there is a need to verify vibrating outputs and open the possibility to other noise types besides white and sinusoidal (e.g., pink and brown).

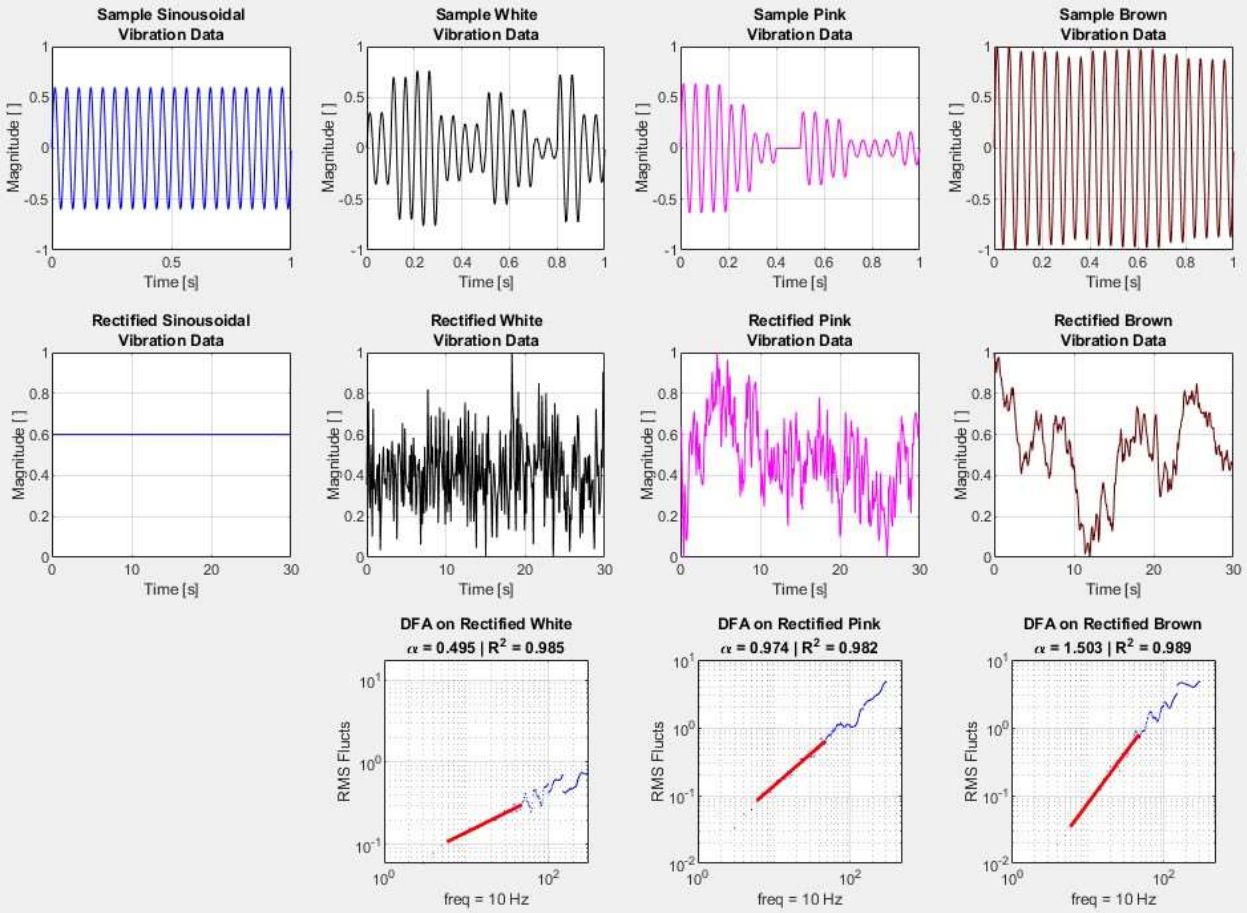

Figure 5: Different types of vibrating data in their simulated-raw, rectified and DFA forms

(Top Row) Simulated raw vibratory outputs for a constant, white, pink, and brown (left to right) vibration. Only 1 second of the time series is displayed; however, the time series is 30 seconds long. (Middle Row) Rectified time series obtained by extracting the Root-Mean-Square every 0.1 seconds from the raw vibratory outputs. (Bottom Row) Log-log plot and linear fits from a Detrended Fluctuation Analysis on the rectified time series.

Determining the Magnitude and Type of a Vibrating Output

Currently, there is not a standard method to test vibratory devices; however, there are three common testing set-ups. Each offers advantages and disadvantages when compared to each other.

- Hanging Test: With a vibrating component and an accelerometer clamped to a hanging platform, the vibrations are recorded through the accelerometer (Figure 6 Left). This low-cost testing set-up offers a fast and easy observation of the vibrating component because it does not require a human or a complete vibratory device. In addition, this testing set-up offers a detailed observation of the vibrating component's vibrations because an accelerometer with a low range

and high resolution can be chosen. However, this testing set-up does not reflect the environment of a plantar vibrotactile study. A participant would normally stand on the vibratory mat or insole that encases the vibrating component(s), which almost completely removes the motion of the vibrating component (i.e., the vibratory mat or insole will not move as the hanging platform minimally does in a hanging test).

- Static Test: A force plate records the ground reaction forces and moments of a manufactured vibratory mat or insole that has a known and static weight on it (e.g., cinder blocks) (Figure 6 Center). The static test offers the non-human feature that the hanging test offers; however, the static test's cost is significantly higher when compared to the hanging test. A force plate costs more than an accelerometer, and the static test requires a manufactured vibratory system. The static test offers a stronger connection between the testing set-up and the environment of a plantar vibrotactile study when compared to the hanging test. However, the accuracy of the static test can be compromised when compared to the hanging test. Force plates are normally manufactured with the intention of testing humans, offering large output ranges (e.g., 0 to 5,000 N). It is common for sensors with large output ranges (i.e., force plates) to have lower sensitivity than sensors with small output ranges (i.e., accelerometers). For example, a 16-bit data acquisition system reads 2^{16} = 65,536 values between 0 and 5,000 N for a force plate, and the same number of values between -3 g and 3 g for an accelerometer. This means that the average sensitivities for the force plate and accelerometer are respectively 0.0763 N/bit and 4.58×10^{-5} g/bit.
- Dynamic Test: A force plate records the ground reaction forces and moments of a manufactured vibratory mat or insole while a human stands on it (Figure 6 Right). The dynamic test being the most complex and expensive of all, offers the most realistic environment (i.e., it is the actual plantar vibrotactile study). The vibrating output is separated from human sway by filtering the

recorded time series with a high- or band-pass filter that has a low cut-off frequency above the maximum frequency found in human sway [21], [27], [49], [55]. Finally, the dynamic and static tests share the sensitivity limitation described for the static test; however, the dynamic test requires more intense data manipulation when compared to the static test. It is easier to remove a static load from a time series, than removing a human's sway from a time series.

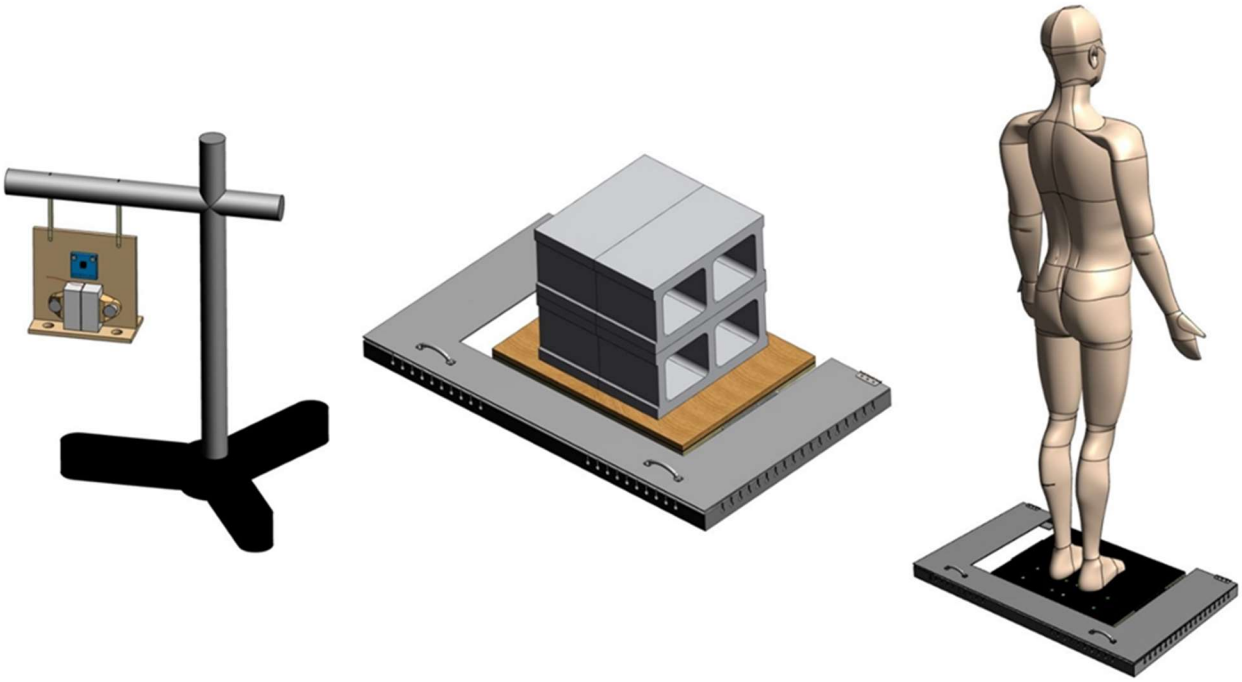

Figure 6: Testing set-ups to record vibrating outputs

(Left) Hanging Test: A vibrating component is clamped to a hanging platform that free to move, and vibrations are recorded by an accelerometer that is attached to the handing platform. (Middle) Static Test: Static weights are placed on a manufactured vibratory device, and the forces exerted by the embedded motors are recorded by a force plate located under the vibratory device. (Right) Dynamic Test: A human is placed on a manufactured vibratory device, and the forces exerted by the embedded motors are recorded by a force plate located under the vibratory device. Filtering techniques are needed to separate human sway from the forces exerted by the motors.

Beyond the testing set-up, determining the magnitude and type of a vibrating output requires the rectification of its raw data, which is comprised of oscillations (Figure 5 Top Row and Figure 7 Left). Before rectifying the raw vibrating data, the raw data need to be band-pass or high-pass filtered using low and high cut-off frequencies that capture the vibration, and no other phenomena such as human sway or a static load [21], [27], [49], [55]. Rectifying the raw vibrating data are needed, otherwise

magnitude and DFA calculations would yield zero or inconclusive results. The average and linear fit of an oscillatory signal are respectively 0 and a line with a 0 slope. Raw vibrating data (Figure 7 Left) are also rectified due to its similarity to raw muscle activity data (Figure 7 Right). The rectification process intended for raw electromyography (EMG) muscle activity data [83] is applied on raw vibrating data with a time-window equivalent to the frequency at which new power levels are sent to the vibrating component. This transforms raw vibrating data (Figure 5 Top Row) into rectified vibrating data (Figure 5 Middle Row), which can be used to determine magnitude and type (Figure 5 Middle and Bottom Rows).

Figure 7: Example of raw vibrating output and raw muscle activity data [83]

Vibration data acquired from a hanging test trial (left), and electromyography data (right) from previous study [83]. Both time series rapidly oscillate around a constant stationary average, and both need to be rectified before their magnitudes are analyzed.

Performance Assessment on Postural Stability

This section initially states the overall methodology of all SR studies that involve vibration at the feet, followed by the overall methodology needed to study the vibratory mat developed in this dissertation. In addition, the section explains the PS metrics used to quantify the effect of SR through vibration under the feet, as well as the statistical analysis that has been done to draw conclusions.

The effect of SR through feet vibration on human PS can be assessed in multiple types of studies that differ on the vibrating output's magnitude given to the participant, the stage at which human PS is assessed, and the biomechanical task chosen to assess PS. The vibrating output can be subthreshold [10]–[24], [26]–[28], [47]–[49], [51]–[53], or suprathreshold [20], [24], [25], [50], [52], [54]–[61], [63], and its effect on human PS can be assessed while the vibration is given to the participant [10]–[17], [20]–[22], [25]–[28], [47]–[55], [57]–[59], [63], immediately-after the vibration [18], [19], [23], [47], [56],

[60], [61], or minutes/days after the vibration was or had been provided [23], [24]. Human PS is needed in everyday life, meaning that it applies to when humans stand, walk, sit down, stand up, etc. That is why SR studies that assess PS have used the body's center of mass (COM) [11], [16], [17], [20], [22], [47], [55], COP [10], [12]–[14], [18], [19], [21], [23]–[27], [47]–[50], [54]–[59], [61], and lower-leg muscles EMG [26], [58] while humans stand, as well as humans' gait [15], [24], [48], [51]–[53], [63]. In addition, all the listed types of studies can be done on different populations such as healthy people in general (Mean Age ≥ 18 years) [11], [16], [17], [20], [52], healthy adults (18 years ≤ Mean Age ≤ 50 years) [26]–[28], [47], [53]–[55], [57]–[59], healthy older adults (Mean Age > 50 years) [14], [15], [18], [19], [48]–[51], [63], people with somatosensory deficiency at the feet [56], diabetes [22], stroke [22] or Parkinson's disease [63], as well as healthy young adults under challenging stances [20], [27], [47], fatigue [27], [28], or cold feet [10], [26] that could simulate aging or a neuromuscular disease (i.e., low PS).

The study to assess the dissertation's vibratory mat must consist of a subthreshold vibrating output, where participants' sway COP is recorded and analyzed before, during and immediately after the vibration is administered. Given that suprathreshold vibrations on humans can reduce cognitive reaction time [62] or produce unexpected reductions on PS [20], [52], it is preferred to assess the vibratory mat as its intended use (i.e., subthreshold). It is not a proven theory; however, SR through subthreshold vibrations might be better for everyday use, since it is believed to train the body to naturally produce better PS, instead of alarming the body, as suprathreshold vibration does during low PS stages [62]. In addition, despite the number of studies and targeted populations that use SR with subthreshold vibration [10]–[14], [16]–[24], [26]–[28], [47]–[49], its effect on PS is still unclear. This suggests that studies that observe how subthreshold vibration affects people's sway during and immediately after the stimulation should take priority. This does not suggest that retention or longitudinal studies are not needed, since these studies [23], [24] and similar ones (whole-body vibration) [84]–[86] have yielded

promising results. Instead, it suggests that they could be improved if the immediate effect of SR is better understood. Finally, since the immediate effect of subthreshold vibration is the priority of this study and a vibratory mat is the device of choice, sway over gait makes more sense as the chosen biomechanical task (i.e., it is not possible to test gait while the participant stands on the vibratory mat). In fact, sway COP will be used over sway COM, since there is an upcoming trend of using sway COP over sway COM in the literature (later explained in Table 4).

Previous non-retention or non-longitudinal sway studies on SR through subthreshold vibration have used either constant or white noise stimulations (Figure 5: Middle row, first two from left to right), and assessed how the participants' COP or COM changed with respect to a control [10]–[12], [14], [16]–[23], [26], [27], [47]–[49]. Using only constant or white vibrations ignores previous design recommendations [68], conclusions [15], [81], [82] and the importance of complexity and predictability in human PS [11], [81], [82]. It is known that healthy humans and other biological systems behave as pink noise; therefore, it is understandable to test whether humans benefit more from a signal that is more natural to them (i.e., Pink, Figure 5: Middle row, third from left to right), or from another signals besides white (e.g., Brown, Figure 5: Middle row, forth from left to right) [82]. However, previous studies have not ignored human predictability and complexity when assessing how people's COP or COM changes in the Anterior-Posterior (AP), Medial-Lateral (ML), or Planar directions. Besides assessing how much in magnitude [14], [16], [17], [20]–[22], [26], [27], [47], [48] COP or COM changes due to SR, observing how the COP or COM changes in terms of predictability and complexity [11], [17]–[20], [22], [27], [47], [49] has also been done. The magnitude of a COP or COM signal can be measured through average, standard deviation, curve length, Root Mean Square (RMS), swept area, range, among others in the AP, ML, or planar directions. Predictability can be measured through entropy calculations, such as Approximate Entropy (AppEn) [87] and Sample Entropy (SampEn) [88] in the AP, ML and planar directions. Both algorithms (AppEn and SampEn) show that a time series is predictable when their values are close to 0, or

unpredictable when their values are large. Complexity can be measured by the slope of the linear fit on the log-log plot (α), resultant of a Detrended Fluctuation Analysis (DFA) [79] in all directions (AP, ML and planar). A white signal (α = 0.5) is interpreted as stationary and anti-persistent signal, a brown signal (α = 1.5) as non-stationary and persistent signal, and a pink signal (α = 1.0) as the mid-point between a white and brown signal [80]. Other accepted methods to measure complexity in all directions are Multiscale Entropy and Stabilogram Diffusion Analysis (SDA). Multiscale Entropy consists of calculating either AppEn or SampEn over the time series' multiple scales, plotting all entropy values vs. the number of scales [89], and determining the area under the curve (Complexity Index) [90]. A scale represents the number of consecutive values averaged in the time series [89]. SDA's calculations are similar to the DFA's ones [91], and it has been shown that DFA covers most of the results of SDA [92], making DFA more common among today's researchers.

Non-retention or non-longitudinal COP or COM sway studies on SR through subthreshold vibration [10]–[12], [14], [16]–[23], [26], [27], [47]–[49] differ in the groups they analyze, when they analyze PS, and which measures they extract from the participants' COP or COM time series (Table 4). However, it is possible to see conclusive trends among all the studies. Most of the studies (10 out of 17) [11], [16], [17], [20]–[23], [47]–[49] ask their participants to stand with their eyes closed, and out of the 7 studies that let their participants keep their eyes open [12], [14], [18], [19], [26], [27], 4 of them [18], [19], [26], [27] reduced their participants' PS through challenging stances, foam under their feet, cold temperatures at the feet or fatigue. This suggests that low levels of PS are needed to observe changes in sway due to SR through subthreshold vibration. Even though the needed low levels of PS might be seen as a negative feature of SR studies (i.e., SR only works in simulated low PS situations), it needs to be pointed out that most of the studies (12 out of 17) involve healthy populations [10]–[12], [14], [16], [17], [20], [26], [27], [47]–[49], which are not the intended users of a vibratory mat. In fact, SR studies on persons with neuromuscular diseases have observed positive results towards subthreshold vibration

without the need of asking participants to close their eyes or perform actions that reduce their PS [18], [19], [21]–[23]. Also, most of the simulated low PS situations (3 out of 4 studies) are in healthy young populations [20], [26], [27], since studies with healthy young populations that do not challenge their PS have a hard time finding significant results towards SR through subthreshold vibration. This shows that a balanced and stable biomechanical system does not get more stable because of an external assist. In other words, someone without a headache does not get a clearer head because they take ibuprofen or acetaminophen. Finally, a common trend on SR studies through subthreshold vibration is that researchers are moving away from body's COM time series and using COP time series.

However, to better understand the effect of SR through subthreshold vibration, studies that observe the effect of vibration while participants stand with respect to no vibration (i.e., During and Pre in Table 4) should be separated from studies that assess how sway changes after a vibration has been provided with respect to how people's sway was before the vibration (i.e., Post and Pre in Table 4).

Table 4: Significant results from subthreshold SR studies assessed through COP or COM

Year & Ref.	Group	Vibration Stages	Sway Time Series	Extracted and Significant Measures
2002 [16]	HO, HY	During, Pre	COM	Mean Radius **(Vib)**, Max Radius, Swept Area **(Vib)**, AP Range **(Vib)**, ML Range, SDA
2003 [17]	HO, HY	During, Pre	COM	Mean Radius **(Vib)**, Max Radius **(Vib)**, Swept Area **(Vib)**, AP Range **(Vib)**, ML Range **(Vib & Group)**, SDA **(Vib & Group)**
2006 [22]	HO, D, S	During, Pre	COM	Mean Radius **(Vib)**, Max Radius **(Vib)**, Swept Area **(Vib)**, AP Range **(Vib)**, ML Range **(Vib)**, SDA **(Vib & Group)**
2007 [11]	HO, HY	During, Pre	COM	AP Multiscale SampEn(m=2, r=0.15) **(Vib & Group)**, ML Multiscale SampEn(m=2, r=0.15) **(Vib & Group)**
2008 [21]	HO, D	During, Pre	COP	Curve Length, AP RMS **(Vib & Group with cognitive task and eyes closed)**, ML RMS
2011 [20]	HO, HY	During, Pre	COM	SDA **(Vib with semi-tandem stance)**
2012 [18]	HY, OF	Post, Pre	COP	AP DFA(n_{min}=5, n_{max}=N/4) **(Vib & Group)**, ML DFA(n_{min}=5, n_{max}=N/4)
2012 [19]	OF	Post, Pre	COP	AP Multiscale SampEn, ML Multiscale SampEn, Multivariate Multiscale SampEn **(Vib)**
2014 [47]	HY	Post, During, Pre	COM, COP	Swept Area **(Vib with foam under feet and eyes closed)**, AP RMS **(Vib with foam under feet and eyes closed)**, ML RMS, AP AppEn, ML AppEn **(Vib with foam under feet and eyes closed)**
2015 [14]	HO, HY	During, Pre	COP	AP Curve Length **(Vib)**, AP AppEn
2015 [48]	HO	During, Pre	COP	Swept Area **(Vib)**, AP Average, ML Average **(Vib)**
2016 [12]	HO, HY	During, Pre	COP	AP RMS, AP AppEn(m=2, r=0.2), AP Curve Length, ML Curve Length, AP Absolute Max, ML Absolute Max
2016 [49]	HO	During, Pre	COP	AP Multiscale SampEn(m=2, r=0.15), ML Multiscale SampEn(m=2, r=0.15) **(Vib)**, Swept Area
2018 [10]	HO, HY	During, Pre	COP	Non-COP or -COM measures
2019 [23]	D	Post, Pre	COP	Swept Area, AP Average, ML Average
2020 [26]	HY	During, Pre	COP, Lower Leg EMG	COP Swept Area **(Vib with cold feet and single stance)**, COP Curve Length **(Vib with cold feet and single stance)**, EMG RMS **(Vib with cold feet and single stance)**
2020 [27]	HY	Post, Pre	COP	DFA(n_{min}=5, n_{max}=N/4) **(Vib with fatigue and single stance)**, Swept Area **(Vib with fatigue and single stance)**

Note: Measures with bolded text in parenthesis correspond to significant results, and the listed factors in the parenthesis create a statistical significance in a comparison.

Abbreviations: HO = Healthy Old; HY = Healthy Young; D = Diabetic; S = Stroke; OF = Old Fallers, Vib = Vibration

Effect of Stochastic Resonance: During- vs. Pre-Vibration

SR studies focused on how people's sway (i.e., COM or COP) is affected while their feet receive a subthreshold vibration have shown that vibration reduces sway's magnitude [14], [16], [17], [21], [26], [47], increases predictability [47], and adds complexity [11], [17], [20], [22]. When searching for significant differences in sway due to vibration among healthy people, it was found that vibration reduced healthy people's sway radius [16], [17], swept area [16], [17], range [16], [17] and curve length

[14]. In fact, a study showed that sway range reductions due to vibration in healthy old people were significantly larger when compared to healthy young people [17]. Besides healthy groups, sway magnitude reductions due to vibration were found in healthy young people with simulated low PS (swept area [26], [47] and curve length [26]), as well as in people with diabetes (RMS [21]). In terms of predictability, one study found that healthy young people's sway under simulated low PS became more predictable due to vibration (i.e., AppEn was reduced due to vibration) [47]. Finally, vibration has shown to increase complexity (i.e., improvement of SDA's measures) in healthy people [17], [20], as well as have a larger improvement in healthy old people when compared to healthy young people [17], or only occur in healthy old people (i.e., increment of multiscale SampEn) [11]. The addition of complexity (i.e., improvement of SDA measures) to sway due to vibration has also been found in diabetic [22] and stroke patients [22].

Effect of Stochastic Resonance: Post- vs. Pre-Vibration

SR studies focused on how people's sway (i.e., COM or COP) is affected after their feet receive a subthreshold vibration have shown that vibration reduces sway's magnitude [27], and adds complexity [18], [19], [27]. Healthy subjects who went through a fatigue protocol had less sway (i.e., lower swept area) when they have had vibration under their feet, compared to when they went through the fatigue protocol and did not have vibration under their feet [27]. In the same study, it was found that complexity (measured through DFA) improved when vibration was present [27]. Similar to healthy young people under simulated low PS, old fallers improved their sway complexity due to vibration when measured through DFA [18] and multiscale SampEn [19].

Statistical Analysis

Non-retention or non-longitudinal COP or COM sway studies on SR through subthreshold vibration [10]–[12], [14], [16]–[23], [26], [27], [47]–[49] have used similar statistical methods that do not focus on the initial state of people's sway. The most common statistical analysis is a 1-Way (vibration) or 2-Way

(vibration and participant's group) Analysis of Variance (ANOVA), followed by multiple comparisons (mostly Tukey). This statistical analysis allows researchers to determine if an input (e.g., vibration or group) has a significant effect on the calculated sway measures. However, the described statistical analysis does not focus on how the subject's sway was at the start of the study, or how much sway changes with respect to the sway's initial state. A study that did DFA on a group of people who received the same type of vibration (i.e., white) found that part of the group benefited from the vibration, while others did not [82]. They concluded that a vibration could or could not benefit a participant depending on the state of the participant's PS before treatment. That is why it was suggested for future vibratory studies to offer different types of vibrations and/or consider the initial state of people's PS in their statistical analysis. The second suggestion was applied in two SR studies that assessed PS through gait [51], [53]. Both studies found that when a linear regression analysis was done on the change due to vibration on a gait measure (gait speed, stance time, etc.) with respect to the gait measure's initial value, a negative slope was obtained. This means that vibration increased certain gait measure among their participants when that measure was below a threshold, or reduced certain gait measure when it was above a threshold, or did not change the gait measure when it was close to a threshold [51], [53].

This concludes the Background and Literature Review needed to conduct the studies that will comprise this dissertation. Given the information on previous vibratory devices and design requirements, vibratory outputs and their features, and the effect of subthreshold vibration under the feet on PS, the following chapters of the dissertation will cover the design and manufacturing (Chapter 3), validation (Chapter 4) and performance assessment (Chapter 5) of a new vibratory mat.

Chapter 3: Design and Manufacturing of a Vibratory Mat

Abstract

Background: Falls in adults over the age of 65 is a problem in need of solutions that becomes more expensive as years pass. Vibratory mats or insoles that introduce stochastic resonance at the feet have been proposed as medical devices that can improve postural stability, thus reduce falls. This study proposed a new vibratory mat and was compared to the most-reported vibratory device using accepted and new design requirements.

Methods: Our new vibratory mat and the most-reported vibratory device were scored on each design requirement, and a final score was given to each device. The accepted design requirements covered the choice and placement of the vibratory components, the power and noise generator, and the overall material. The new design requirements assessed the adaptability to various feet sizes and sensing thresholds, the protocol to determine sensing threshold, cost, and manufacturing.

Findings: The new vibratory mat outperformed the most-reported vibratory device in the already accepted design requirements (8.75 vs. 6.5), and new ones (6 vs. 4).

Interpretation: The study showed that the new vibratory mat, when compared to the most-reported vibratory device, has as much or more potential to improve postural stability through stochastic resonance on people with high risk of falling.

Background

Falls in adults over the age of 65 is an expensive problem in need of solutions. In 2006, $19.3 billion were used to cover injuries created by falls [1], which more than doubled by 2017 ($40 billion) [2]. On average, it is expected for one third of adults over the age of 65 to fall at least once per year [2]. Exercising, home modifications, vitamin D supplements and medical devices are some of the proposed strategies to reduce falls [4], [5]. Referring to medical devices, it is known that users increase their

postural stability (PS) when compared to people who do not use their recommended assistive device such as a cane, walker, wheel-chair, etc. [7]. However, it is also known that medical device cause users to feel *weak* in their social circle, often resulting in them choosing not use their recommended medical device [8]. PS is defined as the integration and processing of all types of sensory feedback's information (visual, proprioceptive, vestibular and somatosensory), and the appropriate execution of a muscular response by the central nervous system to maintain balance [9]. That is why, PS enhancement strategies (medical devices, surgeries, etc.) have targeted both the central nervous system [29] or a specific type of sensory feedback.

Through stochastic resonance (SR), vibratory insoles or mats have shown to be a potential candidate to improve the somatosensory feedback in people with low PS [16]. SR is the addition of noise to a signal below a threshold level, so that the signal with the noise's assistance can cross such threshold level (Figure 2). The attenuation of somatosensory feedback due to aging or neuromuscular diseases is reflected by people not sensing touching stimuli that they used to recognize at younger ages or prior to the onset of negative effects of a disease. Given that sensation in humans is only achieved when neurons at the skin cross the threshold of excitation, vibratory devices that insert SR are ideal medical devices to improve the somatosensory feedback, leading to better PS and a reduction of falls.

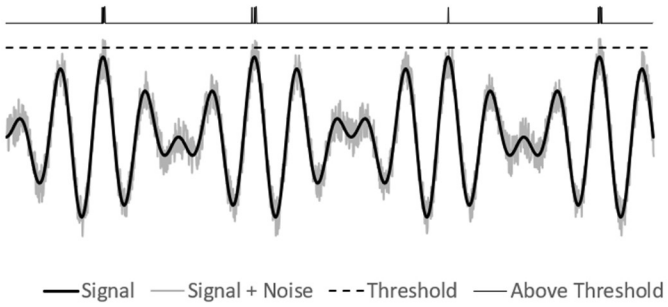

Figure 2: Stochastic resonance graphical description

Stochastic resonance (SR) is the addition of noise to a signal that is below a threshold level so that the signal with the noise's assistance can cross the threshold level that it could not cross before

Various SR studies have assessed the effect of vibration at the feet on PS [10]–[28], [47]–[61], [63]; however, only two studies have focused on the design and necessary features that any vibratory mat or insole should have [68], [69]. The main difference between the design papers and the SR studies that assess the effect of vibration at the feet on PS, is that the design papers go beyond listing the materials of the vibratory device. The current design requirements and suggestions for vibratory devices are listed below.

1. Motor Selection: The vibrating component should not exceed a thickness of 16 mm [68], and they can be either indenters, eccentric rotating masses, or piezo-electric actuators [68], [69].
2. Motor Location: The vibrating components should be placed at the heel, big toe, first and fifth metatarsal of each foot [68], [69].
3. Power Generator: There should not be more than one power generator per foot [68], and possible options are commercial microcontrollers such as Arduino, Raspberry Pi, etc. [69].
4. Noise Generator: The noise generator should be adjustable to different people's sensing thresholds [68], [69], and they should output white noise [69], and other colors (e.g., pink or brown) [68].
5. Material: The material that encases the vibrating components should be a hard silicone (Shore A50). In addition, between the vibratory device and the foot, there should be two thin layers. The one in contact with the top of vibratory device should be slightly harder (e.g., Shore A55, or cork), and the one touching the participant's foot should be slightly softer (e.g., soft leather).

SR studies that successfully assessed the effect of vibration at the feet on PS [10]–[23], [25]–[28], [47]–[49], [51], [52], [54], [55], [57]–[61], [63] followed most of the current design requirements and suggestions [68], [69]. Out of the 31 studies, all studies used an accepted type of vibrating component, 20 studies [10]–[15], [17]–[22], [27], [28], [47]–[49], [51], [52], [63] used thicknesses of 16 mm or less for

their devices, 25 studies [11]–[15], [17]–[23], [26], [27], [47], [51], [52], [54], [55], [57]–[61], [63] placed their vibrating components at the heel, first and fifth metatarsal, all studies had no more than 1 power generator per foot and adjustable noise generators that could produce white noise, and finally, all studies fabricated their devices out of hard silicone or used commercial insoles. When studying the complete vibratory devices reported by the SR studies, common designs have been used multiple times. The most-reported vibratory device [11]–[14], [17], [20], [22] that meets the majority of the current design requirements [68], [69] is a 16-mm thick (or less) vibrating insole made from Shore A50 silicone that has three C-2 Tactors (Engineering Acoustics, FL) per insole under the heel, first, and fifth metatarsal. The vibrating components are powered and controlled by either the Engineering Acoustics Universal Controller (Engineering Acoustics, FL) or a custom-built one. Further details on the most-reported vibratory insoles are given in the Methods, Results and Discussion sections of this chapter.

The current design requirements and suggestions [68], [69] allow the design, development and study of vibratory mats or insoles. However, it is proposed by this chapter that new design requirements and suggestions (listed below) are needed to assure that vibratory mats or insoles can be used by the intended groups on their everyday lives [1], [2], [21]–[28].

1. Multiple Shoe Sizes: Male and female people over the age of 65 wear a wide range of US shoe sizes, creating different positions for the metatarsals with respect to the heel [70]. Sensing threshold at the feet changes with respect to the location where the vibration is applied [71]–[73]. Therefore, vibratory mats or insoles should accommodate for multiple shoe sizes (male and female) to assure that the correct skin mechanoreceptors (heel, first and fifth metatarsals) are targeted [73], and to not modify people's sensing thresholds [71], [72].
2. Multiple Motors: Sensing threshold is sensitive to age [74], body temperature [75], contact area [76], among other factors. Therefore, vibratory mats or insoles should have different motors

that cover a wide range of amplitudes and frequencies. Especially motors that operate between 200 Hz and 300 Hz, since this is the frequency range where Pacinian Corpuscles (Fast Adapting Type II skin mechanoreceptors) respond [71]–[73]. Pacinian Corpuscles are the skin mechanoreceptors that should be targeted by vibratory devices that introduce SR [71]–[73].

3. Cost: The cost that people over 65 [1], [2], or with a neuromuscular disease [21]–[28] are willing to pay to improve their PS should be part of the design process. The goal of any medical device is to be used by as many people as possible, and this is achieved by marketing the product at the correct cost [3]. Therefore, it is suggested for vibratory insoles or mats to cost around $300, since as of right now (November 2020), that sum of money has shown to be an appropriate cost to improve PS (e.g., whole-body vibration equipment, or already available vibratory insoles).
4. Robust Sensing Threshold: Given that sensing threshold is non-constant [71]–[76], and that SR studies that administer suprathreshold vibrations [54], [57], [58] under the feet obtain significantly different results when compared to subthreshold studies [16], [17], [22], a robust method to determine sensing threshold is needed [77].
5. Robust Manufacturing: SR studies should document the manufacturing process of their vibratory mats or insoles (at least on their first publication), so future SR studies can take the current technology and address questions that were not initially considered. It is acknowledged SR studies might not share their manufacturing process, wiring diagrams and codes since they could be Intellectual Property owned by the institution or laboratory. However, listing only the materials in the Methods section of a publication is not enough for future investigators to manufacture and study a vibratory device.

A new vibratory device that we claim to meet the majority of the current [68], [69] and new design requirements is proposed in this chapter (Figure 4). The new vibratory device is a 19.5 in x 15 in x 13.17 mm mat made from Shore A50 silicone that has multiple sets of eccentric rotating mass motors (307-

105, 310-003, 306-10H and 307-103 from Precision Microdrives, UK) under the heel, first and fifth metatarsal of multiple US shoe sizes. Each set of motors follows foot placement recommendations (i.e., heels 17 cm apart, and 14 degrees between the lines formed by each foot's heel and big toe) [93], as well as three locations for the first and fifth metatarsals to accommodate various shoe sizes (Figure 8). The vibrating components are powered and controlled by a 5-Volt and 12-Volt external power supply, DRV2605 Chips (Texas Instruments, TX), and custom-built Arduino UNO codes (Arduino, MA) that include white, pink, and brown noise signals developed in MATLAB (MathWorks, MA) for each motor. Finally, the vibratory mat uses a robust protocol to find participants' sensing thresholds, and it consists of an improved 421 protocol [94], [95]. The details on the new vibratory mat are developed in the Methods, Results and Discussion sections of this chapter. Further details such as manufacturing steps, wiring diagrams, and codes needed to operate the vibratory mat are in the Appendix of this chapter.

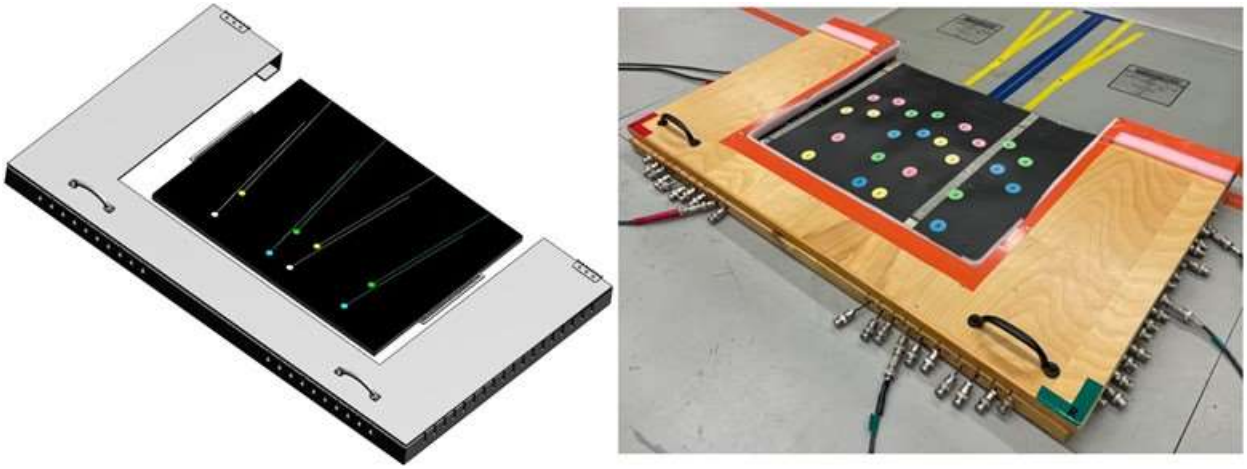

Figure 4: New vibratory mat

Vibratory mat controlled by custom-built Arduino code that uses validated white, pink, and brown inputs for each of the offered motors. Four sets of motors (307-105, 310-003, 306-10H and 307-103 from Precision Microdrives, UK) are embedded in a 10-mm think Shore A50 silicone, and each set of motors accommodate multiple shoe sizes by offering three ranges of shoe sizes. Finally, the mat directs participants to follow a standardized stance.

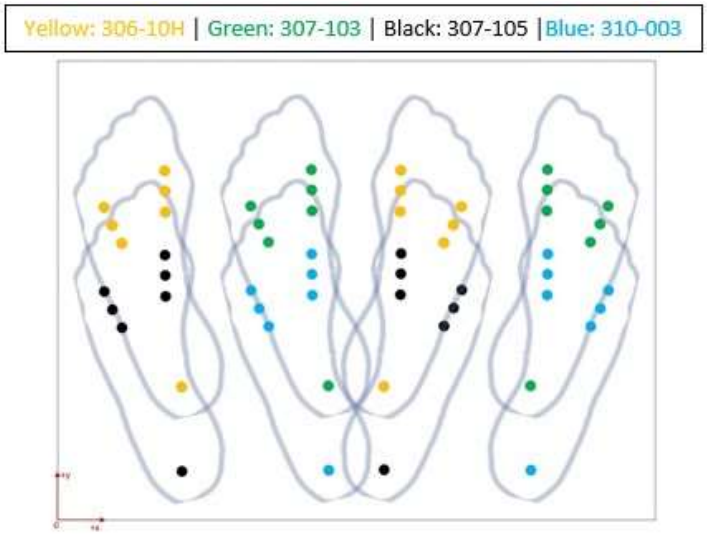

Figure 8: Layout of eccentric rotating motors for the new vibratory mat

Each set of motors (307-105, 310-003, 306-10H, and 307-103 from Precision Microdrives, UK) offers the Short, Middle and Long feet sizes. Short: US men's 7 to 8.5 and women's 6 to 9; Middle: US men's 9 to 10.5 and women's 9.5 to 11.5; Long: US men's 11 to 14 and women's 12 to 14.

The purpose of this chapter is to accomplish a comprehensive design review on the most-reported device and our new vibratory device in the context of the current and new design requirements. The questions to be answered by this chapter are: 1) how do both vibratory devices (most-reported insole and our new mat) meet the current design requirements [68], [69]? 2) How do both vibratory devices meet the new design requirements? 3) How likely are both devices to be used by the intended groups [1], [2], [21]–[28]?

Methods

To assess how the most-reported [11]–[14], [17], [20], [22] and new (Figure 4) vibratory devices meet the current [68], [69] and new design requirements, one or more questions per design requirement will be answered using each vibratory device's design information (Table 5). Each answer will receive a score from 0 to 1, and a final score will be given to each device which will determine how well the design requirements are met.

Table 5: Features and assessment questions of the most-reported and new vibratory devices

Design Requirement	Design Requirement Question(s)	Features of Most-reported Vibratory Device (Insole)	Features of New Vibratory Device (Mat)
Motor Selection	• Is the motor's thickness less than 16 mm? • Is the motor an indenter, eccentric rotating mass, or piezo-electric actuator?	C2-Tactors (EA, FL) • Indenter • Thickness = 7.9 mm	307-105 (PM, UK) • Eccentric rotating mass • Thickness = 2.05 mm 310-003 (PM, UK) • Eccentric rotating mass • Thickness = 3.4 mm 306-10H (PM, UK) • Eccentric rotating mass • Thickness = 7 mm 307-103 (PM, UK) • Eccentric rotating mass • Thickness = 8.7 mm
Motor Location	• Are the motors placed under the heel, big toe, first and fifth metatarsal?	Heel, first and fifth metatarsals	Heel, first and fifth metatarsals following standardized stance [93]
Power Generator	• How many motors can be controlled per power generator? Is this number equal to or less than the number of motors per foot?	EA Universal Controller (Engineering Acoustics, FL)	External power supply (5V and 12V), and Arduino UNO (Arduino, MA)
Noise Generator	• Is the motor's output adjustable? • Can white noise be generated? • Can non-white noises be generated?	EA Universal Controller, TDK software and TAction software (Engineering Acoustics, FL)	Arduino UNO (Arduino, MA) codes that contain white, pink, and brown noises developed in MATLAB (MathWorks, MA) (Chapter's Appendix), as well as DRV2605 Chips (Texas Instruments, TX).
Material	• Is the material that capsules the vibrating components a Shore A50 silicone? • Are there two layers (i.e., cork-like, and soft leather) between the Shore A50 silicone and the participant's feet?	Shore A50 Silicone with soft layer between the insole and people's foot	Shore A50 Silicone, with cork (i.e., Shore A55) and soft layers between the mat and the participant's feet
Multiple Shoe Sizes	• Does the vibratory device accommodate for multiple shoe sizes?	Multiple insole sizes are available.	Short: US men's shoe sizes 7 to 8.5 and women's shoe sizes 6 to 9. Middle: US men's shoe sizes 9 to 10.5 and women's shoe sizes 9.5 to 11.5. Long: US men's shoe sizes 11 to 14 and women's shoe sizes 12 to 14.

Multiple Motors	• Do all motors in the vibratory device cover the frequency range that targets Pacinian Corpuscles (200 Hz to 300 Hz)?	C-2 Tactors (EA, FL) • 0.2 mm ≤ P2P ≤ 0.84 mm • 150 Hz ≤ Freq ≤ 320 Hz	307-105 (PM, UK) • 0.075 g ≤ Acc ≤ 0.46 g • 60 Hz ≤ Freq ≤ 290 Hz 310-003 (PM, UK) • 0.1 g ≤ Acc ≤ 1.2 g • 40 Hz ≤ Freq ≤ 190 Hz 306-10H (PM, UK) • 0.1 g ≤ Acc ≤ 2.4 g • 60 Hz ≤ Freq ≤ 280 Hz 307-103 (PM, UK) • 0.1 g ≤ Acc ≤ 8.5 g • 30 Hz ≤ Freq ≤ 260 Hz
Cost	• Given the cost of the vibratory device's materials, how possible is to market the vibratory device around $300?	Pair of Vibrating Insoles Shore A50 Silicone: $12.70 Soft Layer: $1.80 Motors: $1,260.00 Controller: $3,040.00 **Total: $4,314.50** More detailed cost breakdown in the chapter's Appendix	Complete Vibratory Mat Shore A50 Silicone: $30.96 Cork Layer: $14.54 Soft Layer: $3.59 Motors: $461.44 Controller: $232.45 External Housing: $319.85 **Total: $1,062.83** More detailed cost breakdown in the chapter's Appendix
Robust Sensing Threshold	• Is there a defined and robust protocol to find the participant's sensing threshold?	Method of levels [12]–[14], [77], user's choice through a potentiometer [11], [17], [20], or researcher cues participant on whether they feel vibration [22].	Modified 421 [94], [95]
Robust Manufacturing	• Are the materials listed? • Is a wiring drawing shared? • Are manufacturing steps listed?	Materials are listed. Wiring diagram or manufacturing steps are not shared; however, possible access can be granted by contacting researchers [20].	Materials are listed. Wiring diagram and manufacturing steps in chapter's Appendix.

Abbreviations: EA = Engineering Acoustics; PM = Precision Microdrives; P2P = Peak-to-Peak; Freq = Frequency; Acc = Acceleration

Results

Motor Selection: Both devices use accepted types of vibrating components whose thicknesses are less than 16 mm. The most-reported vibratory device [11]–[14], [17], [20], [22] uses indenters (C-2 Tactors from Engineering Acoustics, FL), while the new vibratory device uses four sets of eccentric rotating mass motors (307-105, 310-003, 306-10H and 307-103 from Precision Microdrives, UK).

Motor Location: Both devices place their vibrating components under the heel, first and fifth metatarsal, ignoring the suggestion of placing a fourth vibrating component under the big toe [68].

Power Generator: The most-reported vibratory device [11]–[14], [17], [20], [22] uses the Universal Controller (Engineering Acoustics, FL), which allows the operation of 8 Engineering Acoustics tactors (e.g., C-2 Tactors), or no more than 4 simultaneously at full power. In the worst-case scenario (i.e., tactors at full power) there would be enough power to operate the 3 vibrating components in each foot, if 2 controllers were available. If the vibrating components are not operated at full power, 1 controller would be enough to operate the 6 vibrating components of both insoles. The new vibratory device uses an external power supply (5V and 12V) shared by the 6 vibrating components that would be operated at once (heel, first and fifth metatarsal per foot), and an Arduino UNO (Arduino, MA) per vibrating component (Wiring diagram is included in this chapter's Appendix). This configuration offers enough power to operate 6 vibrating components simultaneously at full power for any of the four sets of eccentric rotating mass motors (307-105, 310-003, 306-10H or 307-103 from Precision Microdrives, UK).

Noise Generator: Both vibratory devices allow for their outputs to be adjusted to the user's sensing thresholds. The most-reported vibratory device [11]–[14], [17], [20], [22] uses the TDK and TAction software programs (Engineering Acoustics, FL) to control the amplitude and frequency of the vibrating components (i.e., C-2 Tactors from Engineering Acoustics, FL). According to the Engineering Acoustics' documentation, it is possible to build custom sequences through a graphical interface indicating the possibility of outputting white and non-white noises. In fact, the most-reported vibratory device has reported the use of white noise in multiple SR studies [11]–[14], [17], [20], [22]. The new vibratory device uses Arduino UNO (Arduino, MA) codes that have prescribed white, pink, and brown noises for each of the four sets of eccentric rotating mass motors (Chapter's Appendix). The noises are 90-second long, and were developed in MATLAB (MathWorks, MA). The Arduino UNO codes output the prescribed noises through DRV2605 chips (Texas Instruments, TX), and the process used to validate the output color for all vibrating components at multiple power levels is described in Chapter 4 of this dissertation.

Material: Both vibratory devices follow the design recommendation of using a Shore A50 silicone as the main material, as well as the recommendation of placing a soft layer between the vibratory device and participant [68], [69]. However, only the new vibratory device places a cork layer between the vibratory mat and the soft layer [68].

Multiple Shoe Sizes: The SR studies that use the most the reported vibratory device [11]–[14], [17], [20], [22] state that participants stood on vibrating shoe insoles, inferring that the insoles follow the participant's shoe size. Three of these studies [12]–[14] explain that their vibratory insoles were comprised of multiple sections allowing them to "puzzle piece" insoles together to match the shoe size of any participant. The new vibratory device has three sizes per set of eccentric mass motors: Short, Middle, and Long (Figure 8). The Short setting is for US men's shoe sizes from 7 to 8.5, and women's shoe sizes from 6 to 9. The Middle setting is for US men's shoe sizes from 9 to 10.5, and women's shoe sizes from 9.5 to 11.5. Finally, the Long setting is for US men's shoe sizes from 11 to 14, and women's shoe sizes from 12 to 14. The ranges of shoe sizes for men and women in each setting were chosen based on the shoe size distributions described in a study that analyzed the shape of multiple people's feet [70]. This means that the new vibratory device has 56 eccentric rotating motors, since there are 7 motors per foot (1 motor at the heel, and 3 settings of 2 motors at the 1^{st} and 5^{th} metatarsal), 2 feet per set of motors, and 4 sets of motors (Figure 8).

Multiple Motors: The most-reported vibratory device [11]–[14], [17], [20], [22] offers one type of motor (C-2 Tactors from Engineering Acoustics, FL), and this motor operates at frequencies (150 Hz to 320 Hz) where the Pacinian Corpuscles are activated (200 Hz to 300 Hz) [71]–[73]. The new vibratory device offers four sets of motors (307-105, 310-003, 306-10H and 307-107 from Precision Microdrives, UK) that were selected based on their rated amplitude. An exponential increase in amplitude was intended to cover a wide range of sensing thresholds. However, when the motors' operating frequencies are

observed, the motors 307-105 (60 Hz to 290 Hz), 306-10H (60 Hz to 280 Hz) and 307-103 (30 Hz to 260 Hz) are the ones that cover frequencies where Pacinian Corpuscles are activated (200 Hz to 300 Hz) [71]–[73]. The motor 310-003 (40 Hz to 190 Hz) misses the skin mechanoreceptors' frequency range.

Cost: Both vibratory devices' materials cost more than $300, which is more than the acceptable cost intended populations [1], [2], [21]–[28] are willing to pay to improve their PS. In terms of materials, a pair of the most-reported vibratory insoles [11]–[14], [17], [20], [22] is estimated to cost $4,314.50, while the complete new vibratory mat is estimated to cost $1,062.83.

Robust Sensing Threshold: The most-reported vibratory device has used different protocols to find the user's sensing threshold at the foot plantar surface. The utilized protocols are the Method of Levels [12]–[14], [77], the participant's choice through a potentiometer [11], [17], [20], and a researcher cuing the participant on whether or not they feel the vibration [22]. From the utilized protocols, only the Method of Levels [77] can be considered as a robust protocol to find participants' sensing threshold. Letting the participant change the vibration's magnitude as they feel the vibration does not allow studies to control how fast power levels are changed or reduce participants' biases. In addition, having a researcher cuing a participant on whether they feel a vibration can create a temptation on the participant to respond "yes" since they know a stimulus was given to them.

The new vibratory device uses a modified 421 protocol [95], which is an improvement of the original 421 protocol [94]. The original 421 protocol consists of asking the participant 15 times if they feel a stimulus, starting at 50% of the stimulus power range. If the participant senses the stimulation, the stimulus becomes greater, and vice versa. At the start of the protocol, the increment or reduction is equivalent to 4-times the smallest division in power level, and this increment or reduction changes if a turnover occurs. A turnover takes place when the participant goes from feeling the stimulus to not feeling the stimulus (i.e., yes-to-no), or vice versa (i.e., no-to-yes). In the first turnover, the increment or reduction

changes from 4-times to 2-times the smallest division, and when the next turnover happens, the change is from 2-times to 1-time the smallest division. Finally, the sensing threshold is defined as the average of all 1-time turnovers. The modifications to the 421 protocol [94] are described in the chapter's Appendix, and further detailed in a previous study [95]. In the end, the modified 421 reduces biases on the participant since they do not control the vibration or are cued by the researcher. In addition, the modified 421 protocol is a robust calculation since it controls the duration of the protocol (not done by other protocols), holding constant any effect of fatigue in a participant. The algorithm that performs the modified 421 is part of the Arduino codes included in this chapter's Appendix.

Robust Manufacturing: Both vibratory devices list the main materials needed for manufacture. However, only the new vibratory mat documents a wiring diagram and manufacturing steps (Chapter's Appendix).

Table 6 summarizes the results of each vibratory device when answering the questions regarding the current and new design requirements. The maximum number of points per design requirement is equivalent to the number of questions, and full points were given if the design requirement's questions were answered with suitable information. Partial points were given if the vibratory device's information partially met the design requirement.

Table 6: Assessment on how the vibratory devices met the design requirements

Design Requirement	Most-reported Vibratory Device (Insole)	New Vibratory Device (Mat)
Motor Selection	2/2	2/2
Motor Location	0.75/1	0.75/1
Power Generator	1/1	1/1
Noise Generator	3/3	3/3
Material	1.5/2	2/2
Multiple Shoe Sizes	1/1	1/1
Multiple Motors	1/1	0.75/1
Cost	0/1	0/1
Robust Sensing Threshold	0.5/1	1/1
Robust Manufacturing	1/3	3/3
Current Design Requirements	*8.25/9*	*8.75/9*
New Design Requirements	*3.5/7*	*5.75/7*
Current & New Design Requirements	*11.75/16*	*14.5/16*

Discussion

The purpose of this chapter was to assess how both vibratory devices (most-reported insole and new mat) meet the current [68], [69] and new design requirements, as well as to assess how likely they are to be used by the intended groups [1], [2], [21]–[28]. In terms of the current design requirements, the most-reported vibratory insoles [11]–[14], [17], [20], [22] scored 91.67% (8.25/9), while the new vibratory mat scored 97.22% (8.75/9). In terms of the new design requirements, the most-reported and new vibratory devices scored 50% (3.5/7) and 82.14% (8/10) respectively, suggesting that the new vibratory mat has as much or higher potential to be used by the intended populations when compared to the most-reported vibratory insoles.

The performance of both vibratory devices with respect to the current design requirements [68], [69] shows that there are not large differences. However, the most-reported vibratory insoles [11]–[14], [17], [20], [22] and the new vibratory mat (Figure 4) differ in context of the new design requirements.

Motor Selection: Both vibratory devices use thin (less than 16 mm) vibrating components of acceptable types (indenters and eccentric rotating motors). This assures that the thickness of the vibratory device

will not negatively affect the participant's PS [68], and that approved products in human biomechanics are used, making a future FDA approval process more efficient.

Motor Location: Both devices install the vibrating components under the heel, first and fifth metatarsal, ignoring the suggestion of placing a fourth vibrating component under the big toe [68]. However, only one SR study [10], out of 31, that had successfully assessed the effect of vibration at the feet on PS [10]–[23], [25]–[28], [47]–[49], [51], [52], [54], [55], [57]–[61], [63] has installed a vibrating component under the big toe. This could imply that a vibrating component under the big toe is not needed, reducing the cost and manufacturing time of future vibratory devices.

Power Generator: Both devices offer power generators able to operate all vibrating components in both feet (6 in total) [68], [69]. The most-reported one, Universal Controller (Engineering Acoustics, FL), offers a compact and portable power generator that reduces the number of lose wires and connectors. However, this power generator could run into issues if more than 4 vibrating components are needed close to full power. Populations such a diabetic subjects suffer from extreme loss of sensation at the feet (peripheral neuropathy) [21]–[23], which could require the operation of motors close to their maximum capacity. Adding another power generator is a solution to this issue; but this would significantly increase the cost of the vibratory insoles (+ $2,350.00). On the other hand, the power generator of the new vibratory mat can run 6 vibrating components at maximum capacity, regardless of the choice of motors (307-105, 310-003, 306-10H or 307-103). However, the power generator of the new vibratory mat does not offer a compact and portable design.

Noise Generator: The noise generator of the most-reported vibratory insoles [11]–[14], [17], [20], [22] (Universal Controller, TDK software and TAction software from Engineering Acoustics, FL) can adjust the vibrating components' power levels and create custom sequences. The option to create sequences has allowed SR studies to output white noise vibrations; however, it is yet to be reported that a study has

used other colors such as pink or brown. The suggestion to use non-white vibrations has been made various times [15], [68], [81], [82], since it is possible that SR through vibration does not follow the assumption “one size fits all” [82]. In other words, it is possible for some participants to benefit from white noise, while others from pink [82]. It is assumed that the Engineering Acoustics controller can output any sequence created on their software, since no experimental validation on their outputs’ colors is available. On the other hand, the new vibratory mat’s noise generator can generate white, pink, and brown vibrations with any of their motors, and the experimental color validation is described in Chapter 4 of this dissertation.

Material: The new vibratory mat follows all material recommendations [68], while the most-reported insoles ignore the cork layer. It is possible that this layer is not needed, since multiple SR studies have been successful without having a cork layer [11]–[14], [17], [20], [22].

Multiple Shoe Sizes: Three of the studies that used the most-reported vibratory insoles [12]–[14] allow the motion of vibrating components in the insole to accommodate for different shoe sizes. The other studies [11], [17], [20], [22] did not report a mechanism or protocol that accommodated different shoe sizes. It is assumed that multiple sizes of vibratory insoles were available. However, if this were to be the case, the cost to conduct their study significantly increases since the estimated cost to manufacture an extra pair of vibratory insoles is $1,274.50. The new vibratory mat offers 3 sizes (Short, Middle and Long) per set of eccentric rotating mass motors. The Short, Middle and Long configurations were chosen to accommodate the distribution of shoe sizes among female and male participants [70]. Since only three sizes per motors are available, locating exactly the first and fifth metatarsal for all participants is not always possible. It would be feasible if a shuffling mechanism would be available [12]–[14], or if there would be a size configuration for each shoe size. However, given that the location of the first and fifth metatarsals does not change dramatically between each increment of US shoe sizes [70], it is expected

for the dissipation of vibration in the mat to overcome this small error in location. Finally, having 56 eccentric rotating motors (4 sets of motors, 2 feet, 7 motors per foot) increases the possibility of plugging the wrong motor to the controller. That is why, a code that shows researchers the motors that need to be used is recommended (Example of such code is in the chapter's Appendix).

Multiple Motors: The most-reported vibratory insoles [11]–[14], [17], [20], [22] have one type of vibrating component (C-2 Tactors from Engineering Acoustics, FL), which makes a study 100% dependent on one option. If a participant's sensing threshold were to fall outside the vibrating component's magnitude and frequency ranges, it would require the study to dismiss the participant or change the protocol. Even though this is a design limitation, it must be pointed out that the C-2 Tactors (Engineering Acoustics, FL) frequency range (150 Hz to 320 Hz) falls on the frequencies that Pacinian Corpuscles operate (200 Hz to 300 Hz). In addition, the C-2 Tactors (Engineering Acoustics, FL) have been used on healthy subjects, diabetic and stroke populations [22], showing that the vibrating component's amplitude and frequency ranges have met the need of various populations. The new vibratory mat has four sets of eccentric rotating mass motors (307-105, 310-003, 306-10H and 307-103 from Precision Microdrives, UK), offering different amplitude and frequency ranges. The 310-003 motor does not overlap with the Pacinian Corpuscles' frequency range. However, the documented frequency range for all eccentric rotating motors is not the final answer to the question "Which frequencies does the motor cover?". Precision Microdrives tests their eccentric rotating mass motors using a Hanging Test set-up (Further explained in Chapter 4), which is not a test set-up that simulates the compressed environment of a working vibratory insole or mat. That is why further testing for all eccentric rotating mass motors is needed in a set-up that simulates the working environment of a vibratory mat, to decide if the motors target the Pacinian Corpuscles of the foot (i.e., Chapter 4).

Cost: The estimated cost for the most-reported vibratory insoles ($4,314.50) and the new vibratory mat ($1,062.83) are sums of money that the average customer could not afford, and health insurances would not want. As said by the Director of Health Programs at the Office of Management and Budget, “if we get a cure for Alzheimer’s priced at $100,000 a pop, we’re toast” [3]. If vibratory devices are to be in the market, their cost needs to be lowered to around $300. Already available vibratory medical devices (whole-body vibration equipment or vibratory insoles) cost between $200 and $400, suggesting that customers and/or health insurance providers feel comfortable paying around $300 to improve people’s PS through vibration. The largest expenses on the most-reported vibratory insoles [11]–[14], [17], [20], [22] are the vibrating components and controller from Engineering Acoustics, FL. Therefore, unless a bulk deal from Engineering Acoustics on their C-2 Tactors, Universal Controller and software programs is obtained, this vibratory device might be too expensive for customers today. Another possibility to reduce the cost of the most-reported vibratory insoles is to design a cheaper controller. The average customer does not need the TDK and TAction software programs, suggesting that Engineering Acoustics or another manufacturer can design a controller that outputs prescribed, tested, and approved sequences. On the other hand, the new vibratory mat’s cost can be lowered to around $300. The listed cost for the vibratory mat ($1,062.83) is for all sets of eccentric rotating mass motors and all foot sizes. Unless the buyer is a nursing home or hospital where the mat has more than one user, there is no need for a customer to buy the fully instrumented vibratory mat. In fact, the average customer for the vibratory mat would be matched with 6 of the most appropriate vibrating components (307-105, 310-003, 306-10H or 307-103 from Precision Microdrives, UK), since only 6 motors are needed per customer. This reduces the mat size to ¾ of the original area, bringing the Shore A50 Silicone cost to $23.22, as well as it reduces the motors’ cost to approximately $49.44 ($461.44 × 6 / 56). The controller’s, cork and soft layers’ cost would not change, bringing the new total to $323.24. The external housing is not added to this new total since it is only needed if all 56 vibrating components are used. Finally, cost reduction

strategies such as bulk deals of raw materials and a more optimal controller could reduce further the cost of the vibratory mat.

Robust Sensing Threshold: Three studies [12]–[14] that have used the most-reported vibratory insoles followed the Method of Levels [77] to determine the participants' sensing threshold. The Method of Levels is considered a robust protocol since it reduces biases on the participant; however, it requires a researcher to conduct it. The Method of Levels could be conducted without a researcher; however, it brings back the participant's bias. The new vibratory mat uses a modified 421 protocol [94], [95] that reduces biases on the participant and does not require a researcher in the room. Not requiring an additional person to find the participant's sensing threshold increases the device's potential to be used on people's everyday lives.

Robust Manufacturing: The studies that utilize the most-reported vibratory insoles [11]–[14], [17], [20], [22] list the materials of the device; however, they do not share/offer any details on the manufacturing process. New researchers interested in working with the most-reported vibratory insoles must reverse engineer the product or contact the original researchers for manufacturing insights. The later has happened once [20]. However, both these options are not efficient, slowing down innovation. That is why, the new vibratory mat's manufacturing steps, wiring diagram, and codes are available in the chapter's Appendix, which could be accessible by other investigators upon request.

Given the discussion on how both vibratory devices meet the design requirements, Table 6 was revised, and the new scores for the most-reported insoles and new mat are in Table 7. The overall score of both devices did not change dramatically (11.75 to 10.5 for the insoles, and 14.5 to 14.75 for the mat), still showing that the new vibratory mat has as much or higher potential of being used by the interned populations. However, it is worth noticing that few individual scores changed for each device. The most-reported vibratory insoles lost points due to their power generator limitations, and no experimental

validation on their outputs' colors. On the other hand, the new vibratory mat gained points due to its potential to be marketed around $300 for the average customer.

Table 7: Assessment on how the vibratory devices met the design requirements (Revised)

Design Requirement	Most-reported Vibratory Device (Insole)	New Vibratory Device (Mat)
Motor Selection	2/2	2/2
Motor Location	~~0.75/1~~ 1/1	~~0.75/1~~ 1/1
Power Generator	~~1/1~~ 0.5/1	~~1/1~~ 0.75/1
Noise Generator	~~3/3~~ 1/3	3/3
Material	~~1.5/2~~ 2/2	2/2
Multiple Shoe Sizes	~~1/1~~ 0.5/1	~~1/1~~ 0.75/1
Multiple Motors	1/1	0.75/1
Cost	0/1	~~0/1~~ 0.5/1
Robust Sensing Threshold	0.5/1	1/1
Robust Manufacturing	~~1/3~~ 2/3	3/3
Current Design Requirements	*~~8.25/9~~ 6.5/9*	*~~8.75/9~~ 8.75/9*
New Design Requirements	*~~3.5/7~~ 4/7*	*~~5.75/7~~ 6/7*
Current & New Design Requirements	*~~11.75/16~~ 10.5/16*	*~~14.5/16~~ 14.75/16*

Conclusion

The goal of this chapter to propose a new vibratory mat that introduces SR into people's balance was achieved. The new vibratory mat meets better the current and new design requirements when compared to the most-reported vibratory insoles [11]–[14], [17], [20], [22]. In addition, it is expected for the new vibratory mat to have a successful welcome by people seeking to improve PS due to its tentative market cost and its design. Given our working experience with elderly populations, we think it would be easier to ask them to stand on a wall plugged vibratory mat at different times of the day for 90 seconds or so, than to ask them to charge their vibratory insoles every night and swap them between shoes. This does not mean that vibratory insoles should no longer be studied. Instead, we are suggesting that it is worth exploring SR vibratory devices considering the intended user (young, old, or diseased populations). We believe that a vibratory mat is more ideal for fall risk and elderly populations [1], [2], [21]–[28], and vibratory insoles are more ideal for active populations (e.g., athletes) [96].

Chapter 4: Validation of Vibratory Mat's Output

Abstract

Background: Introducing stochastic resonance at the feet through mechanical vibration has shown to improve postural stability in people who are at risk of falling. Most of the previous studies that have used this technology have not quantified their vibration through universal units (e.g., newtons and hertz), or validated their outputs. This chapter quantified the output of the vibratory mat proposed in chapter 3, and experimentally validated its outputs.

Methods: Utilizing three static weights which cover the range of possible participants' weights and varying the power level from the lowest to the highest levels, the exerted forces and frequencies of the vibratory mat were recorded. It was determined whether or not the vibratory mat output the desired input colors of white, pink, and brown vibrations for the three weights tested across all power levels.

Findings: The vibratory mat's forces and frequencies were successfully quantified by quadratic regression models ($R^2 \geq 0.87$ and $R^2 \geq 0.70$ respectively). The vibratory mat was able to produce accurate white, pink, and brown output vibrations. More accurate and reliable vibrations were achieved when stronger motors in the mat were used.

Interpretation: This study successfully quantified the output of the proposed vibratory mat (Chapter 3), which will allow for easier comparisons of results with future studies. It was also shown that the proposed vibratory mat can output white, pink, and brown vibrations, which is a feature needed for studies that investigate the effect of vibration color on postural stability.

Background

Somatosensory feedback is an essential part of human postural stability (PS) [9], and its performance decays as people age [10]–[20], or due to neuromuscular diseases [21]–[28]. Loss of the somatosensory feedback is reflected when humans do not feel touch stimuli that was previously perceptible, leading to

a higher risk of falls. Vibratory devices that introduce stochastic resonance (SR) under the feet is a technology under development that has the potential to improve the performance of the somatosensory feedback in humans, increasing their PS, and reducing falls [30]–[46]. In theory, the goal of SR is to assist a system to cross a threshold level that it could not cross initially by adding noise (Figure 2) [16]. Given that sensation in humans is only perceived by the brain when neurons at the skin cross the sensation threshold, vibratory devices that introduce SR under the feet are ideal candidates to improve sensation, resulting in a lower fall risk and an improved quality of life.

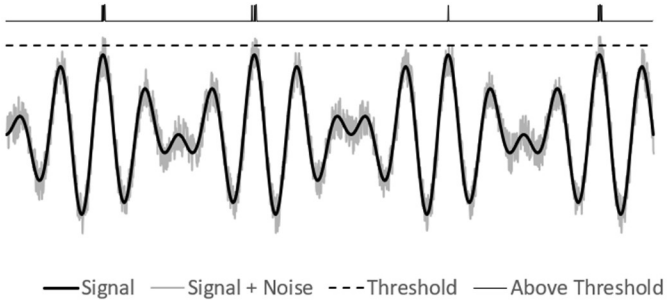

Figure 2: Stochastic resonance graphical description
Stochastic resonance (SR) is the addition of noise to a signal that is below a threshold level so that the signal with the noise's assistance can cross the threshold level that it could not cross before

SR studies that assess the effect of vibration at the feet on PS [10]–[28], [47]–[61], [63] define their outputs based on their magnitude and type. In terms of magnitude, 9 studies used universal units such as indentation depth and frequency [24], [25], [52], [54]–[59]; 21 studies used a percentage of the participant's sensing threshold [10]–[23], [26]–[28], [47]–[49], [51]; and 5 studies used a power level of their system [50], [53], [60], [61], [63]. Regarding the output's type, 19 studies [10]–[18], [20]–[23], [26], [28], [47]–[49], [51] used vibrations that followed a white noise pattern; 15 studies held their power constant yielding sinusoidal vibrations [24], [25], [27], [50], [52]–[61], [63]; and 1 study did not define the type of their vibration [19]. All the claims in these studies regarding the system's output type do not have experimental validation. Given this information, it is suggested that there are two unresolved

issues addressed by this chapter: 1) Most of the vibrating outputs' magnitudes do not use universal units, and 2) The vibrating output types have not been experimentally validated to determine if they are actually constant or white as assumed.

Using universal units to quantify the magnitude of any vibrating output allows comparison among multiple investigators and aligns with practices from neurophysiology studies on human sensing threshold. When SR studies do not use universal units [10]–[23], [26]–[28], [47]–[51], [55], [60], [61], [63], new investigators must replicate previous vibratory systems to compare results. This slows down innovation since new investigators might rather compare their results with previous discoveries, than to develop a new system, repeat the studies that previous investigators have done, and compare any new discoveries with previous ones. However, if SR studies used universal units, as a few have done (e.g., [24], [25], [52], [54]–[59]), it would be possible for new technologies to be proposed since new and old technologies would be measured with units that are not dependent on a system (distance, frequency, contact area, force, etc.). In addition, not using universal units creates a gap between SR studies on PS and neurophysiology studies on human sensing threshold [71]–[76], [78]. Both fields of study share a step on their protocol: measuring the participant's sensing threshold. If both fields of study were to use universal units (distance, frequency, contact area, force, etc.) to quantify the stimulus given to humans, it would be possible to relate both fields' results and discoveries.

Experimentally validating a vibrating output's type removes the assumption that, *whatever is input to the motor, is output by the motor*, as well as yields good practices knowing the sensitivity of human PS towards different noise types. A vibrating component (e.g., eccentric rotating mass motor) is a complex electro-mechanical system, that when embedded in an insole or mat becomes more complex due to the surrounding material, proximity to other vibrating components and the participant's weight compressing them. It is not denied that current technologies allow for the design of highly accurate

controllers for vibrating components. However, given that human PS is sensitive to different types of noises [81], it is justifiable to experimentally validate the vibrating output types using Detrended Fluctuation Analysis (DFA) to determine the vibration's color [79], [80]. DFA on any time series (e.g., vibration) yields a log-log plot that is fitted commonly with a linear regression. The linear regression's slope (α) states the color of the time series (White $\alpha = 0.5$, Pink $\alpha = 1.0$, and Brown $\alpha = 1.5$) [79], [80]. DFA has also been used to investigate postural sway by analyzing the Center of Pressure (COP) time series [17]. It suggested that vibratory devices should output multiple types of vibration (white, pink or brown) because there is evidence that one noise type may not be the most ideal noise to improve all human PS (i.e., one-size-fits-all does not work) [82]. Previous SR studies have only introduced white noise [10]–[18], [20]–[23], [26], [28], [47]–[49], [51] or sinusoidal [24], [25], [27], [50], [52]–[61], [63] vibrations to their participants, ignoring previous design recommendations [68], conclusions [15], [81], [82] and the importance of complexity and predictability in human PS [11], [81], [82]. This shows the necessity to experimentally validate vibrating outputs' types, which will open the possibilities to study SR with vibrations that have not been explored (pink and brown).

There are three common testing set-ups to study the magnitude and type of vibrating outputs, and they are listed below.

1. The Hanging Test (Figure 6 Left) which consists of a vibrating component and an accelerometer clamped to a hanging platform. The output vibrations are recorded using the accelerometer.
2. The Static Test (Figure 6 Center) which consists of a force plate recording the ground reaction forces and moments of a manufactured vibratory device that has a known and static weight on it (e.g., cinder blocks).
3. Finally, the Dynamic Test (Figure 6 Right) being the same as the Static Test with one exception. Instead of having a static weight on the vibratory device, a participant stands on it. The vibrating

output and human sway are separated by filtering techniques, such as low-pass, band-pass or high-pass filters [21], [27], [49], [55]. No experimental data will be acquired in this set-up by this chapter; however, Chapter 5 will acquire data through this test set-up and address their results.

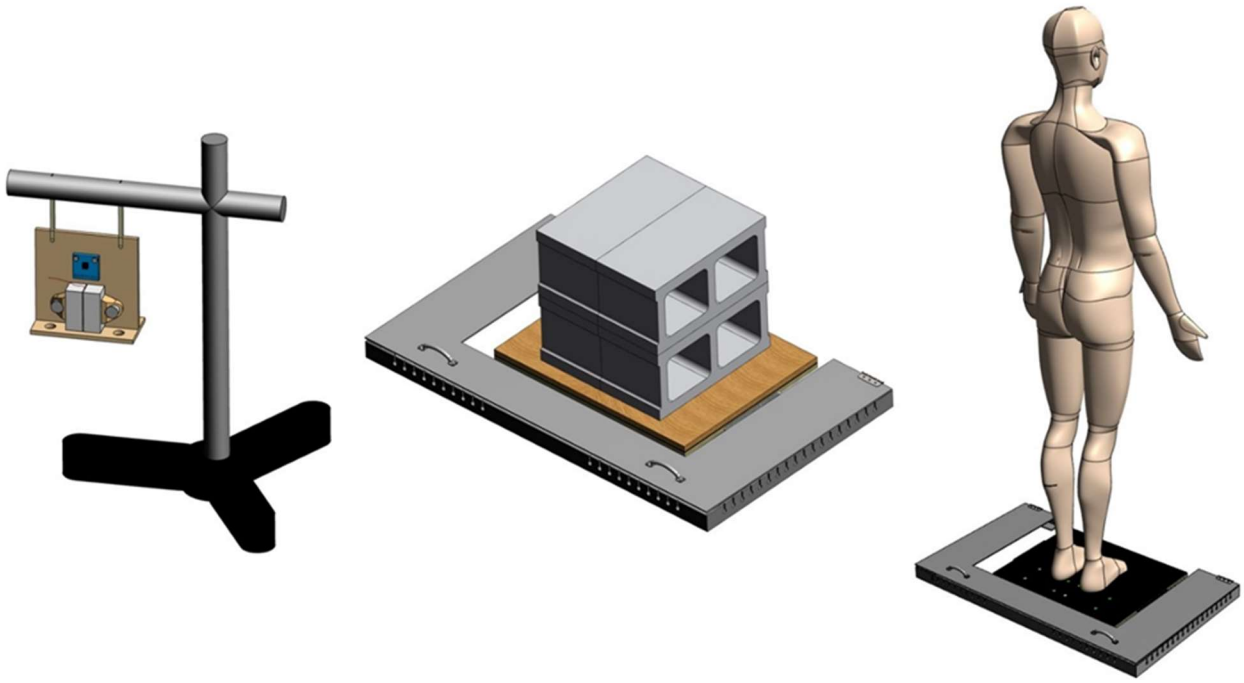

Figure 6: Testing set-ups to record vibrating outputs

(Left) Hanging Test: A vibrating component is clamped to a hanging platform that free to move, and vibrations are recorded by an accelerometer that is attached to the handing platform. (Middle) Static Test: Static weights are placed on a manufactured vibratory device, and the forces exerted by the embedded motors are recorded by a force plate located under the vibratory device. (Right) Dynamic Test: A human is placed on a manufactured vibratory device, and the forces exerted by the embedded motors are recorded by a force plate located under the vibratory device. Filtering techniques are needed to separate human sway from the forces exerted by the motors.

In Chapter 3, a new vibratory mat was designed and manufactured (Figure 6 Center and Right), while meeting all design requirements that the most-reported vibratory insoles have met [11]–[14], [17], [20], [22]. The vibratory mat offers four sets of eccentric rotating mass motors from Precision Microdrives, UK (model # for the weakest to strongest motor: 307-105, 310-003, 306-10H, and 307-103). The vibratory mat can also adjust the power levels of all motors from 0% to 100%, and it can operate the left and right foot separately (LF and RF) or both feet simultaneously (BF). Given this device, the purpose of this chapter is to experimentally validate the new vibratory mat by defining the forces and frequencies that

it exerts given a choice of motor, participant's weight, feet setting and power level, as well as by stating when an accurate vibrating output's type (white, pink, or brown) is obtained given a choice of motor, participant's weight and power level. The chapter's hypotheses are listed under.

- Hypothesis 1: Based on data obtained through **static tests**, it is hypothesized that the participant's weight does not have a significant effect on the forces and frequencies exerted by each motor for a given feet setting.
- Hypothesis 2: Based on data obtained through **static tests**, it is hypothesized that there are repeated forces and frequencies across multiple motors for a given feet setting, as well as across feet settings for a given motor.
- Hypothesis 3: Based on data obtained through **hanging and static tests**, it is hypothesized that more accurate outputs' colors are found as the motor size and power level increase.
- Hypothesis 4: It is hypothesized that there is a relation between the vibrating outputs' colors found through **hanging and static tests**, suggesting that it is possible for future researchers to study motors before they are embedded in a device.

Methods

All data manipulation and statistics were performed in MATLAB R2020b (MathWorks, MA, USA). For all statistical analysis, the level of significance was $p < 0.05$.

Forces and Frequencies Exerted by the Vibratory Mat (Hypotheses 1 and 2)

The ground reaction forces exerted by the vibratory mat were recorded by an OR6 force plate (AMTI, Watertown, MA, USA) from the lowest power (40% for 307-105, 30% for 310-003, and 20% for 306-10H and 307-103) to the highest one when different static loads that represent various participants' weights (34 kg, 75 kg, and 115 kg) were placed on the mat. This was done for all motor choices (307-105, 310-003, 306-10H or 307-103) and feet settings (LF, RF, or BF). The force plate kinetic data were recorded for

10 seconds at 2500 Hz using a 16-bit A/D CED Power mkII and Spike2 (Cambridge Electronic Design, UK), while the vibratory mat's power level was held constant.

To determine the exerted force by the mat given a motor choice, power level, feet setting and simulated participant's weight (Figure 9), the resultant force was calculated using the x, y, z directions, which were previously filtered by a band-pass whose cut-off frequencies were 20 Hz and 400 Hz [21], [27], [49], [55]. The resultant force was then rectified consecutively over time windows equal to 0.1 seconds, frequency (10 Hz) at which new input voltages were given to the motors. The motors' voltage was constant in this part of the study; however, a new constant input voltage was given to the motors every 0.1 seconds (10 Hz). Rectification of vibratory data using methods established for electromyography muscle data [83] was done due to the similarities between both time series, and inconclusive results obtained on unrectified vibration data (i.e., averages and slopes equal to 0 due to sinusoidal behaviors). From the filtered and rectified resultant force, the middle 50% of the time series was extracted, and an average and standard deviation were calculated to quantify the force exerted by the motor. The middle part of the data was used to avoid any transient behavior at the start and at the end of the vibration. The data manipulation explained in this paragraph is further detailed in the Appendix of this chapter.

To determine the exerted frequencies by the mat for a given motor choice, power level, feet setting (LF, BF, or RF) and simulated participant's weight (Figure 10), a power spectrum density analysis was done on each of the ground reaction forces (x, y, and z directions). From each power spectrum density plot (dB/Hz vs. Hz for x, y, and z directions), the frequency at which the highest power occurred was recorded. Among these three recorded frequencies, the one with the highest power spectral density was selected as the exerted frequency by the mat. In addition, the frequencies at which the power spectral density behavior started and ended were recorded. The starting and ending frequencies were included to show the frequency ranges that the vibratory mat covered. The starting and ending

frequencies were not used in any statistical analysis. The data manipulation explained in this paragraph is further detailed in the Appendix of this chapter.

Linear and quadratic regression models in terms of the simulated weight and power level were fitted for the exerted forces and frequencies given a feet setting and motor (Table 8 and Table 9). The linear and quadratic regression models were respectively $y = A_0 + A_1x_1 + A_2x_2$ and $y = A_0 + A_1x_1 + A_2x_2 + A_3x_1^2 + A_4x_1x_2$ where A_n were coefficients, x_1 was power level and x_2 was simulated weight. A quadratic regression model was selected over a linear one if the Adjusted R^2 (R^2_{adj}) and Root Mean Squared Error (RMSE) of the quadratic model were better. A comparison between the linear and quadratic regression models is available in the Appendix of this chapter. On the selected model, the 95% prediction bounds were determined at the tested simulated weights and power levels (Figure 11 to Figure 14). The type of prediction bounds was functional and simultaneous, meaning that the used equation was $y \pm f\sqrt{xSx^T}$ where S is the covariance matrix of the coefficients, and f depends on the coefficients' confidence level and is calculated from the F cumulative distribution function. Finally, using the 95% prediction bounds, the following comparisons ($p < 0.05$) were done for the exerted forces and frequencies at each power level. A detailed description of the comparisons is included in the Appendix of this chapter.

- Within each motor and feet setting (subplots of Figure 11 or Figure 12), it was assessed if the regression's output (force or frequency) differed across simulated weights for a given power level.
- Within each motor (columns of Figure 11 or Figure 12), it was assessed if the regression's output differed across feet settings for a given power level. This was done for each simulated weight.
- Within each feet setting (rows of Figure 11 or Figure 12), it was assessed if the regression's output differed across motors for a given power level. This was done for each simulated weight.

Vibratory Outputs' Colors - Hanging Test (Hypothesis 3)

Before studying the type of the vibratory outputs, input signals had to be chosen for each motor and desired output type. To select the input for each motor (307-105, 310-003, 306-10H, 307-103) and output type (White, Pink and Brown), 10 "perfect" white, pink, and brown input signals (30 in total) were developed in MATLAB, and tested on each motor using the Hanging Test. All input signals were 90-second long and had a frequency of 10 Hz. A "perfect" input signal in MATLAB was one whose DFA (t_{min} = 0.5 s and t_{max} = 15 s, or n_{min} = 5, n_{max} = N/6, N = 900) slope (α) was within ±0.02 from the ideal slope (α_{white} = 0.5, α_{pink} = 1.0, and α_{brown} = 1.5), and whose DFA R^2 was larger than or equal to 0.98 [79], [80]. The accelerations created by the motor on the hanging platform were recorded for 105 seconds in all directions (x, y, and z) by an ADXL335 Accelerometer (Adafruit Industries, NY) at 2500 Hz using a 16-bit A/D CED Power mkII and Spike2. The accelerometer's data received the data manipulation used to determine the force exerted by the vibratory mat, except for one final step. Instead of calculating the exerted force on the middle, filtered and rectified resultant time series, a DFA (t_{min} = 0.5 sec, t_{max} = 15 sec) was performed on the filtered and rectified resultant acceleration when the motor was ON [79], [80]. The input signals on each motor that yielded the closest DFA results to the ideal ones were selected, creating 12 inputs signals in total (4 motors and 3 types, Figure 15). In some motors and vibratory types, a "perfect" input did not yield positive results, requiring the use of "imperfect" inputs. For example, a "perfect" white input yielded DFA α values around 0.57 for the motors 306-10H and 307-103. Therefore, an "imperfect" white input (DFA α = 0.441) was used in motors 306-10H and 307-103 to obtain DFA α values closer to white (DFA α around 0.53).

Using the selected inputs for each motor and type (Figure 15), all motors were tested from their lowest (40% for 307-105, 30% for 310-003, and 20% for 306-10H and 307-103) to the maximum (100%) power levels in a Hanging Test set-up. The accelerometer's data was acquired and manipulated as described in the last paragraph, resulting in DFA α slopes as a function of power level for each motor (Figure 16).

Signal-to-Noise (SN) ratios were included at each power level to graphically represent the reliability of the DFA results. The SN ratios were equal to the RMS of the resultant, filtered and not rectified acceleration while the motor was ON (~90 seconds), divided by the RMS of the resultant, filtered and not rectified acceleration while the motor was OFF (~15 seconds).

Vibratory Outputs' Colors - Static Test (Hypothesis 3)

Using the selected inputs for each motor and type (Figure 15), all motors were tested under the BF setting from their lowest to maximum power levels in a Static Test set-up with simulated weights equivalent to 34 kg, 75 kg, and 115 kg. Except for two steps, the force plate's data was acquired and manipulated as it was done when the exerted force by the mat was calculated. First, instead of acquiring 10 seconds of data, 95 seconds of vibration were recorded. In addition, instead of calculating the exerted force on the middle, filtered and rectified resultant time series, a DFA (t_{min} = 0.5 sec, t_{max} = 15 sec) was performed on the filtered and rectified resultant force when the mat was ON [79], [80]. This yielded DFA α slopes as a function of power level and participant's weight for each motor (Figure 17). SN ratios were included at each power level to graphically represent the reliability of the DFA results. The SN calculation was equivalent to the one described in the last paragraph; however, the OFF time was less (i.e., ~5 seconds).

Vibratory Outputs' Colors - Static vs. Hanging Test (Hypothesis 4)

Finally, the DFA results from the static tests were plotted against the DFA results from the hanging tests to investigate any possible relations between both test set ups (Figure 18). Regression analysis from these comparisons were not included in this chapter, due to the weak relations that were obtained. Instead, comments and observations on the plots will be part of the discussion.

Results

Forces and Frequencies Exerted by the Vibratory Mat (Hypotheses 1 and 2)

The forces exerted by the vibratory mat given a motor, feet setting, power level and simulated participant's weight, are shown in Figure 9. The rows indicate the feet setting that was used (LF: Left foot, BF: Both feet, and RF: Right foot), while the columns represent the motor choice (weakest model # to strongest: 307-105, 310-003, 306-10H and 307-103). The markers and shaded areas in the plots represent the average and standard deviation of the exerted force, respectively. Motor 307-105 showed an unusual behavior under the RF setting, since its exerted force started decaying around 60% for all simulated weights. Also, motor 307-105 did not yield any vibration at 40% for any of the weights under the RF setting, and for weights equal to 75 kg and 115 kg under the LF and BF settings. Finally, as the motor strength increased, the exerted force's variability increased too.

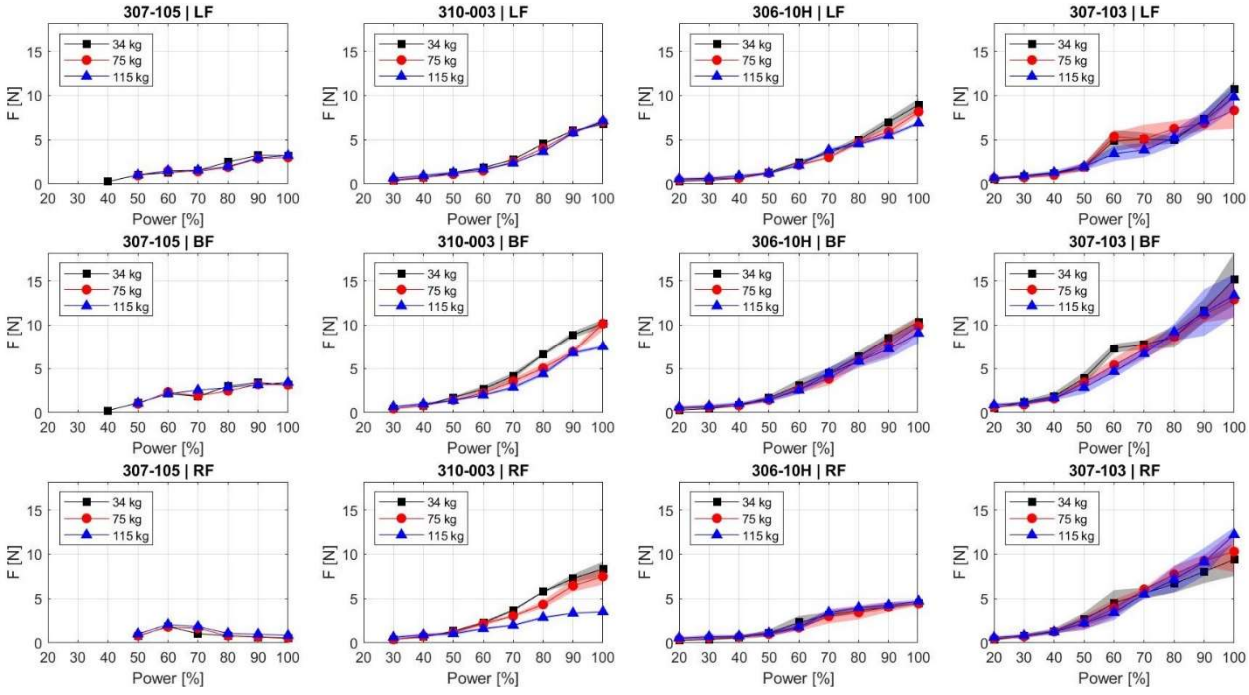

Figure 9: Forces exerted by the mat

Rows represent the feet setting (LF, BF or RF), while columns represent the motor (307-105, 310-003, 306-10H and 307-103). In each subplot, exerted force as a function of power level are displayed under three simulated participants' weights (34 kg, 75 kg, and 11 kg). Black shades, lines and squares represent 34 kg. Red shades, lines and circles represent 75 kg. Blue shades, lines and triangles represent 115 kg. The center line indicates the average exerted force at a power level, while the shaded area represents its variation (standard deviation).

The frequencies exerted by the vibratory mat given a motor, feet setting, power level and simulated participant's weight, are shown in Figure 10. As indicated in Figure 9, rows and columns represent respectively the feet setting and motor used in the mat. The markers in the plot represent the exerted frequency, while the shaded area represents the range of frequencies covered by the mat. The lowest frequency covered by the mat remains mostly constant for motors 307-105, 310-003 and 307-103, regardless of the weight. The highest frequency covered by the mat increases as the power rises for all motors, regardless of the weights. Finally, the exerted frequency is not always at the ends of the ranges, indicating that even though a motor could cover a wide range of frequencies, there will be a frequency inside that range that has a stronger power than the lowest or highest frequencies.

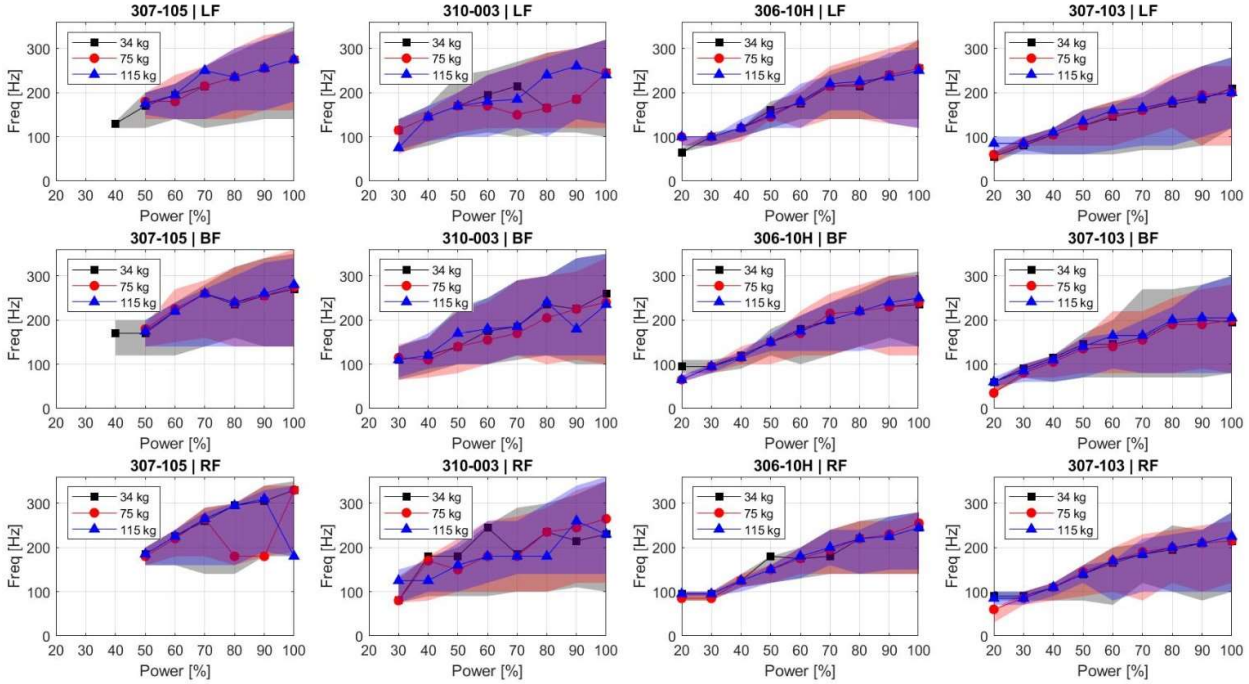

Figure 10: Frequencies exerted by the mat

Rows represent the feet setting (LF, BF or RF), while columns represent the motor (307-105, 310-003, 306-10H and 307-103). In each subplot, exerted frequency as a function of power level are displayed under three simulated participants' weights (34 kg, 75 kg, and 115 kg). Black shades, lines and squares represent 34 kg. Red shades, lines and circles represent 75 kg. Blue shades, lines and triangles represent 115 kg. The center line indicates the exerted frequency at a power level, while the shaded area represents its range.

The coefficients of the regression models for the exerted force (Figure 9) as a function of weight and power, given a feet setting and motor are described by Table 8. A quadratic regression model was

superior in all cases when compared to the linear model. The unusual behavior of 307-105 RF was reflected by the low R^2_{adj} when compared to the rest. However, high R^2_{adj} values were found for all other motors and feet settings reflecting accurate fits (lowest R^2_{adj} was 0.8793). The RMSE increased as the strength of the motor strength increased. Some coefficients were not statistically significant at a 95% confidence, and they are displayed in red (Table 8). Based on the statistical significance of the term A_2, the simulated weight does not have a significant effect on the exerted forces by 307-103 LF, 307-105 BF, 307-103 BF, and 306-10H RF. Power level had a significant impact on the exerted forces since the A_1 and/or A_3 coefficients were always significant. The coefficients A_1 and A_3 were associated with the linear and quadratic values of power.

Table 8: Coefficients and fitting performance of regression models for exerted force

		307-105	310-003	306-10H	307-103
LF	A_0	-1.06E+00 (-1.32E+00 … -8.05E-01)	1.35E+00 (1.17E+00 … 1.52E+00)	-1.34E-01 (-2.88E-01 … 1.86E-02)	-1.05E-01 (-5.62E-01 … 3.52E-01)
	A_1	2.66E-02 (1.94E-02 … 3.39E-02)	-6.95E-02 (-7.44E-02 … -6.47E-02)	-2.91E-02 (-3.34E-02 … -2.48E-02)	7.71E-03 (-5.24E-03 … 2.07E-02)
	A_2	7.65E-03 (5.72E-03 … 9.57E-03)	3.02E-03 (1.57E-03 … 4.48E-03)	1.46E-02 (1.32E-02 … 1.61E-02)	2.79E-03 (-1.59E-03 … 7.17E-03)
	A_3	1.93E-04 (1.42E-04 … 2.45E-04)	1.31E-03 (1.28E-03 … 1.35E-03)	1.24E-03 (1.21E-03 … 1.27E-03)	9.30E-04 (8.32E-04 … 1.03E-03)
	A_4	-1.13E-04 (-1.38E-04 … -8.74E-05)	-6.67E-05 (-8.78E-05 … -4.56E-05)	-3.22E-04 (-3.44E-04 … -3.00E-04)	-1.18E-04 (-1.85E-04 … -5.12E-05)
	R^2_{adj}	0.9307	0.9849	0.9811	0.8793
	RMSE	0.2363	0.2819	0.3595	1.0772
BF	A_0	-4.37E+00 (-4.68E+00 … -4.05E+00)	-1.24E-01 (-3.92E-01 … 1.43E-01)	1.25E-01 (-1.38E-01 … 3.88E-01)	-6.24E-01 (-1.17E+00 … -8.02E-02)
	A_1	1.41E-01 (1.32E-01 … 1.50E-01)	-4.17E-02 (-4.91E-02 … -3.42E-02)	-3.85E-02 (-4.60E-02 … -3.10E-02)	3.29E-02 (1.75E-02 … 4.83E-02)
	A_2	2.21E-03 (-1.67E-04 … 4.59E-03)	2.25E-02 (2.03E-02 … 2.47E-02)	1.08E-02 (8.31E-03 … 1.33E-02)	1.03E-03 (-4.15E-03 … 6.20E-03)
	A_3	-6.50E-04 (-7.14E-04 … -5.87E-04)	1.62E-03 (1.57E-03 … 1.68E-03)	1.47E-03 (1.42E-03 … 1.53E-03)	1.24E-03 (1.12E-03 … 1.36E-03)
	A_4	-1.37E-05 (-4.51E-05 … 1.77E-05)	-5.58E-04 (-5.90E-04 … -5.25E-04)	-2.53E-04 (-2.92E-04 … -2.14E-04)	-1.61E-04 (-2.40E-04 … -8.12E-05)
	R^2_{adj}	0.8973	0.9805	0.9638	0.9239
	RMSE	0.2932	0.4351	0.6228	1.2792
RF	A_0	-2.68E+00 (-3.23E+00 … -2.14E+00)	-2.98E+00 (-3.32E+00 … -2.65E+00)	-6.22E-01 (-8.32E-01 … -4.12E-01)	6.36E-01 (1.86E-01 … 1.09E+00)
	A_1	1.13E-01 (9.91E-02 … 1.27E-01)	5.60E-02 (4.67E-02 … 6.53E-02)	2.62E-02 (2.02E-02 … 3.21E-02)	-1.24E-02 (-2.51E-02 … 3.69E-04)
	A_2	4.29E-03 (1.21E-03 … 7.37E-03)	4.08E-02 (3.80E-02 … 4.36E-02)	1.62E-03 (-4.01E-04 … 3.64E-03)	-1.40E-02 (-1.83E-02 … -9.72E-03)
	A_3	-8.53E-04 (-9.43E-04 … -7.62E-04)	8.23E-04 (7.56E-04 … 8.90E-04)	2.72E-04 (2.27E-04 … 3.17E-04)	1.03E-03 (9.29E-04 … 1.12E-03)
	A_4	3.50E-06 (-3.66E-05 … 4.36E-05)	-9.56E-04 (-9.97E-04 … -9.16E-04)	2.18E-06 (-2.87E-05 … 3.31E-05)	3.04E-04 (2.38E-04 … 3.70E-04)
	R^2_{adj}	0.5200	0.9499	0.9052	0.9167
	RMSE	0.3459	0.5421	0.4960	1.0575

Coefficients are based on $y = A_0 + A_1x_1 + A_2x_2 + A_3x_1^2 + A_4x_1x_2$, where x_1 is power level and x_2 is simulated weight. If A_3 and A_4 have values, then the best model was quadratic, otherwise the best model was linear. Coefficients in red were not statistically significant, and the values in parenthesis represent the 95% confidence interval.

The coefficients of regression models for the exerted frequencies (Figure 10) as a function of weight and power, given a feet setting and motor are described by Table 9. A quadratic regression model was superior in all cases when compared to the linear model. The fitting performance values of R^2_{adj} and RMSE improved as the motor strength increased. In general, all fittings were accurate since the R^2_{adj}

values were mostly above 0.7 for all motors and feet settings. When compared to Table 8, there were more coefficients that were not statistically significant (red text in Table 9). The simulated weight (A_2 coefficient) only had a significant effect on the exerted frequency by 307-103 LF and 306-10H BF. In addition, the power level had a significant impact on the exerted frequencies by most of the motors since the A_1 and/or A_3 coefficients were significant. Only the exerted frequencies of 310-003 LF and 307-105 RF did not have a significant effect from the power level. However, both instances (310-003 LF and 307-105 RF) did not have a significant effect from any of the regression coefficients.

Table 9: Coefficients and fitting performance of regression models for exerted frequency

		307-105	310-003	306-10H	307-103
LF	A_0	-1.49E+01 (-9.60E+01 … 6.62E+01)	9.39E+01 (-2.34E+01 … 2.11E+02)	4.07E+00 (-2.99E+01 … 3.80E+01)	-1.00E+01 (-2.60E+01 … 6.00E+00)
	A_1	4.03E+00 (1.73E+00 … 6.34E+00)	1.78E+00 (-1.46E+00 … 5.02E+00)	3.25E+00 (2.29E+00 … 4.21E+00)	2.99E+00 (2.54E+00 … 3.44E+00)
	A_2	3.43E-01 (-2.68E-01 … 9.54E-01)	-6.98E-01 (-1.67E+00 … 2.74E-01)	2.21E-01 (-1.03E-01 … 5.46E-01)	2.99E-01 (1.46E-01 … 4.52E-01)
	A_3	-1.16E-02 (-2.79E-02 … 4.74E-03)	-8.04E-03 (-3.14E-02 … 1.53E-02)	-6.64E-03 (-1.39E-02 … 6.09E-04)	-8.33E-03 (-1.17E-02 … -4.92E-03)
	A_4	-3.35E-03 (-1.14E-02 … 4.71E-03)	1.21E-02 (-1.96E-03 … 2.62E-02)	-2.89E-03 (-7.85E-03 … 2.08E-03)	-3.39E-03 (-5.73E-03 … -1.05E-03)
	R^2_{adj}	0.946	0.703	0.968	0.988
	RMSE	9.711	25.017	10.622	5.003
BF	A_0	-2.19E+01 (-1.51E+02 … 1.07E+02)	6.17E+00 (-7.27E+01 … 8.51E+01)	2.17E+01 (-3.71E+00 … 4.72E+01)	-1.07E+01 (-4.08E+01 … 1.95E+01)
	A_1	5.85E+00 (2.17E+00 … 9.52E+00)	2.92E+00 (7.35E-01 … 5.10E+00)	3.28E+00 (2.56E+00 … 4.00E+00)	3.68E+00 (2.83E+00 … 4.53E+00)
	A_2	-2.92E-01 (-1.27E+00 … 6.82E-01)	4.11E-01 (-2.43E-01 … 1.07E+00)	-2.93E-01 (-5.36E-01 … -4.98E-02)	-8.42E-02 (-3.72E-01 … 2.04E-01)
	A_3	-3.05E-02 (-5.65E-02 … -4.43E-03)	-3.37E-03 (-1.91E-02 … 1.23E-02)	-1.15E-02 (-1.69E-02 … -6.08E-03)	-1.63E-02 (-2.28E-02 … -9.91E-03)
	A_4	4.28E-03 (-8.56E-03 … 1.71E-02)	-7.05E-03 (-1.65E-02 … 2.44E-03)	4.54E-03 (8.14E-04 … 8.26E-03)	2.07E-03 (-2.34E-03 … 6.48E-03)
	R^2_{adj}	0.819	0.880	0.982	0.966
	RMSE	15.481	16.832	7.961	9.430
RF	A_0	-2.48E+02 (-8.42E+02 … 3.46E+02)	2.19E+01 (-1.04E+02 … 1.48E+02)	3.35E+01 (-3.39E-01 … 6.73E+01)	1.44E+01 (-1.34E+01 … 4.21E+01)
	A_1	1.04E+01 (-4.83E+00 … 2.57E+01)	4.05E+00 (5.56E-01 … 7.55E+00)	2.69E+00 (1.73E+00 … 3.65E+00)	3.13E+00 (2.34E+00 … 3.91E+00)
	A_2	1.67E+00 (-1.69E+00 … 5.03E+00)	-3.07E-01 (-1.36E+00 … 7.40E-01)	-7.03E-02 (-3.93E-01 … 2.53E-01)	-9.25E-02 (-3.58E-01 … 1.73E-01)
	A_3	-4.49E-02 (-1.44E-01 … 5.39E-02)	-1.80E-02 (-4.31E-02 … 7.18E-03)	-5.66E-03 (-1.29E-02 … 1.55E-03)	-1.12E-02 (-1.71E-02 … -5.24E-03)
	A_4	-2.61E-02 (-6.98E-02 … 1.75E-02)	2.12E-03 (-1.31E-02 … 1.73E-02)	1.05E-03 (-3.89E-03 … 6.00E-03)	1.77E-03 (-2.30E-03 … 5.83E-03)
	R^2_{adj}	0.260	0.724	0.964	0.972
	RMSE	48.407	26.960	10.579	8.689

Coefficients are based on $y = A_0 + A_1x_1 + A_2x_2 + A_3x_1^2 + A_4x_1x_2$, where x_1 is power level and x_2 is simulated weight. If A_3 and A_4 have values, then the best model was quadratic, otherwise the best model was linear. Coefficients in red were not statistically significant, and the values in parenthesis represent the 95% confidence interval of each coefficient.

From the quadratic regression models described in Table 8, the 95% prediction bounds are displayed in Figure 11 for the exerted forces as a function of power and simulated weight. The markers indicate the experimental average exerted forces. Using the prediction bounds within each subplot (motor and feet setting), it was found that the simulated weight did not statistically influence the motor 307-105's

exerted force when the power was between 40% and 80% for all feet settings. In motor 310-003, the simulated weight did not statistically influence the exerted force under the LF setting for powers between 40% and 70%. In motor 306-10H, the simulated weight did not statistically affect the exerted force under the LF and BF settings for powers between 20% and 50%, and it did not statistically influence the exerted force at any power under the RF setting. In motor 307-103, the simulated weight did not statistically affect the exerted force under the BF and RF settings for powers between 20% and 60%, and it did not statistically influence the exerted force at any power under the LF setting. Using the prediction bounds within each motor, it was found that the motor 307-105's exerted force did not statistically differ between the LF and RF settings when the simulated weight was 34 kg, and the power was between 40% and 60%. For motor 310-003, the exerted force under the LF and RF settings did not statistically differ for all weights when the power was between 30% and 50%. For motor 306-10H, the exerted force under the LF and RF settings did not statistically differ for all weights when the power was between 20% and 50%. For motor 307-103, the exerted force under the LF and RF settings did not statistically differ for weights equal to 75 kg and 115 kg when the power was between 20% and 40%. However, the motor 307-103's exerted force did not statistically differ between the LF and RF settings for all power levels when the simulated weight was 34 kg. Finally, using the prediction bounds within each feet setting, it was found that under the LF and RF settings motors 306-10H and 307-103 did not statistically differ at 20% for all weights, and that motors 310-003, 306-10H and 307-103 did not statistically differ at 30% for all weights. Under the BF setting, motors 306-10H and 307-103 did not statistically differ at 20% for all weights. In addition, under the BF setting, motors 310-003 and 306-10H did not statistically differ at 30% for weights equal to 75 kg and 115 kg, and they did not statistically differ for all power levels when the weight was 34 kg.

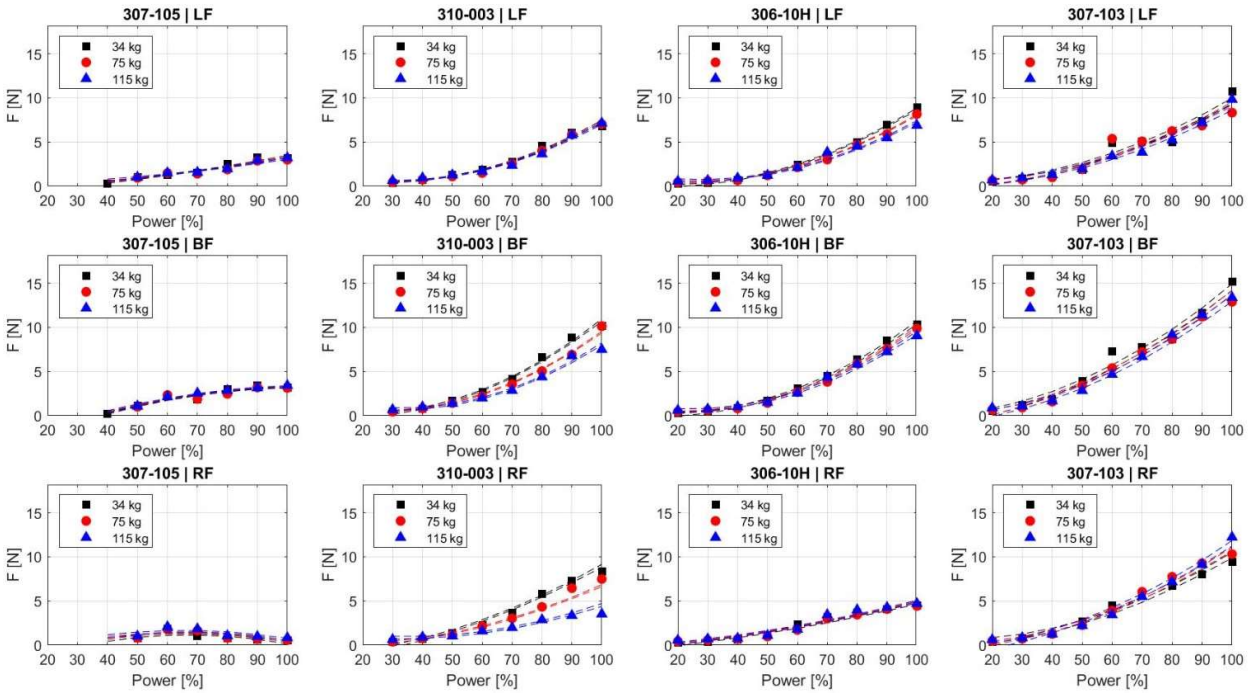

Figure 11: Forces exerted by the mat - Quadratic prediction intervals

Rows represent the feet setting (LF, BF or RF), while columns represent the motor (307-105, 310-003, 306-10H and 307-103). In each subplot, the prediction intervals (dashed lines) of the exerted forces calculated by a quadratic regression model are displayed under three simulated participants' weights (34 kg, 75 kg, and 11 kg), alongside the experimental data (markers). Black lines and squares represent 34 kg. Red lines and circles represent 75 kg. Blue lines and triangles represent 115 kg.

From the quadratic regression models described in Table 9, the 95% prediction bounds are displayed in Figure 12 for the exerted frequencies as a function of power and simulated weight. The markers indicate the experimental exerted frequencies. Using the prediction bounds within each subplot (motor and feet setting), it was found that the simulated weight did not statistically influence any motor's exerted frequencies for all power levels. Using the prediction bounds within each motor, it was found that the motor's exerted frequencies did not statistically differ between feet settings for all power levels and weights. Finally, using the prediction bounds within each feet setting, it was found that under the LF setting the exerted frequency did not statistically differ between motors 307-105, 310-003 and 306-10H, and between motors 310-003 and 307-103 for all power levels and weights. Under the BF setting, the exerted frequencies of motors 307-105 and 310-003, motors 310-003 and 307-103 and motors 307-105 and 306-10H did not statistically differ for all power levels and weights. Under the RF setting, there were

not statistical significances in terms of exerted frequencies across all motors for all power levels and weights.

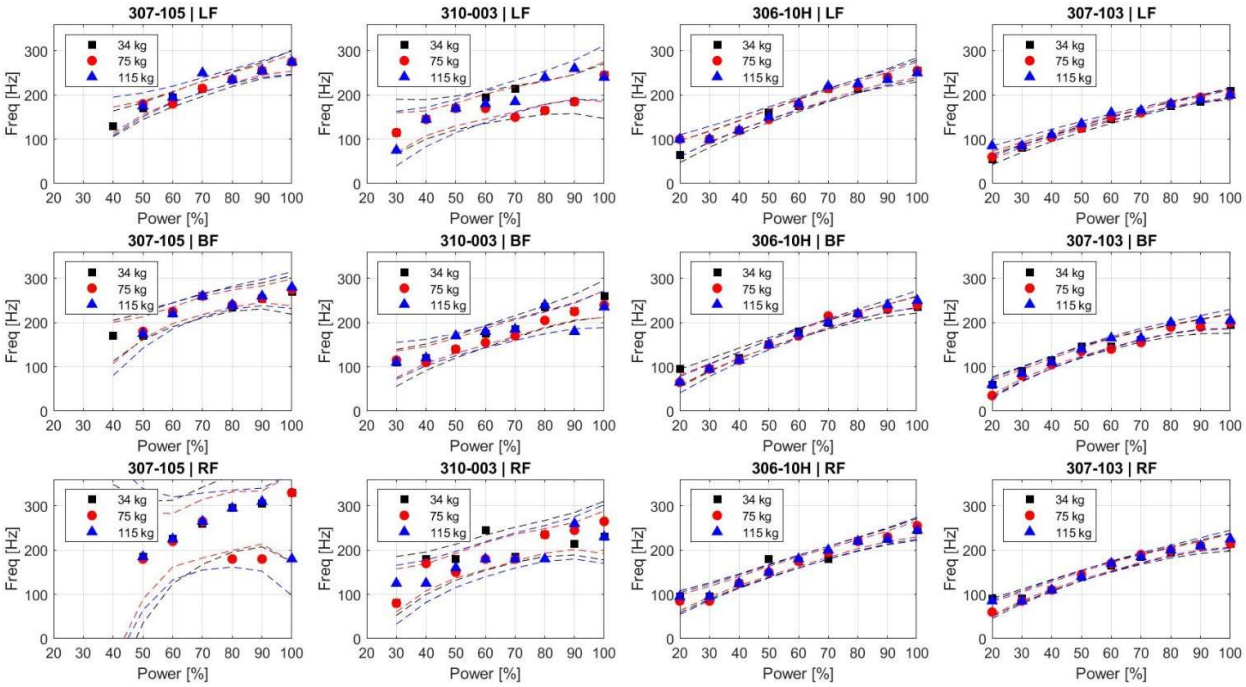

Figure 12: Frequencies exerted by the mat - Quadratic prediction intervals

Rows represent the feet setting (LF, BF or RF), while columns represent the motor (307-105, 310-003, 306-10H and 307-103). In each subplot, the prediction intervals (dashed lines) of the exerted frequencies calculated by a quadratic regression model are displayed under three simulated participants' weights (34 kg, 75 kg, and 11 kg), alongside the experimental data (markers). Black lines and squares represent 34 kg. Red lines and circles represent 75 kg. Blue lines and triangles represent 115 kg. Data for 307-105 RF at 40% is not displayed since it was not possible to visualize a signal at 40%.

Figure 13 and Figure 14 show the exerted forces' prediction bounds plotted against the exerted frequencies' prediction bounds for all simulated weights. Figure 13 shows how various feet settings compare with each other within a motor. From Figure 13, motor 310-003 has a larger variability in terms of frequency when compared to other motors, motor 307-103 shows more uniformity between the LF and RF settings, and all motors show that the BF setting exerts larger forces when compared to the LF and RF settings. Figure 14 shows how various motors compare with each other within a feet setting. From Figure 14, motor 307-103 shows to exert a lower frequency content, but larger forces when compared to the other motors. In addition, motors 310-003 and 306-10H highly overlap with each other

under the LF and BF settings, and not under the RF setting (i.e., 310-003 exerts larger forces when compared to 306-10H).

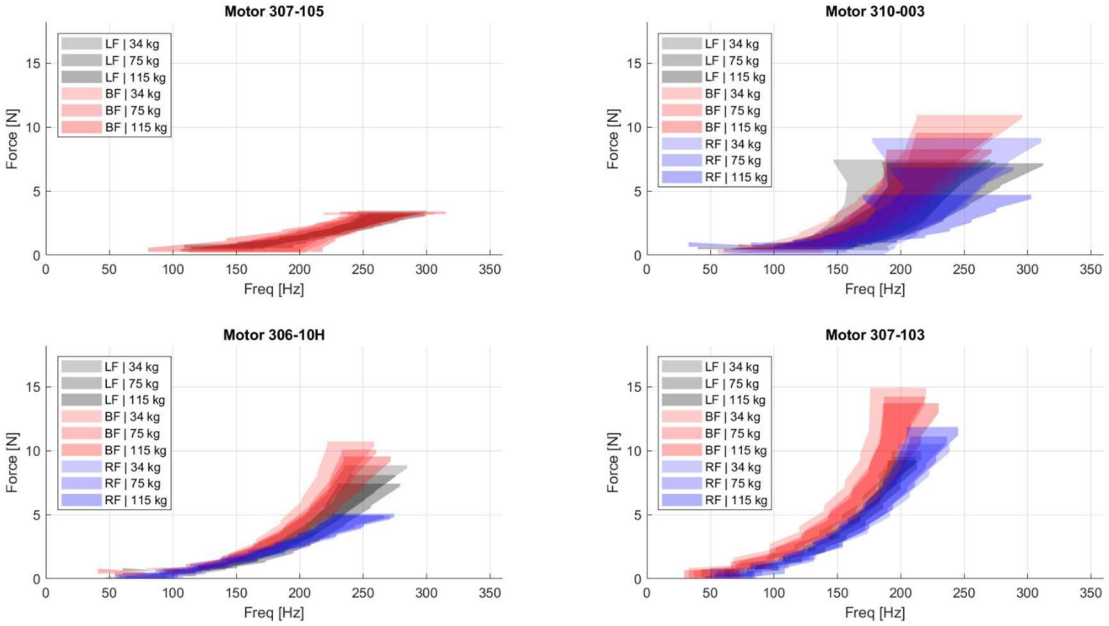

Figure 13: Forces vs. frequency by the mat across motors - Quadratic prediction intervals

Darkness of the shaded area is proportional to the simulated weight (34 kg, 75 kg, and 115 kg). Right foot (RF) data was omitted for the motor 307-105 (top-left plot) due to its unexpected and abnormal exerted force as a function of power. Black, red, and blue colors respectively represent the feet settings LF, BF, and RF. The shape of each plot is defined by the force and frequency prediction intervals obtained from the regression analysis.

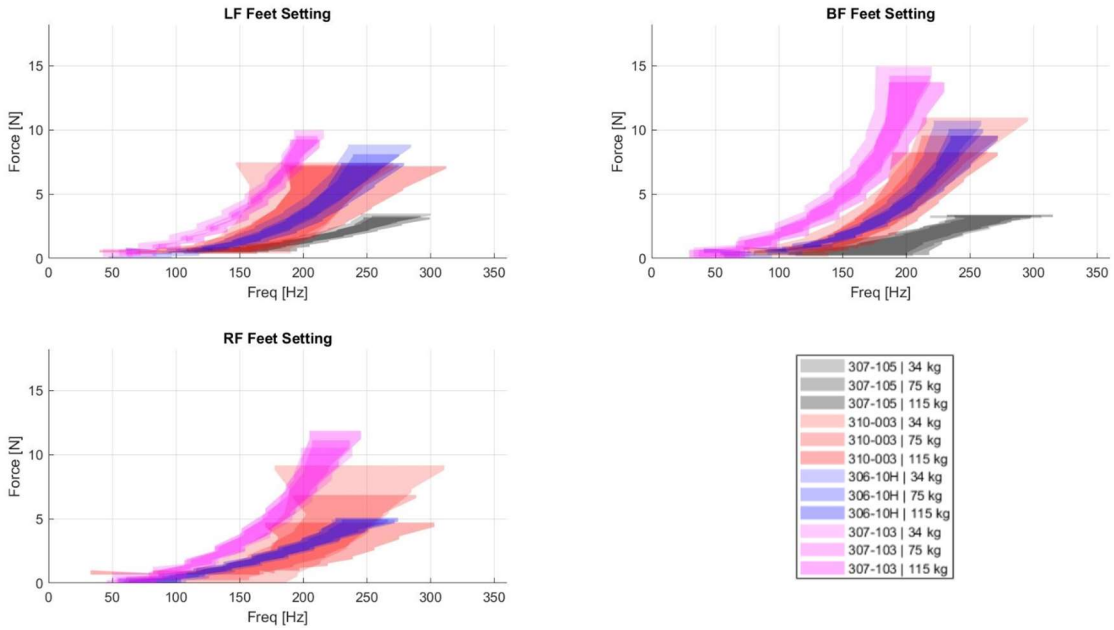

Figure 14: Forces vs. frequency by the mat across feet settings - Quadratic prediction intervals

Darkness of the shaded area is proportional to the simulated weight (34 kg, 75 kg, and 115 kg). Right foot (RF) data was omitted for the motor 307-105 (bottom-left plot) due to its unexpected and abnormal exerted force as a function of power. Black, red, blue, and magenta colors respectively represent the motors 307-105, 310-003, 306-10H, and 307-103. The shape of each plot is defined by the force and frequency prediction intervals obtained from the regression analysis.

Vibratory Outputs' Colors - Hanging Test (Hypothesis 3)

The selected input signals for all motors (307-105, 310-003, 306-10H and 307-103) and types (White, Pink and Brown) are displayed in Figure 15. Except for the white vibration in motors 306-10H and 307-103, there were not repeated input signals between motors and output types. For all motors, a "perfect" white input signal (DFA α_{white} = 0.5) did not yield successful vibrations. All motors required input signals with DFA α values lower than 0.5 to obtain an output vibration close to white (e.g., DFA α equal to 0.303 for 307-105). Similarly, motor 306-10H required an input signal with DFA α equal to 0.880 to obtain a pink vibration (DFA α_{pink} = 1.0). Finally, all motors followed an almost 1-to-1 relation when outputting brown vibrations (DFA α_{brown} = 1.5).

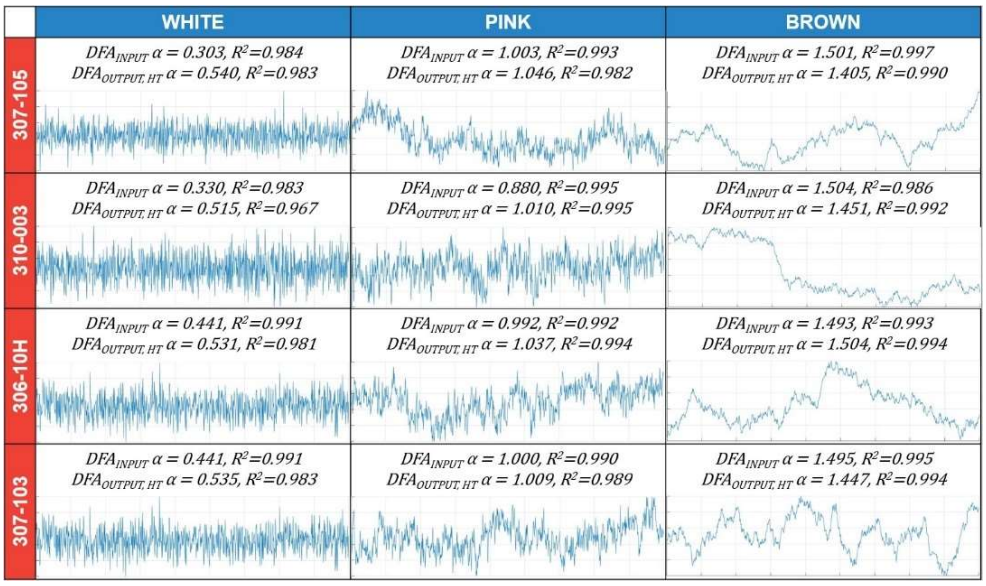

Figure 15: Selected inputs for all motors and vibratory types

All signals are normalized between 0 and 1, and the MATLAB DFA α is stated in the first line of each cell (DFA_{INPUT} α). The DFA α calculated from the hanging test is described in the second line of each cell ($DFA_{OUTPUT,\ HT}$ α), and it corresponds to the best output from all tested input signals.

Using a hanging test set-up, the vibrations' type (White, Pink and Brown) as a function of power for all motors (307-105, 310-003, 306-10H and 307-103) with their respective SN ratios are shown in Figure 16. A stronger SN ratio was found, as motor strength increased (from 307-105 to 307-103), and as power increased within each motor. Across all vibration types, the SN ratios for motors 307-105, 310-003, 306-10H and 307-103 were respectively 1-17, 7-21, 11-45 and 20-71. Each motor's ability to output an acceptable vibration type (white, pink, or brown) was dependent on the power level. Motor 307-105 produced acceptable white, pink, and brown vibrations when the power was larger than or equal to 70%, 50% and 50% respectively. Motor 310-003 produced acceptable white and pink vibrations for all tested powers, and acceptable brown vibrations when the power was larger than or equal to 50%. Motor 306-10H produced acceptable white, pink, and brown vibrations when the power was larger than or equal to 30%, 30% and 40% respectively. Finally, 307-103 produced acceptable white, pink, and brown vibrations for all tested powers.

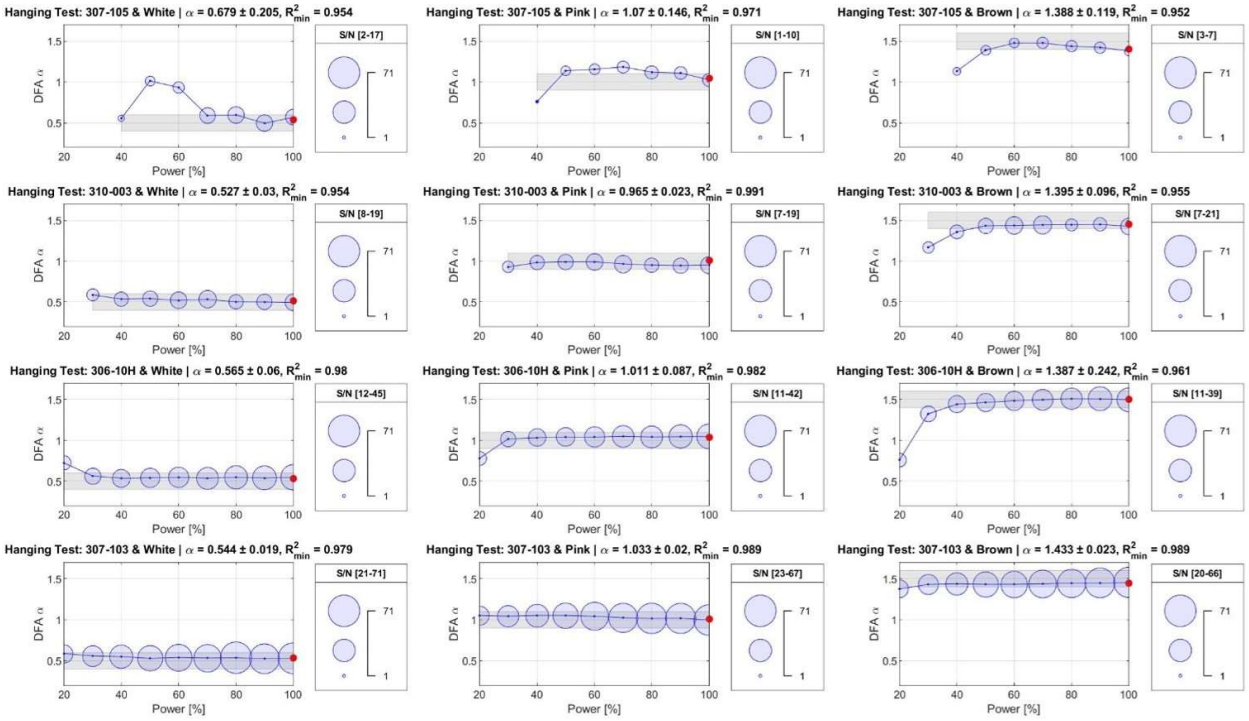

Figure 16: Output's color as a function of power level - Hanging test

The gray shaded and rectangular area represents an acceptable range for the type of outputs (i.e., ±0.1 from the ideal DFA α). The red dot at 100% is the first obtained DFA α, which was the one used to select the input signal for each motor and vibratory type (Figure 15). The first obtained DFA α (red dot) is displayed to show the reliability of the vibratory mat. The signal-to-noise ratio information is directly related to each subplot.

Vibratory Outputs' Colors - Static Test (Hypothesis 3)

Using a static test set-up, the vibrations' type (White, Pink and Brown) as a function of power for all motors (307-105, 310-003, 306-10H and 307-103) and simulated weights (34 kg, 75 kg, and 115 kg) with their respective SN ratios are shown in Figure 17. Even though results are displayed for 307-105 across all power levels in Figure 17, vibrations were not visually available when recording forces at powers equal to or less than 60%. Across all vibration types and simulated weights, the respective SN ratios for motors 307-105, 310-003, 306-10H and 307-103 were 0.9-2.4, 1.1-22.2, 1.1-14.9 and 1.4-18.2. The motor's ability to output an acceptable vibration type (white, pink, or brown) in the static test set-up was dependent on the power level and the simulated weight. Motor 307-105 produced acceptable white vibrations when power was larger than or equal to 80% under a weight of 115 kg, and acceptable pink vibrations when the power was larger than or equal to 70% under weights of 34 kg and 75 kg.

Motor 307-105 did not produce acceptable brown vibrations; however, there was a tendency to approach acceptable brown vibrations starting at 70% power for all weights. Motor 310-003 produced acceptable pink vibrations for powers larger than or equal to 50% under weights of 34 kg and 75 kg, and for powers larger than or equal to 60% under a weight of 115 kg. Motor 310-003 did not produce acceptable white or brown vibrations; however, there was a tendency to achieve white and brown vibrations for all weights starting at powers around 60% and 30% respectively. Motor 306-10H produced acceptable white vibrations for all weights and power levels. Motor 306-10H also produced acceptable pink vibrations starting at 60% for weights of 75 kg and 115 kg and starting at 40% under a weight of 34 kg. Motor 306-10H did not produce acceptable brown vibrations; but from the start, motor 306-10H tended to approach acceptable brown vibrations. Finally, motor 307-103 produced acceptable white vibrations for all powers and weights, and acceptable pink vibrations for all weights starting at 60% power. Motor 307-103 was not able to produce acceptable brown vibrations; but similar to motor 306-10H, motor 307-103 tended to approach acceptable brown vibrations as power increased.

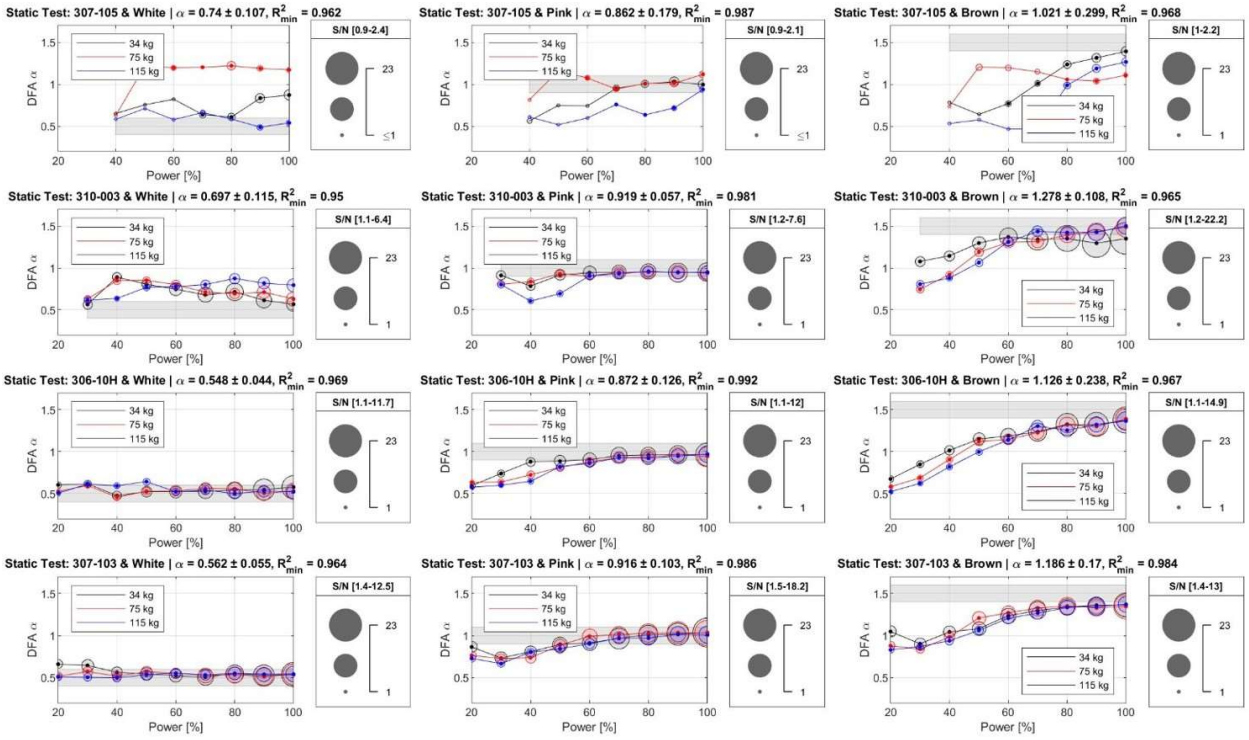

Figure 17: Output's color as a function of power level and simulated weight - Static test

The gray shaded and rectangular area represents an acceptable range for the type of outputs (i.e., ±0.1 from the ideal DFA α). For motor 307-105, it was not possible to visualize a signal under various conditions. In fact, it was not possible to visualize a signal in motor 307-105 when the power level was less than or equal to 60%. The signal-to-noise ratio information is directly related to each subplot. Black, red and blue lines respectively represent a simulated weight of 34 kg, 75 kg, and 115 kg.

Vibratory Outputs' Colors - Static vs. Hanging Test (Hypothesis 4)

Figure 18 shows the DFA results obtained from the static tests (Figure 17) plotted against the DFA results obtained from the hanging tests (Figure 16). No motor showed strong or valuable correlations between the DFA results obtained from the hanging and static test set ups.

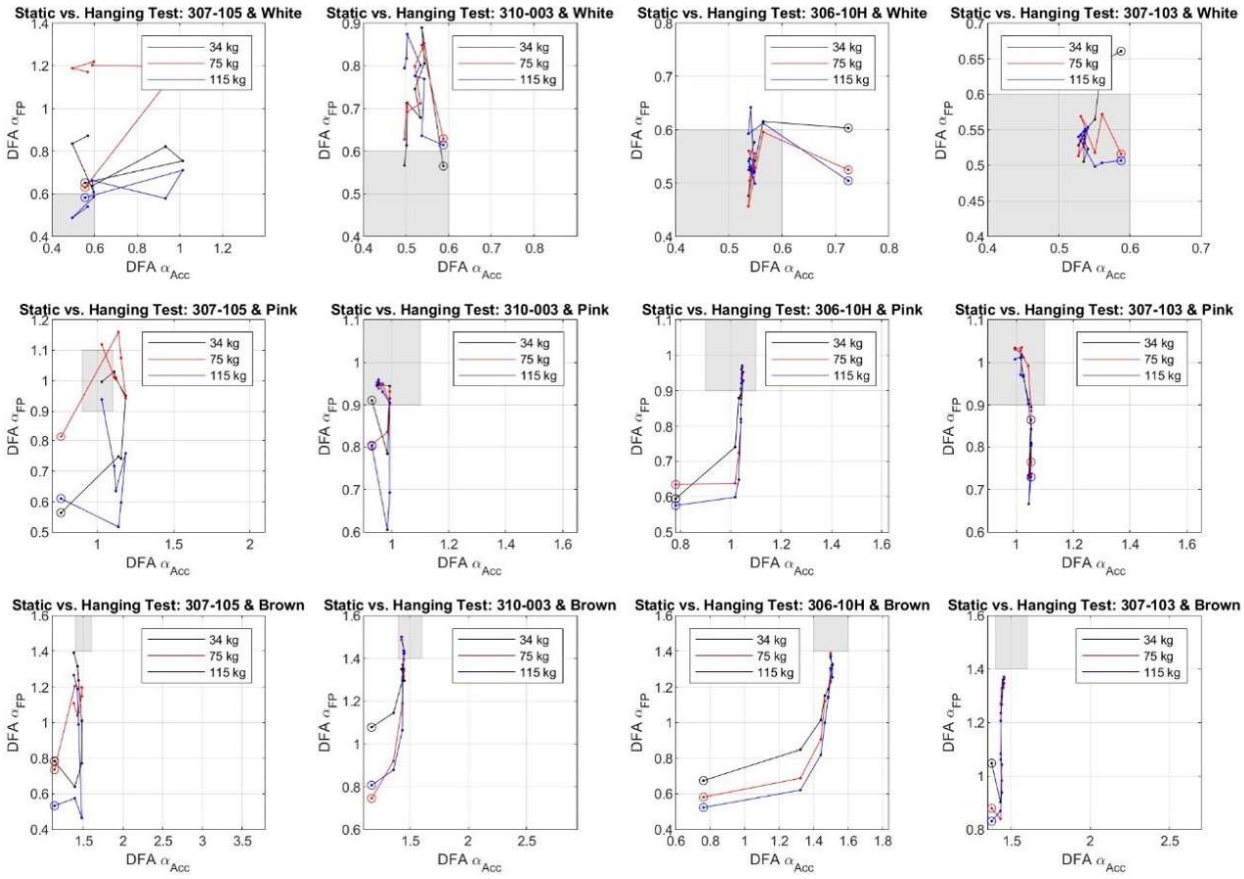

Figure 18: Relation between output colors calculated from static and hanging tests

The gray shaded and rectangular area represents an acceptable range for the type of outputs (i.e., ±0.1 from the ideal DFA α). The circles indicate the lowest power level, which is the start of the relation. DFA α_{FP} indicates results from the Static Test set up (FP: force plate), while DFA α_{Acc} indicates results from the Hanging Test set up (Acc: Accelerometer). Black, red and blue lines respectively represent a simulated weight of 34 kg, 75 kg, and 115 kg.

Discussion

The goal of this chapter was to quantify the vibratory mat's output in universal units (Newtons and Hertz), and to experimentally validate its output types (white, pink, and brown vibrations). The results showed that it was possible to quantify the magnitude of the vibrations generated by the mat, and that acceptable white, pink, and brown vibrations are achievable.

Forces and Frequencies Exerted by the Vibratory Mat (Hypotheses 1 and 2)

Hypothesis 1 stated that the forces and frequencies exerted by the mat were not affected by the participant's weight standing on it, making hypothesis 1 partially valid. Due to the non-significance from the coefficient linked to the simulated weight in the regression equations (Table 8), the vibratory mat's

force was not significantly affected by the simulated weights under the settings 307-103 LF and 306-10H RF. This was supported by the comparisons of prediction bounds in both settings, since the predictions bounds of all simulated weights overlapped with each other at all power levels (Figure 11). On the other hand, the vibratory mat's force under the settings 310-003 BF and 310-003 RF were affected by the simulated weights since the coefficient linked to the weight (Table 8) was significant, and no predictions bounds overlapped with each other (Figure 11). The other settings showed significance in the coefficient linked to the simulated weight and overlaps of prediction bounds at low and middle power levels (i.e., 20% to ~70%). Therefore, one method states that the simulated weight affects the mat's exerted force, and another one states the opposite for a range of powers. The effect of participants' weight on the source of vibration or indentation in the skin at the bottom of the feet has not been investigated before, so it is not possible to compare our results with previous discoveries. Studies that have used indentation [24], [25], [52], [54]–[59] are not expected to be severely affected by the participant's weight, since an indenter will always move the anticipated distance as long as the device is in motion and has enough power.

In terms of the vibratory mat's exerted frequency, the simulated weight did not have a large impact on the exerted frequency when compared to the exerted force. The coefficient linked to the simulated weight in the regression equations (Table 9) was significant only for the settings 307-103 LF and 306-10H BF. However, overlaps of prediction bounds happened in all motors and feet settings at all power levels (Figure 12), indicating that the weight does not affect the vibratory mat's exerted frequency. Due to the almost perfect results, it is possible to claim that the vibratory mat's exerted frequencies are not significantly affected by the participant's weight. The recommended range of frequencies for SR at the feet introduced by vibration is 200 Hz to 300 Hz [71]–[73], which has been achieved by few SR studies [12]–[14], [21], [27]. The ranges of frequencies offered by the vibratory mat are 120 Hz to 360 Hz, 60 Hz to 360 Hz, 60 Hz to 320 Hz, and 30 Hz to 300 Hz respectively for the motors 307-105, 310-003, 306-10H

and 307-103 (Figure 10). Motors 307-105 and 310-003 reach frequencies above 200 Hz when their power level is larger than or equal to 50%, while motors 306-10H and 307-103 reach frequencies over 200 Hz for power levels larger than or equal to 60%. This indicates that our vibratory mat might operate at frequencies that are not physiologically recommended; something that other designs have done. Successful SR studies have introduced vibratory signals between frequencies that do not cover the recommended ones: 40 Hz to 120 Hz [10]; 0 Hz to 100 Hz [11], [15]–[17], [20], [22], [28], [47]–[49], [51], [55], [60], [61]; 0 Hz to 200 Hz [23]; and 0 Hz to 120 Hz [26]. This shows that even though a frequency range is preferable from a physiological point of view, it is still possible to improve postural stability when such frequencies are not used.

Ideally, a vibratory mat's forces and frequencies would not be affected by the participant's weight at any power level or feet setting. The vibratory mat's best performance approached this goal when motor 307-103 was used. However, all motors showed a strong robustness in terms of exerted frequencies. Regarding the exerted forces, statistical results that supported hypothesis 1 were not obtained. Even though it was stated that the simulated weight significantly affected the vibratory mat's exerted forces, it is valid to point out that the differences caused by the simulated weights are expected to be relatively small. Visually in Figure 11, it is only possible to notice differences in the exerted force across weights for 310-003 BF, 310-003 RF and 306-10H LF.

The first part of hypothesis 2 stated that there were repeated forces and frequencies across multiple motors for a given feet setting, making the first part of hypothesis 2 partially valid. Across each feet setting (LF, BF, and RF), exerted forces that were not statistically different between motors were found at low power levels, with the exception of motors 310-003 RF and 306-10H RF under a 34 kg simulated weight, which showed similar exerted forces at all power levels (Figure 11). On the other hand, exerted frequencies that were not statistically different between motors were found across all feet settings and

power levels (Figure 12). The initial intention of the vibratory mat was to offer 4 different motors that were independent of each other. From previous comments, the goal was not 100% achieved. Repeated forces and frequencies were obtained when multiple motors were compared with each other. However, even though it was not a statistically inferred result, Figure 14 shows force-frequency separations between motors 307-103, 306-10H or 310-003, and 307-105. This suggests that the vibratory mat could potentially offer three types of force-frequency groups: high force and medium frequency (307-103), medium force and medium frequency (306-10H or 310-003), and low force and high frequency (307-105). Offering various combinations of force-frequency follows previous results and recommendations [52], since it was found that the optimal vibration that improved gait in humans was defined by both magnitude and frequency. Finally, the results in Figure 14 agreed with the information provided by Precision Microdrives on their motors, except for the overlapping between 306-10H and 310-003. According to Precision Microdrives, 306-10H is stronger than 310-003, which is distinct to our results. However, it must be pointed out that Precision Microdrives rates their motors through the Hanging Test, and our results are based on the Static Test. This potentially suggests that when motors 310-003 and 306-10H are embedded in silicone and compressed, they output similar vibrations.

The second part of hypothesis 2 stated that there were repeated forces and frequencies across various feet settings within a motor, making the second part of hypothesis 2 valid. Within a motor, Figure 11 shows that exerted forces that are not statistical different occur between the feet settings LF and RF. Within a motor choice, an ideal vibratory mat should exert similar forces under the LF and RF settings, and different ones under the BF setting when compared to the LF and RF settings. The uniformity between LF and RF was better achieved as the motor size increased. Motor 307-103 under a weight of 34 kg was able to exert similar forces at all power levels under the feet settings LF and RF. In terms of exerted frequency, the uniformity between LF and RF was not exclusive to a single motor and simulated weight. Figure 12 shows that the exerted frequencies did not statistically differ between feet settings for

all power levels and weights. This suggests that the ideal uniformity between the LF and RF settings was easier to achieve in terms of frequency, compared to force. Although it was not a result inferred from a statistical analysis, the previous observations are visually validated by Figure 13. Motor 307-103 shows uniformity between the LF and RF settings, and differences between the BF and LF/RF settings. When compared to motors 307-105, 310-003 and 306-10H, motor 307-103 visually shows a more defined overlap between LF and RF forces and frequencies, and a more defined separation between BF and LF/RF forces and frequencies. While fabricating the vibratory mat, all motors received equal quality checks and manufacturing techniques, suggesting that motor 307-103 could be the most resilient of the four on this new application (i.e., vibratory mat). This means that future vibratory SR studies have another strong option when selecting their vibrating component, in addition to considering the most common one: C-2 Tactors by Engineering Acoustics, FL [11]–[15], [17], [20], [22], [51], [52].

Vibratory Outputs' Colors - Hanging and Static Tests (Hypothesis 3)

Hypothesis 3 stated that more accurate output colors are obtained as motor size and power increase, making hypothesis 3 valid. Based on both testing set ups (Hanging Test: Figure 16, and Static Test: Figure 17), it was evident that motor 307-105 had the most difficulty in achieving output colors within the acceptable ranges, and that motor 307-103 had the least issues producing output colors within the acceptable ranges. The ability to produce accurate white, pink, or brown vibrations was more evident in the hanging test set-up (Figure 16) than in the static test (Figure 17), which could be explained by the SN ratio of each test. The hanging test had SN ratios between 1 and 71, and that the static test had SN ratios between 0 and 23, making the hanging test results more reliable. Therefore, it is valid to state that the motors used in this study (307-105, 310-003, 306-10H and 307-103 from Precision Microdrives, UK), when isolated, can produce accurate white, pink, and brown vibrations for various power levels (Figure 16). However, it must be reminded that the static test set-up is a more realistic environment for our application, compared to the hanging test. So, whether the hanging test results are applicable when the

motors are embedded in a vibratory mat and compressed by a participant, remains to be determined in a future study. Figure 17 shows strong possibilities that they are applicable since as SN ratios increased in the static test results, vibratory outputs fell more in the acceptable ranges as it happened in the hanging test results. This indicates that our vibratory device has evidence that it can produce different and accurate types of vibrations (white, pink, and brown), following previous recommendations [11], [15], [51], [68], [81], [82], and that such evidence can expand further than what our current results do today.

Despite the reliability importance of SN ratios while indicating if a vibratory output is white, pink, or brown, the output qualities must be considered in the discussion as well (Figure 15). A white signal is the most stationary signal out of the three (i.e., signal's average equal to 0), while a brown signal is the least stationary one [80], [92]. This means that a SN ratio better represents the behavior of a white signal when compared to a brown one. This was reflected in the hanging test results for the brown outputs in motors 307-105, 310-003 and 306-10H (Figure 16). At low powers, the three motors did not yield accurate brown vibrations, showing a heel in their plots. This heel was exaggerated in the static test results (Figure 17), since it was more dominant in the brown outputs, and due to its presence in pink outputs and motor 307-103. This indicates that future studies that validate vibratory outputs in a static test setting should focus on using instrumentation with a higher resolution than the one we used, especially when pink and/or brown vibrations are studied.

Vibratory Outputs' Colors - Static vs. Hanging Test (Hypothesis 4)

Hypothesis 4 claimed that there was a relation between the output colors obtained from the hanging and static tests, making hypothesis 4 invalid. Figure 18 showed no potential of using the hanging test results as a predictor of the static test ones. As previously mentioned, the static test represents a more realistic environment, while the hanging test represents a less expensive and easier to accomplish experiment. That explains our motivation to determine if future studies could test their vibrating

components using a hanging test before manufacturing their vibratory device, thus saving money and time. The current results do not show evidence of this being possible. However, this idea should not be ruled out completely. The hanging test results had better SN ratios when compared to the static test ones, making the comparison not ideal. An ideal comparison that could truly determine if the hanging test results could predict static test results, is the one that has similar SN ratios in both test set ups.

Conclusion

The goals of this study were to quantify the force and frequency exerted by our vibratory mat, and to experimentally validate if the intended output types (white, pink, and brown) were achievable. Both goals were met. The vibratory mat's force and frequency could be described by accurate quadratic regression fits ($R^2 \geq 0.7$), and even though statistical differences were found when various weights were placed on the mat, such differences were relatively small. It was also possible to conclude that all motors were not independent of each other; however, they have the potential to offer three groups of force-frequency relationships. It was possible to conclude that motor 307-103 was the most resilient motor to be embedded in a vibratory mat and compressed by a participant. In terms of the accuracy of the vibratory mat's outputs, motor 307-103 was the best one at producing accurate white, pink, and brown vibrations when it was and was not embedded in the mat. Current evidence shows average confidence levels that the vibratory mat can produce accurate white, pink, and brown vibrations. However, given the low SN ratios that the motors showed when tested inside the mat, and the high SN ratios and positive results that all motors showed when tested outside the mat, it was concluded that our current evidence can improve significantly if more sensitive instrumentation is used. This means that the proposed vibratory mat has experimental evidence that it can produce white, pink, and brown vibrations, and that such evidence could increase by changing the instrumentation that assesses the mat.

Chapter 5: Vibratory Mat's Impact on Postural Stability (Pilot Study)

Abstract

Background: Stochastic resonance through subthreshold vibration under the feet is a strategy that can improve postural stability in people of age and those with a somatosensory deficiency. The effect of constant or white vibrations has been assessed by comparing people's sway during and post stimulation (relative to pre stimulation). Given that no study has investigated the effect of other vibrations on sway (e.g., pink, or brown), this pilot study assessed the change in sway due to subthreshold white, pink and brown vibrations under people's feet.

Methods: Older adults (62.33 ± 1.53 years) and young adults (24.67 ± 3.06 years) who stood on a 1-inch foam to simulate somatosensory deficiency, performed three 90-second sway trials (i.e., Center of Pressure) with their eyes closed. The three sway trials consisted of pre, during and post subthreshold vibration, and four different vibrations (white, pink, brown, and placebo) were administered to all participants across four visits. Center of pressure measures of magnitude (Root Mean Square or 95% Ellipse), predictability (Sample Entropy) and complexity (Detrended Fluctuation Analysis) were extracted.

Findings: The use of a 1-inch foam under young adults' feet simulated aging since it was not possible to statistically differentiate the sensing threshold of both tested groups ($p > 0.05$). The impact of subthreshold vibration on sway was dependent on how people's sway was before, especially in terms of predictability (Sample Entropy).

Interpretation: This pilot study added evidence to the use of external factors that could simulate aging in young people (foam, cold feet, challenging stances, fatigue), which facilitates the experimentation of new assistive technologies (i.e., easier to recruit and test young people than old people). The pilot study also showed that the effect of subthreshold vibration could be dependent on the state of postural

stability before the stimulation, and the type of administered vibration. Meaning that more than one vibration could benefit a person's postural stability, and that it might change from day to day.

Background

Fall prevention among people over the age of 65 is an unresolved goal that negatively affects a country's economy [1]–[3] and people's quality of life [4], [5]. An increase of falls is a consequence of low postural stability (PS), and low PS can be associated with somatosensory feedback deficiency at the feet [9]. The somatosensory feedback in humans decays with aging [10]–[20], and it can be amplified in the presence of neuromuscular diseases such as diabetes [21]–[23] or stroke [22], [24]. Low somatosensory feedback can also be introduced or simulated in young populations who do not suffer from neuromuscular diseases by cooling their feet [26], asking them stand on foam [47], or by inducing fatigue [27], [28]. This simulated reduced somatosensory feedback in healthy young could serve and has been used as a model in experiments focused on understanding the effects of and treatment for sensory deficits in older adults. Introducing stochastic resonance (SR) at the feet through vibratory insoles or mats has shown to improve PS by assisting the somatosensory feedback [30], [31]. SR is the addition of noise to a weak signal that is below a sensory threshold level, so that the signal with the noise's assistance can cross the sensory threshold level, thereby enhancing detection and processing of a weak signal (Figure 2) [16].

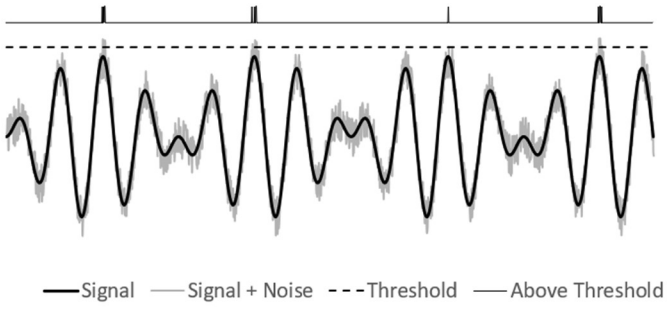

Figure 2: Stochastic resonance graphical description

Stochastic resonance (SR) is the addition of noise to a signal that is below a threshold level so that the signal with the noise's assistance can cross the threshold level that it could not cross before.

The impact of SR in PS through subthreshold vibration under the feet has been assessed in postural sway (Center of Pressure: COP, or Center of Mass) [10]–[12], [14], [16]–[23], [26], [27], [47]–[49], and in other biomechanical tasks such as gait [15], [48], [51], [53]. In sway, the effect of vibrating people's feet below their sensing threshold levels has been significant during [11], [14], [16], [17], [20]–[22], [26], [47] or immediately after the vibration [18], [19], [27]. These studies have focused on the COP and/or center of mass time series in the Anterior-Posterior (AP), Medial-Lateral (ML), and/or spatial directions. The analysis typically consists of quantifying the magnitude [14], [16], [17], [21], [26], [27], [47], predictability [47], and complexity [11], [17]–[20], [22], [27] of the selected time series. Even though previous studies have analyzed the effect of white noise vibration on the COP time series (i.e., sway) predictability and complexity, no study has analyzed the effect of vibrations that differ in predictability and complexity (e.g., white, pink, and brown vibrations). All prior studies used either constant or white vibrations, which does not follow previous design recommendations [68], conclusions [15], [81], [82] and the importance of complexity and predictability in human PS [11], [81], [82].

While white or constant subthreshold vibration was administered under the feet, people's sway reduced in magnitude [14], [16], [17], [21], [26], [47], and increased in both predictability [47] and complexity [11], [17], [20], [22]. Previous studies found that sway radius [16], [17], swept area [16], [17], [26], [47], range [16], [17], curve length [14], [26], and Root Mean Square (RMS) [21] reduced during subthreshold vibration when compared to the sway before the vibration. In addition, subthreshold vibration made people's sway more predictable during subthreshold vibration when compared to the sway before the vibration (reduction of approximate entropy) [47]. Finally, subthreshold vibration increased sway's complexity while vibration was administered, by improving Stabilogram Diffusion Analysis' measures [17], [20], [22], as well as by increasing the complexity index of a multiscale sample entropy analysis [11].

After white or constant subthreshold vibration was administered under the feet, people's sway reduced in magnitude [27] and increased in complexity [18], [19], [27]. It was found that the swept area was less affected after a fatigue test when vibration was administered, in comparison to the swept area when vibration was not administered [27]. Similar to studies that investigated the effect of subthreshold vibration while it was administered, studies that assessed the post-effect of subthreshold vibration found that sway's complexity increased due to vibration [18], [19], [27]. The only difference is that two of them used Detrended Fluctuation Analysis (DFA) to reach such conclusion [18], [27], while the other used the complexity index from a multiscale sample entropy [19].

All previous SR sway studies that used subthreshold vibration [10]–[12], [14], [16]–[23], [26], [27], [47]–[49] derived their conclusions from statistical analysis on the change of sway. However, it has been suggested that the impact of SR through subthreshold vibration could be dependent on the participant's PS before the vibration is applied [82]. That is, a personalized treatment, instead of a one treatment for all. Two gait studies that vibrated people's feet found this idea to be plausible [51], [53]. It was found that the positive or negative change in certain gait parameters was dependent on the value of the gait parameter prior to the vibration [51], [53].

Therefore, the relationship between the initial state of the system, the color of the subthreshold vibration used as a treatment, and the effect of the treatment on the system is unclear. The purpose of this pilot study is to explore the effect of subthreshold vibration in postural sway, when different types of vibrations (white, pink, and brown) are introduced in a healthy old group, and in a healthy young group that is under a balance deficit (1" foam). It is hypothesized that 1) the use of healthy young participants with a simulated sensory feedback deficit (introduced using a 1" foam) is a potential model to simulate age related somatosensory deficits, and 2) the efficacy of utilizing subthreshold vibration of

distinct colors to change postural sway magnitude, predictability and complexity for postural sway depends on their initial values and the color used.

Methods

Vibratory Mat

The vibratory mat whose design and validation are explained respectively in Chapters 3 and 4 was used for this study. Briefly, the vibratory mat has 4 different motors (307-105, 310-003, 306-10H and 307-103) from Precision Microdrives, UK, each offering various ranges of force and frequency. The motors are placed under the heel, first and fifth metatarsal of each foot, and their locations are adjustable to different people's feet sizes. The vibratory mat can output white, pink, or brown vibrations at various power levels, and such feature is independent of the participant's weight. The power level of the mat is controlled by a custom-built circuit and Arduino UNO (Arduino, MA). Finally, the vibratory mat has the feature of determining the participant's threshold through a modified and improved 421 protocol [94], [95].

Participants

Three healthy older adults (HO: 1 male and 2 females; age: 62.33 ± 1.53 years; height: 171.45 ± 12.12 cm; weight: 83.27 ± 13.31 kg), and three healthy young adults (HY: 1 male and 2 females; age: 24.67 ± 3.06 years; height: 167.64 ± 13.44 cm; weight: 61.97 ± 14.85 kg) participated in the pilot study. All participants were free of neuromuscular and cardiovascular diseases and were able to stand for 5 minutes without any assistance while keeping their eyes closed. The study was approved by the Institutional Review Board of The University of Kansas, and all participants consented to participate in the study.

Experimental Protocol

The experimental design consisted of two groups and four vibration color treatments. The participant visited the Biodynamics Laboratory 4 times, separated by at least one night. The same protocol was

used for all visits. Across the four visits, each vibration color (white, pink, brown, and placebo) was used for only one visit, with the color order being random for each participant. Only the HY participants stood on a 1" foam across all sway trials to simulate a somatosensory feedback deficiency [26]–[28], [47].

All sway trials were standardized by keeping people's heels 17 cm apart [93], and their toes pointing forward. In addition, across all sway trials the participants were instructed to close their eyes, stand barefoot, keep their hands at the side, and stand naturally without speaking. Eyes closed were kept across all trials, since it was desired to see how subthreshold vibration assisted both groups when their PS was challenged [11], [16], [17], [20]–[23], [47]–[49].

The vibratory mat was on top of a force plate (AMTI, Watertown, USA) and the participant stood for 90 seconds. The force plate kinetic data were recorded at 2500 Hz using a 16-bit A/D CED Power mkII and Spike2 (Cambridge Electronic Design, UK). The following provides the details for each trial collected.

1. Trial 1 (BL_{Mat}): The participant standing on the vibratory mat without vibration, serving as the baseline trial on the mat.
2. Trial 2 (STIM): The participant's sensing threshold was determined using the modified 421 protocol [94], [95], and the 307-103 motors. After a 2-minute break, the participant stood on the vibratory mat and received the vibration treatment administered at 90% of their sensing threshold [10]–[12], [14], [16], [17], [20]–[23], [27], [47]. The 307-103 motors were used, and the vibration lasted 90 seconds.
3. Trial 3 (T_0): Immediately after the vibration treatment, the participant's sway was recorded while standing on the vibratory mat without any vibration.

Data Analysis

All data analysis was done in MATLAB R2020b (MathWorks, MA, USA). From each sway trial (BL_{Mat}, STIM, and T_0), the COP was calculated in the AP and ML directions. The COP_{AP} and COP_{ML} time series were low-

pass filtered with a cut-off frequency equal to 20 Hz to remove any motor vibration from the sway time series [21], [27], [49]. This was only required in the non-placebo vibration sway trials (3 out of 4 STIM trials); however, it was decided to apply the low-pass filter in all sway trials for consistency. Using the filtered data, the spatial COP was calculated using $COP_{spatial} = \sqrt{COP_{AP}^2 + COP_{ML}^2}$, and all directions (AP, ML, and spatial) were downsampled to 50 Hz in line with best practices for variability measures such as entropy and fractality, which were part of the pilot study. Out of the nine time series ([BL_{Mat}, STIM, T_0] ∩ [COP_{AP}, COP_{ML}, $COP_{spatial}$]), measures of magnitude, predictability and complexity were extracted.

The magnitude of the COP_{AP} and COP_{ML} was represented by the Root Mean Square (RMS) of the time series, and the magnitude of the $COP_{spatial}$ was represented by the 95% ellipse. The predictability in all time series was represented by the Sample Entropy (SampEn) [88], which was calculated with m = 2, and R = 0.1. Finally, the complexity in all time series was represented by the slope of the log-log curve (α) obtained from a Detrended Fluctuation Analysis (DFA) [79], [80], whose t_{min} = 0.5 s and t_{max} = 15 s (or, n_{min} = 25, n_{max} = N/6). Using m = 2 and R = 0.1 for the SampEn, and t_{min} = 0.5 s and t_{max} = 15 s for the DFA followed the suggestions made in previous parameter studies [97], [98].

Only in the non-placebo STIM sway trials, the ground reaction forces were used to determine the rectified force that the motors exerted during the sway trial. This methodology was detailed in Chapter 4, but briefly, it required to band-pass filter the ground reaction forces between 20 Hz and 400 Hz to remove any sway from the data [21], [27], [49]. Next, the filtered data were rectified consecutively over time windows equal to 0.1 seconds. The rectified and filtered forces of the motors was used in a DFA (t_{min} = 0.5 s and t_{max} = 15 s, or n_{min} = 5, n_{max} = N/6) to assess the accuracy of the output's color. These results were included in the Appendix of this chapter and complemented the validation study of Chapter 4.

Statistical Analysis

Three statistical analyses done in MATLAB 2020b (MathWorks, MA, USA) were performed in this study. First, a two-sample t-test was done between the 90% sensing thresholds of the HO and HY groups (HY stood on a 1-inch foam). Second, for each subject group (HO and HY), direction (AP, ML and Spatial) and measure (RMS or 95% Ellipse, SampEn, and DFA α), a linear regression model was fitted between how much a measure changed between trials (STIM vs. BL_{Mat}, T_0 vs. BL_{Mat}, and T_0 vs. STIM), and the initial value of such measure $\left(meas_{final} - meas_{initial} \propto meas_{initial}\right)$. Data from all vibration colors were used in the regressions, meaning that differentiation between the vibration colors did not take place in the statistical analysis. In a future study, the effect of color will be investigated; but given the low number of participants in this pilot study, it was decided to not draw conclusions between the colors. Last, a power analysis to estimate the required number of participants to find statistical differences was done for each direction and measure. This was done between STIM vs. BL_{Mat}, T_0 vs. BL_{Mat}, and T_0 vs. STIM, and separated by vibration color and group. The results of the power analysis were not included in the results of this chapter, but in the appendix. The level of statistical significance across all results was $p < 0.05$.

Due to the low number of participants per group, the four visits per participant were assumed to be independent of each other. It is acknowledged that the results of this study do not consider the connection between visits for each participant. However, for the purpose of this pilot study, which is to provide guidance for a future study, we accepted the limitations of this assumption.

Results

Sensing Thresholds

The 90% of the sensing thresholds for the HO and the HY (who stood on a 1-inch foam) are shown in Figure 19. No significant differences ($p > 0.05$) were found between the two groups.

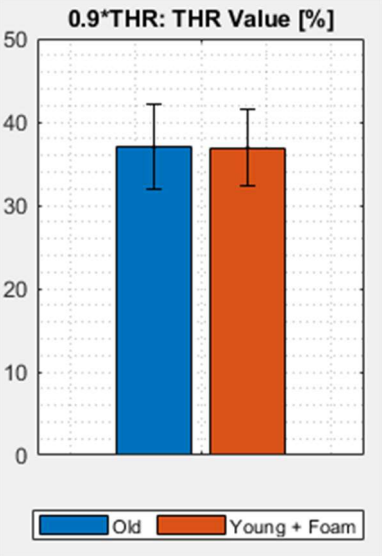

Figure 19: 90% Threshold for old and young plus foam groups

THR = Threshold. Healthy young (HY) and healthy older adults (HO) did not show statistical differences in sensing thresholds ($p > 0.05$). The bar plot includes sensing thresholds from all visits, meaning that there is a connection within each participant across their four visits. Although the sensing threshold is displayed in percent of a sensing threshold, these results can be converted using the regressions and figures provided in Chapter 4.

COP Changes Based on COP Initial Values

All DFA α's that were calculated were considered to be reliable, since the lowest DFA R^2 among all trials and participants was 0.94. The reliability of the DFA α's will not be considered further.

Figure 20 shows the effect of subthreshold vibration on sway while the stimulation was administered (STIM) with respect to the sway before the vibration (BL_{Mat}). Detailed results from the regressions are included in the chapter's appendix, and only the ones with $R^2_{adj} \geq 0.5$ are mentioned in the discussion. Negative relations were found for the 95% ellipse, AP SampEn, and DFA α in the ML and Spatial directions. The indication that the sway 95% ellipse and AP SampEn were reduced during subthreshold vibration when such variables were initially large (and vice versa), was more reliable in the HY (95% Ellipse $R^2_{adj} = 0.631$, AP SampEn $R^2_{adj} = 0.642$) than in the HO (95% Ellipse $R^2_{adj} = 0.111$, AP SampEn $R^2_{adj} = 0.268$). On the other hand, the indication that the ML and Spatial DFA α's were reduced during subthreshold vibration when they were initially large (and vice versa), was more reliable in the HO (ML

DFA α R^2_{adj} = 0.620, Spatial DFA α R^2_{adj} = 0.500) than in the HY (ML DFA α R^2_{adj} = 0.154, Spatial DFA α R^2_{adj} = 0.162).

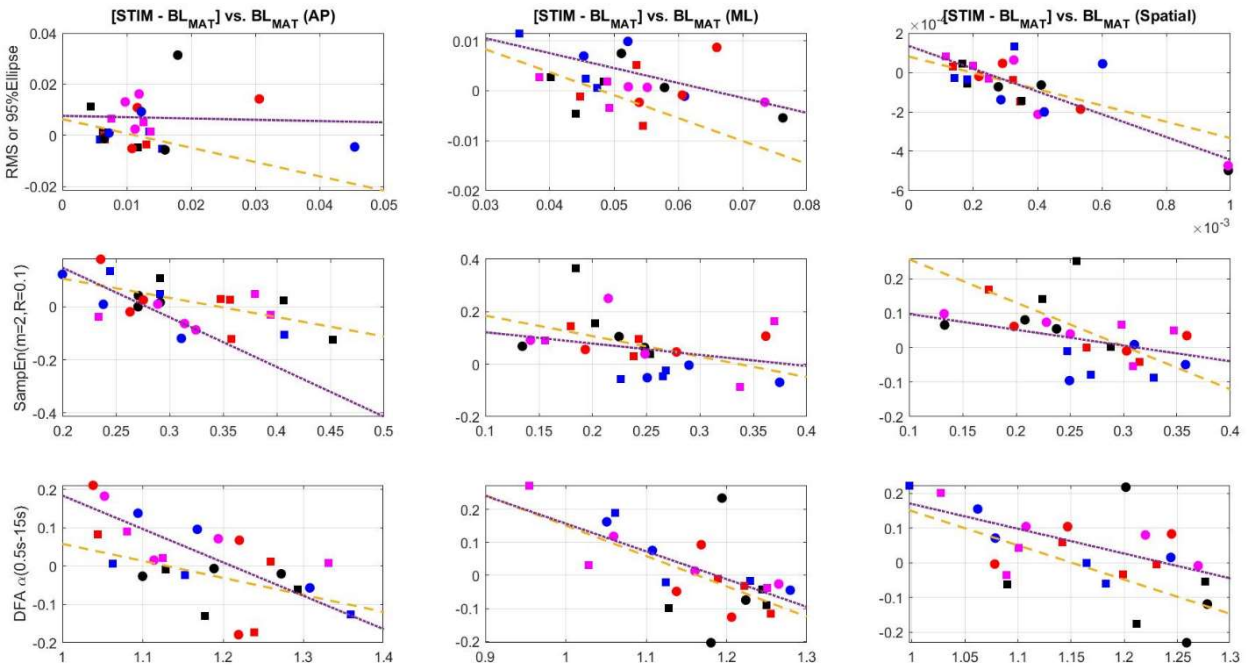

Figure 20: Effect of subthreshold vibration while it was administered relative to pre-vibration

Marker Shape Legend: □ = Heathy Old (HO), ○ = Healthy Young + Foam (HY). Marker Color Legend: ■ = White Vibration, ■ = Pink Vibration, ■ = Brown Vibration, ■ = Sham Vibration. Regression Line Color Legend: ┆ = Healthy Old (HO), ●●● = Healthy Young + Foam (HY). Rows represent the magnitude (RMS or 95% Ellipse), predictability (SampEn), and complexity (DFA α) of COP sway in the AP, ML, and Spatial directions (columns). Units of RMS (AP and ML) are 95% (Spatial) respectively are m and m^2. SampEn and DFA α are unitless measures. In each subplot, the y-axis represents the change in measure between STIM and BL_{Mat}, while the x-axis represents the measure extracted from BL_{Mat}. Although all regressions are displayed, the ones mentioned in the discussion ($R^2_{adj} \geq 0.5$) are Spatial 95% Ellipse HY, AP SampEn HY, ML DFA α HO, and Spatial DFA α HO.

Figure 21 shows the effect of subthreshold vibration on sway after the stimulation was administered (T_0) with respect to the sway before the vibration (BL_{Mat}). Detailed results from the regressions are included in the chapter's appendix, and only the ones with $R^2_{adj} \geq 0.5$ are mentioned in the discussion. Negative relations were found for the sway ML RMS, and SampEn in the ML and Spatial directions. The reduction of RMS in the ML direction between post- and pre- vibration due to initial large ML sway, was present in the HO (ML RMS R^2_{adj} = 0.590); not in the HY (ML RMS R^2_{adj} = 0.002). The reduction of Spatial SampEn between post- and pre- vibration due to initial large Spatial SampEn, was more reliable in the HY (Spatial SampEn R^2_{adj} = 0.581) than in the HO (Spatial SampEn R^2_{adj} = 0.488). Similarly, this also occurred for ML

SampEn; however, more reliability was found in the HO (ML SampEn R^2_{adj} = 0.409) than in the HY (ML SampEn R^2_{adj} = 0.336). Even though similar regression equations were not found between the two groups, it was noticeable that HO showed steeper slopes for ML and Spatial SampEn when compared to HY.

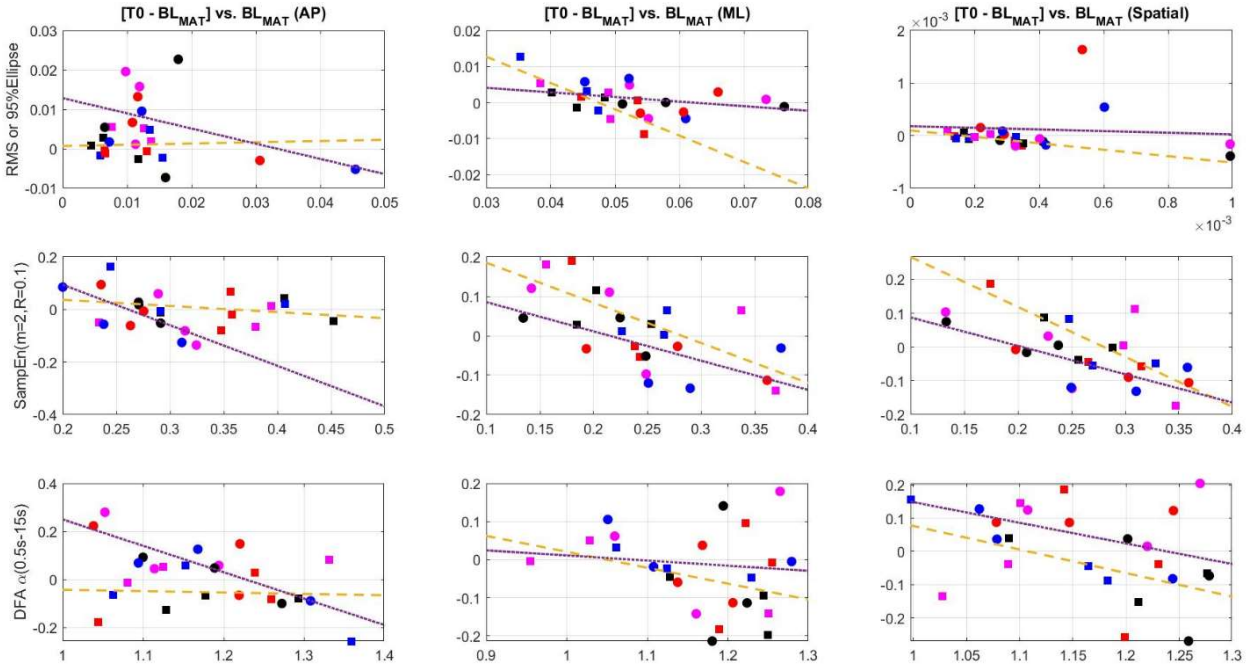

Figure 21: Effect of subthreshold vibration after it was administered relative to pre-vibration

Marker Shape Legend: □ = Heathy Old (HO), ○ = Healthy Young + Foam (HY). Marker Color Legend: ■ = White Vibration, ■ = Pink Vibration, ■ = Brown Vibration, ■ = Sham Vibration. Regression Line Color Legend: ┆ = Healthy Old (HO), ●●● = Healthy Young + Foam (HY). Rows represent the magnitude (RMS or 95% Ellipse), predictability (SampEn), and complexity (DFA α) of COP sway in the AP, ML, and Spatial directions (columns). Units of RMS (AP and ML) are 95% (Spatial) respectively are m and m^2. SampEn and DFA α are unitless measures. In each subplot, the y-axis represents the change in measure between T_0 and BL_{Mat}, while the x-axis represents the measure extracted from BL_{Mat}. Although all regressions are displayed, the ones mentioned in the discussion ($R^2_{adj} \geq 0.5$) are ML RMS HO, ML SampEn HO, Spatial SampEn HO, ML SampEn HY, and Spatial SampEn HY.

Figure 22 shows the effect of subthreshold vibration on sway after the stimulation was administered (T_0) with respect to the sway during the vibration (STIM). Detailed results from the regressions are included in the chapter's appendix, and only the ones with $R^2_{adj} \geq 0.5$ are mentioned in the discussion. In HO, reliable negative relations were found for ML RMS (R^2_{adj} = 0.560), ML SampEn (R^2_{adj} = 0.814), and Spatial SampEn (R^2_{adj} = 0.669). In HY, a negative relation was found for AP RMS (R^2_{adj} = 0.494).

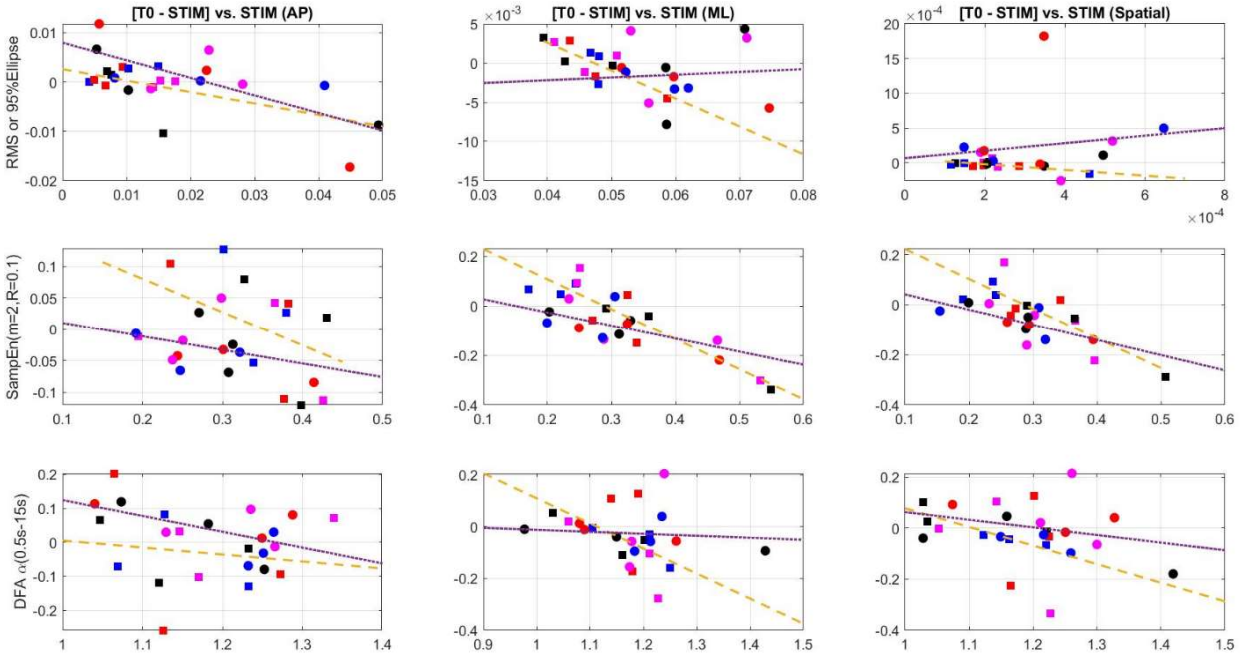

Figure 22: Effect of subthreshold vibration after it was administered relative to while it was administered

Marker Shape Legend: □ = Heathy Old (HO), ○ = Healthy Young + Foam (HY). Marker Color Legend: ■ = White Vibration, ■ = Pink Vibration, ■ = Brown Vibration, ■ = Sham Vibration. Regression Line Color Legend: ┆ = Healthy Old (HO), ●●● = Healthy Young + Foam (HY). Rows represent the magnitude (RMS or 95% Ellipse), predictability (SampEn), and complexity (DFA α) of COP sway in the AP, ML, and Spatial directions (columns). Units of RMS (AP and ML) are 95% (Spatial) respectively are m and m^2. SampEn and DFA α are unitless measures. In each subplot, the y-axis represents the change in measure between T_0 and STIM, while the x-axis represents the measure extracted from STIM. Although all regressions are displayed, the ones mentioned in the discussion ($R^2_{adj} \geq 0.5$) are ML RMS HO, ML SampEn HO, Spatial SampEn HO, and AP RMS HY.

Discussion

The first purpose of this pilot study was to investigate the use of healthy young people with a simulated deficit (1-inch foam) instead of old participants in SR studies. The second purpose was to explore if changes in sway due to subthreshold vibration are dependent on how the participant's sway is before the stimulation. Even though various types of vibration (white, pink, and brown) were used in the pilot study, it was not possible to statistically conclude which vibration type was better at improving postural sway due to our low sample size. However, it was still possible to show that the HY with a simulated sensory deficit (1-inch foam under their feet), is a strong possibility to simulate aging in SR studies. The pilot study also showed that it is likely plausible that some of the changes in sway due to subthreshold vibration are dependent on how the participant's sway is before the stimulation.

Young Participants + 1 Inch Foam = Old Participants?

Hypothesis 1 stated that the HY with a simulated sensory deficit (1-inch foam) could simulate HO in SR studies, and it was found to be mostly valid. It is accepted that older populations have a higher sensing threshold compared to young populations [74], and this has been seen in previous SR studies [12]–[14], [20]. In our SR pilot study, it was not possible to statistically differentiate the sensing thresholds of the HO and HY who stood on a 1-inch foam (Figure 19). When determining the sensing thresholds for all participants in the pilot study, the same protocol was used. Both groups used the 307-103 motor in the vibratory mat, followed the modified 421 protocol [94], [95], and received vibrations at their heels, first and fifth metatarsal. Thus, our inability to find a statistical difference between the sensing threshold of HO and HY participants can be justified by the use of the 1-inch foam. Although our sensing threshold results show high possibilities of using foam as an aging factor in SR studies, our COP results showed differences between the HO and HY participants who stood on a 1-inch foam.

The impact of subthreshold vibration was analyzed through three comparisons: During- vs. Pre-Vibration (Figure 20), Post- vs. Pre-Vibration (Figure 21), and Post- vs. During-Vibration (Figure 22). If foam were to age HY participants in SR studies, similar results should had been found for the HY and HO participants. This ideal case only occurred in the comparison of Post- vs. Pre-Vibration (Figure 21) for the ML and Spatial SampEn measures. However, this result should not be considered as proof that foam or other balance deficiencies are not valid strategies to simulate aging in SR studies. Previous SR studies that used sensory deficiencies in HY participants (cooling feet [26], foam [47], and fatigue [27]) obtained similar results to other SR studies that tested HO participants [14], [16]–[19], [26], [47] or populations with a neuromuscular disease [21]. Therefore, our results show that foam is a strong candidate to simulate aging in SR studies that investigate sensing threshold, and how subthreshold vibration affects the predictability of sway when the post- and pre-stages of vibration are compared.

Impact of Subthreshold Vibration

Hypothesis 2 stated that the impact of subthreshold vibration on sway was dependent on the state of the participant's sway prior to stimulation, and it was found to be valid. Reliable correlations were found in all three comparisons (During vs. Pre, Post vs. Pre, and Post vs. During) for both groups (HO and HY who stood a 1-inch foam).

During vs. Pre: When assessing how subthreshold vibration impacted the participants' sway during the stimulation (relative to how the participants' sway was initially, Figure 20), it was determined that in HY subthreshold vibration reduced sway magnitude (95% Ellipse) and increased predictability (AP SampEn) when initial large values were present. The reduction of sway magnitude during subthreshold vibration in HY is a result obtained by other SR studies [16], [17], [26], [47]. The reduction has also been found in HO [14], [16], [17] and diabetic [21] populations, making our results consistent with others' discoveries. Similarly, a previous SR study determined that subthreshold vibration increased predictability in HY [47]. However, all previous SR studies' conclusions were generic, while ours are dependent on the initial sway values of magnitude and predictability. While most of our results for the HY suggest that subthreshold vibration reduced their sway magnitude and increased predictability, we also obtained results that suggest the opposite (i.e., subthreshold vibration increased sway magnitude and reduced predictability). That is, the obtained correlations showed a "break point" that decided whether subthreshold vibration increased or reduced the sway swept area or AP SampEn in the HY participants who stood on a 1-inch foam.

In HO, it was determined that subthreshold vibration reduced complexity (ML and Spatial DFA) when large initial values were present (Figure 20). At a first glance, our results do not seem to agree with previous SR studies since they had found that subthreshold vibration adds complexity to the sway of HO [11], [17], [22], diabetic [22] and stroke [22] populations. However, consider that complexity in terms of DFA α is defined as how close it is to 1.0 (pink) [92]. The obtained correlations for ML and Spatial DFA

show “break points” around 1.15, and negative slopes. That means that complexity was added when initial small values of DFA α were present, which agrees with previous SR studies [11], [17], [22]. In fact, the “break points” and negative slopes means that the current results are consistent with another SR study that found a reduction of complexity due to subthreshold vibration [20]. Considering that the effect of subthreshold vibration is dependent on initial sway values opens the possibilities of adding [11], [17], [22] and subtracting [20] complexity, instead of choosing one of the two as a conclusion.

Post vs. Pre: When assessing how subthreshold vibration impacted the participants’ sway after the stimulation (relative to how the participants’ sway was initially, Figure 21), it was determined that in HO subthreshold vibration reduced sway magnitude (ML RMS) and increased predictability (ML and Spatial SampEn) when initial large values were present. A SR study that simulated aging in HY through fatigue also obtained a reduction of sway magnitude after subthreshold vibration was administered [27]. Although the agreement of results come from two different groups, it is possible to connect both discoveries if Hypothesis 1 is valid. Other SR studies found significant changes in sway complexity due to vibration [18], [19], [27]; but we did not. However, we found significant changes in sway predictability due to vibration in HO (ML and Spatial SampEn) and HY (Spatial SampEn) participants, and they are dependent on their initial values.

In the Post vs. Pre comparison, sway predictability (Spatial SampEn) was affected by subthreshold vibration for both HY and HO participants. However, it was noticed that the rate of change in Spatial SampEn was steeper for the HO participants when compared to the HY ones. This could indicate that subthreshold vibrations could have a larger impact in old populations who suffer from natural somatosensory deficiencies. In other words, subthreshold vibration has the potential to improve PS in populations who need it most.

Post vs. During: When assessing how subthreshold vibration impacted the participants' sway after the stimulation (relative to how the participants' sway was during the stimulation, Figure 22), it was determined that in HO subthreshold vibration reduced sway magnitude (ML RMS) and increased predictability (ML and Spatial SampEn) when large values were present during the stimulation. Even though post- vs. during vibration analysis on HO were not found, the reduction of sway magnitude and increase of sway predictability seems to be a common conclusion. In HY, it was determined that sway magnitude (AP RMS) was reduced due to subthreshold vibration when large values were present during the stimulation. However, a previous SR study found that subthreshold vibration increased the sway magnitude in HY after it was administered [47]. This is opposite to what other studies had observed (i.e., reduction of sway magnitude); but this observation does not go against our results since our correlation analysis allows for the magnitude to increase or reduce (i.e., break point and negative slope).

Conclusion

In conclusion, this pilot study showed evidence that using young participants under a balance deficit is a valid way to simulate old participants in SR studies [26], [27], [47]. It was also concluded that the effect of subthreshold vibration on sway has a dependency on how the sway is before the stimulation, supporting the statistical analysis used in human gait SR studies [51], [53]. Therefore, future studies should continue the investigation of SR through various vibration colors (white, pink, and brown) [11], [15], [68], [81], [82], and analyze their results from a perspective that targets personalized treatments instead of a global treatment.

Chapter 6: Conclusions

Major Findings

The first goal of this dissertation was to design, manufacture, and validate a vibratory mat that could introduce stochastic resonance (SR) through the plantar surface of people's feet. The second goal was to assess the impact of various subthreshold vibrations (white, pink, and brown) on people' postural sway. All goals were met, and the major findings were:

1. In Chapter 3, it was found that an alternative vibratory mat to the most-reported vibratory device [11]–[14], [17], [20], [22] could be used in future SR studies. The proposed vibratory mat met all current design requirements [68], [69], and new ones that increase the likelihood of being used by the targeted populations. The biggest advantage of our vibratory mat over the most widely reported one, is the cost. Our vibratory mat's manufacturing cost is around $300, while the most-reported one's manufacturing cost is around $4,000.
2. In Chapter 4, we were able to quantify the forces and frequencies that our vibratory mat exerts, allowing the comparison of results with future SR studies that use different vibratory devices. It was also experimentally validated that our vibratory mat could output accurate white, pink, and brown vibrations [79], [80] for various participants' weights and power levels. The accuracy and reliability of the vibratory mat's outputs increased as both the strength of the vibratory components (or motors) and power levels increased. Although it sounds as if our vibratory mat is only reliable when large motors and power levels are used, it must be pointed out that supporting evidence that our vibratory mat exerts accurate white, pink, and brown vibrations was obtained. In fact, it was concluded in Chapter 4 that such evidence can be expanded with further testing. A vibratory mat that accurately outputs white, pink, and brown vibrations follows previous design recommendations [68], conclusions [15], [81], [82] and the importance of complexity and predictability in human postural stability [11], [81], [82]

3. In chapter 5, positive evidence towards the simulated aging effects of young people through foam under their feet was obtained. This finding agrees with other studies that simulated aging, or other postural stability deficiencies, in young populations [26], [27], [47]. It was also found that the effect of subthreshold vibration under the feet could be dependent on the state of sway prior to the vibration [51], [53], as well as the to the type of vibration [82]. Finally, our results indicated that subthreshold vibration has the tendency of reducing sway magnitude and increasing predictability, as other studies have reported [14], [16], [17], [21], [26], [27], [47].

Studies' Limitations

As all studies, this dissertation was presented with limitations, and some of them were accredited to the COVID-19 pandemic which stagnated our recruitment and testing efforts.

In the design of the vibratory mat (Chapter 3), it is acknowledged that the estimated costs and codes could be outdated within a few or many years. It is no secret that the cost of electrical components and building materials change with time. It is also possible that an Arduino or MATLAB update could make our codes and libraries outdated, not allowing our system to run as it is explained in this dissertation. Finally, the time of manufacturing is around 4 days, not allowing this device (as of today) to be largely produced. Further investigations on how to make the manufacturing process more efficient is required.

Regarding the first part of the vibratory mat's validation (Chapter 4), only one vibratory mat was tested, and it was tested once. Best practices in quality/validation studies suggest testing multiple versions of the same product, since they allow reliability analyses that can improve manufacturing and design practices. Due to cost and time constraints, we were only able to manufacture and test one vibratory mat. Also, best practices in regression analysis suggests testing a product more than once to see if their results change over time (i.e., tuning and validation data). The results presented in Chapter 4 required around 72 hours of testing time alone, without counting set-up and time between tests. This reflected

between 6 and 8 weeks of testing. Given the large time commitment to test one vibratory mat, it was agreed by the Biodynamics Laboratory that one session of testing in the manufactured vibratory mat was OK for this dissertation. Therefore, Chapter 4's limitations in terms of quantifying the vibratory mat's outputs are summarized by the following list.

- A quick test that would allow the investigator to know if the vibratory mat's performance changed over time was not available.
- The quality and reliability of the manufacturing process was not tested. Therefore, it is unknown whether a future vibratory mat will behave as described in this dissertation.

In the second part of the vibratory mat's validation (Chapter 4) when using the force plate to determine the color of the vibratory mat's outputs, low signal-to-noise ratios were obtained. This reflected less reliable results when compared to results obtained through an accelerometer (i.e., large signal-to-noise ratios). To address this unbalance, a regression or statistical analysis that used the signal-to-noise ratios as weights could had been performed.

In the assessment of how subthreshold vibration impacted postural sway (Chapter 5), a pilot study on 2 groups, each with 3 participants, was conducted. The low sample size did not allow us to conduct statistical analyses that could indicate which type of vibration (white, pink, or brown) was more beneficial to the participants. However, despite the low sample size in the pilot study, it was concluded that the effect of subthreshold vibration on postural sway was dependent on the state of postural stability prior to the stimulation. Regardless of the low sample size the following list shows some of the analyzes that were not performed, limiting our pilot study.

- A statistical analysis within each participant was not performed, therefore the variability of each participant across visits was not quantified.

- The connection between the four participant's visits was not quantified, which creates a dependency within the data.
- Nine extracted measures were used in the regressions, creating many observations. A more concise list of measures should had been used to draw stronger conclusions.
- A control group was not used in the statistical analysis, which did not allow us to state if the listed conclusions or observations were significant. Control data were available in the pilot study, and it was comprised of the placebo stimulation. The placebo data could be used as the control data either within each participant or across all participants.
- Retention was not quantified or addressed.

Future Projects

Given the studies' limitations listed above, as well as the results obtained in this dissertation, these are proposed future projects that could further investigate the effect of subthreshold vibration in postural stability:

- A second vibratory mat should be manufactured and tested as it was done in Chapter 4. The results from this new vibratory mat should be compared to the results of this dissertation and decide if changes in the manufacturing process should be made to ensure manufacturing reliability.
- The current and future vibratory mats should be tested at least one more time using all or some of the methodology described in Chapter 4 to analyze how repeatable the mats' forces, frequencies, and vibration types (white, pink, and brown) are.
- Current and future vibratory mats that are analyzed by a force plate as described in Chapter 4, should be tested utilizing a force plate (or other force sensing device) whose sensitivity is much higher than the one used in this dissertation.

- The pilot study started in Chapter 5 should be continued to increase the sample size (i.e., 15 to 20 participants). This would allow further statistical analysis that could determine the vibration that most benefits a person's postural stability. A larger sample size would also allow a statistical analysis that accounts for repeated measures across participants, given that a single participant visits the laboratory 4 times.
- In addition to the extracted sway measures in Chapter 5, other sway measures such as recurrent quantification analysis, and other analyses such mechanical modeling of the human body should be considered. Additional data that continues the work started in Chapter 5 is not restricted to the analysis done in the presented pilot study.
- Finally, subthreshold vibration is not the only strategy that could improve postural stability. Future projects could use the developed vibratory mat in suprathreshold vibratory studies, which is another strategy to improve postural stability.

References

[1] J. A. Stevens, P. S. Corso, E. A. Finkelstein, and T. R. Miller, "The costs of fatal and non-fatal falls among older adults," *Inj Prev*, vol. 12, no. 5, pp. 290–295, Oct. 2006, doi: 10.1136/ip.2005.011015.

[2] US HUD, "Overcoming Obstacles to Policies for Preventing Falls by the Elderly," *Healthy Housing Solutions*, Feb. 2017, [Online]. Available: https://www.hud.gov/sites/dfiles/HH/documents/OvercomingObstaclesFalls.pdf

[3] J. H. Gurwitz and S. D. Pearson, "Novel Therapies for an Aging Population: Grappling With Price, Value, and Affordability," *JAMA*, vol. 321, no. 16, pp. 1567–1568, Apr. 2019, doi: 10.1001/jama.2019.2633.

[4] L. D. Gillespie *et al.*, "Interventions for preventing falls in older people living in the community," *Cochrane Database of Systematic Reviews*, no. 9, 2012, doi: 10.1002/14651858.CD007146.pub3.

[5] M. C. Robertson and L. D. Gillespie, "Fall Prevention in Community-Dwelling Older Adults," *JAMA*, vol. 309, no. 13, p. 1406, Apr. 2013, doi: 10.1001/jama.2013.3130.

[6] C. McCrum, "Fall Prevention in Community-Dwelling Older Adults - Correspondence," *The New England Journal of Medicine*, Jun. 2020, doi: 10.1056/NEJMc2005662.

[7] H. S. Kaye, T. Kang, and M. P. LaPlante, "Mobility Device Use in the United States," *National Institute on Disability and Rehabilitation Research*, Jun. 2000, [Online]. Available: https://iwalk-free.com/wp-content/uploads/2015/05/Mobility-Device-Use-in-US_2010.pdf

[8] L. Resnik, S. Allen, D. Isenstadt, M. Wasserman, and L. Iezzoni, "Perspectives on use of mobility aids in a diverse population of seniors: Implications for intervention- ClinicalKey," *Disability and Health Journal*, pp. 77–85, 2009, doi: doi:10.1016/j.dhjo.2008.12.002.

[9] R. J. Peterka, "Sensorimotor Integration in Human Postural Control," *Journal of Neurophysiology*, vol. 88, no. 3, pp. 1097–1118, Sep. 2002, doi: 10.1152/jn.2002.88.3.1097.

[10] A. Aboutorabi, M. Arazpour, F. Farahmand, M. Bahramizadeh, R. Fadayevatan, and E. Abdollahi, "Design and evaluation of vibratory shoe on balance control for elderly subjects: technical note," *Disability and Rehabilitation: Assistive Technology*, vol. 13, no. 2, pp. 173–177, Feb. 2018, doi: 10.1080/17483107.2017.1300346.

[11] M. Costa *et al.*, "Noise and poise: Enhancement of postural complexity in the elderly with a stochastic-resonance–based therapy," *EPL*, vol. 77, no. 6, p. 68008, Mar. 2007, doi: 10.1209/0295-5075/77/68008.

[12] M. Dettmer, A. Pourmoghaddam, B.-C. Lee, and C. S. Layne, "Associations between Tactile Sensory Threshold and Postural Performance and Effects of Healthy Aging and Subthreshold Vibrotactile Stimulation on Postural Outcomes in a Simple Dual Task," *Current Gerontology and Geriatrics Research*, 2016, doi: 10.1155/2016/9797369.

[13] M. Dettmer, A. Pourmoghaddam, B.-C. Lee, and C. S. Layne, "Do Aging and Tactile Noise Stimulation Affect Responses to Support Surface Translations in Healthy Adults?," *Current Gerontology and Geriatrics Research*, vol. 2016, p. e2941964, Apr. 2016, doi: https://doi.org/10.1155/2016/2941964.

[14] M. Dettmer, A. Pourmoghaddam, B.-C. Lee, and C. S. Layne, "Effects of aging and tactile stochastic resonance on postural performance and postural control in a sensory conflict task," *Somatosensory & Motor Research*, vol. 32, no. 2, pp. 128–135, Jun. 2015, doi: 10.3109/08990220.2015.1004045.

[15] A. M. Galica *et al.*, "Subsensory vibrations to the feet reduce gait variability in elderly fallers," *Gait Posture*, vol. 30, no. 3, pp. 383–387, Oct. 2009, doi: 10.1016/j.gaitpost.2009.07.005.

[16] A. Priplata, J. Niemi, M. Salen, J. Harry, L. A. Lipsitz, and J. J. Collins, “Noise-Enhanced Human Balance Control,” *Phys. Rev. Lett.*, vol. 89, no. 23, p. 238101, Nov. 2002, doi: 10.1103/PhysRevLett.89.238101.

[17] A. A. Priplata, J. B. Niemi, J. D. Harry, L. A. Lipsitz, and J. J. Collins, “Vibrating insoles and balance control in elderly people,” *Lancet*, vol. 362, no. 9390, pp. 1123–1124, Oct. 2003, doi: 10.1016/S0140-6736(03)14470-4.

[18] C.-C. Wang and W.-H. Yang, “Using detrended fluctuation analysis (DFA) to analyze whether vibratory insoles enhance balance stability for elderly fallers,” *Arch Gerontol Geriatr*, vol. 55, no. 3, pp. 673–676, Dec. 2012, doi: 10.1016/j.archger.2011.11.008.

[19] Q. Wei *et al.*, “Multivariate Multiscale Entropy Applied to Center of Pressure Signals Analysis: An Effect of Vibration Stimulation of Shoes,” *Entropy*, vol. 14, no. 11, pp. 2157–2172, Nov. 2012, doi: 10.3390/e14112157.

[20] P. Simeonov, H. Hsiao, J. Powers, D. Ammons, T. Kau, and A. Amendola, “Postural stability effects of random vibration at the feet of construction workers in simulated elevation,” *Applied Ergonomics*, vol. 42, no. 5, pp. 672–681, Jul. 2011, doi: 10.1016/j.apergo.2010.10.002.

[21] J. M. Hijmans, J. H. B. Geertzen, W. Zijlstra, A. L. Hof, and K. Postema, “Effects of vibrating insoles on standing balance in diabetic neuropathy,” *Journal of Rehabilitation Research & Development*, vol. 45, no. 9, pp. 1441–1449, Dec. 2008.

[22] A. A. Priplata *et al.*, “Noise-enhanced balance control in patients with diabetes and patients with stroke,” *Annals of Neurology*, vol. 59, no. 1, pp. 4–12, 2006, doi: 10.1002/ana.20670.

[23] S. C. Regueme *et al.*, “A Therapeutic Insole Device for Postural Stability in Older People With Type 2 Diabetes. A Feasibility Study (SENSOLE Part I),” *Front. Med.*, vol. 6, 2019, doi: 10.3389/fmed.2019.00127.

[24] S.-W. Lee, K.-H. Cho, and W.-H. Lee, “Effect of a local vibration stimulus training programme on postural sway and gait in chronic stroke patients: a randomized controlled trial,” *Clinical Rehabilitation; London*, vol. 27, no. 10, pp. 921–31, Oct. 2013, doi: http://dx.doi.org.www2.lib.ku.edu/10.1177/0269215513485100.

[25] C. Maurer, T. Mergner, B. Bolha, and F. Hlavacka, “Human balance control during cutaneous stimulation of the plantar soles,” *Neuroscience Letters*, vol. 302, no. 1, pp. 45–48, Apr. 2001, doi: 10.1016/S0304-3940(01)01655-X.

[26] W.-M. Chen, J.-W. Li, X. Geng, C. Wang, L. Chen, and X. Ma, “The potential influence of stochastic resonance vibrations on neuromuscular strategies and center of pressure sway during single-leg stance,” *Clin Biomech (Bristol, Avon)*, vol. 77, p. 105069, Jul. 2020, doi: 10.1016/j.clinbiomech.2020.105069.

[27] J. Moon *et al.*, “Shoes with active insoles mitigate declines in balance after fatigue,” *Scientific Reports*, vol. 10, no. 1, Art. no. 1, Feb. 2020, doi: 10.1038/s41598-020-58815-9.

[28] D. L. Miranda *et al.*, “Sensory Enhancing Insoles Modify Gait during Inclined Treadmill Walking with Load,” *Med Sci Sports Exerc*, vol. 48, no. 5, pp. 860–868, May 2016, doi: 10.1249/MSS.0000000000000831.

[29] L. Rocchi, L. Chiari, and F. B. Horak, “Effects of deep brain stimulation and levodopa on postural sway in Parkinson’s disease,” *J. Neurol. Neurosurg. Psychiatry*, vol. 73, no. 3, pp. 267–274, Sep. 2002, doi: 10.1136/jnnp.73.3.267.

[30] C. Z.-H. Ma, W.-K. Lam, B.-C. Chang, and W. C.-C. Lee, “Can Insoles Be Used to Improve Static and Dynamic Balance of Community-Dwelling Older Adults? A Systematic Review on Recent Advances and Future Perspectives,” *J Aging Phys Act*, pp. 1–16, Jun. 2020, doi: 10.1123/japa.2019-0293.

[31] O. White, J. Babič, C. Trenado, L. Johannsen, and N. Goswami, “The Promise of Stochastic Resonance in Falls Prevention,” *Front. Physiol.*, vol. 9, 2019, doi: 10.3389/fphys.2018.01865.

[32] F. Viseux, A. Lemaire, F. Barbier, P. Charpentier, S. Leteneur, and P. Villeneuve, “How can the stimulation of plantar cutaneous receptors improve postural control? Review and clinical commentary,” *Neurophysiologie Clinique*, Jan. 2019, doi: 10.1016/j.neucli.2018.12.006.

[33] J. Paton, A. L. Hatton, K. Rome, and B. Kent, “Effects of foot and ankle devices on balance, gait and falls in adults with sensory perception loss: a systematic review,” *JBI Database System Rev Implement Rep*, vol. 14, no. 12, pp. 127–162, Dec. 2016, doi: 10.11124/JBISRIR-2016-003229.

[34] J. Maculewicz, L. B. Kofoed, and S. Serafin, “A Technological Review of the Instrumented Footwear for Rehabilitation with a Focus on Parkinson’s Disease Patients,” *Front. Neurol.*, vol. 7, 2016, doi: 10.3389/fneur.2016.00001.

[35] M. Bagherzadeh Cham, M. A. Mohseni-Bandpei, M. Bahramizadeh, S. Kalbasi, and A. Biglarian, “The clinical and biomechanical effects of subthreshold random noise on the plantar surface of the foot in diabetic patients and elder people: A systematic review,” *Prosthetics and Orthotics International*, vol. 40, no. 6, pp. 658–667, 2016, doi: 10.1177/0309364616631351.

[36] P. B. Shull and D. D. Damian, “Haptic wearables as sensory replacement, sensory augmentation and trainer – a review,” *J NeuroEngineering Rehabil*, vol. 12, no. 1, p. 59, Jul. 2015, doi: 10.1186/s12984-015-0055-z.

[37] B. Lauber and M. Keller, “Improving motor performance: Selected aspects of augmented feedback in exercise and health,” *European Journal of Sport Science*, vol. 14, no. 1, pp. 36–43, Jan. 2014.

[38] N. Murillo, J. Valls-Sole, J. Vidal, E. Opisso, J. Medina, and H. Kumru, “Focal vibration in neurorehabilitation,” *Eur J Phys Rehabil Med*, vol. 50, no. 2, pp. 231–242, Apr. 2014.

[39] A. L. Hatton, K. Rome, J. Dixon, D. J. Martin, and P. O. McKeon, “Footwear InterventionsA Review of Their Sensorimotor and Mechanical Effects on Balance Performance and Gait in Older Adults,” *J Am Podiatr Med Assoc*, vol. 103, no. 6, pp. 516–533, Nov. 2013, doi: 10.7547/1030516.

[40] E. Sejdić and L. A. Lipsitz, “Necessity of noise in physiology and medicine,” *Comput Methods Programs Biomed*, vol. 111, no. 2, pp. 459–470, Aug. 2013, doi: 10.1016/j.cmpb.2013.03.014.

[41] M. D. McDonnell and L. M. Ward, “The benefits of noise in neural systems: bridging theory and experiment,” *Nature Reviews Neuroscience*, vol. 12, no. 7, pp. 415–426, Jul. 2011, doi: 10.1038/nrn3061.

[42] M. D. McDonnell and D. Abbott, “What Is Stochastic Resonance? Definitions, Misconceptions, Debates, and Its Relevance to Biology,” *PLOS Computational Biology*, vol. 5, no. 5, p. e1000348, May 2009, doi: 10.1371/journal.pcbi.1000348.

[43] J. C. Menant, J. R. Steele, H. B. Menz, B. J. Munro, and S. R. Lord, “Optimizing footwear for older people at risk of falls,” *Journal of Rehabilitation Research & Development*, vol. 45, no. 8, pp. 1167–1181, Nov. 2008.

[44] J. M. Hijmans, J. H. B. Geertzen, P. U. Dijkstra, and K. Postema, “A systematic review of the effects of shoes and other ankle or foot appliances on balance in older people and people with peripheral nervous system disorders,” *Gait Posture*, vol. 25, no. 2, pp. 316–323, Feb. 2007, doi: 10.1016/j.gaitpost.2006.03.010.

[45] F. Moss, L. M. Ward, and W. G. Sannita, “Stochastic resonance and sensory information processing: a tutorial and review of application,” *Clinical Neurophysiology*, vol. 115, no. 2, pp. 267–281, Feb. 2004, doi: 10.1016/j.clinph.2003.09.014.

[46] J. J. Collins, A. A. Priplata, D. C. Gravelle, J. Niemi, J. Harry, and L. A. Lipsitz, “Noise-enhanced human sensorimotor function,” *IEEE Engineering in Medicine and Biology Magazine*, vol. 22, no. 2, pp. 76–83, Mar. 2003, doi: 10.1109/MEMB.2003.1195700.

[47] E. A. Keshner, J. C. Slaboda, L. L. Day, and K. Darvish, “Visual conflict and cognitive load modify postural responses to vibrotactile noise,” *J Neuroeng Rehabil*, vol. 11, p. 6, Jan. 2014, doi: 10.1186/1743-0003-11-6.

[48] L. A. Lipsitz, M. Lough, J. Niemi, T. Travison, H. Howlett, and B. Manor, “A Shoe Insole Delivering Subsensory Vibratory Noise Improves Balance and Gait in Healthy Elderly People,” *Archives of Physical Medicine and Rehabilitation*, vol. 96, no. 3, pp. 432–439, Mar. 2015, doi: 10.1016/j.apmr.2014.10.004.

[49] J. Zhou, L. Lipsitz, D. Habtemariam, and B. Manor, “Sub-sensory vibratory noise augments the physiologic complexity of postural control in older adults,” *Journal of NeuroEngineering and Rehabilitation*, vol. 13, no. 1, p. 44, Dec. 2016, doi: 10.1186/s12984-016-0152-7.

[50] Y. Wang, K. Watanabe, and L. Chen, “Effect of plantar cutaneous inputs on center of pressure during quiet stance in older adults,” *Journal of Exercise Science & Fitness*, vol. 14, no. 1, pp. 24–28, Jun. 2016, doi: 10.1016/j.jesf.2016.02.001.

[51] D. G. Stephen, B. Wilcox, J. B. Niemi, J. Franz, D. C. Kerrigan, and S. E. D’Andrea, “Baseline-Dependent Effect of Noise-Enhanced Insoles on Gait Variability in Healthy Elderly Walkers,” *Gait Posture*, vol. 36, no. 3, pp. 537–540, Jul. 2012, doi: 10.1016/j.gaitpost.2012.05.014.

[52] J. H. Chien, V. N. P. Ambati, C.-K. Huang, and M. Mukherjee, “Tactile stimuli affect long-range correlations of stride interval and stride length differently during walking,” *Experimental Brain Research*, vol. 235, no. 4, pp. 1185-, Apr. 2017.

[53] H. Toda, Y. Hashimoto, and M. Tada, “Vibrotactile Stimulation of Nail of Hallux during Walking: Effect on Center-of-Mass Movement in Healthy Young Adults,” *Applied Sciences*, vol. 10, no. 13, Art. no. 13, Jan. 2020, doi: 10.3390/app10134562.

[54] A. Kavounoudias, R. Roll, and J. P. Roll, “The plantar sole is a ‘dynamometric map’ for human balance control,” *Neuroreport*, vol. 9, no. 14, pp. 3247–3252, Oct. 1998.

[55] C. Thompson, M. Bélanger, and J. Fung, “Effects of plantar cutaneo-muscular and tendon vibration on posture and balance during quiet and perturbed stance,” *Human Movement Science*, vol. 30, no. 2, pp. 153–171, Apr. 2011, doi: 10.1016/j.humov.2010.04.002.

[56] L. Bernard-Demanze, N. Vuillerme, M. Ferry, and L. Berger, “Can tactile plantar stimulation improve postural control of persons with superficial plantar sensory deficit?,” *Aging Clin Exp Res*, vol. 21, no. 1, pp. 62–68, Feb. 2009.

[57] A. Kavounoudias, R. Roll, and J.-P. Roll, “Specific whole-body shifts induced by frequency-modulated vibrations of human plantar soles,” *Neuroscience Letters*, vol. 266, no. 3, pp. 181–184, May 1999, doi: 10.1016/S0304-3940(99)00302-X.

[58] A. Kavounoudias, R. Roll, and J.-P. Roll, “Foot sole and ankle muscle inputs contribute jointly to human erect posture regulation,” *The Journal of Physiology*, vol. 532, no. 3, pp. 869–878, 2001, doi: 10.1111/j.1469-7793.2001.0869e.x.

[59] R. Roll, A. Kavounoudias, and J.-P. Roll, “Cutaneous afferents from human plantar sole contribute to body posture awareness,” *Neuroreport*, vol. 13, no. 15, pp. 1957–1961, Oct. 2002.

[60] A. Karimi-Ahmad Abadi, S. Naghdi, N. N. Ansari, Z. Fakhari, and M. Khalifeloo, “A clinical single blind study to investigate the immediate effects of plantar vibration on balance in patients after stroke,” *Journal of Bodywork and Movement Therapies*, vol. 22, no. 2, pp. 242–246, Apr. 2018, doi: 10.1016/j.jbmt.2017.04.013.

[61] M. Khalifeloo *et al.*, “A study on the immediate effects of plantar vibration on balance dysfunction in patients with stroke,” *J Exerc Rehabil*, vol. 14, no. 2, pp. 259–266, Apr. 2018, doi: 10.12965/jer.1836044.022.

[62] C.-C. Lin *et al.*, “The Use of Vibrotactile Feedback During Dual-Task Standing Balance Conditions in People With Unilateral Vestibular Hypofunction,” *Otology & Neurotology: Official Publication of the American Otological Society, American Neurotology Society [and] European Academy of Otology and Neurotology*, vol. 39, no. 5, pp. e349–e356, 2018, doi: 10.1097/MAO.0000000000001764.

[63] P. Novak and V. Novak, “Effect of step-synchronized vibration stimulation of soles on gait in Parkinson’s disease: a pilot study,” *J NeuroEngineering Rehabil*, vol. 3, no. 1, p. 9, May 2006, doi: 10.1186/1743-0003-3-9.

[64] D. Rugelj, M. Vidovič, and R. Vauhnik, “Sensory Sub- and Suprathreshold TENS Exhibit No Immediate Effect on Postural Steadiness in Older Adults with No Balance Impairments,” *BioMed Research International*, vol. 2020, p. e2451291, Feb. 2020, doi: https://doi.org/10.1155/2020/2451291.

[65] D. C. Gravelle *et al.*, “Noise-enhanced balance control in older adults,” *Neuroreport*, vol. 13, no. 15, pp. 1853–1856, Oct. 2002.

[66] R. Suomi and D. M. Koceja, “Effect of Magnetic Insoles on Postural Sway Measures in Men and Women during a Static Balance Test:,” *Perceptual and Motor Skills*, Aug. 2001, doi: 10.2466/pms.2001.92.2.469.

[67] M. R. Hinman, “Effect of Magnetic Insoles on Balance in Older Adults,” *Journal of the American Geriatrics Society*, vol. 52, no. 1, pp. 166–166, 2004, doi: 10.1111/j.1532-5415.2004.52030_6.x.

[68] J. M. Hijmans, J. H. B. Geertzen, B. Schokker, and K. Postema, “Development of vibrating insoles,” *Int J Rehabil Res*, vol. 30, no. 4, pp. 343–345, Dec. 2007, doi: 10.1097/MRR.0b013e3282f14469.

[69] M. Bagherzadeh Cham, M. A. Mohseni-Bandpei, M. Bahramizadeh, S. Kalbasi, and A. Biglarian, “The effects of vibro-medical insole on sensation and plantar pressure distribution in diabetic patients with mild-to-moderate peripheral neuropathy,” *Clinical Biomechanics*, vol. 59, pp. 34–39, Nov. 2018, doi: 10.1016/j.clinbiomech.2018.08.007.

[70] K. J. Mickle, B. J. Munro, S. R. Lord, H. B. Menz, and J. R. Steele, “Foot shape of older people: implications for shoe design,” *Footwear Science*, vol. 2, no. 3, pp. 131–139, Sep. 2010, doi: 10.1080/19424280.2010.487053.

[71] N. D. J. Strzalkowski, J. J. Triano, C. K. Lam, C. A. Templeton, and L. R. Bent, “Thresholds of skin sensitivity are partially influenced by mechanical properties of the skin on the foot sole,” *Physiological Reports*, vol. 3, no. 6, p. e12425, 2015, doi: 10.14814/phy2.12425.

[72] N. D. J. Strzalkowski, R. L. Mildren, and L. R. Bent, “Thresholds of cutaneous afferents related to perceptual threshold across the human foot sole,” *Journal of Neurophysiology*, vol. 114, no. 4, pp. 2144–2151, Aug. 2015, doi: 10.1152/jn.00524.2015.

[73] P. M. Kennedy and J. T. Inglis, “Distribution and behaviour of glabrous cutaneous receptors in the human foot sole,” *J. Physiol. (Lond.)*, vol. 538, no. Pt 3, pp. 995–1002, Feb. 2002, doi: 10.1113/jphysiol.2001.013087.

[74] R. T. Verrillo, “Age related changes in the sensitivity to vibration,” *J Gerontol*, vol. 35, no. 2, pp. 185–193, Mar. 1980, doi: 10.1093/geronj/35.2.185.

[75] R. T. Verrillo and S. J. Bolanowski, “Effects of temperature on the subjective magnitude of vibration,” *Somatosensory & Motor Research*, vol. 20, no. 2, p. 133, Jun. 2003, doi: 10.1080/089902203100105163.

[76] R. T. Verrillo, “Effect of Contactor Area on the Vibrotactile Threshold,” *The Journal of the Acoustical Society of America*, vol. 35, no. 12, pp. 1962–1966, Dec. 1963, doi: 10.1121/1.1918868.

[77] M. E. Shy *et al.*, “Quantitative sensory testing: report of the Therapeutics and Technology Assessment Subcommittee of the American Academy of Neurology,” *Neurology*, vol. 60, no. 6, pp. 898–904, Mar. 2003, doi: 10.1212/01.wnl.0000058546.16985.11.

[78] N. D. J. Strzalkowski, A. V. Incognito, L. Bent, and P. J. Millar, “Cutaneous mechanoreceptor feedback from the hand and foot can modulate muscle sympathetic nerve activity,” *Front. Neurosci.*, vol. 10, 2016, doi: 10.3389/fnins.2016.00568.

[79] C.-K. Peng, S. V. Buldyrev, S. Havlin, M. Simons, H. E. Stanley, and A. L. Goldberger, “Mosaic organization of DNA nucleotides,” *Phys. Rev. E*, vol. 49, no. 2, pp. 1685–1689, Feb. 1994, doi: 10.1103/PhysRevE.49.1685.

[80] C. -K. Peng, S. Havlin, H. E. Stanley, and A. L. Goldberger, “Quantification of scaling exponents and crossover phenomena in nonstationary heartbeat time series,” *Chaos*, vol. 5, no. 1, pp. 82–87, Mar. 1995, doi: 10.1063/1.166141.

[81] N. Hunt, D. McGrath, and N. Stergiou, “The influence of auditory-motor coupling on fractal dynamics in human gait,” *Scientific Reports*, vol. 4, no. 1, Art. no. 1, Aug. 2014, doi: 10.1038/srep05879.

[82] D. G. Kelty-Stephen and J. A. Dixon, “Temporal correlations in postural sway moderate effects of stochastic resonance on postural stability,” *Human Movement Science*, vol. 32, no. 1, pp. 91–105, Feb. 2013, doi: 10.1016/j.humov.2012.08.006.

[83] C. J. De Luca, “The Use of Surface Electromyography in Biomechanics,” *Journal of Applied Biomechanics*, vol. 13, no. 2, p. 135, May 1997.

[84] K. Stambolieva, D. Petrova, and M. Irikeva, “Positive effects of plantar vibration training for the treatment of diabetic peripheral neuropathy: A pilot study,” *Somatosensory & Motor Research*, vol. 34, no. 2, pp. 129–133, Jun. 2017, doi: 10.1080/08990220.2017.1332585.

[85] F. S. Wanderley, F. Alburquerque-Sendín, N. A. Parizotto, and J. R. Rebelatto, “Effect of Plantar Vibration Stimuli on the Balance of Older Women: A Randomized Controlled Trial,” *Archives of Physical Medicine and Rehabilitation*, vol. 92, no. 2, pp. 199–206, Feb. 2011, doi: 10.1016/j.apmr.2010.10.014.

[86] K. Oku *et al.*, “Immediate effects of plantar vibration stimuli during static upright posture following total hip arthroplasty in females,” *Somatosensory & Motor Research*, vol. 0, no. 0, pp. 1–7, Jun. 2020, doi: 10.1080/08990220.2020.1784129.

[87] S. M. Pincus, “Approximate Entropy as a Measure of System Complexity,” *Proceedings of the National Academy of Sciences of the United States of America*, vol. 88, no. 6, pp. 2297–2301, 1991.

[88] J. S. Richman and J. R. Moorman, “Physiological time-series analysis using approximate entropy and sample entropy,” *American Journal of Physiology-Heart and Circulatory Physiology*, vol. 278, no. 6, pp. H2039–H2049, Jun. 2000, doi: 10.1152/ajpheart.2000.278.6.H2039.

[89] M. Costa, A. L. Goldberger, and C.-K. Peng, “Multiscale Entropy Analysis of Complex Physiologic Time Series,” *Phys. Rev. Lett.*, vol. 89, no. 6, p. 068102, Jul. 2002, doi: 10.1103/PhysRevLett.89.068102.

[90] M. Costa, C.-K. Peng, A. L. Goldberger, and J. M. Hausdorff, “Multiscale entropy analysis of human gait dynamics,” *Physica A: Statistical Mechanics and its Applications*, vol. 330, no. 1, pp. 53–60, Dec. 2003, doi: 10.1016/j.physa.2003.08.022.

[91] J. J. Collins and C. J. De Luca, “Open-loop and closed-loop control of posture: a random-walk analysis of center-of-pressure trajectories,” *Exp Brain Res*, vol. 95, no. 2, pp. 308–318, 1993, doi: 10.1007/BF00229788.

[92] D. Delignières, K. Torre, and P.-L. Bernard, “Transition from Persistent to Anti-Persistent Correlations in Postural Sway Indicates Velocity-Based Control,” *PLOS Computational Biology*, vol. 7, no. 2, p. e1001089, Feb. 2011, doi: 10.1371/journal.pcbi.1001089.

[93] W. E. McIlroy and B. E. Maki, “Preferred placement of the feet during quiet stance: development of a standardized foot placement for balance testing,” *Clin Biomech (Bristol, Avon)*, vol. 12, no. 1, pp. 66–70, Jan. 1997, doi: 10.1016/s0268-0033(96)00040-x.

[94] P. J. Dyck, P. C. O’Brien, J. L. Kosanke, D. A. Gillen, and J. L. Karnes, “A 4, 2, and 1 stepping algorithm for quick and accurate estimation of cutaneous sensation threshold,” *Neurology*, vol. 43, no. 8, pp. 1508–1512, Aug. 1993.

[95] B. Whorley, C. W. Luchies, S. Wilson, and E. Friis, “A Physiology-Based Approach for Detecting Vibration Perception Threshold in the Plantar Foot,” M.S. Thesis, University of Kansas, Lawrence, KS, 2020.

[96] D. L. Miranda *et al.*, “Sensory enhancing insoles improve athletic performance during a hexagonal agility task,” *Journal of Biomechanics*, vol. 49, no. 7, pp. 1058–1063, May 2016, doi: 10.1016/j.jbiomech.2016.02.022.

[97] P. Nichols, C. W. Luchies, H. Fang, and E. Friis, “The Use of Sample Entropy and Fuzzy Sample Entropy to Analyze Somatosensory Deficit in the COP of Quiet Standing,” Thesis, University of Kansas, Lawrence, KS, 2020.

[98] M. Weilert, C. W. Luchies, H. Fang, and S. Shontz, “The Application of Detrended Fluctuation Analysis and Adaptive Fractal Analysis on Center of Pressure Time Series in Parkinson’s Disease,” Thesis, University of Kansas, Lawrence, KS, 2017. Accessed: May 21, 2021. [Online]. Available: https://kuscholarworks.ku.edu/handle/1808/25868

Appendices

Chapter 2 Appendix

Table 10: Summary of vibratory studies at the feet

Year & Ref	Design	Output	Participants & Conditions	Postural Stability Measures	Vibratory Significant Results
1998 [54]	• Vibrating mat • Heel, and metatarsals • Electromagnetic indenters type 201 (Ling Dynamic Systems) • Thickness does not apply • Metallic • Adjustable sizes	• Suprathreshold • Sinusoidal • Custom-built amplifier	• 10 healthy adults (38.5 years) • 10 vibrations at 100 Hz while standing: heel or metatarsal per foot (4x), heels, metatarsals, all left, all right, both feet, and no vibration.	3-second COP at 500 Hz while standing with eyes closed • Average direction and magnitude (i.e., polar coordinates)	• Vibration made humans sway in opposite direction to the point where vibration was applied (i.e., anterior-right vibration made humans sway towards the posterior-left direction) • Vibration in both feet using all motors increased sway; however, it did not have a defined direction.
1999 [57]	• Refer to [54]	• Refer to [54]	• 9 healthy adults (38.5 years) • While standing, no vibration, both metatarsals, both heels, and all motors at 20 Hz, 60 Hz and 100 Hz	3-second COP at 500 Hz while standing with eyes closed • Average position and velocity	• Vibration created an opposite sway (i.e., frontal vibration made subjects leaned back) that increases as frequency increases • Reaction time on sway from vibration was 0.9 ± 0.4 seconds
2001 [25]	• Vibrating mat • Forefoot • 3-mm diameter indenters • Thickness does not apply • Metallic • Adjustable sizes	• Suprathreshold • Sinusoidal (0.05, 0.1, 0.2 and 0.4 Hz) • Custom-built amplifier	• 8 healthy young (36.6 years) • 4 vestibular deficiency subjects (35 years) • 0.05/0.1/0.2/0.4 Hz indentations while standing • 0.05/0.1/0.2/0.4 Hz ground tilt (+/- 2 degrees) while standing • In-phase/constant/ counter-phase ground tilt while standing	Undefined duration of AP hip and shoulder position, and undefined duration of COP were used to calculate: • Phase • Gain	• None

Table 10: Summary of vibratory studies at the feet

Year & Ref	Design	Output	Participants & Conditions	Postural Stability Measures	Vibratory Significant Results
2001 [58]	• Refer to [54]	• Refer to [54]	• 9 healthy adults (38 years) • Control (no vibration) and all 24 frequency combinations (20, 40, 60, and 80 Hz) of vibration at the tibialis anterior and metatarsals while standing	3-second COP at 500 Hz while standing with eyes closed • Average (AP and ML) 3-second EMG from the soleus and tibialis anterior at 1000 Hz while standing with eyes closed • Average of Tibialis - Soleus	• Vibration created an opposite sway (i.e., metatarsal vibration made subjects leaned back, tibialis vibration made subjects leaned forward). • EMG and COP activity happened first than body angle (i.e., after a vibration, muscle and COP activity reacted first than ankle angle). • When tibialis and metatarsal vibration happened at the same time, the input with the highest vibration dominated the body reaction.
2002 [16]	• Vibrating mat • Entire feet's soles • 3.2-mm diameter nylon indenters • Box of undefined thickness • Metallic or another strong material that could hold an adult • Adjustable sizes	• Subthreshold (90%) • Random/White (100 Hz) • Power amplifiers + Linear actuators + Signal generator	• 16 healthy old (72 years) • 14 healthy young (23 years) • Yes/no vibration while standing	30-second shoulder position while standing with eyes closed • Mean radius • Swept area • Maximum radius • Range (AP and ML) • SDA's critical value, short-term and long-term diffusion coefficients	• When the old and young groups are combined, it is found that vibration reduced mean radius, swept area and AP range.

Table 10: Summary of vibratory studies at the feet

Year & Ref	Design	Output	Participants & Conditions	Postural Stability Measures	Vibratory Significant Results
2002 [59]	• Vibrating mat • Heels, metatarsals, and lateral side of the feet • 30 micro-vibrators per foot • Undefined thickness • Undefined material • No adjustable sizes	• Suprathreshold • Sinusoidal (0-100 Hz) • Custom-built amplifier	• 10 healthy adults (37.5 years) • Control (no vibration) and 5 vibrating conditions: both metatarsals, both heels, all left, all right, and both feet while standing	13-second COP while standing with eyes closed and immobilized at the hips and shoulders • Average direction and magnitude (i.e., polar coordinates)	• Vibration made subjects sway towards the vibration application point (i.e., metatarsal vibration made subjects leaned forward).
2003 [17]	• Shoe insole • Heel, first, and fifth metatarsal • C-2 Tactors (Engineering Acoustics, FL) • 16-mm thick • Silastic T-2 Moldmaking Rubber • No adjustable sizes	• Subthreshold (90%) • Random/White (0-100 Hz) • Noise generator ISD2560P (Winbound Electronics, Taiwan)	• 12 healthy old (73 years) • 15 healthy young (23 years) • Yes/no vibration while standing	• Refer to [16]	• When the old and young groups are combined, vibration reduced all parameters except for the long-term diffusion coefficient • The interaction of vibration and subject group reduced the ML range and critical value
2006 [22]	• Refer to [17]	• Refer to [17]	• 15 subjects with diabetic neuropathy (60 years) • 15 post-stroke subjects (61 years) • 12 healthy old (73 years) • Yes/no vibration while standing	• Refer to [16]	• Vibration reduced all extracted measures (Mean radius, Swept area, Maximum radius, AP and ML Range, and SDA's critical value, short-term and long-term diffusion coefficients) for everybody. • For diabetic and stroke participants, vibration reduced the short-term and long-term diffusion coefficients.

Table 10: Summary of vibratory studies at the feet

Year & Ref	Design	Output	Participants & Conditions	Postural Stability Measures	Vibratory Significant Results
2006 [63]	• Shoe insole • Heel, first, and fifth metatarsals • Optect 2890W11 (Optec Co., Japan) • Dr. Scholl's massaging gel insoles thickness • Dr. Scholl's massaging gel insoles material • Adjustable sizes	• Suprathreshold • Sinusoidal (70 Hz) • Custom-built amplifier	• 8 Parkinson's disease subjects (61.4 years) • 8 healthy adults (58.9 years) • Yes and no vibration while walking and while the feet were in contact with the ground (i.e., step synchronized vibration)	6-minute walks with eyes open at the subject's speed were used to identify walking distance, velocity, cadence, stride length, as well as the duration and coefficient of variation of the stride, stance, swing and double support • Average	• In PD subjects, vibration improved walking distance, velocity, cadence, all stride measures, and stance duration • In healthy subjects, vibration improved walking distance, speed, and stride coefficient of variance. • Vibration and group influenced walking distance, velocity, stride coefficient of variance, and stance duration.
2007 [11]	• Refer to [17]	• Refer to [17]	• Refer to [17]	30-second shoulder position while standing with eyes closed • Multiscale SampEn (m=2, r=0.15) 30-second COP velocity at 60 Hz • Multiscale SampEn (m=2, r=0.15)	• Vibration increased multiscale SampEn in healthy old's COP and COP velocity for both directions (AP and ML).
2008 [21]	• Shoe insole • Heel, first, and fifth metatarsal • EPZ35-MS29, 35-mm diameter (Karl/Heinz Mauz GMBH, Germany) • 6-mm thick • Cork and leather • Adjustable sizes	• Subthreshold (90%) • Random/White (25-500 Hz) • Custom-built amplifier + LabVIEW and USB-DAQ (National Instruments)	• 17 subjects with diabetic neuropathy (52.1 years) • 15 healthy old (51.8 years) • Yes/no vibration while standing • Yes/no cognitive task defined as eyes closed and subtracting numbers	25-second COP at 100 Hz while standing • Mean velocity • Curve length • RMS (AP and ML)	• Vibration during the cognitive test reduced the mean COP velocity and the AP RMS for the diabetic group

Table 10: Summary of vibratory studies at the feet

Year & Ref	Design	Output	Participants & Conditions	Postural Stability Measures	Vibratory Significant Results
2009 [15]	• Shoe insole • Heel, first, and fifth metatarsal • C-2 tactors (Engineering Acoustics, FL) • Thickness larger than 9 mm • Commercial sandals' material • Adjustable sizes	• Subthreshold (90%) • Random/White (100 Hz) • Engineering Acoustics controller (Engineering Acoustics, FL)	• 18 old fallers (77 years) • 18 healthy old (78 years) • 12 healthy young (26 years) • Yes/no vibration while walking	3-minute walks with eyes open at the subject's speed were used to identify heel-strike and toe-liftoff events, which were used to extract timing of stride, stance, and swing phase • Standard deviation	• Vibration on old fallers reduced the standard deviations of stride time, stance time and swing time. • Vibration on healthy old reduced the standard deviations of stride time and stance time
2009 [56]	• Vibrating mat • Medial arch region • Rotating ball bearings (Remington FM 3000) • Remington FM 3000 dimensions • Remington FM 3000 material • Adjustable sizes	• Suprathreshold • Sinusoidal (5 Hz) • Remington FM 3000 controller	• 8 healthy young (30.3 years) • 13 healthy old (64.6 years) • 9 old subjects with plantar sensory deficiency (64.2 years) • Before/after 10-minute vibration while subjects were sitting on a chair	32-second COP at 64 Hz while standing with eyes open • 90% ellipse • Mean velocity • RMS (AP and ML)	• Vibration reduced sway area and RMS ML for the old subjects with plantar sensory deficiency.
2011 [20]	• Refer to [17]	• Subthreshold (90%) • Suprathreshold (120%) • Random/White (100 Hz) • Noise generator ISD2560P (Winbound Electronics, Taiwan)	• 6 old construction workers (51.2 years) • 6 young construction workers (27.2years) • No/subthreshold/ suprathreshold vibration while standing • Normal/semi-tandem stance • Eyes open/closed	30-second shoulder position at 10 Hz while standing • Mean velocity (AP and ML) • SDA's critical value, short-term and long-term diffusion coefficients (ML and Radial) 30-second trunk angular position at 10 Hz • Range (ML and Radial)	• Sensory threshold was larger for the old group than for the young group • Subthreshold vibration increased the ML critical value for everybody during semi-tandem stance. • Suprathreshold vibration increased Radial sway velocity, ML and Radial critical values, Radial short-term diffusion coefficient, and ML and Radial trunk range for everybody during semi-tandem stance.

Table 10: Summary of vibratory studies at the feet

Year & Ref	Design	Output	Participants & Conditions	Postural Stability Measures	Vibratory Significant Results
2011 [55]	• Shoe insole • Heel, metatarsals and Achilles tendon • Eccentric rotating motors • Undefined thickness • Undefined material • Adjustable sizes	• Suprathreshold • Sinusoidal (80 Hz) • Custom-built amplifier	• 12 healthy young (26.8 years) • All combinations of vibration while standing at Achilles, metatarsal, and heel in either no, thumbs up or down surface tilt	14-second COP (AP), COM (AP), and angles of trunk, hips, knees and ankles at 10 Hz while standing with eyes closed • Average	• During no surface tilt, vibration at the Achilles and heels made subject leaned backwards and forwards respectively. • During toes up surface tilt, vibration at the Achilles reduced COP and increased COM. • During toes down surface tilt, vibration reduced the angle motion of hips and knees.
2012 [18]	• Shoe insole • Heel, first, and fifth metatarsal • Eccentric rotating motors • Undefined thickness • Commercial insoles • Adjustable sizes	• Subthreshold • Random/White • Custom-built controller and noise generator	• 26 old fallers (83.3 years) • 16 healthy young (25.2 years) • Before/after 10-minute vibration while walking	65-second COP at 40 Hz while standing without shoes and with eyes open • DFA and α (n_{min}=5, n_{max}=N/4) (AP and ML)	• When the first 30 seconds of data are used, vibration reduced α (i.e., from brownish to pinkish) on old fallers.
2012 [19]	• Shoe insole • Heel, first, and fifth metatarsal • Eccentric rotating motors • Undefined thickness • Commercial insoles • Adjustable sizes	• Undefined threshold level • Undefined color • Custom-built controller and noise generator	• 26 old fallers (84.1 years) • Before/after 6-minute vibration while walking	60-second COP at 31.25 Hz while standing with eyes open • Multiscale SampEn (AP and ML) • Multivariate multiscale SampEn	• Vibration increased the multivariate multiscale SampEn (i.e., added complexity).
2012 [51]	• Refer to [15]	• Subthreshold (90%) • Random/White (0-100 Hz) • LabVIEW controller (National Instruments, TX)	• 29 healthy old (71.9 years) • Yes/no vibration while walking	30-second walks at 1.4 m/s on a treadmill were recorded with force plates and motion capture, and step width and length were extracted • Coefficient of variance	• Post-vibration coefficient of variance has a negative correlation with pre-vibration (i.e., subjects with low coefficient of variance increase their variability, and vice versa)

Table 10: Summary of vibratory studies at the feet

Year & Ref	Design	Output	Participants & Conditions	Postural Stability Measures	Vibratory Significant Results
2013 [24]	• Motor taped to body • Heel and Achilles tendon • Indenter motors • Thickness does not apply • Material does not apply • Adjustable sizes do not apply	• Subthreshold and/or suprathreshold • Sinusoidal (90 Hz) • Custom-built amplifier	• 17 stroke subjects (53.31 years) who did physical therapy with vibration • 17 stroke subjects (55.73 years) who did physical therapy without vibration • Before/after physical therapy training (i.e., 30-minute sessions, 5x per week, for 6 weeks) • Eyes open/closed	30-second COP while standing • Average (AP) • Mean velocity (AP) 3-meter walk with eyes open was used to extract gait speed, cadence, paretic sidestep length and single limb support time • Average	• Vibration reduced all sway measures (eyes open and closed) when both groups were analyzed together, as well as when each group was analyzed separately. • Vibration increased all gait measures when both groups were analyzed together, and all gait measures (except step length) when each group was analyzed separately. • Vibration increased all physical therapy's benefits.
2014 [47]	• Shoe insole • Heel, first and fifth metatarsal • DC vibrating motors • Thickness of commercial sandals • Material of commercial sandals • Adjustable sizes	• Subthreshold (90%) • Random/White (10-55 Hz) • MATLAB noise generator + Custom-built amplifier	• 21 healthy young (24.5 years) • Eyes closed/open with virtual reality • Before/during/after vibration whiles standing • Yes/no mental calculation	20-second COP and COM at 200 Hz while standing on 6.5-cm foam • 95% ellipse area • RMS (AP and ML) • AppEn (AP and ML)	• COP and COM areas and ML entropies were reduced for eyes closed and no mental calculation when before and during vibration were compared. • COP and COM AP RMS were increased for eyes closed and no mental calculation when during and after vibration were compared.

Table 10: Summary of vibratory studies at the feet

Year & Ref	Design	Output	Participants & Conditions	Postural Stability Measures	Vibratory Significant Results
2015 [14]	• Vibrating mat • Heel, first, and fifth metatarsal • C-2 tactors (Engineering Acoustics, FL) • Thickness larger than 9 mm • Silicone (Shore A50) • Adjustable sizes	• Subthreshold (90%) • Sinusoidal + Random/White noise (1-500 Hz) • Engineering Acoustics controller (Engineering Acoustics, FL)	• 9 healthy old (78.6 years) • 10 healthy young (25.1 years) • Yes/no vibration while standing	20-second COP at 100 Hz while standing with eyes open. Surrounding moved in-phase with the subject's sway • Equilibrium score • Curve length (AP) • AppEn (AP) • Strategy score	• Sensory threshold was larger for the old group than for the young group • When motors were ON, no significant differences were found in curve length and equilibrium score between the old and young groups. • Vibration reduced curve length and equilibrium score in the old group. • Vibration increased strategy score in the old group.
2015 [48]	• Shoe insole • Medial arch region • Two 2.5-cm diameter piezoelectric actuators • Thickness of commercial insoles • Urethane foam with double electrical insolation • Adjustable sizes	• Subthreshold • Random/White (0-100 Hz) • Custom-built noise generator and amplifier	• 12 healthy old (77.5 years) • 0%/70%/85% vibration while standing or walking • Eyes open/closed	60-second COP while standing • Mean velocity • 95% ellipse area • Average (AP and ML) 4.9-walks at the subject's speed were used to extract gait speed, stride time (left and right), step width and double support time • Average • Coefficient of variation TUG test time	• Vibration for both visual conditions reduced sway area and ML COP average. • Vibration reduced TUG time, average stride time (left), stride time coefficient of variation (left and right), and double support time coefficient of variation. • There were not differences between 70% and 85% vibration.

Table 10: Summary of vibratory studies at the feet

Year & Ref	Design	Output	Participants & Conditions	Postural Stability Measures	Vibratory Significant Results
2016 [12]	• Refer to [14]	• Subthreshold (90%) • Random/White (1-500 Hz) • Engineering Acoustics controller (Engineering Acoustics, FL)	• 10 healthy young (25.1 years) • 10 healthy old (78.6 years) • Yes/no vibration while standing	20-second COP at 100 Hz while standing with eyes open and performing cognitive test (listen and repeat words) • Integrated time-to-boundary (AP) • RMS (AP) • AppEn (m=2, r=0.2) (AP) • Equilibrium score • Curve length (AP and ML) • Absolute maximum (AP and ML) • Strategy score	• Sensory threshold was larger for the old group than for the young group
2016 [13]	• Refer to [14]	• Refer to [12]	• Refer to [12]	3-second COP at 100 Hz while standing with eyes open. Force plate translated backwards for a distance scaled to each subject's height • Curve length (AP) • Temporal latency • Absolute maximum (AP)	• Sensory threshold was larger for the old group than for the young group
2016 [28]	• Refer to [48]	• Subthreshold (90%) • Random/White (0-100 Hz) • Custom-built noise generator and amplifier	• 27 healthy recreational athletes (22.4 years) • Baseline, max effort (fatigue based) and post-max effort • Yes/no vibration while walking	1-minute walks (1.1 m/s) recorded with motion capture at 120 Hz were used to extract double support time, as well as stride time, length and width • Average • Coefficient of variance	• Vibration increased the coefficient of variance for stride width in all conditions (baseline, max and post).

Table 10: Summary of vibratory studies at the feet

Year & Ref	Design	Output	Participants & Conditions	Postural Stability Measures	Vibratory Significant Results
2016 [49]	• Refer to [48]	• Subthreshold • Random/White (0-100 Hz) • Custom-built noise generator and amplifier	• 12 healthy old (73.8 years) • 0%/70%/85% vibration while standing • Eyes open/closed	60-second COP at 240 Hz while standing • Multiscale SampEn (m=2, r=0.15) (AP and ML) • Mean velocity • 95% ellipse area TUG test time	• Sensing threshold and TUG time had a negative correlation with ML multiscale SampEn • Vibration (70% and 85%) increased ML multiscale SampEn when compared to no vibration
2016 [50]	• Motor between force plate and feet soles • Heel • 26.5-mm diameter coin motor • Thickness does not apply • Material does not apply • Adjustable sizes	• Suprathreshold by inducing pressure point (i.e., increasing height of motor) • Sinusoidal • Custom-built amplifier	• 8 healthy old (72.3 years) • Yes/no vibration while standing	30-second COP at 1000 Hz while standing with eyes closed • 95% ellipse • Mean velocity (AP and ML) • Rambling and trembling (AP and ML)	• Vibration reduced the 95% ellipse area, mean velocity (AP and ML), and the AP trembling.
2017 [52]	• Shoe insole • Heel, first, and fifth metatarsal • C-2 tactors (Engineering Acoustics, FL) • Thickness of commercial insoles • Material of commercial insoles • Adjustable sizes	• Sub and suprathreshold • Sinusoidal • Engineering Acoustics controller (Engineering Acoustics, FL)	• 10 healthy adults • No vibration and all combination of 30, 150, and 250 Hz frequencies with 8, 12, and 17.5 dB amplitudes while walking	5-minute walks on a treadmill at the subject's speed recorded by motion capture at 100 Hz and by force plates at 300 Hz, were used to extract stride length and interval • Standard deviation • DFA and α (n_{min}=4, n_{max}=N/4)	• For stride length, vibration at 250 Hz increased α when compared to 30 Hz and 150 Hz (i.e., from whiteish to pinkish). • For stride interval, vibration at 12 dB increased α when compared to 8 dB and 17.5 dB (i.e., from whiteish to pinkish). • For stride interval, vibrations at 250Hz/12dB, 250Hz/17.5 dB and no vibration were different in terms of α. In fact, 250Hz/12dB approached pinkness, while 250Hz/17.5dB approached whiteness.

Table 10: Summary of vibratory studies at the feet

Year & Ref	Design	Output	Participants & Conditions	Postural Stability Measures	Vibratory Significant Results
2018 [10]	• Shoe insole • Heel, first and fifth metatarsal, and under big toe • 6-mm cylindrical motors (Korea) • 11 to 17 mm thick • Silicone (Shore A55) with 1-mm leather top layer • Adjustable sizes	• Subthreshold (90%) • Random/White (40-120 Hz) • Arduino Nano (Arduino LLC, MA) + MATLAB (MathWorks, MA)	• 2 healthy old (70 years) • 2 healthy young (28.5 years) with feet under hypothermic anesthesia • Eyes open/closed • Single/dual stance • Yes/no vibration while standing	25-second COP at 100 Hz while standing • Stability Index TUG test time	• Vibration reduced the healthy old's stability index (i.e., improvement) for all conditions, except single stance with eyes closed. • Vibration reduced the healthy old's TUG time.
2018 [60]	• Vibrating mat • Heel and metatarsals • Undefined vibrating devices • Width x Length x Height = 30 x 45 x 20 cm • Undefined polymer • No adjustable sizes	• Suprathreshold • Sinusoidal (100 Hz) • Custom-built amplifier	• 22 post-stroke subjects (55.8 years) • Before vibration and after yes/no 5-minute vibration	Postural scales • Mini-BESTest • Ankle flexor spasticity MMAS • Ankle dorsiflexion PROM	• Vibration improved all scales more with respect to the baseline when compared to the change made by the no vibration with respect to the baseline.
2018 [61]	• Refer to [60]	• Refer to [60]	• 18 post-stroke subjects (26 years) • Before/After 5-minute vibration • Eyes open/closed (only for COP)	20-second COP at 100 Hz while standing • Mean velocity • Average (AP and ML) • Surface area Postural scales • TUG test time • Functional reach test • Ankle flexor spasticity MMAS • Ankle dorsiflexion PROM	• Vibration reduced TUG test time.

Table 10: Summary of vibratory studies at the feet

Year & Ref	Design	Output	Participants & Conditions	Postural Stability Measures	Vibratory Significant Results
2019 [23]	• Shoe insole • Heel, first and fifth metatarsal • Vibrating micro-motors • Undefined thickness • Undefined material • Adjustable sizes	• Subthreshold (90%) • Random/White (0-200 Hz) • Custom-built controller and signal generator	• 29 diabetic subjects (84.3 years) • Before/immediately after/15 minutes after a siting 14-minute vibration	25.6-second COP while standing with eyes closed • 95% ellipse • Average (AP and ML) • Mean COP velocity • COP velocity variance TUG test time	• None
2020 [26]	• Shoe insole • Heel, first, and fifth metatarsal • Miniature actuators • Undefined thickness • HI-POLY foam • Adjustable sizes	• Subthreshold • Random/White (0-120 Hz) • Custom-built controller and signal generator	• 14 healthy young (23.9 years) • No vibration + No ice/No vibration + Yes ice/Yes vibration + Yes ice	60-second COP while standing with one leg and eyes open • 95% ellipse • Curve length • Mean velocity 60-second EMG at medial gastrocnemius, tibialis anterior, peroneus longus, and extensor digitorum longus while standing with one leg and eyes open • RMS	• Vibration reduced all COP measures and the tibialis anterior activity when standing on ice without and with vibration are compared, as well as vibration tended to bring all COP measures and the tibialis anterior activity back to their natural state (i.e., No vibration or ice). • Regression fits between COP area and muscle activity shows that vibration tended to bring subjects back to their natural state.

Table 10: Summary of vibratory studies at the feet

Year & Ref	Design	Output	Participants & Conditions	Postural Stability Measures	Vibratory Significant Results
2020 [27]	• Shoe insole • Heel (x2), first, and fifth metatarsals • Piezoelectric actuators (Disc Benders-Bimorphs Model 20-2225) • Thickness of commercial insoles • Material of commercial insoles • Adjustable sizes	• Subthreshold (90%) • Sinusoidal (1-350 Hz) • Custom-built controller (app in cellphone) and amplifier	• 21 healthy young (27 years) • Before/after inclined walking fatigue • Yes/no vibration while standing	30-second COP at 100 Hz while standing on non-dominant leg with eyes open • DFA and α (n_{min}=5, n_{max}=N/4) on planar displacement COP • 95% ellipse	• After fatigue, vibration reduced ellipse area and brough it closer to the value before the fatigue. In fact, after fatigue and no vibration yielded a larger area when compared to yes and no vibration before fatigue. • After fatigue, vibration kept the baseline (i.e., before fatigue) α. In fact, after fatigue and no vibration, α was reduced when compared to the baseline, and when compared to after fatigue with vibration (i.e., reduced it from pinkish to whitish).
2020 [53]	• Motor taped on body • Foot's big toenail • LD14-002, Nidec Copal Co., Japan • Thickness does not apply • Material does not apply • Adjustable sizes	• Subthreshold • Sinusoidal (150 Hz) • Custom-built controller (app in tablet) and DRV2605 amplifier	• 13 healthy young (23.8 years) • Yes and no vibration while walking and while the feet were in contact with the ground (i.e., step synchronized vibration)	10-meters walks at subject's speed recorded by motion capture at 200 Hz and by force plates at 1000 Hz, were used to extract walking speed, stance time, and COM displacement in the vertical, progression and lateral directions. • Average • Coefficient of variation	• Vibration reduced average walking speed and COM in the progression direction. • When change due to vibration is plotted vs. initial without vibration for the coefficient of variation walking speed, stance time and COM in the lateral direction, a negative correlation is found (i.e., subjects with low initial coefficient of variation increase variation and vice versa).

Listed ages correspond to the average of all ages across a group
Abbreviations: TUG = Timed Up and Go.

Chapter 3 Appendix

Cost Breakdown

The approximate cost of materials for the most-reported vibratory insoles (USD $4,314.50) is broken down in Table 11. From the papers that reference the most-reported vibratory device, it is not possible to know the actual cost for the vibratory insoles, since their specific suppliers are not known. All listed costs are based on quotes and information obtained throughout the period of the project (2018 - 2020).

Table 11: Cost breakdown for most-reported vibratory device

Part	Explanation	Cost
Shore A50 Silicone	The cost for 16 lbs of Shore A50 Silicone (https://shop.smooth-on.com/reoflex-50) is $117.88 and its specific volume is 27.4 in^3/lb. Assuming a rectangular area for a large shoe insole (12 in x 5 in), and a thickness of 10 mm (i.e., enough to cover C-2 Tactors whose thickness is 7.9 mm), the volume per insole is 23.62 in^3. This means that the weight for both insoles is 1.724 lbs = 2 × 23.62 in^3 ÷ 27.4 in^3/lb, which yields the cost of silicone for both vibratory insoles to $12.70 = 1.724 lbs × $117.88/16 lbs.	$12.70
Soft Layer	The cost for a sheet of soft-cushioning foam (Thickness = 1/16 in) with dimensions 24 in x 24 in is $3.59 (https://www.mcmaster.com/8722K6/). Knowing that each insole's area is around 12 in x 5 in, only half of the raw material's area is needed for a set of 2 insoles. This means that the total cost for the soft layer is $1.80.	$1.80
Motors	According to a quote from Engineering Acoustics provided on February 8, 2018, each C-2 Tactor was prized at $210.00. This means that 6 C-2 Tactors (Heel, 1st and 5th metatarsal for two insoles) would cost $1,260.00.	$1,260.00
Controller	According to a quote from Engineering Acoustics provided on February 8, 2018, the cost for the Universal Controller and TAction Creator Software are respectively $2,350.00 and $690.00. This yields a total cost for the controller equal to $3,040.00.	$3,040.00

The total cost of materials for the new and proposed vibratory mat (USD $1,062.83) is broken down in Table 12. All listed costs are based on quotes and information obtained throughout the period of the project (2018 - 2020).

Table 12: Cost breakdown for new and proposed vibratory device

Part	Explanation	Cost
Shore A50 Silicone	The cost for 16 lbs of Shore A50 Silicone (https://shop.smooth-on.com/reoflex-50) is $117.88 and its specific volume is 27.4 in^3/lb. Knowing that the dimensions of the vibratory mat are 19.5 in x 15 in x 10 mm, the volume of the mat is 115.16 in^3. This means that the weight of the vibratory mat is 4.203 lbs = 115.16 in^3 ÷ 27.4 in^3/lb, which yields the cost of silicone for the mat to $30.96 = 4.203 lbs × $117.88/16 lbs.	$30.96
Cork Layer	The cost for a sheet of cork (Thickness = 1/32 in) with dimensions 12 in x 36 in is $14.54 (https://www.mcmaster.com/9607K61/). Knowing that a 12 in x 36 in sheet will be mostly used to cover the area of the vibratory mat (19.5 in x 15 in), the total cost for the cork layer is assumed to be $14.54.	$14.54
Soft Layer	The cost for a sheet of soft-cushioning foam (Thickness = 1/16 in) with dimensions 24 in x 24 in is $3.59 (https://www.mcmaster.com/8722K6/). Knowing that a 24 in x 24 in sheet will be mostly used to cover the area of the vibratory mat (19.5 in x 15 in), the total cost for the soft layer is assumed to be $3.59.	$3.59
Motors	To manufacture the complete vibratory mat which includes 4 sets of eccentric rotating motors (307-105, 310-003, 306-10H and 307-103 from Precision Microdrives, UK), and three different shoe sizes per set of motors (Short, Middle and Long), 14 motors are needed per set. The 14 motors per set consist of 2 heels, and three sets (Short, Middle and Long) of 2 1st metatarsals and 2 5th metatarsals. With that said, the unit costs for the motors 307-105 (https://www.precisionmicrodrives.com/product/307-105-7mm-vibration-motor-2mm-type), 310-003 (https://www.precisionmicrodrives.com/product/310-003-10mm-vibration-motor-3mm-type), 306-10H (https://www.precisionmicrodrives.com/product/306-10h-7mm-vibration-motor-25mm-type), and 307-103 (https://www.precisionmicrodrives.com/product/307-103-9mm-vibration-motor-25mm-type) are respectively $6.89, $7.85, $9.68 and $8.54. These costs when added and multiplied by 14 yields $461.44.	$461.44
Controller	The parts needed to manufacture the controller are: • Large Breadboard (x1) at $19.95 (https://www.adafruit.com/product/443) • Arduino UNO (x6) at $23.00 (https://store.arduino.cc/usa/arduino-uno-rev3?gclid=Cj0KCQiAzZL-BRDnARIsAPCJs73x5w46QOBMSWtf3cXUehXQXE4XKJF1euucnWlZf38SmAaXUkYT4TAaAsQlEALw_wcB) • DRV2605 Chips (x6) at $7.95 (https://www.adafruit.com/product/2305?gclid=Cj0KCQiAzZL-BRDnARIsAPCJs71VHIXW5wN3dSIas8pfQyquwEkKeyP21yE6zAdeJyzINLwRyv1flTwaAvdpEALw_wcB) • Push Buttons (x3) at 1.60 for 4 (https://www.sparkfun.com/products/14460) • 3-Pin Switches (x2) at 1.50 (https://www.sparkfun.com/products/102) • Potentiometers (x5) at $0.95 (https://www.sparkfun.com/products/9806) • Wires (x1) at $15.95 (https://www.adafruit.com/product/1311) • PCB Board (x1) at $19.95 for 3 (https://www.adafruit.com/product/590)	$232.45

External Housing	The parts needed to manufacture the external housing of the vibratory mat are: • BNC Wall Mount (x62) at $2.247 (https://www.digikey.com/en/products/detail/amphenol-rf-division/031-10-RFXG1/2643384?utm_adgroup=Connectors%20and%20Interconnects&utm_source=google&utm_medium=cpc&utm_campaign=Shopping_Supplier_Amphenol%20RF_0115_Co-op&utm_term=&utm_content=Connectors%20and%20Interconnects&gclid=Cj0KCQiAzZL-BRDnARIsAPCJs70wIIXagbPvcqk-WEiwCJL9tcHaPz9rG5webq7hRiXNxDijuUsTw5oaAiA-EALw_wcB) ○ 56 for all the inputs in the external housing, and 6 for the outputs of the controller • Male-Male BNC Cord 10’ (x6) at $16.59 (https://www.digikey.com/en/products/detail/tpi-test-products-int/58-120-1M/268027?s=N4IgjCBcoLQdIDGUAuAnArgUwDQgPZQDaIATAJwAMIAugL516nEgCsAHHKZXALK10gA) • Angle Steel 1/8” x 1.5” x 36” (x1) at $11.99 (https://www.menards.com/main/hardware/sheet-metal-rods/hillman-reg-steel-angle/11707/hardware/sheet-metal-rods/hillman-reg-steel-angle/11697/hardware/sheet-metal-rods/hillman-reg-steel-angle/11709/p-1444432405334.htm) • Angle Steel 1/8” x 1.5” x 72” (x1) at $13.99 (https://www.menards.com/main/hardware/sheet-metal-rods/hillman-reg-steel-angle/11707/hardware/sheet-metal-rods/hillman-reg-steel-angle/11697/hardware/sheet-metal-rods/hillman-reg-steel-angle/11709/hardware/sheet-metal-rods/hillman-reg-steel-angle/11711/p-1444432400703.htm) • Sheet Metal Gauge 16 24” x 48” at $54.99 (https://www.menards.com/main/hardware/sheet-metal-rods/hillman-reg-steel-plain-sheet-metal/11758/hardware/sheet-metal-rods/hillman-reg-steel-plain-sheet-metal/11769/hardware/sheet-metal-rods/hillman-reg-steel-plain-sheet-metal/11779/hardware/sheet-metal-rods/hillman-reg-steel-plain-sheet-metal/11769/p-1444432403703.htm)	$319.85

Wiring Diagram

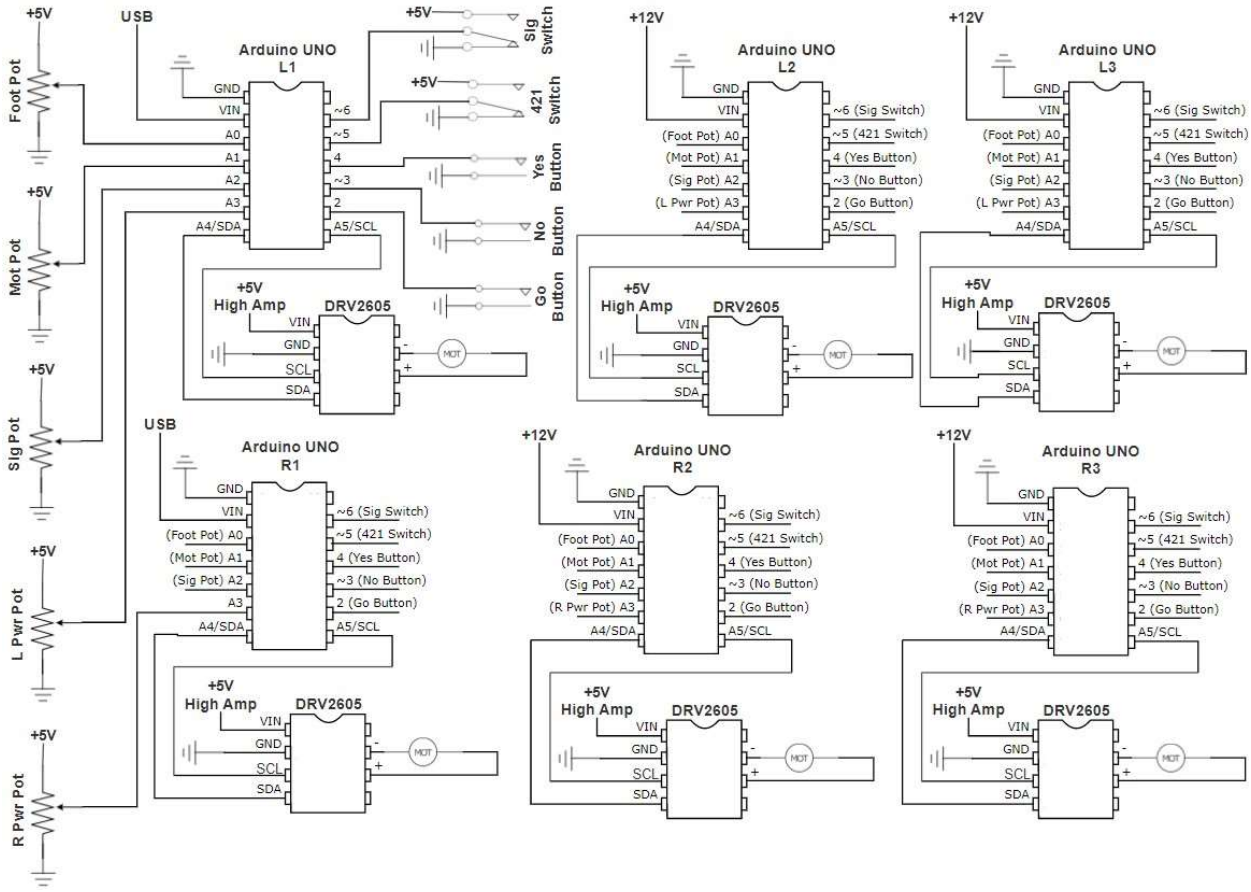

Figure 23: New vibratory mat's wiring diagram

Abbreviations: Pot = Potentiometer, Mot = Motor, Sig = Signal, L = Left, R = Right, Pwr = Power

Figure 23 shows the wiring diagram needed to operate the Arduino codes, and thus the vibratory mat. The Arduino UNOs L1 and R1 are powered by an USB connection that offers Serial Print messages that guide the operation of the vibratory mat. However, if an USB connection and Serial Print messages are not desired, Arduino UNOs L1 and R1 can be powered with 12V (i.e., same power supply used for the other Arduino UNOs). The 5V High Amp used to power the vibratory components' drivers require more amperage when compared to the 12V and 5V power suppliers that operate the Arduino UNOs and hardware (i.e., potentiometers and buttons). It is recommended that the 5V High Amp power supply allows amperage levels up to 200 mA, since the motor 307-103 (strongest motor) can draw up to 180 mA when is at full capacity.

Arduino Codes

The codes that need to be uploaded to the three Arduino UNOs that control the left foot's vibrating components (Arduino_Left_Master.ino), and three Arduino UNOs that control the right foot's vibrating components (Arduino_Right_Master.ino) are given below. In both codes, motors labeled as Mini, Small, Medium and Large correspond respectively to 307-105, 310-003, 306-10H and 307-103.

Arduino_Left_Master.ino

```
/*
 * Master Arduino Code - Left Foot
 * University of Kansas - Biodynamics Lab
 * Written by Camilo Giraldo on August 19, 2019
 * Last Update by Camilo Giraldo on September 20, 2020
 *
 * Comments:
 *    - The circuit is meant to be powered by a 5V and 12V voltage suppliers. 12V to power the Arduino
 *      chip, and 5V to power the potentiometers, switches, and motors. The 5V supply for the motors
 *      must have a high level of current since the large motors draw a decent amount.
 *    - The arduino that is connected to the PC does not need the Vin pin, so unplug it.
 *
*/

// Library to move motor and motor's variable
#include "Adafruit_DRV2605.h"
Adafruit_DRV2605 drv;               //Name of the motor
int m_signal_dec;                   //Value given to the motor drv

// General variables
int system_delay = 100;             //Delta time of 100 ms per loop
int ii; int jj; int kk;             //For-loop counters

// Defining pins and values for potentiometers, switches and buttons
int Foot_Pot_Pin = A0;              //Pin number for potentiometer that selects the foot to be tested
int Foot_Pot_Value;                 //Value of reading from potentiometer that selecs the foot to be tested
    //-- Off -- Left -- Right -- Both --

int Motor_Pot_Pin = A1;             //Pin number for potentiometer that selects the motor to be used
int Motor_Pot_Value;                //Value of reading from potentiometer that selecs the motor to be used
    //-- Off -- Mini -- Small -- Medium -- Large

int Signal_Pot_Pin = A2;            //Pin number for potentiometer that selects the signal to be used
int Signal_Pot_Value;               //Value of reading from potentiometer that selecs the signal to be used
    //-- Off -- White -- Pink -- Brown --

int Pwr_Pot_Pin = A3;               //Pin number for potentiometer that selects the power of the motors
float Pwr_Pot_Value;                //Value of reading from potentiometer that selects the power of the motors
    //0% -- 100%

int Buzz_Button_Pin = 2;            //Pin number for button that sends a signal/buzz to the motors
int Buzz_Button_Value;              //Value of reading from button that sends a signal/buzz to motors

int No_Button_Pin = 3;              //Pin number for button that says No
int No_Button_Value;                //Value of reading from button that says No
    //This will be a push button given to the subject to claim feeling (pressed = LOW), or no feeling (not pressed = HIGH)

int Yes_Button_Pin = 4;             //Pin number for button that says Yes
int Yes_Button_Value;               //Value of reading from button that says Yes

int Test421_Switch_Pin = 5;         //Pin number for switch that selects the 421 code
int Test421_Switch_Value;           //Value of reading from switch that selecs the 421 code

int TestSignal_Switch_Pin = 6;      //Pin number for switch that selects the signal code
int TestSignal_Switch_Value;        //Value of reading from switch that selecs the signal code

int LED_pin = 13;                   //Pin number for LED that confirms entry

// ---------------------------- Signal Code Variables ----------------------------
int m_signal_idx_low;               //Low index for motor signal
int m_signal_idx_high;              //High index for motor signal
int m_signal_curr;                  //Current value from motor signal
float m_signal_curr_float;          //Current value from motor signal in float format
float m_Vmax;                       //Maximum voltage allowed in motor
float m_Vmin;                       //Minimum voltage allowed in motor
float m_Vdelta;                     //Accuracy of voltage in motor
float m_pwr;                        //Power for motor signal

// Declaring all signals - Row order:
//  1)  m307105 White   Signal  2 from all_signals_v4   idx:    0 to   900
//  2)  m307105 Pink    Signal 10 from all_signals      idx:  901 to  1801
//  3)  m307105 Brown   Signal  9 from all_signals      idx: 1802 to  2702
//  4)  m310003 White   Signal  3 from all_signals_v3   idx: 2703 to  3603
//  5)  m310003 Pink    Signal  3 from all_signals_v3   idx: 3604 to  4504
//  6)  m310003 Brown   Signal  2 from all_signals      idx: 4505 to  5405
//  7)  m30610H White   Signal  2 from all_signals_v2   idx: 5406 to  6306
//  8)  m30610H Pink    Signal  5 from all_signals      idx: 6307 to  7207
//  9)  m30610H Brown   Signal  7 from all_signals      idx: 7208 to  8108
//  10) m307103 White   Signal  2 from all_signals_v2   idx: 8109 to  9009
```

```
//  11) m307103 Pink    Signal  7 from all_signals      idx: 9010 to  9910
//  12) m307103 Brown   Signal 10 from all_signals      idx: 9911 to 10811
const int m_signal[] PROGMEM =
{404,484,475,346,429,404,575,399,418,478,480,0,293,519,598,352,498,265,206,533,577,361,443,407,512,492,316,826,364,367,331,567,424,447,654,35
9,317,388,304,268,604,609,465,663,195,294,593,679,413,442,572,464,357,359,504,367,272,501,514,509,590,369,500,292,791,438,343,365,532,308,433
,368,443,564,407,488,278,627,457,579,351,555,414,582,457,490,584,363,473,333,460,40,391,505,302,414,339,522,476,488,431,320,460,245,408,531,2
56,474,708,556,420,404,309,461,470,400,422,366,542,567,185,515,531,259,478,393,467,639,537,676,495,366,677,312,348,345,700,382,369,605,216,53
8,418,345,345,475,574,373,331,599,434,622,464,462,418,395,419,226,419,182,575,408,74,435,676,703,373,552,409,571,331,453,385,547,438,373,328,
246,503,600,709,447,307,447,503,291,479,371,411,467,417,349,320,404,364,562,398,548,521,384,190,595,470,467,695,229,663,275,289,332,570,334,5
63,450,340,556,558,588,172,370,480,299,636,416,380,469,364,549,347,421,526,366,337,427,403,434,493,355,560,525,380,489,415,513,385,496,463,49
6,340,267,502,485,236,584,586,352,329,398,348,415,499,446,611,331,294,447,601,574,242,348,620,544,218,248,615,395,282,489,592,609,140,658,426
,331,499,502,382,567,431,570,547,418,636,443,324,489,364,457,393,465,610,582,506,432,299,426,410,487,401,474,577,626,447,261,307,433,523,494,
469,276,309,624,426,423,276,559,439,418,609,338,295,462,833,383,303,356,490,542,267,535,389,543,452,464,609,404,231,683,448,470,489,421,209,5
00,329,603,308,632,377,210,483,631,487,310,523,93,805,534,672,187,511,535,302,377,189,588,264,652,457,305,538,421,492,549,536,460,440,597,636
,433,680,200,254,647,406,273,433,397,404,502,450,306,373,536,678,527,317,431,491,282,427,395,497,476,522,341,426,378,500,484,389,716,185,267,
286,507,373,323,522,336,376,480,477,363,294,322,670,351,468,359,571,462,597,550,535,504,213,408,393,573,406,336,558,304,416,299,577,398,375,4
25,392,451,440,695,562,384,417,387,444,586,313,461,393,388,591,559,496,327,551,426,419,384,272,410,402,656,81,337,579,207,717,443,559,423,676
,337,398,474,538,585,529,271,510,415,407,558,413,483,528,453,236,563,357,414,513,290,342,524,474,305,606,464,535,452,477,426,323,554,669,373,
516,253,447,524,415,426,319,284,565,360,219,455,496,664,445,288,400,175,497,600,587,317,395,593,524,455,545,459,449,597,196,196,577,474,406,4
81,248,564,393,606,480,468,307,395,249,344,568,306,583,610,526,225,668,322,253,375,513,513,519,396,488,407,496,415,375,441,497,653,439,263,47
4,488,517,335,345,558,292,445,488,557,465,267,316,549,364,507,540,510,585,238,662,284,444,461,632,455,401,227,410,619,442,235,538,518,487,152
,484,505,309,377,370,232,494,632,377,407,552,639,552,220,203,592,452,314,604,480,252,614,535,376,680,201,434,464,471,212,229,356,516,483,564,
641,247,455,597,380,342,351,554,589,208,501,494,518,341,777,391,443,270,462,582,457,287,464,616,153,450,479,368,571,414,634,408,576,286,456,4
91,276,315,279,1000,360,362,525,416,460,278,435,338,489,395,367,415,589,506,363,501,384,420,378,429,271,382,363,331,598,449,215,400,386,636,5
07,598,281,446,309,615,380,536,518,364,545,409,412,298,263,609,355,136,477,402,427,439,453,231,788,202,497,477,243,357,454,462,723,505,666,21
3,436,309,461,368,453,408,484,523,564,377,587,280,421,511,620,339,341,600,499,464,516,612,357,413,367,446,358,360,385,363,703,496,365,331,434
,588,278,384,613,488,197,312,458,401,303,493,466,489,551,293,351,602,441,359,328,561,417,465,337,684,542,427,469,512,568,216,272,402,484,471,
347,282,586,399,467,498,618,165,470,452,413,456,607,231,230,553,202,473,381,748,454,427,501,289,411,366,550,345,433,278,650,569,220,433,406,4
98,499,294,456,390,592,402,419,203,598,450,381,523,564,628,532,331,553,394,
                                    463,586,512,590,552,567,632,642,523,660,466,471,660,659,678,580,635,648,636,546,504,535,495,657,605,633,626,6
63,694,649,780,635,582,698,597,785,705,794,785,913,698,656,813,929,1000,845,639,724,584,806,759,793,687,657,715,701,890,644,783,854,725,813,5
77,733,722,654,668,685,549,625,675,820,697,760,866,783,828,816,819,895,765,759,812,681,758,585,741,779,573,667,768,752,700,772,626,631,651,80
0,833,794,815,647,665,506,690,478,610,497,658,721,767,597,686,566,598,540,548,537,572,639,678,595,626,465,609,583,697,658,619,699,611,635,791
,738,594,743,728,590,643,679,478,525,525,368,523,385,401,361,458,389,612,571,574,452,399,330,564,568,478,570,328,348,218,489,364,221,454,302,
364,297,516,419,446,428,444,473,565,635,428,457,383,238,351,187,223,170,211,241,268,306,287,166,354,289,338,338,281,389,376,509,527,645,687,5
89,681,599,461,524,520,372,403,442,462,418,364,520,420,575,511,351,401,396,209,390,192,286,435,310,253,266,432,304,267,289,148,248,276,210,26
9,228,345,313,209,211,218,411,334,233,320,160,205,70,98,398,289,268,269,267,327,119,122,145,291,247,309,418,357,271,293,340,244,349,338,376,3
65,238,193,284,498,291,359,334,404,318,275,346,353,366,401,474,486,376,405,357,351,344,359,380,390,339,438,371,371,376,353,563,311,345,387,28
2,338,475,430,257,397,562,443,291,489,329,382,492,460,416,424,359,324,243,278,295,521,500,503,517,511,501,550,591,565,613,560,686,432,345,375
,335,338,371,220,288,389,544,471,429,255,244,417,329,276,417,294,309,272,369,244,261,277,340,372,263,243,252,475,432,377,285,104,174,366,197,
233,119,269,139,222,196,239,87,153,288,395,251,309,262,244,341,393,376,114,455,505,372,386,451,180,168,84,187,73,247,302,183,157,188,121,266,
265,135,299,88,42,121,40,167,255,253,335,377,436,506,231,337,300,256,320,297,369,351,202,171,334,473,503,400,284,377,155,218,308,317,350,276,
208,297,153,98,282,233,355,393,376,321,305,253,201,111,254,282,302,97,153,348,323,370,311,394,515,346,356,531,543,408,494,373,226,372,512,411
,558,380,333,457,282,339,198,189,300,394,331,314,354,528,416,348,300,409,355,403,398,215,258,245,157,256,171,235,260,230,289,302,147,315,223,
285,331,316,325,356,442,369,250,325,181,145,272,233,123,269,188,267,383,197,305,423,205,279,285,328,295,377,389,439,254,132,249,143,248,296,2
04,130,119,294,140,196,217,194,134,143,39,218,101,244,142,59,90,214,137,274,176,188,211,142,395,328,324,330,339,412,210,305,416,370,332,355,3
85,197,273,283,292,295,204,359,398,282,268,300,204,220,62,242,234,358,219,308,407,371,292,282,257,243,311,410,327,311,255,303,273,251,319,386
,328,212,272,168,83,0,92,258,215,220,285,350,174,288,200,168,261,286,308,76,303,447,195,233,463,453,505,392,531,446,308,101,211,251,333,353,3
41,108,195,306,262,138,238,319,222,285,272,336,417,501,544,382,452,333,499,439,220,380,534,460,251,343,405,285,507,359,509,634,401,342,320,41
6,369,483,476,439,455,431,374,349,470,478,309,429,484,478,505,549,411,424,445,416,564,689,520,406,521,401,444,467,409,491,419,545,733,637,550
,783,768,722,592,546,465,602,612,426,463,472,494,529,456,572,708,522,411,425,410,419,355,377,399,319,367,571,599,560,467,455,522,529,515,357,
537,509,727,578,439,550,548,453,395,215,474,290,329,353,366,377,384,482,271,259,250,207,140,275,181,379,299,369,269,104,81,306,309,418,363,35
1,355,292,367,496,586,591,554,308,342,219,208,456,292,195,258,389,385,285,369,444,411,443,424,376,279,285,462,434,395,371,320,351,366,337,415
,249,238,325,381,460,383,498,413,346,531,397,436,496,261,200,212,426,306,473,391,393,259,349,382,294,183,349,317,272,252,142,268,290,113,85,8
8,48,200,290,362,248,169,208,184,112,186,75,249,249,273,229,86,77,145,211,241,310,304,
                                    304,279,263,302,291,283,285,326,341,335,362,382,403,379,391,397,403,397,400,394,375,373,384,394,372,396,387,3
81,403,355,348,349,374,389,409,429,425,412,450,484,506,516,514,483,469,516,508,493,466,481,484,480,478,493,483,514,485,498,491,478,459,478,49
3,490,479,446,468,448,453,455,451,464,450,464,477,497,484,473,478,483,480,452,437,367,386,387,386,398,377,354,387,369,400,420,402,402,422,448
,461,457,488,458,458,483,471,476,453,502,524,519,555,543,517,550,592,557,568,530,528,558,541,516,494,539,538,542,552,589,554,565,548,506,526,
499,497,484,441,424,427,396,427,441,444,423,415,408,396,407,389,394,394,449,445,417,453,433,404,397,368,393,377,373,345,313,306,314,357,307,3
14,315,350,409,372,399,366,313,327,309,296,273,252,262,276,261,224,213,189,221,238,243,233,224,261,258,226,208,215,193,188,194,195,193,251,22
8,228,218,219,217,181,146,133,108,107,108,123,102,66,73,52,84,98,105,70,66,82,59,82,92,96,102,115,68,60,87,39,57,86,75,69,72,48,84,92,78,79,9
0,104,85,62,29,31,39,48,44,83,87,71,76,92,70,78,53,35,26,24,0,71,63,59,75,77,60,71,78,42,55,23,24,18,5,32,60,76,80,89,124,128,135,148,222,213
,239,234,237,289,270,271,275,302,345,381,408,372,334,335,311,323,345,343,333,308,305,310,307,285,273,279,245,206,175,176,171,169,171,168,142,
151,168,137,117,100,84,87,133,115,120,118,97,93,113,118,134,133,139,120,117,133,168,192,145,118,131,137,158,154,170,164,156,167,167,163,142,1
41,153,136,167,190,154,175,193,187,200,224,242,240,225,235,212,248,276,293,296,278,270,275,247,232,215,179,192,222,255,291,289,272,282,292,30
9,291,290,262,276,306,335,362,363,370,352,357,374,379,378,376,369,375,412,405,386,393,417,395,397,390,364,336,288,291,365,355,374,401,375,357
,355,381,397,390,413,411,425,455,477,494,476,471,414,432,437,405,364,380,369,370,391,372,389,361,342,328,320,306,329,347,380,375,435,449,437,
456,466,490,506,508,525,525,520,501,516,532,528,574,522,516,529,507,479,472,453,436,467,481,501,510,506,499,503,526,525,486,487,464,497,490,5
01,518,538,529,510,469,467,480,489,491,503,534,579,616,586,575,556,587,583,589,574,565,569,530,561,581,538,530,544,574,593,572,609,634,673,67
3,685,677,648,650,655,637,603,566,538,525,537,503,540,501,535,514,525,537,540,518,544,563,527,566,568,598,598,595,615,603,590,577,577,578,568
,575,636,584,585,563,594,598,599,577,559,560,586,591,558,571,567,560,602,611,576,577,577,559,544,555,570,546,522,533,535,524,491,453,457,450,
433,415,406,370,344,342,311,345,370,402,406,392,399,422,449,418,420,438,507,495,486,488,451,455,452,422,434,446,439,451,420,425,397,421,393,4
20,420,425,432,468,449,416,402,423,398,393,413,393,368,379,375,338,360,333,333,305,311,304,296,314,310,286,260,249,246,225,229,226,254,209,19
6,173,193,148,132,148,132,99,108,100,63,79,76,50,48,44,61,71,104,92,69,98,90,120,162,210,224,245,249,218,205,255,246,269,265,264,246,255,249,
252,270,302,312,311,315,283,329,318,341,348,376,376,369,372,333,323,337,304,315,328,300,304,299,325,350,362,325,329,330,320,292,321,362,363,3
37,322,289,311,306,303,257,262,290,310,264,310,335,340,351,364,375,385,381,382,398,405,414,426,460,484,523,494,509,499,503,494,539,540,529,53
8,510,503,500,505,506,536,543,533,505,520,521,535,552,571,587,567,536,529,537,526,508,506,520,507,512,501,518,564,607,598,565,544,551,543,550
,521,505,511,517,500,513,492,497,506,543,546,542,517,528,520,501,528,555,574,595,586,606,567,541,526,553,569,564,574,542,575,637,651,666,674,
672,660,658,662,661,686,720,757,756,757,754,746,727,728,745,729,773,794,773,779,791,781,779,800,830,836,825,828,859,880,888,880,905,926,955,9
66,993,997,993,974,1000,988,
                                    454,496,352,268,561,695,387,761,410,427,702,468,571,376,489,586,645,374,287,811,639,529,643,349,258,550,572,2
06,524,460,396,686,348,355,325,516,448,466,774,647,447,738,347,39,771,396,418,700,738,137,630,209,448,610,519,540,689,309,420,533,488,642,462
,605,347,654,453,484,327,505,383,375,469,591,295,549,682,432,647,408,488,148,309,416,402,310,213,133,751,585,697,645,276,678,272,640,393,567,
480,641,432,198,639,594,516,339,488,379,470,575,520,218,573,642,387,578,365,191,638,329,260,68,635,686,324,309,611,398,369,321,662,417,477,39
2,912,548,307,363,629,470,375,300,605,590,352,427,100,409,450,640,495,520,552,460,280,340,498,551,467,470,613,439,389,412,136,648,1000,406,54
2,295,258,433,544,513,323,488,543,347,398,438,331,520,415,653,364,601,466,532,376,400,302,619,336,117,710,211,504,557,183,583,527,553,333,252
,740,456,277,342,592,510,357,484,640,540,466,200,439,625,493,413,758,367,362,508,826,625,217,570,623,340,363,325,367,164,434,659,399,773,214,
529,393,510,460,343,495,720,343,472,569,562,439,598,526,616,581,547,734,391,494,381,530,416,293,228,637,554,431,433,719,500,357,439,477,328,4
87,858,434,499,693,398,360,518,602,528,560,418,221,496,522,498,507,316,428,434,443,394,383,719,677,340,413,297,486,712,724,407,550,193,722,65
0,92,452,647,192,462,381,626,537,360,490,658,375,380,661,497,327,263,518,621,428,565,784,179,263,739,493,581,680,496,267,389,670,210,505,595,
568,366,522,494,318,126,583,379,693,328,517,569,553,629,454,779,212,835,540,187,557,574,334,222,619,185,441,914,348,497,697,399,423,589,360,3
52,469,785,835,189,282,508,558,434,566,500,551,222,451,772,354,367,584,705,501,493,346,546,654,746,331,324,623,363,548,548,331,494,508,753,29
4,493,329,409,738,470,200,666,210,379,369,422,304,645,321,239,194,693,561,327,581,700,388,409,309,718,265,482,347,456,245,583,527,176,744,684
,188,155,583,390,509,303,773,570,670,499,541,351,563,249,759,381,91,373,363,527,400,326,370,702,659,394,392,606,275,676,388,395,796,479,376,4
93,386,493,467,626,499,414,262,370,761,742,239,710,209,246,650,354,537,576,276,381,463,312,516,546,327,542,548,423,131,708,548,388,624,567,50
5,378,508,357,254,551,324,604,478,522,333,495,463,458,597,342,357,201,593,547,399,421,287,716,431,512,408,641,169,649,229,303,492,292,742,216
,659,617,208,799,216,412,900,714,168,561,365,567,701,563,397,454,564,625,570,596,368,656,403,485,242,754,593,247,255,760,473,236,704,481,563,
393,347,610,524,674,260,785,566,575,135,672,705,209,837,463,196,657,579,601,55,420,594,593,211,571,424,513,395,265,657,175,580,390,571,571,45
8,622,440,644,379,133,474,196,971,349,522,121,597,895,499,112,413,640,624,377,737,335,312,347,647,320,474,408,652,303,520,412,963,646,664,378
,362,580,195,444,244,532,693,488,467,262,291,501,589,643,522,728,478,385,739,473,808,694,0,405,87,356,663,433,634,307,587,426,431,672,279,409
,794,793,580,331,2,333,426,509,450,315,960,145,762,709,570,109,458,415,579,677,236,765,681,142,574,242,688,548,381,428,352,239,343,454,914,18
2,670,251,486,495,280,256,617,738,388,696,455,532,366,56,527,391,543,546,418,398,587,364,525,592,411,602,419,437,671,532,342,562,466,401,341,
434,578,264,576,547,541,576,506,62,639,640,797,139,757,327,478,247,380,566,350,196,705,388,634,243,532,642,231,565,413,268,683,971,263,669,40
```

2,485,526,425,242,615,547,479,543,334,563,772,711,324,495,407,516,596,451,402,759,144,318,545,657,378,472,311,367,581,594,416,479,598,608,455
,529,202,273,517,651,822,286,551,459,642,463,812,575,348,408,357,474,684,264,664,579,292,629,596,768,292,182,309,609,662,755,176,678,591,333,
448,896,254,560,357,360,806,423,510,272,546,205,269,560,386,667,317,677,415,354,425,797,556,631,676,
616,513,356,665,365,72,116,377,397,481,475,749,308,498,419,357,487,538,488,547,676,360,559,683,468,317,288,41
1,476,324,240,460,266,376,367,283,287,244,264,197,258,528,510,333,231,311,451,267,67,222,55,300,134,399,591,174,403,124,266,541,607,378,539,2
84,32,407,389,578,425,528,320,379,449,807,470,641,402,400,106,419,131,267,301,523,515,609,436,419,587,461,469,295,331,317,513,714,688,508,626
,296,332,401,501,393,673,599,611,686,509,332,285,404,275,319,37,135,347,497,435,393,340,543,460,570,501,433,374,453,315,476,482,653,261,637,6
40,494,509,515,674,735,722,831,726,493,629,325,446,513,567,527,641,610,515,490,642,514,820,442,352,555,432,507,653,543,623,537,654,369,484,43
9,295,94,233,400,416,585,462,647,557,357,238,502,507,547,272,356,536,405,455,536,524,479,511,441,410,170,309,423,463,553,321,481,480,654,742,
490,737,477,687,409,228,325,457,448,372,604,495,284,398,617,551,482,353,322,438,690,303,191,292,69,172,355,665,278,293,261,415,630,565,466,60
8,642,504,687,636,644,402,462,500,439,359,535,731,720,566,735,515,655,539,556,335,440,573,344,523,497,344,528,406,355,312,524,614,750,575,565
,693,523,426,564,608,822,578,696,741,893,788,696,904,786,622,786,447,523,401,486,582,458,469,783,695,541,486,520,733,616,582,496,563,336,597,
534,490,371,581,683,470,572,505,408,534,603,590,170,436,385,624,547,515,522,301,374,327,579,636,418,380,445,650,369,729,446,431,577,313,189,5
03,618,691,208,478,285,398,163,175,480,359,552,352,120,0,400,496,362,437,327,200,460,153,204,266,344,119,547,407,344,130,42,229,266,388,212,1
12,121,245,115,96,47,249,149,172,248,706,385,520,662,352,440,469,579,457,701,382,444,326,483,581,421,478,420,336,517,411,730,739,442,589,364,
607,311,394,568,420,426,441,694,524,499,323,499,625,673,793,640,548,640,1000,729,751,685,821,843,648,774,716,745,698,467,800,657,490,141,283,
163,423,463,486,306,452,652,426,587,382,467,527,239,691,649,517,811,750,686,630,667,325,369,601,339,364,537,366,466,583,793,533,804,701,641,4
13,438,515,521,325,412,593,445,425,511,697,457,318,220,340,333,704,160,458,427,621,646,497,880,796,768,630,341,409,162,543,432,316,344,230,68
,16,102,124,272,287,552,403,111,172,220,385,117,169,117,362,482,578,507,488,397,439,288,358,270,591,791,533,455,486,587,653,427,373,242,373,2
63,327,348,689,689,423,529,642,494,467,417,622,593,622,727,515,556,186,583,609,690,575,718,449,418,391,277,368,528,450,687,665,611,578,440,77
2,555,512,569,672,566,392,630,700,630,532,572,492,644,553,547,586,510,379,615,467,896,615,797,683,843,763,590,501,488,742,771,699,623,350,704
,459,530,603,448,395,405,405,503,629,402,257,499,393,590,577,339,646,543,340,490,574,721,698,544,508,208,389,364,579,395,338,399,301,297,382,
466,634,469,528,145,132,278,467,578,559,345,549,277,522,465,300,580,520,801,383,562,575,656,513,585,324,466,297,333,327,280,261,476,396,457,5
58,511,490,522,507,273,591,560,770,703,363,605,618,625,367,325,583,502,427,394,179,540,607,454,835,543,290,147,122,36,164,279,475,429,399,447
,565,419,638,628,328,511,402,449,304,475,822,772,654,770,683,702,529,520,556,616,634,504,707,810,843,817,829,780,577,706,522,761,907,497,646,
459,681,566,298,341,532,492,603,654,556,847,582,544,407,572,507,601,232,462,591,499,659,500,179,348,376,354,692,529,214,430,435,736,498,700,6
17,625,778,676,688,652,650,797,525,422,395,895,656,624,380,639,523,500,514,556,533,614,397,475,456,757,656,539,608,472,646,696,741,564,536,66
2,575,521,347,630,606,540,716,693,569,357,640,749,656,779,697,693,666,569,583,686,376,458,746,684,866,462,373,503,537,736,813,584,695,767,790
,701,848,614,734,967,661,600,687,665,658,608,680,508,565,584,432,421,646,938,686,773,750,459,640,
898,909,886,903,932,936,954,939,956,945,922,937,918,917,908,891,889,903,887,869,811,838,850,857,843,833,841,8
57,848,866,873,882,852,859,883,895,893,921,919,921,894,867,875,845,835,826,822,826,832,838,837,829,802,814,835,857,863,909,868,862,888,881,90
0,909,896,908,858,870,899,906,894,896,879,865,875,883,865,864,839,836,803,798,790,814,813,777,763,764,746,788,788,767,755,741,743,736,729,714
,718,751,779,745,764,800,810,796,802,801,819,832,846,856,880,880,873,870,878,881,915,921,929,933,948,944,960,962,955,960,982,963,982,971,990,
1000,995,956,962,970,977,982,975,987,965,966,943,937,933,916,927,962,986,981,938,933,939,932,935,906,889,881,907,908,929,932,910,898,891,873,
899,924,935,926,920,939,946,968,949,924,919,900,937,946,968,972,952,987,979,957,922,931,923,892,888,868,912,891,894,903,900,898,912,932,925,9
30,931,955,938,933,926,948,917,924,927,894,919,866,900,876,862,867,908,916,933,959,926,898,897,884,879,865,893,898,880,883,880,870,830,823,82
7,813,808,821,820,824,817,835,840,856,877,836,825,826,824,828,837,863,861,861,861,867,883,883,856,866,852,856,851,822,874,876,860,858,823,831
,845,867,837,842,864,862,863,856,849,830,819,840,816,788,789,806,785,786,784,801,820,833,811,798,796,761,811,806,790,771,774,766,734,700,700,
666,665,649,633,650,626,567,578,582,546,555,550,533,539,525,517,480,461,413,406,402,395,403,393,340,337,338,339,319,354,348,345,332,348,349,3
33,351,311,283,259,260,253,217,216,262,300,313,318,307,292,291,305,317,323,314,331,318,332,348,381,354,352,361,346,358,369,353,381,366,355,35
1,366,358,324,329,315,281,256,242,245,260,264,273,277,271,298,308,335,314,319,325,297,298,283,261,246,258,247,244,265,272,289,290,256,241,230
,240,255,236,240,216,211,182,208,241,260,264,226,243,206,204,176,168,171,187,211,249,233,210,220,187,198,241,244,230,233,178,196,192,224,220,
223,274,240,207,196,196,205,221,234,233,247,201,198,211,235,263,250,242,258,221,203,206,216,230,248,278,305,291,281,274,273,275,273,281,303,2
95,268,249,242,219,218,197,170,162,189,208,195,236,226,240,239,207,200,194,213,206,195,171,163,180,210,235,190,187,197,202,191,177,168,145,12
5,159,141,125,137,146,135,138,144,159,143,135,145,180,165,189,165,170,201,189,185,201,210,203,218,227,249,228,223,210,197,192,167,152,143,120
,129,137,143,145,134,164,171,178,167,161,155,150,147,164,183,209,233,218,227,223,197,192,212,223,189,183,205,214,208,206,214,248,219,199,208,
174,186,195,239,227,210,191,179,162,157,129,129,132,124,95,88,119,99,82,38,57,60,65,55,67,59,78,57,14,8,2,0,11,7,10,14,51,76,44,27,28,40,55,6
2,60,71,93,87,86,106,115,111,118,88,80,71,89,108,132,178,155,180,164,158,189,184,200,181,179,207,195,168,144,150,127,139,103,115,98,90,83,54,
53,68,76,88,118,123,111,117,115,92,98,93,107,135,130,135,139,116,116,106,110,102,71,59,38,45,58,19,52,51,66,50,71,61,69,104,84,86,63,44,50,50
,58,38,19,12,37,51,48,71,89,87,84,63,79,99,108,129,157,189,193,187,161,163,144,121,152,162,138,125,153,175,180,179,149,148,167,187,215,229,24
5,226,230,239,258,262,250,255,261,280,264,286,283,260,250,275,270,255,258,236,259,280,258,292,301,299,290,264,272,250,235,212,210,211,198,214
,227,222,237,274,261,257,236,265,256,265,289,298,334,321,293,294,280,292,259,271,272,276,278,296,314,324,294,327,346,345,342,355,357,395,400,
413,415,407,378,357,341,318,322,312,317,301,282,263,276,309,332,353,316,299,322,293,272,235,266,245,210,239,212,212,178,174,180,162,169,196,1
92,193,190,173,187,176,165,197,218,247,267,256,240,244,248,232,251,227,230,223,234,230,213,225,205,234,254,247,247,256,249,230,225,252,265,29
2,268,268,245,187,210,216,
475,571,675,612,342,505,377,332,474,597,586,137,166,477,440,338,384,371,472,791,596,570,470,745,504,427,315,4
90,504,699,414,480,586,278,538,508,360,781,281,379,237,646,496,463,693,498,498,492,548,712,767,691,414,404,357,503,636,569,255,635,223,520,51
6,255,570,440,312,603,194,613,185,356,379,600,461,386,240,292,544,618,437,435,359,638,375,482,307,435,633,525,692,451,127,576,504,565,215,436
,434,473,374,462,630,429,706,492,513,216,541,567,552,301,120,497,679,438,389,607,559,316,579,532,386,384,356,275,733,376,340,438,552,467,532,
504,589,419,509,762,610,401,117,355,526,495,332,402,212,458,405,509,243,375,255,248,318,876,563,527,476,304,397,410,209,435,142,297,276,471,3
65,471,478,495,524,432,242,532,604,178,324,411,467,558,649,334,664,512,384,467,296,677,355,282,558,304,416,198,656,437,695,230,506,413,501,54
4,528,530,198,301,414,534,315,458,393,81,574,555,388,359,450,602,231,332,221,678,422,658,308,291,486,299,432,411,572,115,577,547,406,681,378,
319,241,554,485,738,556,492,503,603,263,748,613,59,490,475,431,366,560,420,0,496,570,289,451,355,552,229,386,502,487,153,420,400,551,705,652,
389,507,270,688,212,451,640,348,503,331,582,735,407,544,389,430,141,223,530,345,391,734,466,234,406,323,486,631,352,233,691,424,797,361,459,2
06,606,530,183,375,514,400,400,583,490,385,251,371,270,496,414,300,332,479,643,499,385,455,544,879,430,511,497,479,544,757,338,255,640,546,40
0,587,516,231,297,452,363,477,476,435,1000,373,409,737,433,427,442,234,741,245,450,656,466,383,429,474,559,328,309,432,302,536,390,451,530,18
4,301,324,734,733,593,217,277,518,333,370,421,567,544,325,114,479,363,349,415,639,596,438,268,574,545,117,349,687,144,568,431,533,445,242,285
,417,337,568,550,460,375,519,397,398,612,513,471,431,177,643,292,143,558,466,439,544,489,376,492,442,578,548,525,341,297,423,354,336,408,480,
441,540,446,397,633,492,603,622,460,626,229,376,426,316,480,315,438,446,589,573,582,660,362,496,375,496,421,467,544,451,363,361,144,454,646,6
54,476,288,505,651,341,546,237,408,413,502,451,170,124,406,545,476,590,644,264,315,391,550,249,532,498,341,400,293,304,481,507,517,536,363,55
3,454,357,711,252,621,651,575,204,384,483,340,642,546,650,504,542,393,293,591,275,332,397,713,494,487,250,500,237,431,350,380,480,396,254,391
,243,135,453,398,416,594,538,437,294,512,148,530,454,637,586,490,430,201,415,421,545,683,559,515,203,607,188,399,602,496,366,628,459,371,360,
402,600,628,185,425,340,400,172,503,484,231,605,592,439,379,325,540,585,489,506,401,530,252,442,442,319,270,303,419,263,550,561,299,426,423,5
09,543,413,439,398,198,625,657,598,506,322,538,424,359,433,254,549,440,134,668,512,510,554,150,567,223,576,210,416,527,422,361,550,358,644,68
4,532,382,275,513,395,275,703,636,376,332,317,381,373,675,308,318,273,569,580,666,442,486,136,362,331,296,726,617,232,470,420,395,389,541,468
,549,438,514,865,495,415,550,561,432,530,300,458,450,566,239,706,449,440,237,671,541,624,465,475,469,747,576,524,436,461,339,660,378,669,608,
509,578,429,407,483,342,619,758,439,280,339,480,407,269,651,674,578,343,487,433,293,375,646,420,591,232,411,415,523,473,580,202,371,570,576,3
68,551,444,511,407,511,522,556,454,572,429,226,515,490,546,341,401,472,524,430,396,420,394,389,614,527,771,362,659,478,515,291,369,768,353,48
1,552,413,412,423,307,239,481,529,409,472,667,594,767,241,403,279,351,538,568,572,540,571,498,176,519,707,281,662,618,203,562,359,404,317,577
,754,358,349,526,470,369,700,618,422,651,539,348,247,416,358,511,466,543,439,617,494,650,71,243,496,108,482,401,70,637,671,406,485,459,551,68
0,358,425,731,648,426,462,280,841,404,533,345,639,431,372,449,586,226,353,490,502,371,635,486,237,489,510,
460,441,482,471,644,343,420,566,616,458,795,717,722,756,681,504,558,672,563,443,566,511,529,523,660,455,488,4
61,499,420,599,616,642,693,703,719,664,538,480,729,574,657,577,608,557,628,446,429,447,467,454,570,473,520,488,434,674,335,390,435,462,537,46
3,555,614,545,620,767,620,808,823,763,558,616,634,555,609,421,340,493,808,526,627,400,402,314,421,325,399,298,470,747,463,363,571,494,440,425
,668,655,502,574,696,558,579,545,521,693,436,420,465,506,486,488,555,439,575,596,648,786,663,707,728,933,716,855,811,730,628,676,586,595,668,
640,480,418,425,389,480,563,478,603,637,695,589,357,534,514,593,548,463,438,484,557,570,639,580,790,716,456,414,341,458,658,324,416,325,202,2
05,222,271,109,222,366,353,265,292,404,260,261,237,258,200,340,350,314,113,224,418,521,619,488,110,373,329,286,309,468,516,480,426,398,442,46
7,305,383,243,353,320,148,347,318,362,406,408,339,296,511,286,259,411,333,269,372,387,442,413,376,344,259,389,329,113,197,37,70,0,215,60,55,0
,115,213,196,252,310,318,158,135,272,336,275,33,214,251,191,103,52,3,194,197,98,286,156,329,298,360,321,149,164,149,221,9,348,340,408,210,244
,448,291,254,621,316,455,323,202,278,321,160,109,324,239,200,83,75,270,323,500,552,656,421,438,274,237,463,164,314,483,564,387,354,290,278,33
2,174,327,244,271,431,446,488,539,533,513,597,435,476,324,339,223,125,328,313,399,229,74,123,245,312,465,471,370,359,463,390,504,604,624,688,
651,481,416,345,507,497,596,411,465,529,422,679,477,516,318,375,415,529,486,492,317,492,574,425,331,292,305,388,220,188,266,361,321,373,127,2
66,319,201,349,294,400,423,637,653,389,665,625,461,488,359,301,556,513,410,522,704,513,564,535,438,224,523,403,435,394,288,317,152,196,108,31
5,99,218,76,165,343,335,304,283,401,309,169,98,165,407,305,457,466,589,405,481,364,314,260,459,533,296,296,238,255,189,232,390,430,490,485,45
7,408,533,515,695,581,582,613,582,684,649,615,398,665,650,592,610,555,693,717,599,723,615,652,712,884,646,597,596,595,768,477,537,459,289,506
,514,641,550,703,556,559,473,403,479,661,526,623,446,519,619,618,538,542,386,369,490,379,399,430,468,569,365,294,46,267,86,178,244,312,460,24
7,283,398,166,217,392,380,455,635,650,690,731,646,548,572,556,450,504,391,634,250,432,439,459,453,580,637,571,391,522,371,304,387,385,553,409
,373,504,530,551,541,537,708,571,538,589,432,280,201,355,418,525,435,465,344,230,201,229,448,371,237,270,408,364,441,364,406,340,501,473,493,
500,598,263,406,525,522,513,622,701,572,584,686,783,881,830,791,735,630,617,698,578,506,704,616,641,522,705,626,578,531,573,713,589,699,649,7
34,566,642,724,674,659,676,643,566,670,724,681,675,582,804,565,761,659,488,560,637,718,580,668,770,782,668,648,732,671,680,505,652,762,818,68
0,707,680,534,455,619,659,556,793,866,752,791,781,664,724,744,742,827,842,732,870,808,796,661,675,816,663,701,669,722,629,644,624,664,618,527
,692,642,680,771,696,637,582,825,832,970,1000,702,556,593,470,535,604,679,733,614,386,477,362,480,439,418,361,393,364,312,432,437,567,476,542
,517,592,664,487,351,310,619,695,638,688,575,466,631,746,609,684,765,654,555,710,567,782,729,673,622,541,711,674,636,893,817,734,495,842,843,
713,633,555,462,535,405,626,530,596,696,717,509,303,702,609,664,704,511,589,338,292,495,605,554,675,637,617,541,451,388,487,716,588,529,466,3

81,462,435,628,426,621,598,623,663,605,628,572,523,737,710,715,655,543,556,729,616,479,635,694,738,660,804,830,718,736,698,810,722,681,468,55
7,530,583,557,770,764,656,721,649,817,727,838,698,698,698,504,548,698,623,786,799,796,600,631,863,712,559,620,687,484,726,407,646,629,580,704
,789,613,686,702,655,607,726,699,597,556,643,920,692,642,689,793,587,566,714,794,876,820,
0,66,69,124,127,104,84,76,71,93,100,108,160,213,166,199,172,173,158,166,183,197,202,175,207,207,252,223,233,1
99,167,153,139,183,190,202,228,220,270,269,259,304,276,293,313,330,315,319,343,341,315,312,292,339,345,346,369,365,413,424,437,475,526,506,51
2,495,490,519,532,572,584,609,596,615,658,608,638,648,597,573,566,570,543,540,556,506,509,505,487,476,497,497,531,523,485,499,471,422,411,418
,456,482,423,422,402,371,399,396,362,429,438,402,379,423,389,388,380,407,418,434,407,408,417,450,448,455,427,400,404,383,403,367,323,353,361,
364,388,326,309,343,352,373,372,348,346,344,333,320,318,276,276,310,297,333,359,392,416,390,331,323,331,299,303,354,362,347,318,278,298,279,2
37,259,271,240,203,211,208,191,212,207,164,174,161,141,174,185,187,195,215,221,228,205,199,224,234,237,240,230,247,247,238,281,296,241,247,21
6,218,263,317,281,246,190,160,147,103,110,98,127,161,185,157,172,194,177,197,200,208,197,210,198,238,249,271,280,237,216,200,183,170,140,166,
234,224,227,223,311,332,325,328,269,260,294,282,221,250,292,290,264,243,232,231,277,289,325,288,292,297,319,295,352,352,324,320,325,272,294,3
13,355,345,318,335,333,358,337,372,337,346,324,331,303,326,384,400,428,430,422,386,379,371,341,315,356,357,379,354,389,348,324,329,305,265,23
8,275,278,253,267,214,235,273,231,206,207,141,166,166,188,182,189,178,204,242,208,242,254,233,282,310,286,372,368,397,440,339,359,331,359,354
,348,350,367,386,396,387,421,399,434,455,502,504,548,541,500,527,545,515,552,556,598,629,594,597,577,593,552,547,512,494,498,486,488,516,496,
494,481,474,447,468,535,569,581,598,542,521,509,505,540,593,579,563,548,543,543,535,546,563,570,556,547,535,541,564,550,506,537,479,456,458,4
71,500,454,467,438,492,448,443,475,492,460,434,439,407,416,423,409,409,478,495,510,540,539,537,576,603,628,663,665,692,728,764,778,772,780,79
3,799,800,799,863,829,818,833,884,923,925,927,937,908,947,976,907,937,949,948,956,1000,962,916,911,895,900,884,892,878,890,892,911,899,946,99
1,969,966,958,979,924,918,833,850,886,908,893,881,900,910,892,879,886,909,887,878,840,845,835,829,826,821,850,868,912,883,911,911,848,832,809
,818,833,828,811,825,816,864,883,897,846,810,782,823,817,861,825,840,832,828,846,870,853,857,822,798,761,751,692,699,695,675,689,706,711,705,
674,658,713,687,708,714,714,730,756,761,728,718,693,691,699,743,730,744,774,756,733,705,690,725,680,681,664,650,599,569,598,573,571,562,528,5
20,504,535,508,536,573,586,589,553,554,552,584,583,641,585,617,641,640,609,619,584,592,607,625,598,546,560,562,573,562,513,506,544,495,489,50
7,496,532,515,499,581,602,576,564,566,597,551,548,517,545,519,526,529,527,563,609,565,561,536,550,556,523,511,472,485,526,517,510,537,501,487
,483,476,483,473,467,494,507,540,568,586,608,558,549,556,514,515,539,511,556,584,549,537,536,525,535,520,535,535,507,516,499,501,459,445,446,
456,404,430,423,469,502,533,587,609,584,551,563,547,576,543,541,539,444,461,494,468,511,475,481,514,502,522,528,516,519,472,454,461,482,474,4
71,485,458,456,456,375,359,396,438,426,383,354,353,326,325,312,314,346,374,365,361,360,364,397,429,412,439,421,422,352,360,357,328,329,297,31
9,295,276,296,241,247,217,289,243,219,220,229,241,227,222,274,333,352,305,335,272,289,265,222,241,253,238,226,206,273,265,261,271,307,262,272
,241,275,298,263,276,248,248,245,208,242,166,221,233,247,241,236,260,227,236,259,263,245,230,273,269,210,213,213,184,161,185,202,194,185,163,
97,90,67,59,63,17,55,60,70,146,142,75,56,104,107,159,172,133,126,149,175,239,260,255,252,270,255,223,195,180,221,257,230,175,219,235,280,239,
211,218,220,245,256,213,216,155,162,162,171,215,183,227,215,216,241,219,270,280,298,295,330,
475,571,675,612,342,505,377,332,474,597,586,137,166,477,440,338,384,371,472,791,596,570,470,745,504,427,315,4
90,504,699,414,480,586,278,538,508,360,781,281,379,237,646,496,463,693,498,498,492,548,712,767,691,414,404,357,503,636,569,255,635,223,520,51
6,255,570,440,312,603,194,613,185,356,379,600,461,386,240,292,544,618,437,435,359,638,375,482,307,435,633,525,692,451,127,576,504,565,215,436
,434,473,374,462,630,429,706,492,513,216,541,567,552,301,120,497,679,438,389,607,559,316,579,532,386,384,356,275,733,376,340,438,552,467,532,
504,589,419,509,762,610,401,117,355,526,495,332,402,212,458,405,509,243,375,255,248,318,876,563,527,476,304,397,410,209,435,142,297,276,471,3
65,471,478,495,524,432,242,532,604,178,324,411,467,558,649,334,664,512,384,467,296,677,355,282,558,304,416,198,656,437,695,230,506,413,501,54
4,528,530,198,301,414,534,315,458,393,81,574,555,388,359,450,602,231,332,221,678,422,658,308,291,486,299,432,411,572,115,577,547,406,681,378,
319,241,554,485,738,556,492,503,603,263,748,613,59,490,475,431,366,560,420,0,496,570,289,451,355,552,229,386,502,487,153,420,400,551,705,652,
389,507,270,688,212,451,640,348,503,331,582,735,407,544,389,430,141,223,530,345,391,734,466,234,406,323,486,631,352,233,691,424,797,361,459,2
06,606,530,183,375,514,400,400,583,490,385,251,371,270,496,414,300,332,479,643,499,385,455,544,879,430,511,497,479,544,757,338,255,640,546,40
0,587,516,231,297,452,363,477,476,435,1000,373,409,737,433,427,442,234,741,245,450,656,466,383,429,474,559,328,309,432,302,536,390,451,530,18
4,301,324,734,733,593,217,277,518,333,370,421,567,544,325,114,479,363,349,415,639,596,438,268,574,545,117,349,687,144,568,431,533,445,242,285
,417,337,568,550,460,375,519,397,398,612,513,471,431,177,643,292,143,558,466,439,544,489,376,492,442,578,548,525,341,297,423,354,336,408,480,
441,540,446,397,633,492,603,622,460,626,229,376,426,316,480,315,438,446,589,573,582,660,362,496,375,496,421,467,544,451,363,361,144,454,646,6
54,476,288,505,651,341,546,237,408,413,502,451,170,124,406,545,476,590,644,264,315,391,550,249,532,498,341,400,293,304,481,507,517,536,363,55
3,454,357,711,252,621,651,575,204,384,483,340,642,546,650,504,542,393,293,591,275,332,397,713,494,487,250,500,237,431,350,380,480,396,254,391
,243,135,453,398,416,594,538,437,294,512,148,530,454,637,586,490,430,201,415,421,545,683,559,515,203,607,188,399,602,496,366,628,459,371,360,
402,600,628,185,425,340,400,172,503,484,231,605,592,439,379,325,540,585,489,506,401,530,252,442,442,319,270,303,419,263,550,561,299,426,423,5
09,543,413,439,398,198,625,657,598,506,322,538,424,359,433,254,549,440,134,668,512,510,554,150,567,223,576,210,416,527,422,361,550,358,644,68
4,532,382,275,513,395,275,703,636,376,332,317,381,373,675,308,318,273,569,580,666,442,486,136,362,331,296,726,617,232,470,420,395,389,541,468
,549,438,514,865,495,415,550,561,432,530,300,458,450,566,239,706,449,440,237,671,541,624,465,475,469,747,576,524,436,461,339,660,378,669,608,
509,578,429,407,483,342,619,758,439,280,339,480,407,269,651,674,578,343,487,433,293,375,646,420,591,232,411,415,523,473,580,202,371,570,576,3
68,551,444,511,407,511,522,556,454,572,429,226,515,490,546,341,401,472,524,430,396,420,394,389,614,527,771,362,659,478,515,291,369,768,353,48
1,552,413,412,423,307,239,481,529,409,472,667,594,767,241,403,279,351,538,568,572,540,571,498,176,519,707,281,662,618,203,562,359,404,317,577
,754,358,349,526,470,369,700,618,422,651,539,348,247,416,358,511,466,543,439,617,494,650,71,243,496,108,482,401,70,637,671,406,485,459,551,68
0,358,425,731,648,426,462,280,841,404,533,345,639,431,372,449,586,226,353,490,502,371,635,486,237,489,510,
426,536,393,291,630,660,722,779,835,643,388,339,337,180,142,328,248,275,169,238,156,224,217,239,394,403,572,4
58,390,364,227,450,349,341,396,473,325,342,350,314,369,267,398,259,259,373,302,471,173,250,285,198,268,293,325,196,252,220,162,172,234,384,23
6,341,480,496,412,440,602,519,464,278,303,362,231,262,446,574,608,548,612,825,713,791,818,776,652,635,772,568,636,613,714,750,501,390,415,639
,454,519,421,413,328,498,634,514,455,460,543,335,579,645,500,495,618,477,471,620,448,205,357,397,377,434,523,418,353,394,315,444,595,561,746,
662,582,534,546,595,585,493,366,187,324,390,304,340,561,559,456,309,493,447,463,529,449,597,447,480,577,574,677,498,585,375,466,510,373,477,4
04,630,707,619,638,604,664,497,654,665,584,585,721,569,753,604,459,445,518,469,325,559,652,432,294,477,427,378,422,341,435,375,325,134,264,44
1,340,538,241,476,175,339,327,320,301,109,221,377,436,473,379,404,502,358,379,354,383,284,246,231,382,330,326,418,353,388,463,613,450,282,420
,299,324,232,353,390,359,115,271,435,487,423,304,250,476,300,287,417,141,273,225,275,233,277,382,252,563,523,467,405,552,626,658,478,462,614,
526,451,513,490,320,373,528,439,340,431,483,358,540,476,637,485,616,490,389,41,229,379,377,256,235,410,317,198,150,318,393,554,354,433,242,41
7,265,228,329,326,164,340,399,384,234,458,293,132,283,412,347,251,464,443,343,486,440,395,510,524,352,356,452,219,130,147,283,184,368,472,297
,240,67,241,492,439,566,419,453,360,604,496,405,303,182,283,0,69,8,197,102,229,262,212,261,339,404,241,335,360,399,494,521,466,443,784,577,59
1,445,551,567,641,672,489,613,537,570,543,603,237,172,442,538,586,553,609,702,693,646,472,601,636,596,688,797,649,821,741,677,563,404,577,736
,764,587,690,858,762,847,677,579,704,811,565,699,658,637,657,736,846,823,725,802,700,821,648,618,695,565,628,560,715,691,685,645,559,736,664,
516,609,596,601,585,517,609,697,424,619,727,848,837,885,899,595,678,749,859,660,619,493,318,504,601,552,620,608,435,442,575,720,637,380,555,3
77,234,438,399,418,512,338,337,365,256,296,456,302,409,382,488,601,384,640,516,652,477,463,440,402,384,334,264,368,396,322,364,455,386,406,44
9,436,536,691,666,547,495,634,616,744,602,595,557,334,401,383,487,594,551,543,518,544,614,448,552,433,548,442,737,669,477,686,775,856,546,576
,526,515,391,463,337,431,535,451,462,609,251,425,451,359,335,230,162,268,347,304,568,554,538,547,489,368,346,371,435,257,339,361,466,515,451,
354,326,373,402,419,445,443,573,382,389,233,272,171,219,113,166,158,231,261,57,228,167,120,412,487,458,301,317,319,516,361,336,301,326,264,32
8,293,384,283,193,490,208,378,498,262,244,420,491,329,262,127,274,257,370,340,346,381,428,390,635,544,372,560,362,439,594,601,495,456,349,501
,513,505,349,456,497,577,316,517,586,716,563,509,522,441,330,434,612,552,314,453,522,668,443,516,610,617,641,470,436,638,550,542,469,392,546,
469,508,515,424,511,740,371,525,484,437,635,427,528,496,433,344,196,203,267,124,269,516,544,324,436,633,658,651,627,336,504,481,517,413,413,2
93,298,462,339,436,708,556,657,718,733,638,730,704,578,611,537,633,555,598,404,525,590,707,535,411,607,518,444,284,452,436,473,446,546,669,61
8,596,625,613,548,567,893,378,447,450,546,499,686,636,623,574,666,673,621,718,510,751,523,679,604,640,682,703,706,878,603,738,580,589,725,733
,746,692,600,586,641,638,766,666,724,698,572,604,735,778,721,709,750,661,655,649,524,558,470,390,250,355,280,390,371,478,477,565,436,580,636,
696,633,799,773,739,627,855,699,788,597,684,999,893,876,988,853,796,775,606,841,831,592,711,750,739,833,1000,636,574,861,831,979,875,996,884,
878,884,711,702,627,634,548,596,596,462,533,411,524,568,603,658,481,510,551,609,506,487,516,592,534,544,
422,442,458,456,485,514,540,494,490,511,497,416,442,420,434,460,523,511,560,554,575,531,514,556,515,543,519,5
37,460,446,443,428,463,448,488,591,582,605,576,587,620,592,580,554,549,518,511,551,566,508,487,470,495,477,442,375,369,406,409,403,392,366,40
7,418,414,404,382,387,369,382,334,303,270,184,150,123,143,181,168,205,195,180,222,222,230,198,296,329,334,306,297,311,246,265,305,296,280,235
,315,383,403,418,426,459,482,456,428,424,405,437,363,411,442,471,486,485,477,528,548,530,558,481,432,474,521,559,534,500,474,460,447,469,458,
465,520,475,481,477,492,475,473,471,502,545,534,578,630,605,652,636,695,696,722,683,691,703,735,804,839,820,844,792,770,774,734,744,729,667,6
26,648,617,594,662,674,684,725,692,725,712,709,683,699,735,727,720,734,678,724,742,684,691,676,666,694,733,727,760,774,787,844,860,839,821,84
5,855,850,867,843,806,796,795,677,715,685,643,653,553,554,592,556,555,574,592,552,529,505,468,495,473,510,446,521,551,549,506,521,511,432,443
,408,472,437,444,401,378,402,386,406,417,417,440,456,480,544,555,552,542,515,548,548,553,480,428,467,451,418,401,353,404,404,427,400,424,407,
393,456,451,410,423,421,413,417,468,447,459,422,519,555,555,561,626,659,639,649,683,687,706,715,626,586,548,588,577,571,588,567,583,518,448,3
79,375,402,435,469,484,408,407,425,403,396,427,410,425,409,404,331,403,447,459,513,557,559,589,601,589,592,570,538,545,600,623,645,669,707,75
6,746,733,690,698,720,767,781,758,769,694,708,756,749,813,813,820,889,841,857,849,795,798,761,795,779,755,706,768,774,800,792,840,870,872,892
,851,932,974,962,964,905,947,1000,986,936,921,950,955,927,923,906,898,873,934,883,890,878,894,891,930,907,942,916,865,839,910,853,887,929,933
,909,846,847,813,820,823,796,776,775,767,805,796,781,808,729,676,674,643,625,654,661,715,729,803,785,738,714,693,693,751,784,735,758,760,739,
735,729,687,690,648,593,557,572,563,581,566,506,523,438,451,474,472,462,518,536,573,589,554,561,625,711,747,772,853,878,820,836,888,885,815,8
07,847,835,911,853,786,794,765,695,654,608,587,610,593,519,490,524,486,403,439,404,377,375,401,387,323,392,393,395,362,351,334,330,331,302,29
5,273,285,315,295,340,344,320,320,257,214,163,222,203,171,175,126,122,179,189,203,137,213,179,155,165,138,184,232,243,310,335,354,407,397,354
,395,432,399,431,444,473,531,557,577,540,493,512,524,549,530,567,499,551,524,500,511,541,567,537,532,577,627,618,548,540,542,596,573,602,589,
561,607,639,602,587,609,611,626,619,614,567,619,677,694,707,671,653,715,680,723,700,685,690,651,631,580,578,566,490,493,486,444,478,478,443,4
31,425,398,397,373,412,539,538,477,472,400,417,387,380,378,462,479,419,385,426,452,478,416,408,395,406,414,428,385,319,275,281,279,312,289,26
5,174,217,261,321,365,375,415,443,426,422,390,402,417,428,510,528,514,493,462,433,413,442,447,453,513,557,517,464,462,512,528,522,568,576,578
,604,576,549,575,524,539,491,472,438,480,566,595,546,558,623,560,575,574,569,539,561,593,606,610,581,530,512,488,545,537,467,484,502,554,514,
589,614,546,552,601,586,640,653,668,702,728,742,721,684,721,661,646,588,534,511,518,517,512,463,389,342,290,248,267,274,271,264,260,289,308,3
05,297,286,291,271,281,283,276,272,260,266,273,226,248,183,148,174,157,138,97,77,114,163,141,131,122,99,19,94,68,51,64,45,35,29,63,49,42,41,1

```
1,0,22,84,64,83,106,167,156,168,165,169,133,143,156,173,177,118,140,203,220,224,208,253,231,215,239,258,221,248,340,357,290,279,294,361,400,4
16,438,475,478,494,524,543,570,581,578,626,622,670,660,648,569,609,611,653,646,628,642,645,660,812,815,805,817,853,847,821,820,821,840,877,88
7,862,897,914,903,918,867,816,837,878,864,826,846,855,829,855,867,833,823,795,812,843,854};

// ---------------------------- 421 Code Variables ----------------------------
// Variables for Yes or No to a stimulus
int Level_421 = 0;                              //Index that decides if we are on the 4,2,1 change
int Stimulus_Response_Current = -1;             //Response to current stimulus (Dummy intialization for coding)
int Stimulus_Response_Last = -1;                //Response to last stimulus (Dummy intialization for coding)
int Stimulus_Number = 15;                       //Number of stimuli in the test

// Variables for power variables
int Motor_Power_Input_Initial;                  //Initial power input for the threshold test
int Motor_Level_421[3];                         //Array that has the decimal changes for each motor based on 4,2,1

void setup() {

  // Serial port
  Serial.begin(9600);

  // Starting motor
  drv.begin();
  drv.setMode(DRV2605_MODE_REALTIME);

  // Setting up input pins for switches
  pinMode(Test421_Switch_Pin,INPUT);
  pinMode(TestSignal_Switch_Pin,INPUT);

  // Setting up pins for buttons
  pinMode(Buzz_Button_Pin,INPUT); digitalWrite(Buzz_Button_Pin,HIGH);
  pinMode(No_Button_Pin,INPUT); digitalWrite(No_Button_Pin,HIGH);
  pinMode(Yes_Button_Pin,INPUT); digitalWrite(Yes_Button_Pin,HIGH);

  // Setting up LED
  pinMode(LED_pin,OUTPUT); digitalWrite(LED_pin,LOW);

}

// Function that makes sure all pins and potentiometers are off
void everything_off() {
  digitalWrite(LED_pin,HIGH);
  Serial.println("All OFF");
  Test421_Switch_Value = digitalRead(Test421_Switch_Pin); TestSignal_Switch_Value = digitalRead(TestSignal_Switch_Pin);
  Foot_Pot_Value = analogRead(Foot_Pot_Pin); Motor_Pot_Value = analogRead(Motor_Pot_Pin); Signal_Pot_Value = analogRead(Signal_Pot_Pin);
  Pwr_Pot_Value = analogRead(Pwr_Pot_Pin); m_pwr = map(Pwr_Pot_Value,0,1023,0,100); m_pwr = m_pwr/100;
  while (Test421_Switch_Value == HIGH or TestSignal_Switch_Value == HIGH or Foot_Pot_Value > 122 or
         Motor_Pot_Value > 22 or Signal_Pot_Value > 122 or m_pwr > 0.15) {
    Test421_Switch_Value = digitalRead(Test421_Switch_Pin); TestSignal_Switch_Value = digitalRead(TestSignal_Switch_Pin);
    Foot_Pot_Value = analogRead(Foot_Pot_Pin); Motor_Pot_Value = analogRead(Motor_Pot_Pin); Signal_Pot_Value = analogRead(Signal_Pot_Pin);
    Pwr_Pot_Value = analogRead(Pwr_Pot_Pin); m_pwr = map(Pwr_Pot_Value,0,1023,0,100); m_pwr = m_pwr/100;
  }
  Serial.println("All OK");
  digitalWrite(LED_pin,LOW);
}

// Function that blinks to confirm entry
void LED_blink() {
  for (kk = 1; kk <= 5; kk++) {
    digitalWrite(LED_pin,HIGH); delay(system_delay);
    digitalWrite(LED_pin,LOW);  delay(system_delay);
  }
}

void loop() {

  // Selecting test to be done
  Test421_Switch_Value = digitalRead(Test421_Switch_Pin); TestSignal_Switch_Value = digitalRead(TestSignal_Switch_Pin);
  Yes_Button_Value = digitalRead(Yes_Button_Pin);
  while (Yes_Button_Value == HIGH or (Test421_Switch_Value == HIGH and TestSignal_Switch_Value == HIGH) or
         (Test421_Switch_Value == LOW and TestSignal_Switch_Value == LOW)) {
    Test421_Switch_Value = digitalRead(Test421_Switch_Pin); TestSignal_Switch_Value = digitalRead(TestSignal_Switch_Pin);
    Yes_Button_Value = digitalRead(Yes_Button_Pin);
  }

  // Printing test selection in Serial Monitor
  if (Test421_Switch_Value == HIGH) {
    Serial.print("421,");
  } else {
    Serial.print("Sig,");
  }

  // Confirming entry by blinking
  LED_blink();

  // Selecting feet or foot to be tested, and interpreting the selection
  Foot_Pot_Value = analogRead(Foot_Pot_Pin); Yes_Button_Value = digitalRead(Yes_Button_Pin);
  while (Yes_Button_Value == HIGH or Foot_Pot_Value <= 122) {
    Foot_Pot_Value = analogRead(Foot_Pot_Pin); Yes_Button_Value = digitalRead(Yes_Button_Pin);
  }
  if (Foot_Pot_Value >= 123 and Foot_Pot_Value < 423) {                //Left foot was chosen
    Foot_Pot_Value = 1;
  } else if (Foot_Pot_Value >= 423 and Foot_Pot_Value < 723) {         //Right foot was chosen
    Foot_Pot_Value = 0;
  } else {                                                             //Left and right feet were chosen
    Foot_Pot_Value = 1;
  }

  // Printing feet selection in Serial Monitor
  if (Foot_Pot_Value == 1) {
    Serial.print("L1,");
  } else {
    Serial.print("L0,");
  }
```

```
// Confirming entry by blinking
LED_blink();

// Selecting motor to be used, and interpreting the selection
Motor_Pot_Value = analogRead(Motor_Pot_Pin); Yes_Button_Value = digitalRead(Yes_Button_Pin);
while (Yes_Button_Value == HIGH or Motor_Pot_Value <= 22) {
  Motor_Pot_Value = analogRead(Motor_Pot_Pin); Yes_Button_Value = digitalRead(Yes_Button_Pin);
}
if (Motor_Pot_Value >= 23 and Motor_Pot_Value < 273) {                //Mini motor was chosen
  Motor_Pot_Value = 1;
} else if (Motor_Pot_Value >= 273 and Motor_Pot_Value < 523) {        //Small motor was chosen
  Motor_Pot_Value = 2;
} else if (Motor_Pot_Value >= 523 and Motor_Pot_Value < 773) {        //Medium motor was chosen
  Motor_Pot_Value = 3;
} else {                                                              //Large motor was chosen
  Motor_Pot_Value = 4;
}

// Printing motor selection in Serial Monitor
if (Motor_Pot_Value == 1) {
  Serial.println("Mi");
} else if (Motor_Pot_Value == 2) {
  Serial.println("Sm");
} else if (Motor_Pot_Value == 3) {
  Serial.println("Me");
} else {
  Serial.println("La");
}

// Confirming entry by blinking
LED_blink();

// The signal test was selected
while (TestSignal_Switch_Value == HIGH) {

  // Selecting the signal to be used, and interpreting the selection
  Signal_Pot_Value = analogRead(Signal_Pot_Pin); Yes_Button_Value = digitalRead(Yes_Button_Pin);
  TestSignal_Switch_Value = digitalRead(TestSignal_Switch_Pin);
  while ((Yes_Button_Value == HIGH or Signal_Pot_Value <= 122) and TestSignal_Switch_Value == HIGH) {
    Signal_Pot_Value = analogRead(Signal_Pot_Pin); Yes_Button_Value = digitalRead(Yes_Button_Pin);
    TestSignal_Switch_Value = digitalRead(TestSignal_Switch_Pin);
  }
  if (TestSignal_Switch_Value == LOW) {                               //Reset was pressed
    break;
  }
  if (Signal_Pot_Value >= 123 and Signal_Pot_Value < 423) {           //White signal was chosen
    Signal_Pot_Value = 1;
  } else if (Signal_Pot_Value >= 423 and Signal_Pot_Value < 723) {    //Pink signal was chosen
    Signal_Pot_Value = 2;
  } else {                                                            //Brown signal chosen
    Signal_Pot_Value = 3;
  }

  // Priting color selection in Serial Monitor
  if (Signal_Pot_Value == 1) {
    Serial.println("Wh");
  } else if (Signal_Pot_Value == 2) {
    Serial.println("Pi");
  } else {
    Serial.println("Br");
  }
  Serial.print("\n");

  // Confirming entry by blinking
  LED_blink();

  // Selecting the power to be used, and interpreting the selection
  Pwr_Pot_Value = analogRead(Pwr_Pot_Pin); m_pwr = map(Pwr_Pot_Value,0,1023,0,100); m_pwr = m_pwr/100;
  Yes_Button_Value = digitalRead(Yes_Button_Pin);
  TestSignal_Switch_Value = digitalRead(TestSignal_Switch_Pin); kk = 1;
  while ((Yes_Button_Value == HIGH or m_pwr <= 0.15) and TestSignal_Switch_Value == HIGH) {
    Pwr_Pot_Value = analogRead(Pwr_Pot_Pin); m_pwr = map(Pwr_Pot_Value,0,1023,0,100); m_pwr = m_pwr/100;
    Yes_Button_Value = digitalRead(Yes_Button_Pin);
    TestSignal_Switch_Value = digitalRead(TestSignal_Switch_Pin);
    if (kk == 20) {
      Serial.println(100*m_pwr); kk = 0;
    } else {
      Serial.print(100*m_pwr); Serial.print(",");
    }
    delay(system_delay); kk = kk + 1;
  }
  Serial.print("\n");
  if (TestSignal_Switch_Value == LOW) {                               //Reset was pressed
    break;
  }

  // Confirming entry by blinking
  LED_blink();

  // Based on the motor selection, select m_Vmax and mVmin, and calculate m_Vdelta
  if (Motor_Pot_Value == 1) {                                         //Mini motor was chosen
    m_Vmax = 3.6; m_Vmin = 1.3;
  } else if (Motor_Pot_Value == 2) {                                  //Small motor was chosen
    m_Vmax = 1.8; m_Vmin = 0.4;
  } else if (Motor_Pot_Value == 3) {                                  //Medium motor was chosen
    m_Vmax = 3.6; m_Vmin = 0.6;
  } else {                                                            //Large motor was chosen
    m_Vmax = 3.6; m_Vmin = 0.3;
  }
  m_Vdelta = m_Vmax/127.0;

  // Selecting low and high index values
  m_signal_idx_low = 901*(3*(Motor_Pot_Value-1)+Signal_Pot_Value)-901;
  m_signal_idx_high = 901*(3*(Motor_Pot_Value-1)+Signal_Pot_Value)-1;
```

```
  // Confirming to start the test
  Buzz_Button_Value = digitalRead(Buzz_Button_Pin); TestSignal_Switch_Value = digitalRead(TestSignal_Switch_Pin);
  while (Buzz_Button_Value == HIGH and TestSignal_Switch_Value == HIGH) {
    Buzz_Button_Value = digitalRead(Buzz_Button_Pin); TestSignal_Switch_Value = digitalRead(TestSignal_Switch_Pin);
  }
  if (TestSignal_Switch_Value == LOW) {                                 //Reset was pressed
    break;
  }

  // Signal is sent!!!
  ii = m_signal_idx_low; kk = 1; Serial.print("\n");
  while (ii <= m_signal_idx_high and TestSignal_Switch_Value == HIGH) {

    // Calculating the input for the motor
    m_signal_curr = pgm_read_word(&m_signal[ii]);
    m_signal_curr_float = m_signal_curr/1000.0;
    m_signal_curr_float = m_signal_curr_float*(m_Vmax*m_pwr-m_Vmin)+m_Vmin;
    m_signal_curr_float = m_signal_curr_float/m_Vdelta;
    m_signal_dec = floor(m_signal_curr_float);
    m_signal_dec = Foot_Pot_Value*m_signal_dec;

    // Driving the motor
    drv.setRealtimeValue(m_signal_dec);

    // Printing motor signal
    if (kk == 20) {
      Serial.println(m_signal_dec); kk = 0;
    } else {
      Serial.print(m_signal_dec); Serial.print(",");
    }

    // Checking for reset
    TestSignal_Switch_Value = digitalRead(TestSignal_Switch_Pin);

    // Updating counters and applying delay
    ii++; kk++; delay(system_delay);

  }
  drv.setRealtimeValue(0);                                              //Stopping motor
  if (TestSignal_Switch_Value == LOW) {                                 //Reset was pressed
    break;
  }
  Serial.print("\n"); Serial.print("\n");

  // Making sure everything is turned off before starting new test
  everything_off();

}

// The 421 test was selected
Serial.print("\n");
while (Test421_Switch_Value == HIGH) {

  // Selecting the initial power input and levels for the 421 based on motor's selection
  if (Motor_Pot_Value == 1) {                                           //Mini motor was chosen
    Motor_Power_Input_Initial = 102;
    Motor_Level_421[0]=8; Motor_Level_421[1]=4; Motor_Level_421[2]=2;
  } else if (Motor_Pot_Value == 2) {                                    //Small motor was chosen
    Motor_Power_Input_Initial = 97;
    Motor_Level_421[0]=9; Motor_Level_421[1]=5; Motor_Level_421[2]=2;
  } else if (Motor_Pot_Value == 3) {                                    //Medium motor was chosen
    Motor_Power_Input_Initial = 95;
    Motor_Level_421[0]=10; Motor_Level_421[1]=5; Motor_Level_421[2]=2;
  } else {                                                              //Large motor was chosen
    Motor_Power_Input_Initial = 93;
    Motor_Level_421[0]=11; Motor_Level_421[1]=5; Motor_Level_421[2]=2;
  }

  // This is a buzz.................
    // Pressing the buzz button
    Buzz_Button_Value = digitalRead(Buzz_Button_Pin); Test421_Switch_Value = digitalRead(Test421_Switch_Pin);
    while (Buzz_Button_Value == HIGH and Test421_Switch_Value == HIGH) {
      Buzz_Button_Value = digitalRead(Buzz_Button_Pin); Test421_Switch_Value = digitalRead(Test421_Switch_Pin);
    }
    if (Test421_Switch_Value == LOW) {                                    //Reset button was pressed
      break;
    }

    // Confirming entry by blinking
    LED_blink();

    // Calibration buzz for 10 seconds, followed by 5 seconds of nothing
    kk = 1;
    for (ii = 1; ii <= 150; ii++) {
      if (ii <= 100) {
        drv.setRealtimeValue(Foot_Pot_Value*Motor_Power_Input_Initial);
        if (kk == 20) {
          Serial.println(Foot_Pot_Value*Motor_Power_Input_Initial); kk = 0;
        } else {
          Serial.print(Foot_Pot_Value*Motor_Power_Input_Initial); Serial.print(",");
        }
      } else {
        drv.setRealtimeValue(0);
        if (kk == 20) {
          Serial.println(0); kk = 0;
        } else {
          Serial.print(0); Serial.print(",");
        }
      }
      kk++;
      delay(system_delay);
    }
    Serial.print("\n");
```

```
// 421 Threshold test starts
for (ii = 1; ii <= Stimulus_Number; ii++) {

  // LED ON on odd numbers
  if (ii == 1 or ii == 3 or ii == 5 or ii == 7 or ii == 9 or ii == 11 or ii == 13 or ii == 15) {
    digitalWrite(LED_pin,HIGH);
  } else {
    digitalWrite(LED_pin,LOW);
  }

  // For the first trial, just use Motor_Power_Input_Initial with the foot selection
  if (ii == 1) {
    m_signal_dec = Foot_Pot_Value*Motor_Power_Input_Initial;
  }

  // Driving motors for 6 seconds, and counting the number of seconds the feeling button is pressed
  kk = 0;
  for (jj = 1; jj <= 60; jj++) {

    // Moving the motor
    drv.setRealtimeValue(m_signal_dec);

    // Checking if it was felt and adding to the counter
    No_Button_Value = digitalRead(No_Button_Pin);
    if (No_Button_Value == LOW) {
      kk++;
    }

    // Printing motor input in the command window
    if (jj == 20 or jj == 40 or jj == 60) {
      Serial.println(m_signal_dec);
    } else {
      Serial.print(m_signal_dec); Serial.print(",");
    }

    // Applying system's delay
    delay(system_delay);

  }

  // Recording last response
  if (Stimulus_Response_Current != -1) {
    Stimulus_Response_Last = Stimulus_Response_Current;
  }

  // Did the participant feel it? Analysis based on the answer
  if (kk >= 45) {                                    //Yes to sensation

    // Modifying the current response
    Stimulus_Response_Current = 1;

    // Updating 421 level and calculating next motor input (it goes down)
    if (Stimulus_Response_Last == 0 and Level_421 != 2) {              //Went from No to Yes, and Level_421 changes
        Level_421 = Level_421 + 1;
    }
    m_signal_dec = Foot_Pot_Value*(m_signal_dec - Motor_Level_421[Level_421]);

  } else {                                            //No to sensation

    // Modifying the current response
    Stimulus_Response_Current = 0;

    // Updating 421 level and calculating next motor input (it goes up)
    if (Stimulus_Response_Last == 1 and Level_421 != 2) {              //Went from Yes to No, and Level_421 changes
        Level_421 = Level_421 + 1;
    }
    m_signal_dec = Foot_Pot_Value*(m_signal_dec + Motor_Level_421[Level_421]);

  }

  // Check if test is terminated
  Test421_Switch_Value = digitalRead(Test421_Switch_Pin);
  if (Test421_Switch_Value == LOW) {
    break;
  }

}

if (Test421_Switch_Value == LOW) {                                  //Reset button was pressed
  drv.setRealtimeValue(0);                                          //Turning off the motors
  break;
}

// Almost Successfull test!!!!
while (ii == Stimulus_Number+1 and Stimulus_Response_Last == Stimulus_Response_Current) {

  // LED indication
  digitalWrite(LED_pin,LOW);

  // Driving motors for 6 seconds, and counting the number of seconds the feeling button is pressed
  kk = 0;
  for (jj = 1; jj <= 60; jj++) {

    // Moving the motor
    drv.setRealtimeValue(m_signal_dec);

    // Checking if it was felt and adding to the counter
    No_Button_Value = digitalRead(No_Button_Pin);
    if (No_Button_Value == LOW) {
      kk++;
    }

    // Printing motor input in the command window
```

```
      if (jj == 20 or jj == 40 or jj == 60) {
        Serial.println(m_signal_dec);
      } else {
        Serial.print(m_signal_dec); Serial.print(",");
      }

      // Applying system's delay
      delay(system_delay);

    }

    // Did the participant feel it? Analysis based on the answer
    if (kk >= 45) {                                     //Yes to sensation

      // Modifying the current response
      Stimulus_Response_Current = 1;

      // Updating 421 level and calculating next motor input (it goes down)
      if (Stimulus_Response_Last == 0 and Level_421 != 2) {              //Went from No to Yes, and Level_421 changes
         Level_421 = Level_421 + 1;
      }
      m_signal_dec = Foot_Pot_Value*(m_signal_dec - Motor_Level_421[Level_421]);

    } else {                                             //No to sensation

      // Modifying the current response
      Stimulus_Response_Current = 0;

      // Updating 421 level and calculating next motor input (it goes up)
      if (Stimulus_Response_Last == 1 and Level_421 != 2) {              //Went from Yes to No, and Level_421 changes
         Level_421 = Level_421 + 1;
      }
      m_signal_dec = Foot_Pot_Value*(m_signal_dec + Motor_Level_421[Level_421]);

    }

    // Check if test is terminated
    Test421_Switch_Value = digitalRead(Test421_Switch_Pin);
    if (Test421_Switch_Value == LOW) {
      break;
    }

    // Finishing with extra step
    ii = ii + 1;

  }

  //Turning off the motors
  drv.setRealtimeValue(0);

  if (Test421_Switch_Value == LOW) {                                  //Reset button was pressed
    break;
  }

  // Fake vibration to know if the last stimulus was felt
  for (jj = 1; jj <= 60; jj++) {

    // Printing motor input in the command window
    if (jj == 20 or jj == 40 or jj == 60) {
      Serial.println(m_signal_dec);
    } else {
      Serial.print(m_signal_dec); Serial.print(",");
    }

  }
  Serial.print("\n");

  // Making sure everything is turned off before starting new test
  everything_off();

}

// Making sure everything is turned off before starting new test
everything_off();

// Reseting all variables
Level_421 = 0; Stimulus_Response_Current = -1; Stimulus_Response_Last = -1;

// Delay
delay(system_delay);

}
```

Arduino_Right_Master.ino

The code for the three Arduino UNOs that control the right foot's vibrating components is almost the same as the one used for the three Arduino UNOs that control the left foot's vibrating components. The only differences are two if-statements located lines 180 and 189 under the comments "`// Selecting`

feet or foot to be tested, and interpreting the selection", and "// Printing feet selection in Serial Monitor". Instead of using the left foot's if-statements:

```
if (Foot_Pot_Value >= 123 and Foot_Pot_Value < 423) {                //Left foot was chosen
    Foot_Pot_Value = 1;
  } else if (Foot_Pot_Value >= 423 and Foot_Pot_Value < 723) {        //Right foot was chosen
    Foot_Pot_Value = 0;
  } else {                                                           //Left and right feet were chosen
    Foot_Pot_Value = 1;
  }


  if (Foot_Pot_Value == 1) {
    Serial.print("L1,");
  } else {
    Serial.print("L0,");
  }
```

Use the right foot if-statements:

```
if (Foot_Pot_Value >= 123 and Foot_Pot_Value < 423) {                //Left foot was chosen
    Foot_Pot_Value = 0;
  } else if (Foot_Pot_Value >= 423 and Foot_Pot_Value < 723) {        //Right foot was chosen
    Foot_Pot_Value = 1;
  } else {                                                           //Left and right feet were chosen
    Foot_Pot_Value = 1;
  }


  if (Foot_Pot_Value == 1) {
    Serial.print("R1,");
  } else {
    Serial.print("R0,");
  }
```

Motor Selector MATLAB Code

The code requires investigators to number their eccentric rotating motors at the external housing, and to know what each number corresponds to. That means that it is needed to have a table that shows the motor number and its respective motor size (307-105, 310-003, 306-10H, or 307-103), foot size (Short, Middle or Long), and foot location (Heel, first or fifth metatarsal). In the example code below, motors labeled as Mini, Small, Medium and Large correspond respectively to 307-105, 310-003, 306-10H and 307-103.

Main Code

```
%% Biodynamics Research Lab, University of Kansas
%Brett Whorley, November 2019

%This code determines which motors should be connected for vibrotactile
%testing on the BRL custom-manufactured silicone mat.

%In Section 2, the user enters the participant's foot length (LINE 31)
%and the current motor size (LINE 36). The program outputs the six (6)
```

```
%motors to connect for testing, three (3) per foot. Motors are located
%at the base of the 1st and 5th metatarsals, and the heel of each foot.

%Foot length guide:                          (Source: Mickleetal, 2010)
    %Eligbility Criteria:
    %   Womens Shoe Size >= 6      Mens Shoe Size <= 14

    %   Mens Shoe Size          Womens Shoe Size      Foot Length Class
    %      M 6-8.5                W 7-9.5                Short
    %      M 8.5-10.5             W 9.5-11.5             Middle
    %      M 10.5-13              W 11.5-14              Long

clear; clc; close all; format compact;

%% Section 1: Motor Groupings (1-56)
%%% USER SHOULD NOT ALTER ANYTHING IN THIS SECTION ***
h = 1;
[Heels,First_Mets,Fifth_Mets,Short,Middle,Long, Mini, Small,...
    Medium, Large, Right, Left] = motor_groupings(h);

%% Section 2: *** This is the ONLY User Input Section ***

%Enter Foot Length based on shoe size guide above:
%Options: Short, Middle, Long
%Do NOT change variable name
valid_length = Middle;

%Enter Motor Size for Vibration:
%Options: Mini (307-105), Small (310-003), Medium (306-10H), Large (307-103)
%Do NOT change variable name
valid_size = Mini;

%%% USER DOES NOT NEED TO ENTER ANYTHING BEYOND THIS POINT ***

%% Section 3: Process User Inputs and Output Motors to Turn On
%%% USER SHOULD NOT ALTER ANYTHING IN THIS SECTION ***
[Motors_On, Motors_On_Right, Motors_On_Left] = motor_connections(valid_length,valid_size,Heels)

%% Section 4: Display Prompt for Participant

if valid_size == Mini           %307-105
    disp('Place heels on the WHITE dots, and align big toes with WHITE lines')
elseif valid_size == Small      %310-003
    disp('Place heels on the BLUE dots, and align big toes with BLUE lines')
elseif valid_size == Medium     %306-10H
    disp('Place heels on the YELLOW dots, and align big toes with YELLOW lines')
elseif valid_size == Large      %307-103
    disp('Place heels on the GREEN dots, and align big toes with GREEN lines')
end

%% End Program
```

Functions

```
function [Heels,First_Mets,Fifth_Mets,Short,Middle,Long, Mini, Small,...
    Medium, Large, Right, Left] = motor_groupings(h)

%Group by Anatomical Location
Heels = sort([30 29 34 33 25 27 26 28]);
First_Mets = sort([49 48 47 40 39 38 52 51 50 43 42 41 1 2 3 11 22 24 5 ...
    7 12 14 15 16]);
Fifth_Mets = sort([56 45 44 46 32 31 55 54 53 37 36 35 6 10 4 20 21 23 ...
    8 9 13 17 18 19]);
```

```
%Group by Foot Length
Short = sort([44 31 47 38 53 35 50 41 3 24 4 23 12 16 13 19]);
Middle = sort([45 32 48 39 54 36 51 42 2 22 10 21 7 15 9 18]);
Long = sort([56 46 49 40 55 37 52 43 1 11 6 20 5 14 8 17]);

%Group by Motor Size
Mini = sort([37 36 35 33 43 42 41 14 15 16 17 18 19 28]);
Small = sort([46 32 31 29 38 39 40 11 22 24 27 20 21 23]);
Medium = sort([55 54 53 50 51 52 34 5 7 12 26 8 9 13]);
Large = sort([56 45 44 30 47 48 49 1 2 3 25 4 6 10]);

%Group by Rt/Lf Foot
Right = [1:28];
Left = [29:56];

end     %end function

%%%%%%%%%%%%%%%%%%%%%%%%%%%%%%%%%%%%%%%%%%%%%%%%%%%%%%%%%%%%%%%%%%%%%%%

function [Motors_On, Motors_On_Right, Motors_On_Left] = ...
    motor_connections(valid_length,valid_size,Heels)

%Identify Metatarsal Motors
for i = 1:length(valid_length)
    for j = 1:length(valid_size)
        if valid_length(i) == valid_size(j)
            valid_overlap(i) = valid_length(i);
        end
    end
end

Motors_Mets_idx = find(valid_overlap > 0);
Motors_Mets = valid_overlap(Motors_Mets_idx);

clear valid_overlap;

%Identify Heel Motors
for i = 1:length(Heels)
    for j = 1:length(valid_size)
        if Heels(i) == valid_size(j)
            valid_overlap(i) = Heels(i);
        end
    end
end

Motors_Heels_idx = find(valid_overlap > 0);
Motors_Heels = valid_overlap(Motors_Heels_idx);

%Assemble Array of Six Motors
Motors_On_Unadjusted = sort([Motors_Mets,Motors_Heels]);

%Adjust for broken motors with nearest neighbors (If needed)
for i_counter = 1:length(Motors_On_Unadjusted)
    if Motors_On_Unadjusted(i_counter) == 56    %Large Motor, Lf 5M Long
        Motors_On_Unadjusted(i_counter) = 45;
    elseif Motors_On_Unadjusted(i_counter) == 44   %Large, Lf 5M Short
        Motors_On_Unadjusted(i_counter) = 45;
    elseif Motors_On_Unadjusted(i_counter) == 43   %Mini, Lf 1M Long
        Motors_On_Unadjusted(i_counter) = 42;
    elseif Motors_On_Unadjusted(i_counter) == 1    %Large, Rt 1M Long
        Motors_On_Unadjusted(i_counter) = 2;
    elseif Motors_On_Unadjusted(i_counter) == 4    %Large, Rt 5M Short
        Motors_On_Unadjusted(i_counter) = 10;
    end
end
```

```
%Identify Six Motors to Turn On
Motors_On = sort(Motors_On_Unadjusted);

%Identify Right/Left Foot Motors for Reference
Motors_On_Right_idx = find(Motors_On < 29);
Motors_On_Right = Motors_On(Motors_On_Right_idx);

Motors_On_Left_idx = find(Motors_On > 28);
Motors_On_Left = Motors_On(Motors_On_Left_idx);

end   %end function
```

Modified 421 Protocol

The modified 421 [95] uses the original stepping protocol, number of stimuli and starting point [94]. However, instead of having the researcher cue the participant on whether they feel vibration, the participant presses and holds a button every time they feel vibration. Also, the stimulus length in the original 421 was never defined, so it was decided for the modified 421 to use 6 seconds per stimulus. This allowed the protocol to control for the duration of the protocol, which is approximately 2 minutes. The original 421 protocol did not define neither if the stimuli had to be continuous, or intermittent. In other words, if the power level is meant to go from 90 to 94, is the power level meant to go to 0 in between 90 and 94? Or, is it meant to go from 90 to 94 without stopping the motors? Since, it was not defined, it was decided for the modified 421 protocol to keep the motors moving continuously to avoid any transient behavior (i.e., sudden starts and stops) that could affect the participant's sensing threshold. Given that each stimulus lasts 6 seconds, a positive response towards vibration is recorded if the button is pressed for more than 4.5 seconds in each stimulus. Finally, the sensing threshold is calculated as originally proposed (i.e., average of all 1-steps turnovers). Further details in the modifications and their justifications are described in a previous study [95].

Manufacturing Documentation

Step 1: Build the mold for the vibratory mat, insert the pedestals for all vibrating component, and spray plenty on non-stick fluid. Next, pour half of the Shore A50 silicone (Height = 5 mm) without overflowing

the mold's sides or pedestals. Make sure a flat working table or bench is used for this step and throughout the entire manufacturing process. Let the silicone rest for at least 24 hours

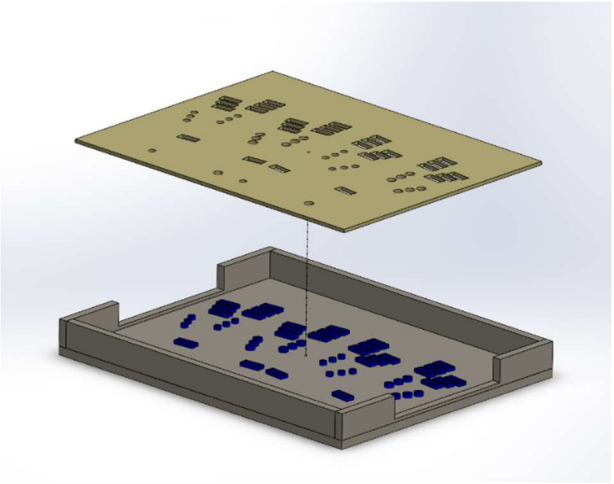

Figure 24: Manufacturing step 1 for new vibratory mat

Step 2: Place eccentric rotating motors on their respective pedestals, as well as the two halves of the PCB board on the sides of the mold. In the next step, soldering the wires of all motors to the PCB boards will be required, so aim the motors' wires with the goal of making next step easier.

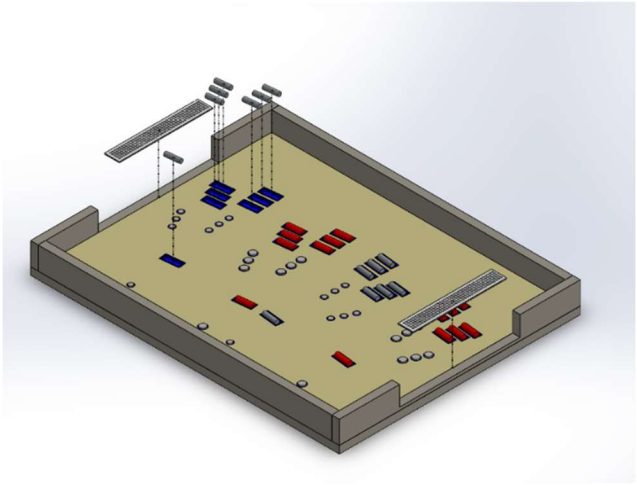

Figure 25: Manufacturing step 2 for new vibratory mat

Step 3: Solder all motors to the PCB boards and record the pin numbers that are getting connected to all wires (negative and positive of each motor). It is acceptable to use the entire area of the mat; however,

avoid placing wires on other eccentric rotating motors. To keep wires from moving during this step, place a small piece of tape on any wires that have been soldered to the PCB boards.

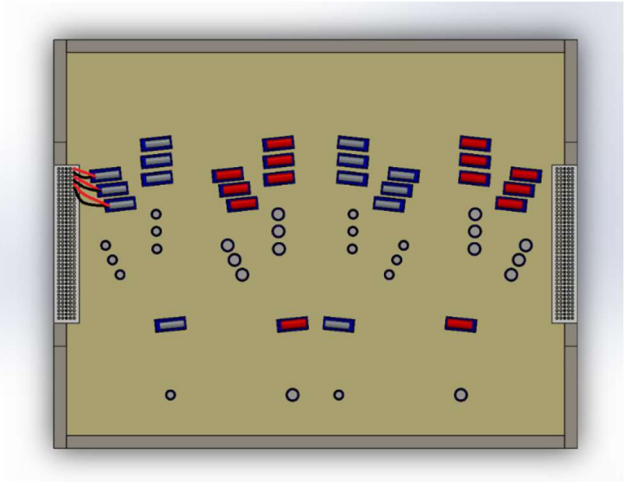

Figure 26: Manufacturing step 3 for new vibratory mat

Step 4: Clamp the mold side sliders (A), spray the sides that will touch the mat with non-sticking spray, and cover any gaps created between the side sliders and the mold. Due to the thickness of the PCB boards, a small gap will be created on each side that must be covered with a moldable and non-permanent material (e.g., Play Dough). Next, pour the second half of Shore A50 silicone (other 5 mm) on top of the vibratory mat, and let is rest again for at least 24 hours.

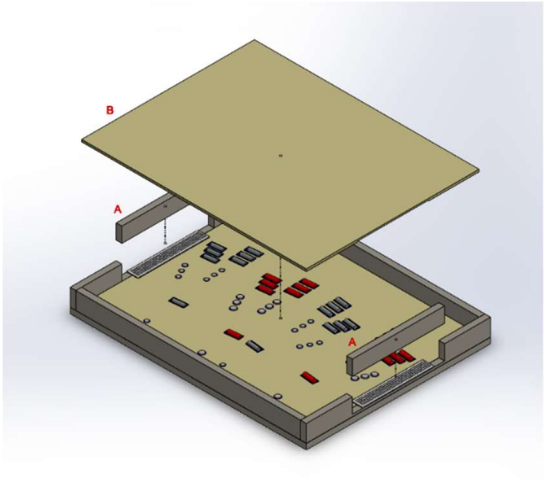

Figure 27: Manufacturing step 4 for new vibratory mat

Step 5: Remove mat and the mold side sliders from the mold. The mat should easily leave the mold, if enough non-stick spray was used. The pedestals might not stay on the mold's bottom. If this happens, use pliers to remove them from the mat, and attach them again to the mold's bottom.

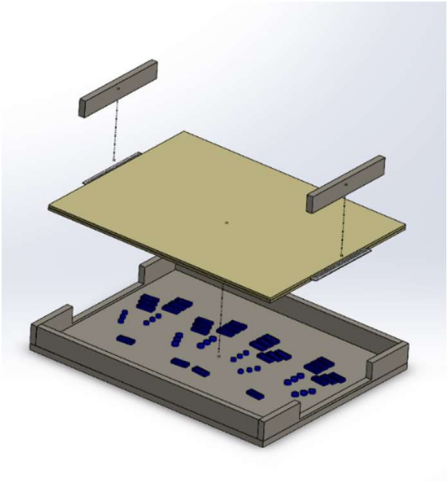

Figure 28: Manufacturing step 5 for new vibratory mat

Step 6: Flip the mat, and fill with enough Shore A50 silicone any holes created by the pedestals. Let eh silicone rest for at least 24 hours, and in case small bumps are created when filling the holes, sand them down with sandpaper.

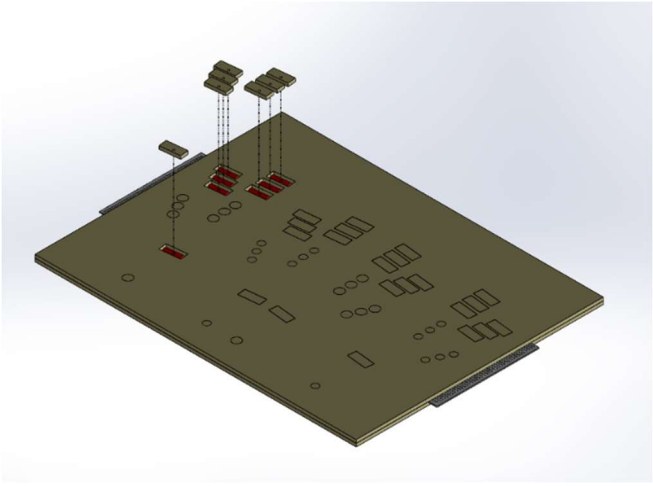

Figure 29: Manufacturing step 6 for new vibratory mat

Step 7: Attach the cork and soft layers to the top of the vibratory mat and draw the feet placement instructions. A small circle is needed for all heels, as well as lines that indicate a 14-degree angle between the participants' big toes.

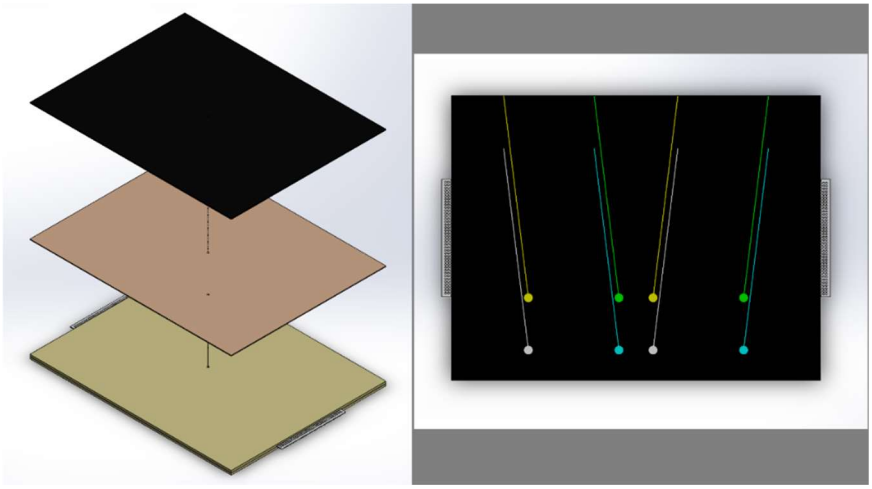

Figure 30: Manufacturing step 7 for new vibratory mat

Step 8: Put together the external housing for the vibratory mat and connect the PCB boards to the side of the external housing. To do so for each motor, solder two wires (negative and positive) to the PCB following the connections created in Step 3. The wires must be long enough that when twisted, they go passed the side of the external housing. Insert the nut and washer of the BNC wall mount through the twisted wires and solder the wall BNC mount to the other end of the wires. Finally, slide the twisted wires through the slot of the external housing's side and clamp the BNC wall mount. Number the BNC wall mount, so it is possible to tell which motor will be operated, if that BNC wall mount is connected to the controller.

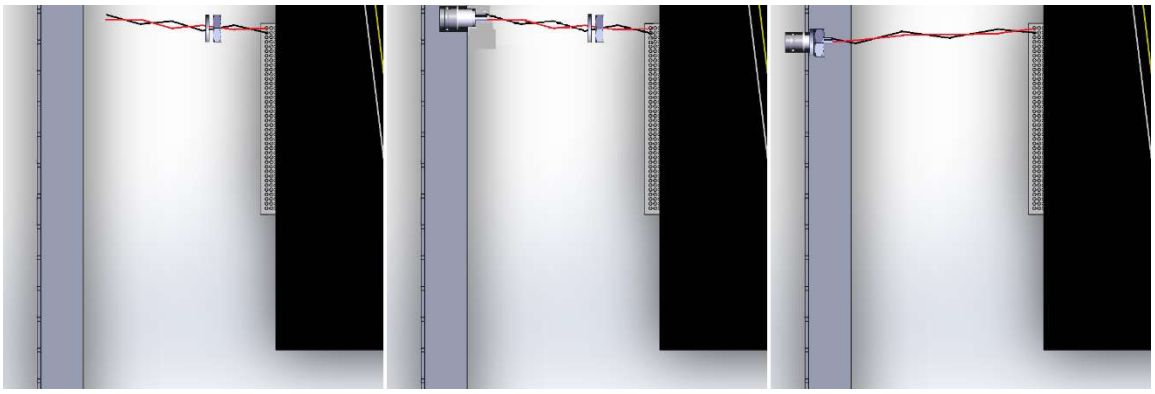

Figure 31: Manufacturing step 8 for new vibratory mat

After all steps are completed, the final product is described by the image below. A final recommendation is to add strong fabric or string nylons under the external housing, allowing the movement of the entire device without putting unnecessary tension on wires.

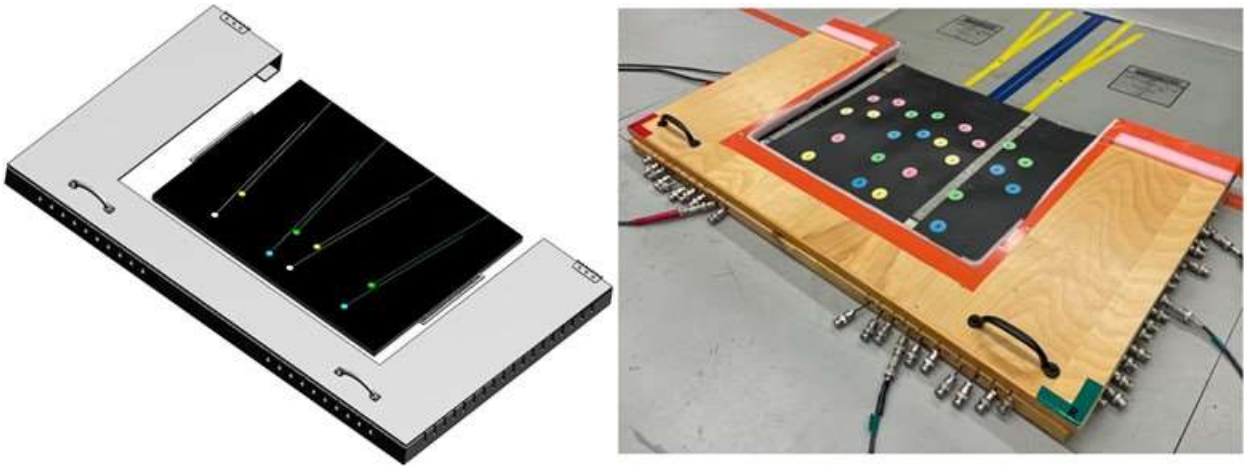

Figure 4: New vibratory mat

Vibratory mat controlled by custom-built Arduino code that uses validated white, pink, and brown inputs for each of the offered motors. Four sets of motors (307-105, 310-003, 306-10H and 307-103 from Precision Microdrives, UK) are embedded in a 10-mm think Shore A50 silicone, and each set of motors accommodate multiple shoe sizes by offering three ranges of shoe sizes. Finally, the mat directs participants to follow a standardized stance. Further details in Chapter 3 of this dissertation.

Chapter 4 Appendix

Data Manipulation to Determine Exerted Force

For every motor, feet setting, simulated participant's weight, and power level, the following data manipulation was required to determine the exerted force by the vibratory mat. Motor 307-103, Feet Setting BF, Simulated Weight = 34 kg, and Power Level = 60% will be used as example.

Step 1: The force plate (AMTI, Watertown, MA, USA) kinetic data was recorded for 10 seconds at 2500 Hz using a 16-bit A/D CED Power mkII and Spike2 (Cambridge Electronic Design, UK), while the vibratory mat's power level was held constant. The recording period was longer than 10 seconds (~15 seconds); however, the motor was only in motion for 10 seconds as the green highlight at the top of Figure 32 shows it.

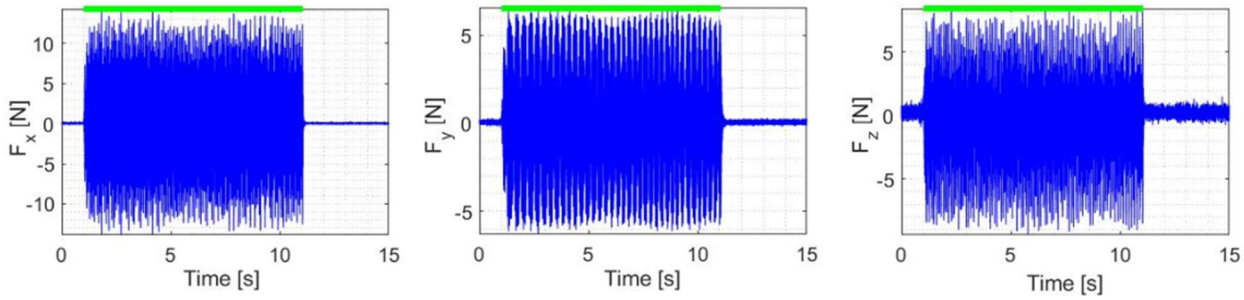

Figure 32: Step 1 to determine exerted force or frequency by vibratory mat

Kinetic data of Motor 307-103, Feet Setting BF, Simulated Weight = 34 kg, and Power Level = 60% under the Static Test set-up, used to determine the exerted force of the vibratory mat. Green highlight shows when the motor was ON.

Step 2: The resultant ground reaction force was calculated using the x, y, z directions $\left(F_{xyz} = \sqrt{F_x^2 + F_y^2 + F_z^2}\right)$, which were filtered previously with a band-pass whose cut-off frequencies were 20 Hz and 400 Hz [21], [27], [49], [55]. The unfiltered (blue data) and filtered (orange) data are displayed to show that the band-pass filter did not alter the vibration exerted by the motors; but removed any system's noise (Figure 33).

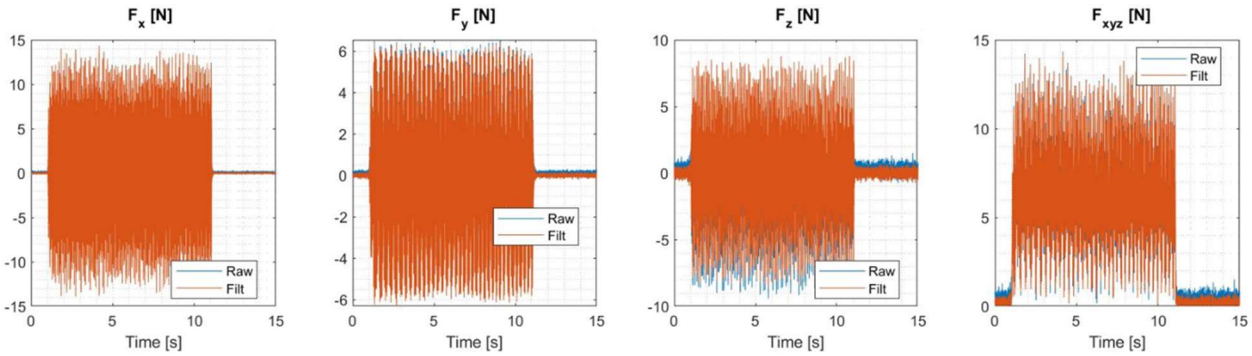

Figure 33: Step 2 to determine exerted force by vibratory mat

Raw (Blue) and 40-200Hz band-pass filtered (Orange) kinetic data of Motor 307-103, Feet Setting BF, Simulated Weight = 34 kg, and Power Level = 60% under the Static Test set-up.

Step 3: The resultant ground reaction force was then rectified with a 10 Hz time window (i.e., frequency at which new inputs were given to the motors) over the period that the motors were activated $\left(F_{rect} = \sqrt{\frac{1}{0.1}\int_{t-0.1}^{t}\left[F_{xyz}(t)\right]^2 dt}\right)$. The middle 50% of the time series was extracted, and an average and standard deviation were calculated to quantify the force exerted by the motor at a given power level. The middle part of the data was used to avoid any transient behavior at the start and end of the vibration (Figure 34).

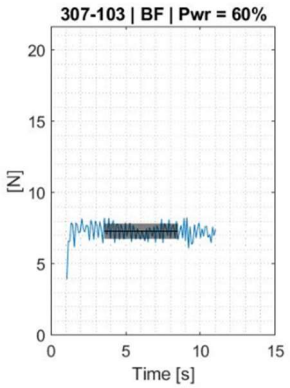

Figure 34: Step 3 to determine exerted force by vibratory mat

Rectified resultant force every 0.1-second windows (Blue), and average and standard deviation (black line and shade) that quantify the force exerted by the motor at a given power level. Graph is for Motor 307-103, Feet Setting BF, Simulated Weight = 34 kg, and Power Level = 60% under the Static Test set-up.

These steps were then repeated for all motors (307-105, 310-003, 306-10H and 307-103), feet settings (LF, BF and RF), simulated participants' weights (34 kg, 75 kg, and 115 kg), and power levels (20% to

100% increments of 10%) to obtain the figure that shows all exerted forces by the vibratory mat (Figure 9).

Data Manipulation to Determine Exerted Frequency

For every motor, feet setting, simulated participant's weight, and power level, the following data manipulation was required to determine the exerted frequency by the vibratory mat. Motor 307-103, Feet Setting BF, Simulated Weight = 34 kg, and Power Level = 60% will be used as example.

Step 1: The force plate (AMTI, Watertown, MA, USA) kinetic data was recorded for 10 seconds at 2500 Hz using a 16-bit A/D CED Power mkII and Spike2 (Cambridge Electronic Design, UK), while the vibratory mat's power level was held constant. The recording period was longer than 10 seconds (~15 seconds); however, the motor was only in motion for 10 seconds as the green highlight at the top of Figure 32 shows it. Step 1 to determine the exerted frequency by the vibratory mat is the same Step 1 to determine the exerted force by the vibratory mat, meaning that both data manipulations can be done in parallel.

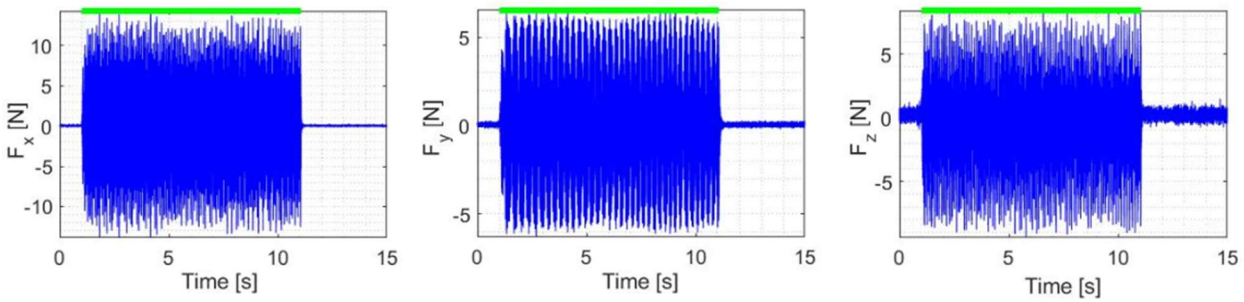

Figure 32: Step 1 to determine exerted force or frequency by vibratory mat

Kinetic data of Motor 307-103, Feet Setting BF, Simulated Weight = 34 kg, and Power Level = 60% under the Static Test set-up, used to determine the exerted force of the vibratory mat. Green highlight shows when the motor was ON.

Step 2: Power spectrum density plots were developed for each of the ground reaction forces (x, y, and z directions). Figure 35 shows the power spectrum generated by the vibratory mat (i.e., Blue lines), static weight that simulates the participant's weight (i.e., Red lines), and force plate when no load is on it or the vibratory mat is operated (i.e., Black Lines).

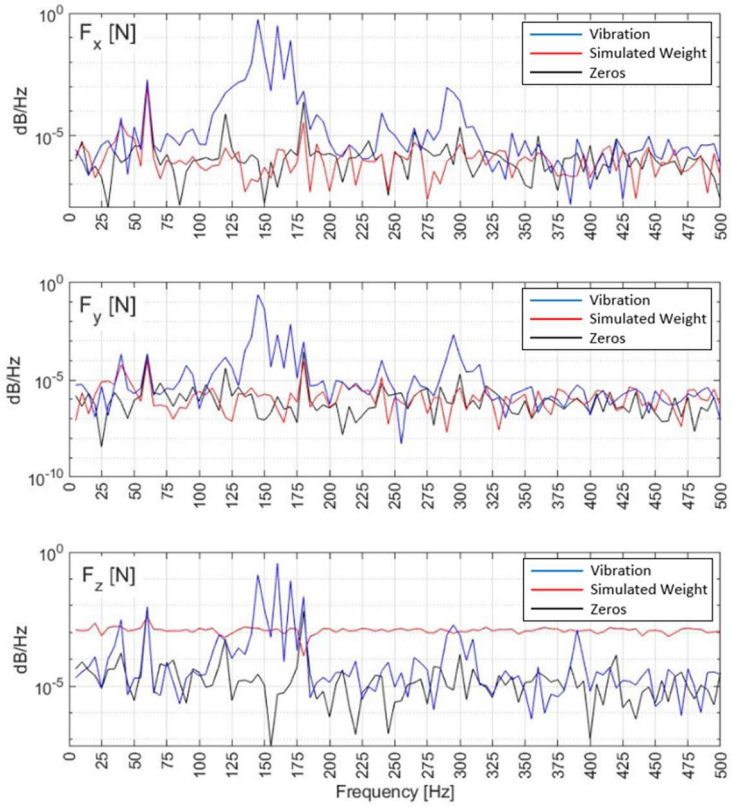

Figure 35: Step 2 to determine exerted frequency by vibratory mat

Power spectrum density plots for all ground reaction forces of Motor 307-103, Feet Setting BF, Simulated Weight = 34 kg, and Power Level = 60% under the Static Test set-up. Blue, red and black lines represent the power spectrum for the vibration, simulated weight and zeros (i.e., force plate without weight or vibration).

Step 3: The frequencies at which power spectral density behavior started and ended were recorded using visual inspection (Figure 35). The visual inspection consisted on determining when the power spectrum of the vibration (Blue line in Figure 35) significantly diverged from the power spectrum of the simulated weight and/or zeros (Red and/or Black lines in Figure 35).

Step 4: The power spectrum of the vibration with respect to the power spectrum of the force plate alone (i.e., Zeros) was calculated for each direction (Figure 36). Given that this subtraction could yield negative values (not mathematically possible), the smallest positive value in each direction was used as the lowest possible answer. Among the three directions, the frequency at which the largest difference occurred was selected and labeled as the frequency exerted by the vibratory mat. It must be pointed out that this selection was only done between the starting and ending frequencies determined in Step 3.

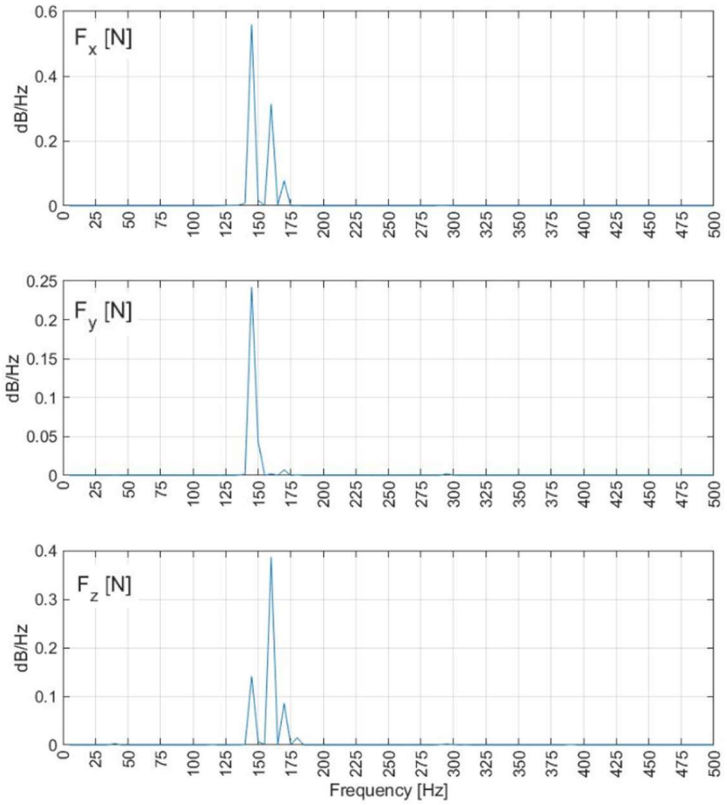

Figure 36: Step 4 to determine exerted frequency by vibratory mat

Power spectrum density plots of the vibration with respect to zeros for all ground reaction forces of Motor 307-103, Feet Setting BF, Simulated Weight = 34 kg, and Power Level = 60% under the Static Test set-up.

These steps were then repeated for all motors (307-105, 310-003, 306-10H and 307-103), feet settings (LF, BF and RF), simulated participants' weights (34 kg, 75 kg, and 115 kg), and power levels (20% to 100% increments of 10%) to obtain the figure that shows all exerted frequencies by the vibratory mat (Figure 10).

Regression Analysis on Exerted Magnitude and Frequency

Linear and quadratic regression models were fitted into the exerted forces (Figure 9) and frequencies (Figure 10) for a given feet setting and motor. The liner and quadratic regression models respectively consisted of $y = A_0 + A_1x_1 + A_2x_2$ and $y = A_0 + A_1x_1 + A_2x_2 + A_3x_1^2 + A_4x_1x_2$ where A_n are coefficients, x_1 is power level and x_2 is simulated weight. A comparison between the linear and quadratic models through Adjusted R^2 and RMSE is given in Table 13. It is possible to see that a quadratic regression model yielded better fits for all exerted forces and frequencies when compared to the linear

regression models (i.e., R^2_{adj} was closer to 1, and RMSE was lower for the quadratic models when compared to all linear models). Column "Lin vs. Qua" in Table 13 indicates in the first letter from left-to-right the model had a better R^2_{adj}, while in the second letter the model had a better RMSE. The estimates (without their prediction bounds) for the exerted forces and frequencies calculated by the quadratic regression models are displayed respectively in Figure 37 and Figure 38.

Table 13: Comparison of linear and quadratic regression fits

	Motor	Feet	Lin: R^2_{adj}	Lin: RMSE	Qua: R^2_{adj}	Qua: RMSE	Lin vs. Qua
Exerted Magnitude	307-105	LF	0.9233	0.2486	0.9307	0.2363	QQ
		BF	0.8497	0.3547	0.8973	0.2932	QQ
		RF	0.3389	0.4059	0.5200	0.3459	QQ
	310-003	LF	0.9159	0.6659	0.9849	0.2819	QQ
		BF	0.9045	0.9633	0.9805	0.4351	QQ
		RF	0.8360	0.9808	0.9499	0.5421	QQ
	306-10H	LF	0.8925	0.8568	0.9811	0.3595	QQ
		BF	0.8898	1.0873	0.9638	0.6228	QQ
		RF	0.8956	0.5207	0.9052	0.4960	QQ
	307-103	LF	0.8476	1.2106	0.8793	1.0772	QQ
		BF	0.8986	1.4765	0.9239	1.2792	QQ
		RF	0.8849	1.2430	0.9167	1.0575	QQ
Exerted Frequency	307-105	LF	0.9387	10.3453	0.9460	9.7109	QQ
		BF	0.7702	17.4366	0.8188	15.4812	QQ
		RF	0.2284	49.4248	0.2599	48.4066	QQ
	310-003	LF	0.6775	26.0475	0.7025	25.0166	QQ
		BF	0.8763	17.0787	0.8798	16.8320	QQ
		RF	0.7197	27.1653	0.7239	26.9600	QQ
	306-10H	LF	0.9644	11.2794	0.9684	10.6218	QQ
		BF	0.9649	11.2231	0.9823	7.9611	QQ
		RF	0.9630	10.7633	0.9642	10.5790	QQ
	307-103	LF	0.9726	7.6871	0.9884	5.0034	QQ
		BF	0.9278	13.7061	0.9658	9.4302	QQ
		RF	0.9550	10.9433	0.9716	8.6886	QQ

Adjusted R^2 and RMSE for linear (Lin) and quadratic (Qua) regression models. Column "Lin vs. Qua" shows in the first letter (left to right) which model has a better Adjusted R^2, while the second letter displays which model has a better RMSE.

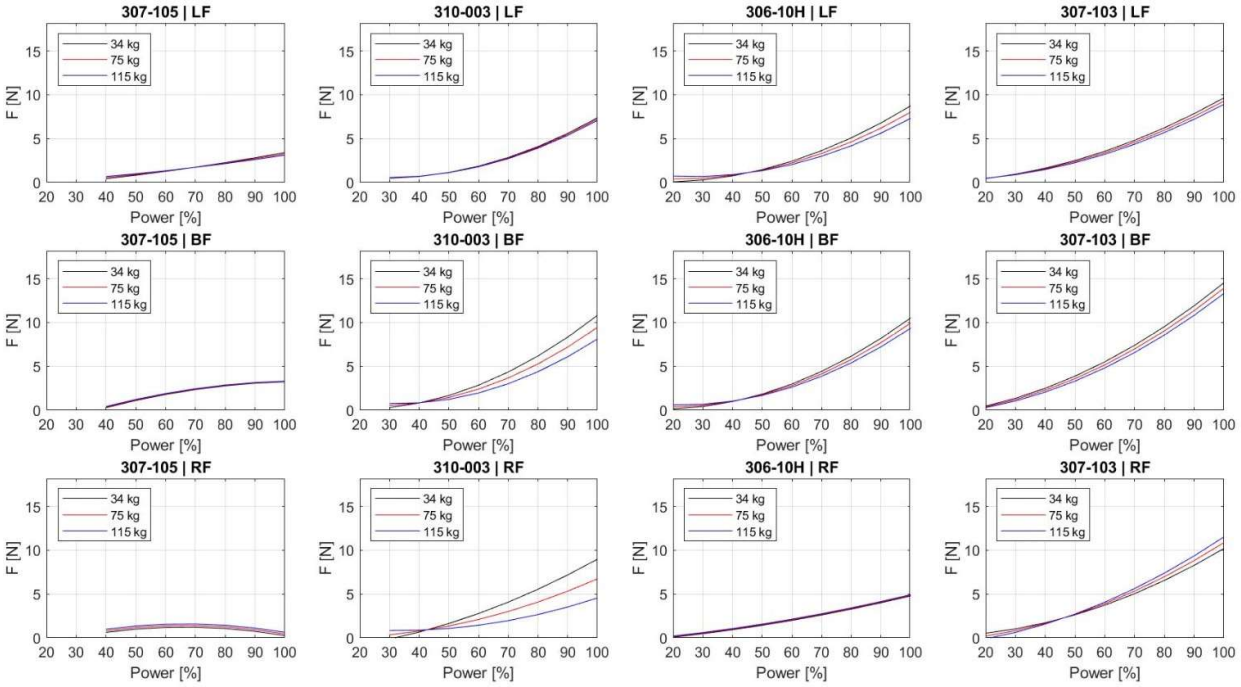

Figure 37: Forces exerted by the mat - Quadratic regression estimates

Rows represent the feet setting (LF, BF or RF), while columns represent the motor (307-105, 310-003, 306-10H and 307-103). In each subplot, the predicted exerted force by a quadratic regression model are displayed under three simulated participants' weights (34 kg, 75 kg, and 11 kg).

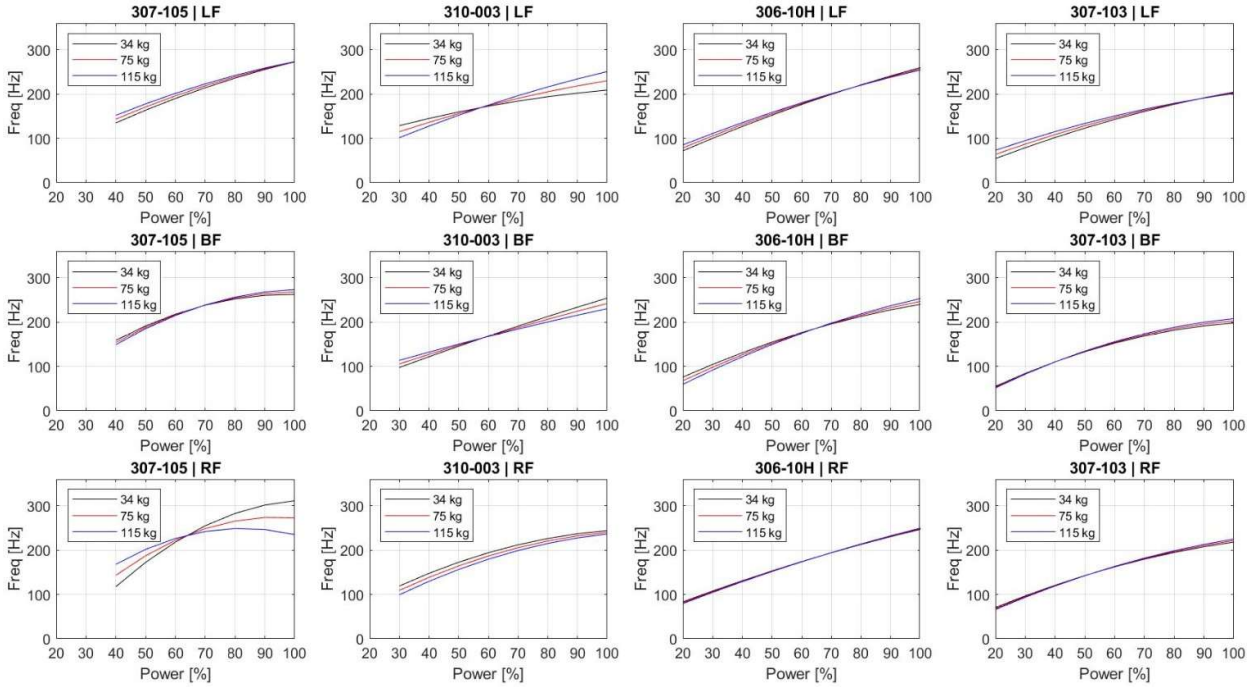

Figure 38: Frequencies exerted by the mat - Quadratic regression estimates

Rows represent the feet setting (LF, BF or RF), while columns represent the motor (307-105, 310-003, 306-10H and 307-103). In each subplot, the predicted exerted frequency by a quadratic regression model are displayed under three simulated participants' weights (34 kg, 75 kg, and 11 kg).

Using the 95% functional and simultaneous prediction intervals displayed in Figure 11 and Figure 12, the following comparisons were done for the exerted forces and frequencies. From Figure 39 to Figure 42, it is displayed by a line when two or more prediction bounds overlap, stating that the regression outputs were not statistically different based on a 95% confidence level. If there is a line for a single case in the y-axis, this indicates that it was not possible to overlap such case's prediction bounds with other ones.

- Within each motor and feet setting (i.e., subplots of Figure 11 or Figure 12), it was assessed if the regression's output (force or frequency) for a given power level differed across simulated weights. Results in Figure 39 and Figure 40.
- Within each motor (i.e., columns of Figure 11 or Figure 12), it was assessed if the regression's output for a given power level differed across feet settings. This was done for each simulated weight. Results in Figure 41 and Figure 42.
- Within each feet setting (i.e., rows of Figure 11 or Figure 12), it was assessed if the regression's output for a given power level differed across motors. This was done for each simulated weight. Results in Figure 43 and Figure 44.

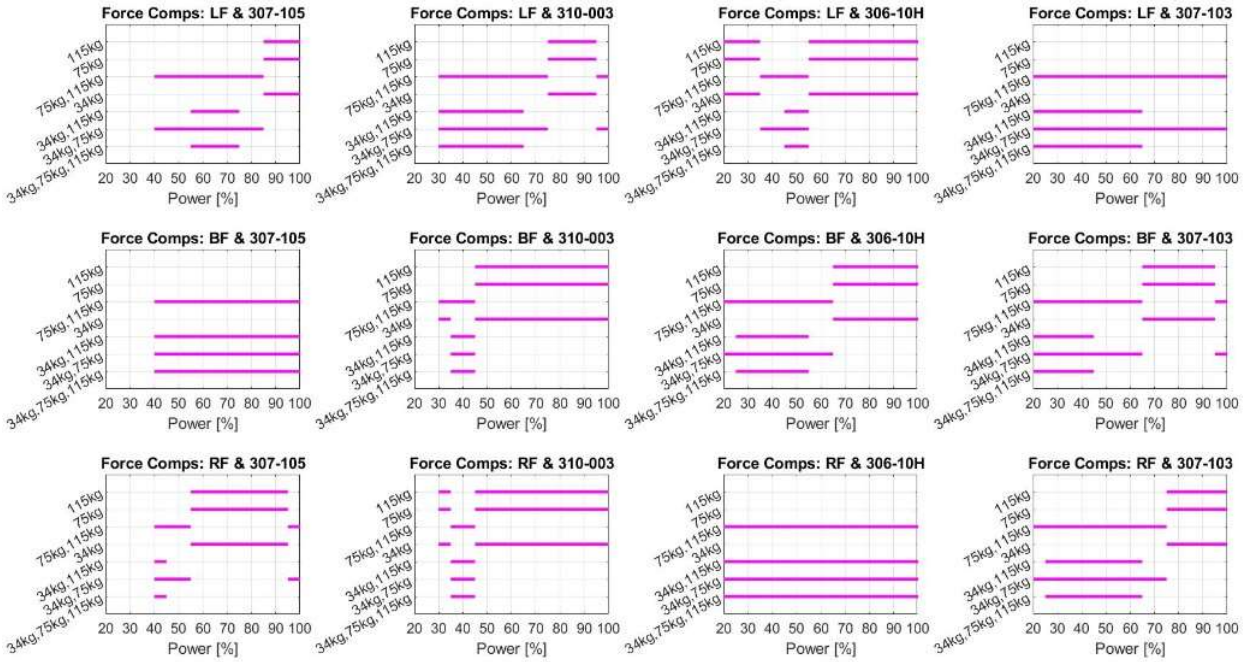

Figure 39: Comparison of forces for simulated weights within motor and feet setting

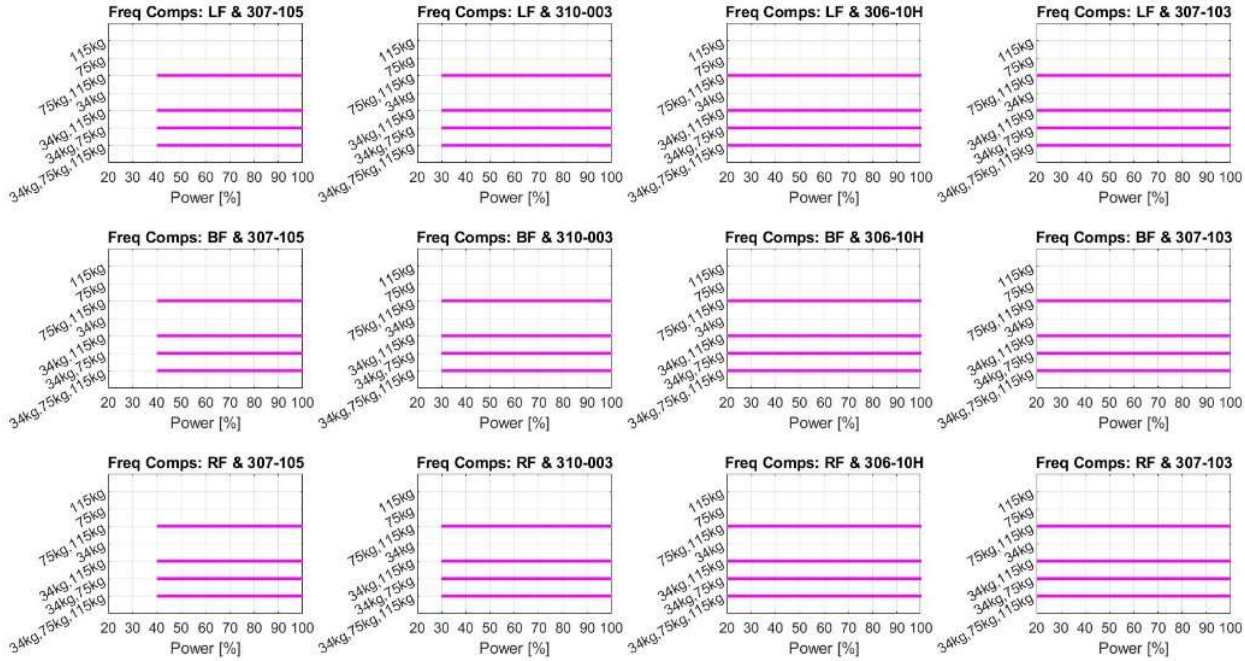

Figure 40: Comparison of frequencies for simulated weights within motor and feet setting

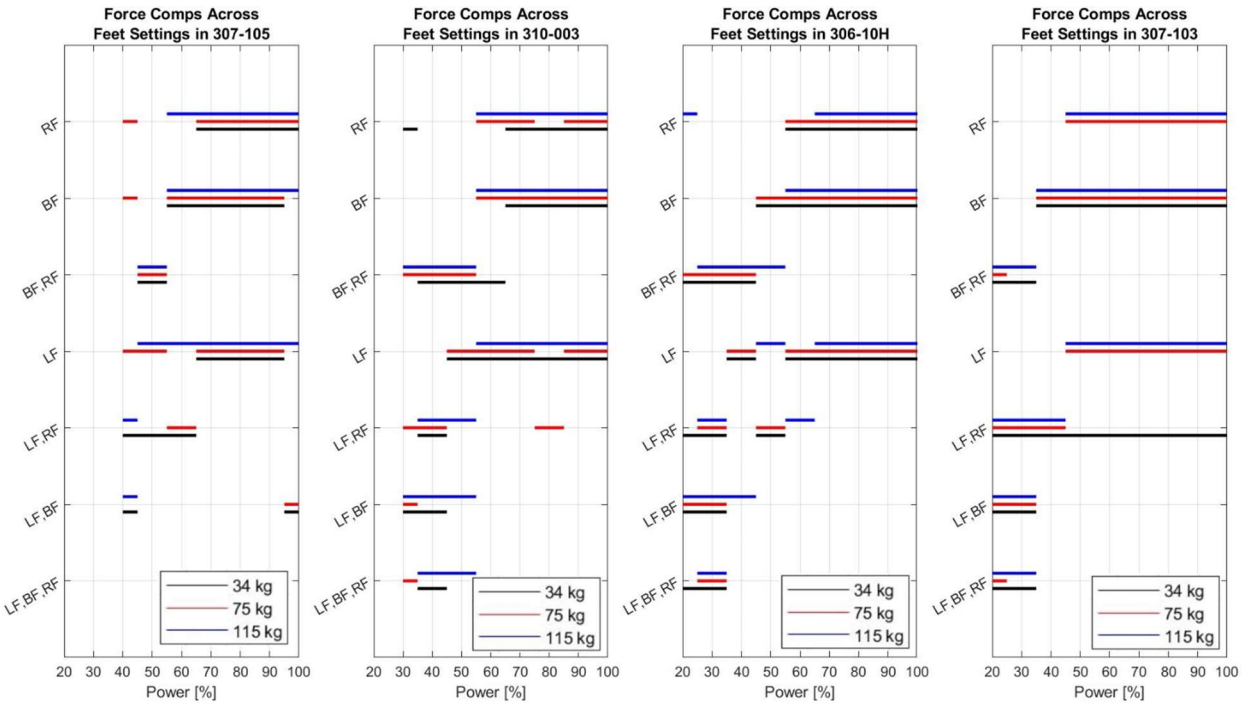

Figure 41: Comparison of forces for feet settings and simulated weights within a motor

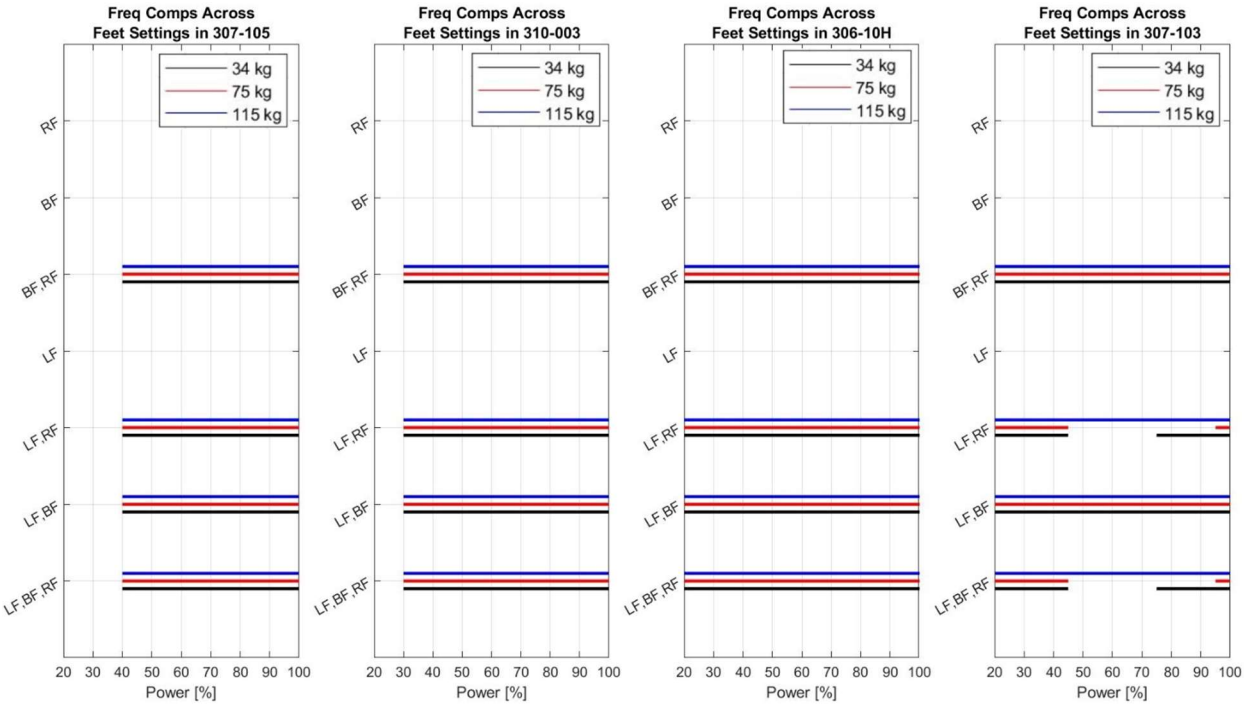

Figure 42: Comparison of frequencies for feet settings and simulated weights within a motor

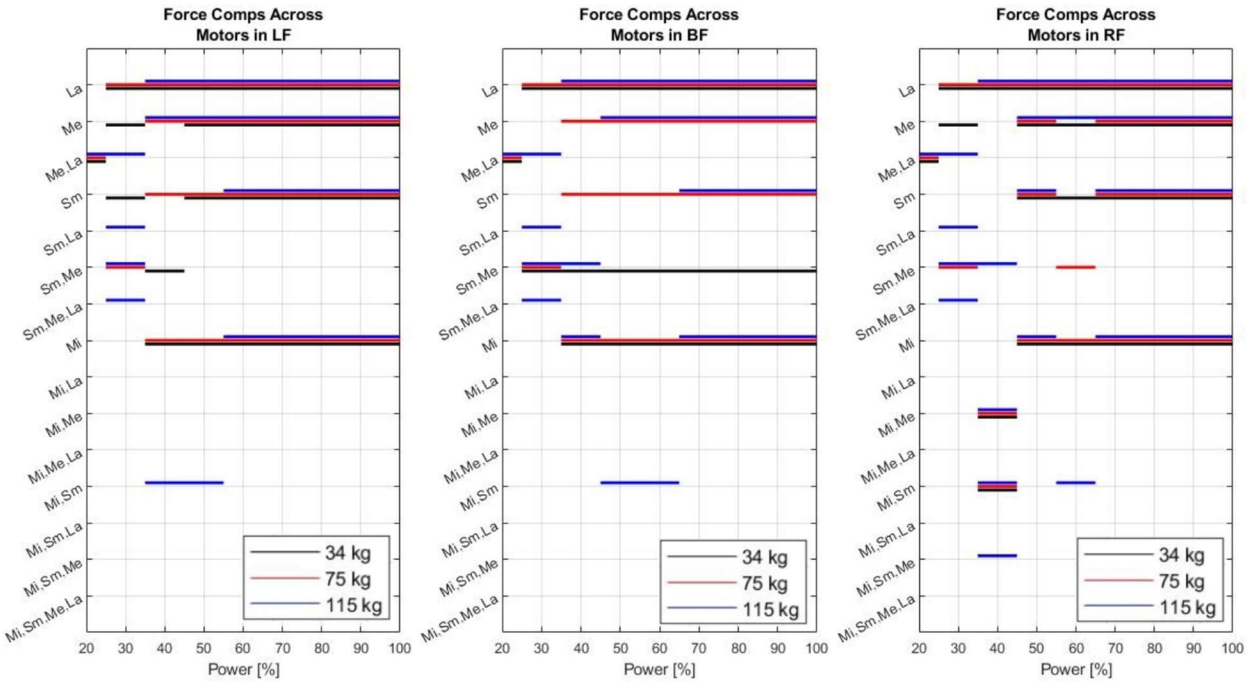

Figure 43: Comparison of forces for motors and simulated weights within feet setting
Mi: 307-105, Sm: 310-003, Me: 306-10H, and La: 307-103

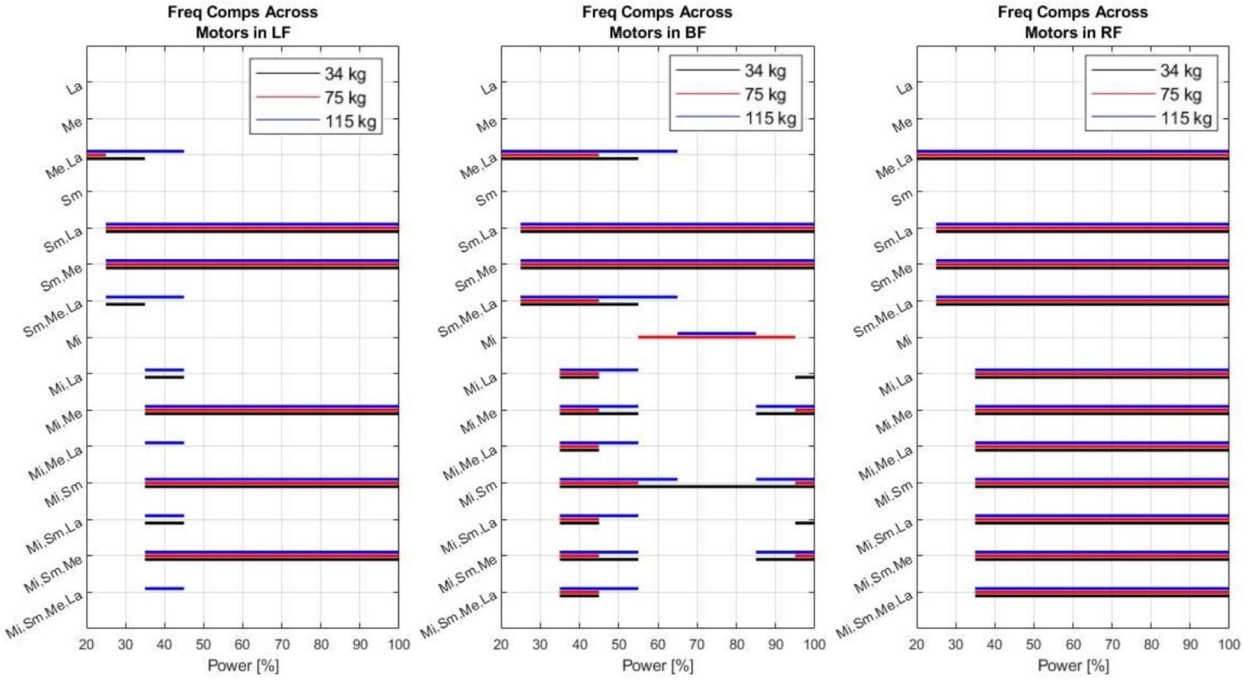

Figure 44: Comparison of frequencies for motors and simulated weights within feet setting
Mi: 307-105, Sm: 310-003, Me: 306-10H, and La: 307-103

Chapter 5 Appendix

Reliability of Vibratory Mat's Outputs

It was determined in Chapter 4 that the hanging and static tests yielded almost perfect results for the 307-103 motor. According to the handing test (Figure 6 Left), it was found that motor 307-103 could output accurate white, pink, and brown vibrations from its lowest power (20%) to its maximum power. According to the static test (Figure 6 Middle), it was found that motor 307-103 could output white vibrations, and that the ability to output a pink or brown vibration became more plausible as larger powers were used. However, this inability to produce accurate pink and brown vibrations at low power levels was justified by the obtained low signal-to-noise ratios and the non-stationary qualities that pink and brown signals have.

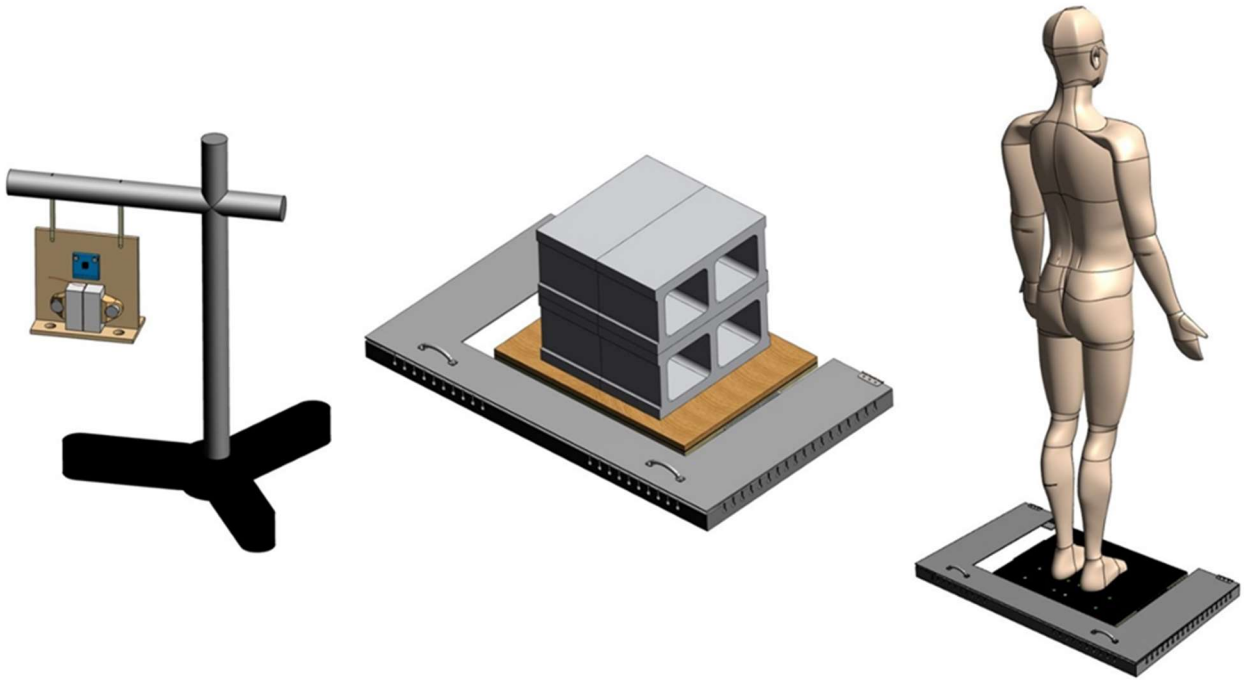

Figure 6: Testing set-ups to record vibrating outputs

(Left) Hanging Test: A vibrating component is clamped to a hanging platform that free to move, and vibrations are recorded by an accelerometer that is attached to the handing platform. (Middle) Static Test: Static weights are placed on a manufactured vibratory device, and the forces exerted by the embedded motors are recorded by a force plate located under the vibratory device. (Right) Dynamic Test: A human is placed on a manufactured vibratory device, and the forces exerted by the embedded motors are recorded by a force plate located under the vibratory device. Filtering techniques are needed to separate human sway from the forces exerted by the motors.

Figure 45 (left) shows that the vibratory mat using motor 307-103 was able to output white vibrations for all participants. It was also possible to notice that the hanging, static and dynamic tests (Figure 6) results agreed in terms of the signal's color and quality. The high similarities between all tests could allow future investigators to test white vibrations without manufacturing a vibratory mat or insole and have confidence that their results are going to be replicated once their motors are embedded in their devices.

Figure 45 (center) shows that according the hanging and dynamic tests, the vibratory mat using motor 307-103 was able to output pink vibrations for all participants. It was also possible to notice that the difference between the hanging and static results is larger, when compared to the difference between the hanging and dynamic results. Even though it is outside the scope of this pilot study or dissertation, pressure distribution is a possible explanation to why the dynamic results were better than the static results. Empirically while testing various motors, it was noticed that a motor's amplitude could be "muted" if high compressions were applied. The static test set-up places a dead weight on the vibratory mat, which is a time-invariant pressure distribution across the vibratory mat. On the other hand, when a participant stands on the vibratory mat and sways, pressure distributions in the feet change during the trial. It is possible that for some time, the participant applies more pressure at the heel than at the metatarsals, allowing the metatarsals motors "breathe" while the motors at the heel are "muted". Possible moments like this one could allow one or more motors be more noticeable by the force plate, increasing the signal-to-noise ratio; thus, fixing one of the possible limitations listed in Chapter 4. In fact, Figure 45 (center) shows a possible instance where this could had happened.

Referring to Figure 45 (center), participants s1003 and s2001 received similar power levels in their pink vibration visit (33% and 30% respectively). The closeness in power levels was reflected on how close the static test results were. However, this closeness was not reflected in the dynamic results. Participant

s1003, according to the dynamic results, received a more accurate pink vibration than participant s2001, when the hanging and static results state that s1003 and s2001 should had received similar pink vibrations. Given this observation, it is possible that the pressure distributions created by s1003 favored the signal-to-ratio in the dynamic test, allowing the DFA yields better results. It is possible to claim that the participant's sway (not pressure distribution) altered the DFA; however, we negate this possibility. The low-pass filter with cut-off frequency equal to 20 Hz [21], [27], [49] was set because from personal and other investigators' experience, human sway normally stays under 10 Hz. In addition, when testing all motors in the vibratory mat through hanging, static and dynamic test set-ups, frequency analysis content was done to make sure the motors were only present above 20 Hz. Therefore, band-pass filtering the motor data between 20 Hz and 400 Hz [21], [27], [49] removed all sway data, which follows our experimental frequency analysis results, as well as the motors' specifications set by Precision Microdrives, UK (motors' manufacturers).

Figure 45 (right) also shows the possible influence of pressure distribution in the accuracy of a signal. Participants s1003 and s2001 received the same power level during their brown vibration visit (33%), which according to the hanging results, both participants should had received similar brown vibrations. Based on the static results, a difference in favor of s2001 was expected. However, participant s1003 ended up receiving a vibration closer to brown. Figure 45 (right) also shows an amplified version of the behavior seen in the pink vibration (Figure 45, center). That is, a larger difference between the hanging and static results, when compared to the difference between the hanging and dynamic results. This amplified behavior can be explained again by the conclusions drawn from Chapter 4: low signal-to-noise ratios in brown vibrations output, and the non-stationarity feature that a brown signal has.

The observations derived from Figure 45, plus the conclusions drawn from Chapter 4 recommend future investigators interested in the validation of their vibratory outputs to consider the following:

- The nature of their vibratory signals, since more stationary signals (e.g., white) allow more constant readability by the force plate while it records vibrations.
- The signal-to-noise ration of the experiment, which will dictate the choice of sensor (accelerometer, force plate, etc.).
- The possible influence of pressure distribution in the motors, since the dynamic results were better than the static results for pink and brown vibrations in our pilot study.

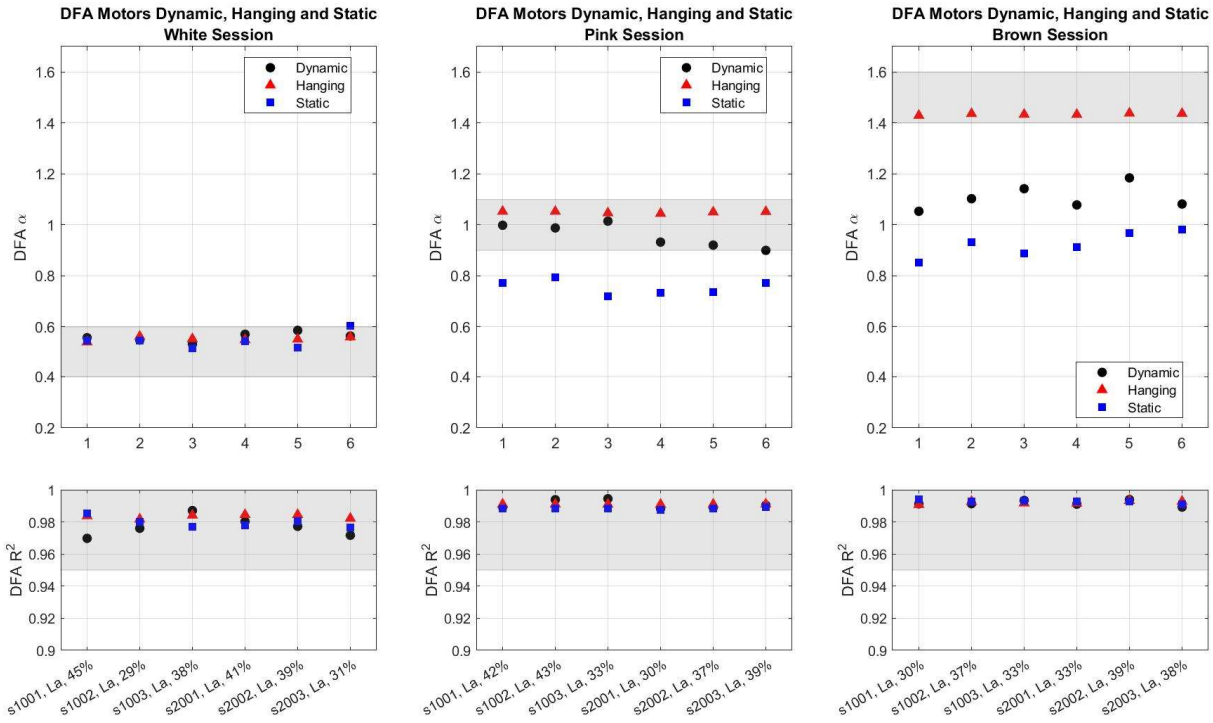

Figure 45: Vibratory mat's colors according to hanging, static and dynamic tests for the pilot study

Left, center and right columns represent respectively the white, pink, and brown sessions for the participants of the pilot study. The top plots represent the DFA α, while the bottom plots represent the DFA R^2. In all plots, the acceptable range is shown as a gray shaded area.

Regressions' Parameters and Information

Table 14 to Table 16 show the coefficients of the regression equations displayed from Figure 20 to Figure 22, as well as the fitting parameters for such regressions. The coefficients have the average value, as well as their confidence intervals inside parenthesis. The information on the regression equations was

separated by the participant's group (old and young), as well as by the COP direction (AP, ML, and Spatial) and COP measure (RMS or 95% Ellipse, SampEn, and DFA α).

Table 14: STIM - $BL_{Mat} \propto BL_{Mat}$ Regression Coefficients and Fitting

		AP		ML		Spatial	
		Old	**Young**	**Old**	**Young**	**Old**	**Young**
RMS or 95% Ellipse	**m**	-0.56 (-1.35 ... 0.23)	-0.051 (-0.75 ... 0.64)	-0.46 (-0.95 ... 0.03)	-0.30 (-0.62 ... 0.02)	-0.41 (-1.01 ... 0.18)	-0.58 (-0.87 ... -0.29)
	b	0.006 (-0.002 ... 0.015)	0.0076 (-0.006 ... 0.021)	0.022 (-0.001 ... 0.045)	0.019 (0.001 ... 0.038)	8.1e-05 (-6.3e-05 ... 0.0002)	0.0001 (-2.2e-05 ... 0.0003)
	R^2_{adj}	0.119	-0.097	0.232	0.236	0.111	0.631
	RMSE	4.554E-03	1.163E-02	4.242E-03	4.379E-03	7.847E-05	1.138E-04
SampEn (m=2, R=0.1)	**m**	-0.72 (-1.44 ... -0.004)	-1.87 (-2.78 ... -0.95)	-0.78 (-2.09 ... 0.53)	-0.43 (-1.16 ... 0.30)	-1.26 (-2.53 ... 0.01)	-0.46 (-0.89 ... -0.03)
	b	0.25 (-0.003 ... 0.5)	0.52 (0.27 ... 0.77)	0.26 (-0.06 ... 0.59)	0.16 (-0.02 ... 0.35)	0.38 (0.02 ... 0.74)	0.14 (0.03 ... 0.25)
	R^2_{adj}	0.268	0.642	0.065	0.063	0.260	0.298
	RMSE	0.0733	0.0494	0.1222	0.0803	0.0911	0.0480
DFA α (0.5s - 15s)	**m**	-0.44 (-0.89 ... 0.004)	-0.87 (-1.54 ... -0.21)	-0.92 (-1.39 ... -0.45)	-0.84 (-1.92 ... 0.24)	-0.99 (-1.62 ... -0.35)	-0.71 (-1.61 ... 0.18)
	b	0.50 (-0.03 ... 1.04)	1.06 (0.28 ... 1.83)	1.07 (0.52 ... 1.62)	1.00 (-0.27 ... 2.26)	1.14 (0.41 ... 1.86)	0.88 (-0.18 ... 1.95)
	R^2_{adj}	0.260	0.406	0.620	0.154	0.500	0.162
	RMSE	0.0713	0.0845	0.0713	0.1161	0.0793	0.1106

Table 15: T_0 - $BL_{Mat} \propto BL_{Mat}$ Regression Coefficients and Fitting

		AP		ML		Spatial	
		Old	**Young**	**Old**	**Young**	**Old**	**Young**
RMS or 95% Ellipse	**m**	0.032 (-0.51 ... 0.57)	-0.38 (-0.93 ... 0.16)	-0.73 (-1.12 ... -0.33)	-0.13 (-0.41 ... 0.15)	-0.61 (-1.07 ... -0.15)	-0.15 (-1.58 ... 1.27)
	b	0.0007 (-0.005 ... 0.006)	0.013 (0.002 ... 0.02)	0.034 (0.016 ... 0.053)	0.008 (-0.009 ... 0.024)	9.8e-05 (-1.2e-05 ... 0.0002)	0.0002 (-0.0006 ... 0.0009)
	R^2_{adj}	-0.098	0.117	0.590	0.002	0.419	-0.094
	RMSE	3.101E-03	9.150E-03	3.417E-03	3.869E-03	5.976E-05	5.590E-04
SampEn (m=2, R=0.1)	**m**	-0.2 (-0.9 ... 0.43)	-1.54 (-2.6 ... -0.48)	-1.02 (-1.79 ... -0.24)	-0.74 (-1.39 ... -0.10)	-1.48 (-2.45 ... -0.51)	-0.84 (-1.3 ... -0.37)
	b	0.083 (-0.15 ... 0.32)	0.40 (0.11 ... 0.69)	0.29 (0.093 ... 0.48)	0.16 (-0.01 ... 0.32)	0.41 (0.14 ... 0.69)	0.17 (0.052 ... 0.29)
	R^2_{adj}	-0.037	0.465	0.409	0.336	0.488	0.581
	RMSE	0.0680	0.0569	0.0722	0.0712	0.0696	0.0521
DFA α (0.5s - 15s)	**m**	-0.057 (-0.73 ... 0.61)	-1.10 (-1.68 ... -0.52)	-0.42 (-0.98 ... 0.14)	-0.13 (-1.31 ... 1.05)	-0.71 (-1.73 ... 0.31)	-0.62 (-1.62 ... 0.37)
	b	0.015 (-0.78 ... 0.81)	1.35 (0.67 ... 2.03)	0.44 (-0.22 ... 1.09)	0.14 (-1.24 ... 1.53)	0.79 (-0.38 ... 1.95)	0.77 (-0.4 ... 1.9487)
	R^2_{adj}	-0.096	0.603	0.137	-0.093	0.114	0.080
	RMSE	0.1064	0.0739	0.0849	0.1269	0.1271	0.1220

Table 16: T_0 - STIM $\propto$ STIM Regression Coefficients and Fitting

		AP		ML		Spatial	
		Old	**Young**	**Old**	**Young**	**Old**	**Young**
RMS or 95% Ellipse	**m**	-0.23 (-0.75 ... 0.29)	-0.36 (-0.59 ... -0.12)	-0.35 (-0.56 ... -0.15)	0.035 (-0.32 ... 0.39)	-0.41 (-0.72 ... -0.1)	0.54 (-1.84 ... 2.92)
	b	0.002 (-0.003 ... 0.008)	0.008 (0.002 ... 0.014)	0.017 (0.007 ... 0.026)	-0.004 (-0.025 ... 0.018)	6.0e-05 (-1.0e-05 ... 0.0001)	6.5e-05 (-0.0008 ... 0.0009)
	R^2_{adj}	-0.001	0.494	0.560	-0.095	0.420	-0.073
	RMSE	3.611E-03	5.299E-03	1.557E-03	4.074E-03	4.155E-05	5.515E-04
SampEn (m=2, R=0.1)	**m**	-0.53 (-1.27 ... 0.21)	-0.21 (-0.67 ... 0.24)	-1.21 (-1.60 ... -0.82)	-0.53 (-0.99 ... -0.07)	-1.19 (-1.73 ... -0.64)	-0.61 (-1.12 ... -0.09)
	b	0.18 (-0.07 ... 0.45)	0.032 (-0.1 ... 0.16)	0.35 (0.22 ... 0.48)	0.08 (-0.07 ... 0.22)	0.34 (0.16 ... 0.52)	0.1 (-0.04 ... 0.25)
	R^2_{adj}	0.122	0.008	0.814	0.335	0.669	0.348
	RMSE	0.0798	0.0387	0.0673	0.0601	0.0716	0.0473
DFA α (0.5s - 15s)	**m**	-0.2 (-1.17 ... 0.76)	-0.46 (-0.95 ... 0.02)	-0.97 (-2.00 ... 0.06)	-0.077 (-0.64 ... 0.49)	-0.73 (-1.86 ... 0.41)	-0.30 (-0.91 ... 0.31)
	b	0.2 (-0.91 ... 1.34)	0.59 (0.002 ... 1.18)	1.08 (-0.12 ... 2.28)	-0.065 (-0.61 ... 0.74)	0.81 (-0.5 ... 2.11)	0.36 (-0.39 ... 1.11)
	R^2_{adj}	-0.076	0.244	0.234	-0.090	0.087	0.017
	RMSE	0.1296	0.0589	0.1052	0.0937	0.1278	0.0982

Sample Size Power Analysis

A power analysis to determine the number of participants required to find statistically significant results was done using the data of the pilot study. The needed sample size to find a significant effect due to vibration (white: WH, pink: PK, and brown: BR) between STIM vs. BL_{Mat}, T_0 vs. BL_{Mat}, and T_0 vs. STIM was performed for each group (old and young), COP direction (AP, ML, and Spatial), and measure (RMS or 95% Ellipse, SampEn, and DFA α). The selected sample size was the one that yielded an 80% power. For the placebo (PB) vibration, the needed sample size to not find statistical significance was determined, still using an 80% power. Table 17 to Table 19 summarize the needed sample size for each case. There were instances where either it was not possible to find the needed sample size or the sample size was larger than 100, and these instances were marked as #N/A.

Table 17: Needed Sample Size for Power = 80%
Between STIM and BL_{Mat}

		AP		ML		Spatial	
		Old	**Young**	**Old**	**Young**	**Old**	**Young**
RMS or 95% Ellipse	**WH**	80	50	#N/A	#N/A	26	14
	PK	4	5	#N/A	#N/A	33	16
	BR	14	20	#N/A	#N/A	24	42
	PB	30	#N/A	15	12	#N/A	16
SampEn (m=2, R=0.1)	**WH**	#N/A	12	9	3	10	3
	PK	#N/A	12	44	4	80	4
	BR	#N/A	23	6	9	57	15
	PB	#N/A	#N/A	5	9	5	14
DFA α (0.5s - 15s)	**WH**	9	4	4	#N/A	5	#N/A
	PK	12	9	30	37	25	11
	BR	#N/A	#N/A	11	#N/A	#N/A	9
	PB	19	25	44	22	61	8

Table 18: Needed Sample Size for Power = 80% Between T_0 and BL_{Mat}

		AP		ML		Spatial	
		Old	Young	Old	Young	Old	Young
RMS or 95% Ellipse	WH	#N/A	40	40	15	35	8
	PK	3	8	#N/A	#N/A	22	4
	BR	4	19	60	#N/A	8	19
	PB	#N/A	#N/A	23	43	3	48
SampEn (m=2, R=0.1)	WH	#N/A	#N/A	8	#N/A	#N/A	40
	PK	16	34	#N/A	61	#N/A	#N/A
	BR	#N/A	#N/A	#N/A	8	#N/A	7
	PB	20	92	16	5	#N/A	3
DFA α (0.5s - 15s)	WH	3	#N/A	4	70	22	20
	PK	14	11	80	#N/A	#N/A	7
	BR	17	19	#N/A	24	#N/A	2
	PB	26	80	80	52	#N/A	#N/A

Table 19: Needed Sample Size for Power = 80% Between T_0 and STIM

		AP		ML		Spatial	
		Old	Young	Old	Young	Old	Young
RMS or 95% Ellipse	WH	80	#N/A	29	#N/A	#N/A	#N/A
	PK	#N/A	60	43	#N/A	#N/A	#N/A
	BR	36	#N/A	92	10	3	20
	PB	9	#N/A	#N/A	4	16	10
SampEn (m=2, R=0.1)	WH	#N/A	40	18	6	17	13
	PK	70	#N/A	#N/A	13	#N/A	16
	BR	#N/A	5	27	5	42	4
	PB	60	7	3	22	6	15
DFA α (0.5s - 15s)	WH	#N/A	83	43	7	20	33
	PK	#N/A	19	16	#N/A	70	46
	BR	#N/A	7	#N/A	33	#N/A	17
	PB	62	38	17	30	4	4

Table 17 to Table 19 show a wide variety of sample sizes for a future study that wishes to expand the preliminary results found in this pilot study. However, to come up with a more practical sample size, Table 20 shows the median sample size across various variables of Table 17 to Table 19. When looking at Table 20, it is possible to see that an achievable and justifiable sample size for a future study is between

15 and 20 participants, which agrees with sample sizes used in similar SR studies [10]–[12], [14], [16]–[23], [26], [27], [47]–[49].

Table 20: Summary of Needed Sample Size

	STIM vs. BL_{Mat}	T_0 vs. BL_{Mat}	T_0 vs. STIM	RMS or 95% Ellipse	SampEn (m=2, R=0.1)	DFA α (0.5s - 15s)	WH	PK	BR	PB
Old	17	17	27	24	17	19	18	28	21	17
Young	12	19	15	16	11	20	15	12	15	16